



Provided by the author(s) and University of Galway in accordance with publisher policies. Please cite the published version when available.

Title	Beyond Lolium perenne: the impact of grassland biodiversity on butyric acid and biomethane production in a forage-based anaerobic biorefinery
Author(s)	Coelho, Fabiana Maria Bastos
Publication Date	2024-02-22
Publisher	NUI Galway
Item record	http://hdl.handle.net/10379/18064

Downloaded 2024-04-29T02:05:18Z

Some rights reserved. For more information, please see the item record link above.





OLLSCOIL NA GAILLIMHÉ
UNIVERSITY OF GALWAY

**Beyond *Lolium perenne*: the impact of
grassland biodiversity on butyric acid and
biomethane production in a forage-based
anaerobic biorefinery**

Fabiana Maria Bastos Coelho

*A thesis presented in fulfilment of the requirements for the degree of Doctor of
Philosophy*

Head of Department: Prof. Conor O'Byrne

Research supervisor: Prof. Vincent O'Flaherty

Microbial Ecology Laboratory
Microbiology, School of Natural Sciences

University of Galway

November, 2023

Table of Contents

Acknowledgements	iii
Abstract	v
List of Figures	viii
List of Tables	xi
Chapter 1: Introduction	1
1.1 Thesis Scope	2
1.2 References	4
Chapter 2: Current Trends in Biological Valorisation of Waste-Derived Biomass: The Critical Role of VFAs to Fuel a Biorefinery	8
2.1 Introduction	9
2.2 Methods of Valorising Low-value Feedstocks	10
2.2.1 Thermochemical approach	10
2.2.2 Biological approach	11
2.2.3 Valorisation - selecting a method	11
2.3 Sustainable Feedstock Types	11
2.3.1 Food waste	11
2.3.2 Agricultural residues	12
2.3.3 Animal residues	13
2.4 State-of-the-art System Designs	14
2.4.1 Single-stage system design and application	14
2.4.2 Multi-stage system design and application	15
2.5 Process optimisation for Carboxylic Acid Production	16
2.5.1 Producing carboxylic acids	16
2.5.2 Inoculum - providing an appropriate microbial community	16
2.5.3 Two-stage design for optimised carboxylic acid production	17
2.5.4 Leachate dilution in LBRs affects VFA production	18
2.5.5 pH directly affects biomass degradability and VFA profile	19
2.5.6 Temperature implications for VFA accumulation	19
2.5.7 Organic loading rate and hydraulic retention time	19
2.5.8 Feedstock choice influences VFA profile	20
2.5.9 The challenge: VFA recovery and concentration	20
2.6 Innovative VFA Applications	22
2.6.1 VFAs for bioplastic production	22
2.6.2 VFAs for chain elongation chemicals	23
2.6.3 VFAs for bioenergy and biofuel	23
2.7 Fermentative Microbial Communities	23
2.7.1 Microbial communities – why bother?	23
2.7.2 Key fermentative groups	24
2.8 Future Perspectives: Biorefinery Concept, Application, and Challenges	24
2.9 Conclusions	26

2.10	Acknowledgement and contributions	26
2.11	References	27

Chapter 3: Synergistic and antagonistic effects in the anaerobic digestion of permanent

	grassland biomass species	40
3.1	Introduction	40
3.2	Materials and Methods	42
3.2.1	Substrate	42
3.2.2	Inoculum	43
3.2.3	Biomethane potential experimental setup	43
3.2.4	Analytical methods	44
3.3	Chemical Parameters and Modelling	45
3.3.1	Volatile solids degradation	45
3.3.2	Theoretical chemical oxygen demand	46
3.3.3	Theoretical methane potential and biodegradability index	46
3.3.4	Biomethane production	47
3.3.5	Empirical kinetic models	47
3.3.6	DI model	49
3.4	Results	50
3.4.1	A similar VS degradation was observed in the digestion of all monocultures and mixtures, regardless of chemical composition	50
3.4.2	First order kinetics selected to model the methane production from grassland species	50
3.4.3	Grassland species varied in methane potential with similar lag phase times and hydrolysis constant rates	52
3.4.4	Antagonistic and synergistic effects identified with the Diversity-interaction models	54
3.5	Discussion	58
3.5.1	Biodegradability and methane yield varied between and within species, indicating the biomass heterogeneity	58
3.5.2	Improved methane yield in monocultures species resulted from balanced C:N ratio and fibre content	58
3.5.3	Synergistic/antagonistic effects were dependent on species, not functional groups	60
3.5.4	A comparable area-specific methane yield was observed when digesting <i>L. perenne</i> , the six-species mixture, and <i>L. perenne</i> mixed with <i>T. pratense</i>	61
3.6	Conclusions	61
3.7	Acknowledgement and contributions	62
3.8	References	62
A.1	Appendices	69

Chapter 4: Producing butyric acid and VFAs from permanent grassland monocultures: the potential of *Lolium perenne*, *Trifolium pratense* and *Trifolium repens*

	potential of <i>Lolium perenne</i>, <i>Trifolium pratense</i> and <i>Trifolium repens</i>	75
4.1	Introduction	76
4.2	Materials and Methods	78
4.2.1	Substrates	78
4.2.2	Biomethane potential assay	78

4.2.3	One-stage fermentation assay	79
4.2.4	Two-stage fermentation assay	80
4.2.5	Analytical methods	81
4.3	Chemical Parameters	82
4.3.1	Volatile solids degradation	82
4.3.2	Biomethane production	83
4.3.3	Acidification yield and VFA production	83
4.4	Results and Discussion	84
4.4.1	Clover's buffering capacity can be associated with its higher volatile solids degradation under fermentation conditions	84
4.4.2	A balanced C:N ratio for <i>L. perenne</i> as effective as a higher nitrogen fertilisation rate	89
4.4.3	Weed intrusion as factor hindering the accumulation of methane from clover fields	90
4.4.4	Selective production of butyric acid mainly obtained from the fermentation of <i>L. perenne</i>	92
4.4.5	Sharp pH drop in the two-stage fermentation of all substrates was associated to lactic acid, but two-stage and one-stage fermentation had the same VFA yield	95
4.5	Conclusions	98
4.6	Acknowledgement and contributions	98
4.7	References	98
B.1	Appendices	105

Chapter 5: Silage fermentation for butyric acid production in leach-bed reactors: the impact of silage pH and inoculum source in the fermentation process **106**

5.1	Introduction	107
5.2	Materials and Methods	109
5.2.1	Seed-inoculum	109
5.2.2	Substrate	109
5.2.3	Selecting a seed-inoculum for the reactor trial (First stage)	110
5.2.4	Silage fermentation in leach-bed reactors (Second stage)	111
5.2.5	Influence of inoculum approaches in silage fermentation (Third stage)	113
5.2.6	Analytical methods	113
5.2.7	Microbial community sampling	115
5.2.8	DNA/RNA co-extraction and cDNA synthesis	115
5.2.9	Sequencing, bioinformatics and statistical analysis	116
5.3	Chemical Parameters	117
5.3.1	Volatile solids degradation	117
5.3.2	Lignocellulosic degradation	118
5.3.3	Biomethane production	118
5.3.4	COD of solid materials	119
5.3.5	Acidification yield and VFA production	120
5.4	Results	120
5.4.1	Mixing granular sludge with other seed-inocula improved the conversion of silage	120
5.4.2	Silage degradation was not influenced by the inoculum source during its fermentation	121

5.4.3	The fermentation of silage resulted in a VFA mixture dominated by butyric acid in all Phases but Phase IV	122
5.4.4	Digestate is important for the degradation of silage and production of VFAs	128
5.4.5	Combining seed-inocula and silage was important to compose a richer microbial community	129
5.4.6	Shifts in microbial composition were correlated to the different silages	132
5.4.7	Prevotella and Lactobacillus as the most abundant genera, irrespective of the seed-inocula used	134
5.5	Discussion	137
5.5.1	Efficient silage degradation achieved using a mixture of granular sludge with rumen material and cattle slurry	137
5.5.2	Silage degradation evidenced by the reduction of cellulose and hemicellulose content	137
5.5.3	Silage pH was an important process indicator for acid accumulation efficiency and acid profile	138
5.5.4	Butyric acid was the primary VFA produced from silage, with a significant accumulation of caproic acid	140
5.5.5	Silage indigenous community and pH were the driving forces shifting the reactor performance	143
5.5.6	Combining digestate and leachate as inoculum is more important for biomass degradation than acids production	146
5.6	Conclusions	147
5.7	Acknowledgement and contribution	147
5.8	References	148
C	Appendices	155
C.1	Quality-check for the microbial community extraction: Sonication and RNAlater	158

Chapter 6: Conclusions and Perspective **161**

6.1	Final Discussion and Conclusions	161
6.1.1	Permanent grassland for the production of methane	161
6.1.2	Permanent grasslands in the production of butyric acid and other VFAs	163
6.1.3	Silage pH – an important process indicator for VFA accumulation	164
6.2	Future Recommendations and Perspectives	167
6.3	References	167

Declaration of Authorship

I, **Fabiana Maria Bastos Coelho**, certify that the thesis:

Beyond *Lolium perenne*: the impact of grassland biodiversity on butyric acid and biomethane production in a forage-based anaerobic biorefinery

is based on my own work and has been generated by me, unless stated otherwise. No other person's work has been used without due acknowledgement in this thesis. Collaborations that made this work possible have been clearly stated where appropriate. All references have been quoted and all source of information, including graphs and datasets, have been acknowledged accordingly.



A handwritten signature in black ink, reading "Fabiana Maria Bastos Coelho", is written over a horizontal line.

A gente é uma contradição, e esperar um ser humano perfeito é a forma mais eficiente de desumanizar um ser humano. ‘Tá todo mundo errando o tempo todo, a gente é um processo de erros.

We are a paradox, expecting a human being to be perfect is the most efficient way to dehumanize a human being. We’re all making mistakes all the time, we’re a process of (making) mistakes.

Guilherme Terreri, Rita von Hunty

For my mom (Fatima), my dad (Fernando) and my brother (Felipe) - who always supported me no matter what I stubbornly decided to do, and who taught me that knowledge was the strongest tool in my toolbox.

For my partner, Otavio, who designed this PhD adventure with me and who believed in me from day 1.

Acknowledgements

To start this (personal, but important) part, I would like to acknowledge that a PhD was a lifelong goal for me, but I did not fully understand what it meant when I started. I've made some of the mistakes everybody does and I've created some of my own. However, it would be impossible to write here without expressing my gratitude to the people that surrounded me in this adventure. This is an ungrateful task, as I will most definitely forget someone (and only realise after the PhD is done).

I believe a big factor in any PhD is who you choose as your supervisor, and I am very happy that prof. Vincent and I got to work together. He gave me an opportunity that I wanted very much, while showing me the reality behind it all. Thanks, Vince, for being supportive, empathetic, kind, and for helping me see things through. Especially when you said, 'Life is long and there is time for everything in life'. I think this was a lesson we all had to face, understand and appreciate after the COVID-19 Pandemic.

Dr. Corine guided me through it all, showing me that I needed to stand up for what I believed was right. I appreciate the trust and guidance, brainstorming, revisions, but especially our conference trips. It was really funny! I learned a lot from you, Corine. Still on guidance, I would like to acknowledge my GRC members - Dr. Piet Lens, Dr. Florence Abraham, and Dr. Gavin Collins. I would also like to acknowledge Bioeconomy Research Centre (BiOrbic), and the funding bodies Science Foundation Ireland (SFI) and Enterprise Ireland that made this research possible.

On the road, I had an amazing group of colleagues with me – they've become friends, but that is another topic. I would like to acknowledge all the VOF lab crew, for the chats and support. In special, I would like to say thanks to (Papa) Andrew Bartle, Alejandra Villa, Sandra O'Connor, Shaun Connolly, and Caroline O'Donnell. These people helped me through the PhD in so many ways and they were so kind, thanks for it all! I would like to thank my 4th year students, Stephanie Curtin, Aaron Talt, and Adam Jones as well as my master student Aaron Nolan, for the confidence and support during my studies. Special thanks to Anna Trego, for her incredible support with the bioinformatics, revising this thesis and for all the great advice, talks and laughs. I would also like to thank Dr. Umer Ijaz for the patience during our bio-informatics sessions and his guidance. I also made some good friends in the neighbouring labs – Borja Tamayo (and Rosalia Lopez), Simone Pau, Armando Oliva, Lea Tan, Federica Carboni, Carlos Sanchez, Laura Cutugno, Paolo Dessi, Jialun Wu and Marco Prevedello – who would remind me every so often the way to the pub.

A PhD is a very lonely journey, but I was lucky to find a place (6 Glenmore) with people that became a very integral part of my family - Claribel Buenano, Yuchen Liu, Jara Buena, Lee Doyle, John Gostage, and Agnese Lucchetti. Looking from distance, now, it feels even more incredible that we have met each other in Galway. I learned a lot from all of you, and I hope I could share a bit of the love and friendship I've received from you. And let's not forget about Isi! The give-me-food-at-4-am and where-is-my-food-human cat that made me realise maybe I should be a pet-sitter and not a researcher!

The PhD was a bittersweet experience – it brought me so much joy, but it was hard sometimes. I think the biggest challenge was to be physically away from my support group, especially my partner Otavio. When we made this crazy plan of going separate ways to get a PhD, I knew it was going to be hard. Let's just say, we don't recommend, but we don't regret. So I appreciate the love, friendship, and support throughout the years, Otavio. I would also like to thank our biggest supporters: my parents (Fatima and Fernando), my brother (Felipe), and my in-laws (Francisco, Janne and Raphaela), who dealt with the distance and cheered for us from across the ocean. In that support group, on the other side of the ocean (and some in the snowy Norway), there are also people I would like to acknowledge for the sweet and strong support – Pablo Campos, Carolina Genuncio, Cecilia Leite, Mellyssa Soares, Lucas Ferreira, Allyne Machado, Shreya Gopalakrishnan, Germana Viana, Nadia Oliveira, Joakim

Andersen and Ricardo Wanderley.

And last, but definitely, not least... I would like to acknowledge myself for embracing an opportunity in another country, far away from home, friends and partner. For being kind (mostly to others) and brave to face so many challenges, personally and professionally. But also for recognising that fear is a part of the process, that it can be a powerful weapon - and as powerful weapons go, they can both protect you and harm you. Kudos to me.

Abstract

Permanent grassland fields are complex ecosystems consisting of graminoids (e.g., grasses) and forbs (e.g., legumes and herbs), which are crucial for environmental health and food production. Forbs are important players in this ecosystem to the maintenance of grassland's biodiversity and functionality. In the context of biorefinery, graminoids and forbs represent a low-cost, abundant and renewable source of feedstock, which can be used for the production of a myriad of products (e.g., biogas, biomethane, volatile fatty acids [VFAs] and fertiliser). In the past 20 years, grasses have been extensively evaluated as a potential feedstock for anaerobic digestion (AD) due to their sustainability and abundance. However, forbs have been overlooked, despite their importance to the environment and their higher nutritional value compared to grasses. Beyond biogas, the AD process can be tailored to improve the production of selected acids with a higher market value than biogas/biomethane, such as butyric acid and caproic acid. Shifting the process to the accumulation of VFAs would be important to associate resource recovery, sustainability and competitiveness. Few works have studied the use of grassland biomass, fresh or ensiled, to selectively accumulate butyric acid, and none have studied the potential of clovers for VFA production. Moreover, silage quality and its effect in the fermentation of grassland biomass is still unclear despite the importance of feedstock type and quality to VFA production.

Therefore, this Ph.D. investigates the use of AD technology in the valorisation of permanent grasslands, evaluating biomethane production and the selective accumulation of butyric acid. This work also aims to elucidate the microbial community dynamics in the fermentation of grass, especially considering different types of silage. The thesis was structured in five chapters. In the first chapter, an introduction to the motivation of this thesis, its research questions and objectives are outlined. In the second chapter, a critical review published in the special issue 'Anaerobic Fermentation' – *A Biological Route Towards Achieving Net Neutrality* (Fermentation, August 2022) is presented in its original form. The review explored the potential for resource recovery from food waste, agricultural and animal residues and some of the recent advances in the production of VFAs from these substrates. The important notes on chemical parameters, state-of-art systems, and applications were also provided. The main drawback in VFA production, VFA recovery, was also discussed, highlighting a range of challenges and opportunities, which are the current drivers in the field.

In the third chapter, a study was designed to evaluate the methane potential of six grassland species adapted to temperate climate: *Lolium perenne*, *Phleum pratense*, *Trifolium pratense*, *Trifolium repens*, *Chicorium intybus*, and *Plantago lanceolata*. The influence of nitrogen fertilisation rates on the methane production was investigated using plots of *L. perenne* supplied with two levels of nitrogen fertiliser. A biomethane potential assay was performed to elucidate the species identity effects and interspecific interaction effects of mono-digesting those species and co-digestion two or six of those species. Those effects were evaluated using a diversity-interaction model. Synergistic effects were observed in the co-digestion of both *T. repens* and *C. intybus*, and *L. perenne* and *T. pratense*. Antag-

onistic effects, though, were observed in the co-digestion of grass species. Improved methane yield was observed in the mono-digestion of *L. perenne* with a higher dose of nitrogen fertiliser. However, a comparable area-specific methane yield was reached in the co-digestion of an equi-proportional mixture of six grassland species.

In the fourth chapter, two fermentation assays were designed to investigate the production of VFAs and butyric acid from *L. perenne* (two doses of nitrogen fertiliser), *T. pratense* and *T. repens*. The co-fermentation of *L. perenne* and *T. repens* was also evaluated. Leachate and digestate from a pilot-scale leach-bed reactor producing VFAs from grass silage and cattle slurry were used as inoculum. The one-step fermentation assay was performed in batch-mode at mesophilic temperatures for 7 and 14 days. In the two-step fermentation assay, the substrate was immersed in water for 6 days before introducing the inoculum to the fermented liquid and fermented solid for further 7 days. The buffering capacity of clovers was an important asset for the biomass degradation, but favoured the accumulation of methane instead of VFAs. Doubling the dose of nitrogen fertiliser did not improve the production of VFAs or butyric acid from *L. perenne*, but improved the total product yield due to a higher accumulation of methane. No difference in VFA production was observed between the one-stage fermentation and the two-stage fermentation, but results from the two-stage correlated the lactic acid consumption to butyric acid production. The best performance in terms of butyric acid was observed in the one-stage fermentation of *L. perenne* (low dose of nitrogen fertiliser) or its mixture with *T. repens*.

In the fifth chapter, the microbial community dynamics in the fermentation of grass, and the influence of silage pH were investigated using three leach-bed reactors. Each was inoculated with a seed-inoculum based on their potential for silage degradation: rumen fluid, rumen solid and granular sludge (reactor 1); cattle slurry and granular sludge (reactor 2); and granular sludge (reactor 3). Silages with pH 4.3, 4.6, 6.7 and 8.1 were tested. The leach-bed reactors were assembled with 5 L working volume and a pH control system, one for each seed-inoculum mixture. The system was operated with a solid retention time of 6 days in sequential batch mode for 8-9 months with constant pH at approximately 5.5. Silage pH was responsible for the shift in VFA profile and yield, with a lower pH (4.3 and 4.6) favouring the accumulation of acids and a high pH (8.1) leading to a very low concentration of VFAs. Higher concentrations of butyric acid were reached by consuming the lactic acid accumulated in the leachate due to the fermentation of the low pH silage. High-throughput sequencing of the 16S rRNA gene in genomic DNA samples and cDNA (synthesised from RNA) samples extracted from digestate and leachate samples reinforced the hypothesis that silage pH was a driving force in the reactor performance. In all reactors, *Prevotella* and *Lactobacillus* were the most abundant genera. The higher presence of *Lactobacillus* associated with the presence of *Caproiciproducens* may explain the accumulation of butyric acid and caproic acid by the end of the trial. After the reactor trial, a small batch was performed to investigate the influence of using digestate, leachate or a mixture of both as inoculum in the semi-continuous fermentation of silage. It was concluded that the solid digestate was an important for the degradation of silage, but the combination of leachate and digestate led to a faster VFA production.

In summary, this thesis demonstrates the importance of permanent grassland biodiversity and

silage preservation in AD, paving the way for potential developments that associate sustainable forage production with VFA production.

List of Figures

2.1	Potential biorefinery process focusing on maximising VFA production. The process begins with the valorisation of residual feedstocks and culminates in the potential production of various high-value end-products (highlighted in pink).	10
2.2	Processes used to separate VFAs from fermentation liquors. Sankey plot showing the variety of VFA harvesting processes as a flow of stages (1st, 2nd, 3rd and 4+). Technologies using similar principles and materials were grouped together; for example, electro dialysis and membrane electrolysis were grouped together since they both use membranes and current driven separation of solutes. Technologies were classified as ‘other’ if they were used by only a single study at any given stage. References: 1 - [110]; 2 - [69]; 3 - [106]; 4 - [111]; 5 - [112]; 6 - [41]; 7 - [105]; 8 - [113]; 9 - [114]; 10 - [89]; 11 - [115]; 12 - [97]; 13 - [116]; 14 - [82]; 15 - [74]; 16 - [117]; 17 - [118]; 18 - [119]; 19 - [120]; 20 - [104]; 21 - [103]; 22 - [121].	22
2.3	Challenges and opportunities for future research. The promise of a biorefinery-based bioeconomy will rely on innovative and interdisciplinary solutions. The literature suggests that key challenges with respect to feedstock variability, VFA production and recovery, process integration and scalability all need to be tackled.	26
3.1	Average volatile solids degradation reached in the digestion of monocultures and mixtures of grassland species. Substrates were labelled according to Table 3.2. The degradation of each plot of grassland species is represented in Figure A.1.	51
3.2	Model prediction based on the digestion of <i>L. perenne</i> (plot 40). An average of the experimental observations (red dots) are presented with its standard deviation.	52
3.3	Interspecific contribution to the substrate-specific (a) and area-specific (b) maximum methane yield. Error bars presented as standard error, and substrates were labelled according to Table 3.2.	56
3.4	Substrate-specific (a) and area-specific (b) maximum methane yield based on the coefficients predicted for the FULL DI model 3.6. Error bars are presented as standard error, and substrates were labelled according to Table 3.2. Lp300 is equivalent to Lp*.	57
A.1	Volatile solids degradation of monocultures (green bars, a), and mixtures of two species (purple bars, b) and six species (orange bars,c). Substrates were labelled according to Table 3.2.	69
4.1	Setup for the one-stage fermentation assay.	80
4.2	Setup for the two-stage fermentation assay.	81
4.3	pH profile and volatile fatty acids production in the one-stage fermentation of <i>L. perenne</i> (150, 150 kgN.ha ⁻¹ .yr ⁻¹), <i>L. perenne</i> (300, 300 kgN.ha ⁻¹ .yr ⁻¹), <i>T. pratense</i> , <i>T. repens</i> , and a mixture of <i>L. perenne</i> and <i>T. repens</i> . Results for the inoculum (negative control) are also displayed.	86

4.4	Profile of pH, lactic acid and volatile fatty acids in the two-stage fermentation of <i>L. perenne</i> , <i>T. repens</i> , and a mixture of <i>L. perenne</i> and <i>T. repens</i> . LF stands for liquid fraction and SF stands for solid fraction.	88
4.5	Maximum methane yield observed from <i>L. perenne</i> (150 kgN.ha ⁻¹ .yr ⁻¹), <i>L. perenne</i> (300 kgN.ha ⁻¹ .yr ⁻¹), <i>T. pratense</i> , <i>T. repens</i> , and a mixture of <i>L. perenne</i> and <i>T. repens</i> after 28 days.	90
4.6	Acidification (orange dot) and total product yield – as VFA (pink bar) and methane (green bar) – in the one-stage fermentation of <i>L. perenne</i> (150 kgN.ha ⁻¹ .yr ⁻¹) after 7 and 14 days); and <i>L. perenne</i> * (300 kgN.ha ⁻¹ .yr ⁻¹), <i>T. pratense</i> , <i>T. repens</i> , and a mixture of <i>L. perenne</i> and <i>T. repens</i> (after 7 days).	93
4.7	VFA yield (bars) and acidification (dots) in the second-stage fermentation of <i>L. perenne</i> , <i>T. repens</i> , and a mixture of <i>L. perenne</i> with <i>T. repens</i> – the light orange represents the production from the solid fraction while the darker orange represents the production from the liquid fraction after the pre-treatment.	96
4.8	Comparison between the one-stage and second-stage fermentation of <i>L. perenne</i> , <i>T. repens</i> , and a mixture of <i>L. perenne</i> with <i>T. repens</i> in terms of VFA yield (bars) and butyric acid yield (black dots).	97
B.1	Profile of volatile solids degradation (on the left) and Total ammonia nitrogen (TAN, on the right) for each substrate during the biomethane potential assay. The * represents the substrate supplied with 300 kgN.ha ⁻¹ .yr ⁻¹	105
5.1	Schematic representation of the seed-inoculum selection experiment using rumen fluid (RF), rumen solid (RS), cattle slurry (CS), and granular sludge (GS) as seed-inoculum.	110
5.2	Reactor setup for the fermentation of silage using different seed-inoculum.	112
5.3	Volatile solids degradation (a) and gas production (b) in the seed-inoculum selection experiment for rumen fluid (RF ^a and RF ^b), rumen solid (RS), cattle slurry (CS), and granular sludge (GS). The error bars represent standard deviations.	121
5.4	Volatile solids degradation in the fermentation of silage over the phases in Reactor 1 (left-bar), Reactor 2 (middle-bar), and Reactor 3 (right-bar). The error bars represent standard deviations – Phase I (n=4), Phases II and III (n=3), Phase IV and V (n=6).	122
5.5	Profile of volatile fatty acids, lactic acid, ethanol, and pH profile at Phase I (Batch 3, a); Batch 16 (b); Phase IV (Batch 20, c); and Phase V (Batch 30, d). For Phase I, pH control started at day 1, while at the other phases it started at day 0.	124
5.6	Production of VFAs and methane from the fermentation of silage through Phases I-V in Reactors 1, 2 and 3. The error bars represent standard deviations of the total production (VFAs and methane) – Phase I (n=4), Phases II and III (n=3), Phase IV and V (n=6).	125
5.7	Methane production detected during the fermentation of silage in Reactor 1 (left-bar, orange), Reactor 2 (middle-bar, green), and Reactor 3 (right-bar, purple)	126

5.8	Net production of volatile fatty acids (VFA) from silage over phases in reactors 1, 2, and 3. Triangles mark batches that had a problem with the control system (e.g., overdosing of base or acids).	127
5.9	Silage degradation (in %VS) resulting from its fermentation using Batch 30's digestate + leachate, leachate, and digestate as inoculum. The error bars represent standard deviations.	128
5.10	VFA production in the fermentation of silage using different inoculum approaches. The error bars represent standard deviations.	129
5.11	Rarefied richness profile based on the 16s rRNA sequences (DNA level) extracted from silage (triangle), seed-inocula (star), leachate (round) and digestate (square) samples – Reactor samples were extracted from the three reactors in the Start Up and Phases I, IV and V.	130
5.12	Shannon Entropy based on the 16s rRNA sequences (DNA level) extracted from silage (triangle), seed-inocula (star), leachate (round) and digestate (square) samples – Reactor samples were extracted from the three reactors in the Start Up and Phases I, IV and V.	131
5.13	Principal Coordinate Analysis (PCoA) plot based on Bray-Curtis distance of 16s rRNA sequences (DNA level) extracted from seed-inocula (pink), Start Up (purple), Phase I (green), Phase IV (orange), and Phase V (red). Silage colour is represented according to the phase it was fed; p-value<0.001.	133
5.14	Taxonomic composition of the microbial community 16s rRNA gene (DNA level) extracted from silage, seed-inocula, leachate and digestate samples – Reactor samples were extracted from the three reactors in the Start Up and Phases I, IV and V.	135
5.15	Taxonomic composition of the microbial community 16s rRNA gene (cDNA level) extracted from silage, seed-inocula, leachate and digestate samples – Reactor samples were extracted from the three reactors in Phase V.	136
C.1	Schematic diagram illustrating the feeding regime for all phases of silage fermentation in LBRs: Phase I, IV and V (a), Phase II (b) and Phase III (c). Batch 16 was fed in a similar way to Phase II, but with two washes.	155
C.2	Principal Coordinate Analysis (PCoA) plot based on Hierarchical Meta-Storms distances of the 16s rRNA sequences (DNA level) extracted from seed-inocula (pink), Start Up (purple), Phase I (green), Phase IV (orange), and Phase V (red). Silage colour is represented according to each phase it was fed (I, IV and V); p-value<0.001.	156
C.3	Electrophoresis gel after the DNA/RNA co-extraction of samples testing different sonication times (1 to 6), and the use of RNeasy [®] in digestate and leachate samples.	158
C.4	Taxonomic composition of the microbial community 16s rRNA gene (DNA level) extracted from Phase I Batch 4 leachate and digestate with and without RNeasy [®]	160

List of Tables

2.1	Chemical characteristics of feedstocks and inoculum sources used for VFA production.	15
2.2	Summary of the operational conditions for VFA production using the raw materials described in Table 2.1.	18
3.1	Summary of the total and volatile solids for each species.	43
3.2	Grassland species composition for each substrate based on its volatile solids content.	44
3.3	Field yield and chemical characteristics for substrates used in this experiment. Substrates were labelled according to Table 3.2.	51
3.4	Information criteria to select the model with the best fit to the experimental data. . .	52
3.5	Theoretical BMP (TBMP), biodegradability index (B_d), area-specific maximum methane yield (Bo_{area}), substrate-specific maximum methane yield (Bo_{sub}), hydrolysis constant rate (k) and lag phase time (λ) observed in the digestion of permanent grasslands.	53
3.6	Estimated values for species identity effects and interspecific interaction effects using the pairwise interaction (FULL) DI model.	55
A.1	Results of the elemental analysis (in %TS) for each substrate. Data is reported in average (and standard deviation) of duplicate measurements.	70
A.2	Standard deviations for the mean values of C:N ratio, ash and crude protein displayed in Table 3.3.	71
A.3	Statistics for the First order kinetics model fitting the experimental data present at Table 3.5.	72
A.4	Total ammonia nitrogen, C:N ratio, pH and substrate-specific maximum methane yield (Bo_{sub}) for selected substrates in the digestion of grassland species.	73
A.5	Comparison between DI models when investigating <i>interactions</i> using the <i>autoDI</i> function. DI models compared: STR (structures), ID (species identity), AV (average interactions), FG (functional group effects), and FULL (pairwise interactions).	73
A.6	Comparison between DI models when investigating <i>interactions</i> using the <i>autoDI</i> function. DI models compared: STR (structures), ID (species identity), AV (average interactions), FG (functional group effects), and FULL (pairwise interactions).	73
A.7	Predictions for maximum methane yield (Predicted Bo_{sub} and Predicted Bo_{area}), and for the contribution of species interaction to maximum methane yield (Interactions) using the pairwise-interaction DI model	74
4.1	Chemical parameters for the grassland biomass used in this study.	78
4.2	Volatile solids degradation for each experiment: in the one-stage fermentation (after 7 and 14 days); in each stage of the two-stage fermentation (6 and 14 days); and in the biomethane potential assay (after 28 days).	84
4.3	Net production of Volatile fatty acids (VFAs) in the one-stage fermentation of grassland biomass.	93

5.1	Chemical parameters for the four silages used in this study.	110
5.2	Seed composition, in %VS, fed to batch bottles in the seed-inoculum selection experiment. RF ^a was collected from a local abattoir in Co. Mayo, while RF ^b was collected from a cannulated cattle experiment (Teagasc Grange, Co. Meath).	111
5.3	Summary of the operational conditions per phase in the fermentation of grassland biomass silage – number of batches ^a , solid retention time (SRT), organic loading rate OLR.	112
5.4	Reactor performance over phases in volatile solids (VS) degradation, acidification yield, and yield of VFAs, butyric acid and caproic acid.	123
5.5	Average net production and profile of VFAs from reactors 1, 2, and 3 at the end of the batch in each fermentation phase.	123
C.1	Lignocellulosic and total solids degradation of silage and the starting mix of silage and digestate during Phase V Batch 30.	156
C.2	Relative abundances (% , at DNA-level) of the phylum observed in the fermentation of silage over phases and reactors.	157
C.3	Mean values (and standard deviation) for the net production and profile of VFAs obtained in the fermentation of silage using Batch30’s digestate and leachate as inoculum.	157
C.4	Quality check of sonication and RNeasy [®] samples in terms of DNA concentration (Qubit [®]) and Nanodrop ratios.	159

List of Acronyms

- AD** Anaerobic digestion.
- ADF** Acid detergent fibre.
- AF** Acidogenic fermentation.
- AIC** Akaike information criterion.
- AOMC** Atlantic meridional overturning circulation.
- ASV** Amplicon Sequencing Variants.
- BIC** Bayesian information criterion.
- BMP** Biomethane potential.
- CAZymes** Carbohydrate active enzymes.
- CE** Chain–elongation.
- CHP** Combined heat and power.
- CMG** Corrected modified gompertz.
- COD** Chemical oxygen demand.
- CS** Cattle slurry.
- CSTR** Continuous–stirred tank reactor.
- CTAB** Cetyl–trimethylammonium bromide.
- DI** Diversity–interaction.
- EGSB** Expanded granular sludge bed.
- FG** Functional group.
- FOK** First order kinetics.
- FW** Fresh weight.
- GHG** Greenhouse gas.
- GS** Granular sludge.
- HMS** Hierarchical Meta–Storms.

HRT hydraulic retention time.

KO KEGG Orthologs.

LAB Lactic acid bacteria.

LBR Leach-bed reactor.

LBRs Leach-bed reactors.

MCCA Medium-chain carboxylic acid.

MG Modified gompertz.

NDF Neutral detergent fibre.

NIRS Near-infrared spectroscopy.

NSTI Nearest Sequenced Taxon Index.

OFMSW Organic fraction of municipal solid waste.

OLR Organic loading rate.

PBS Phosphate Buffered Saline.

PCoA Principal Coordinate Analysis.

PEG Polyethylene glycol.

PHA Polyhydroxyalkanoate.

RF Rumen fluid.

RMSE Root mean squared error.

RS Rumen solid.

RSS Residual sum of squares.

SCCA Short-chain carboxylic acid.

SQP Sequential quadratic programming.

SRT Solid retention time.

TAN Total ammonia nitrogen.

TBMP Theoretical biomethane potential.

ThCOD Theoretical chemical oxygen demand.

TS Total solids.

TSS Total suspended solids.

VFA Volatile fatty acids.

VS Volatile solids.

VSS Volatile suspended solids.

Nomenclature

χ	Acidification yield (%)
λ	Lag phase time (<i>days</i>)
μ_{max}	Maximum methane production rate ($NL.kgVS^{-1}.day^{-1}$)
VFA(0)	Concentration of Volatile fatty acids (VFA)s (or any specific acid) in the leachate at the beginning of the batch (gCOD.L ⁻¹)
VFA(<i>t</i>)	Concentration of VFAs (or any specific acid) in the leachate at a time <i>t</i> (gCOD.L ⁻¹)
VFA _{<i>t</i>}	Concentration of VFAs, in total, at the end of each batch (gCOD.L ⁻¹)
VFA _{net} (<i>t</i>)	Net concentration of VFAs (or any specific acid) at a time <i>t</i> (gCOD.L ⁻¹)
B_o	Maximum methane yield ($NL.kgVS^{-1}$)
B_{oarea}	Area-specific maximum methane yield ($NL.kgVS^{-1}$)
B_{osub}	Substrate-specific maximum methane yield ($NL.kgVS^{-1}$)
η_{i}/η_a	Degradation level of a lignocellulosic component (<i>i</i> , %)
k	Hydrolysis constant rate ($days^{-1}$)
$l_{29,i}$	Lignocellulosic composition of a component <i>i</i> in Batch 29's digestate (%TS)
$l_{30,i}$	Lignocellulosic composition of a component <i>i</i> in Batch 30's digestate (%TS)
$l_{s,i}$	Lignocellulosic composition of a component <i>i</i> in silage (%TS)
m_{29}	Mass of Batch 29's digestate supplied to the reactor (gTS)
m_{30}	Mass of Batch 30's digestate collected from the reactor (gTS)
m_{sil}	Mass of silage supplied to the reactor (gTS)
n	Shape factor (CONE model)
$N_{K_2Cr_2O_7}$	Normality of the potassium dichromate solution (<i>N</i>)
N_{Mohr}	Normality of the Mohr's salt solution (<i>N</i>)
P	Operational pressure (<i>kPa</i>)
p_o	Standard pressure (<i>kPa</i>)
P_w	Vapour pressure of water (<i>kPa</i>)

T	Operational temperature (K)
t	Time (<i>days</i>)
T_o	Standard temperature (K)
V_{biogas/CH_4}	Cumulative production of biogas or methane (NL)
v_b	Volume of gas sampled from gas bags (NL)
v_{dry}	Volume of dry gas in standard conditions (NL)
v_h	Volume of the headspace (NL)
$V_{K_2Cr_2O_7}$	Volume of potassium dichromate (mL)
$V_{Mohr,blank}$	Volume of Mohr's salt solution used to titrate the remaining dichromate in blank bottles (mL)
$V_{Mohr,sample}$	Volume of Mohr's salt solution used to titrate the remaining dichromate in sample bottles (mL)
V_{Mohr}	Volume of Mohr's salt solution used in the titration of dichromate - COD (mL)
V_r	Reactor volume at takedown (L)
v_{wet}	Volume of wet gas (L)
$VS_{deg_i}(t)$	VS degradation of a seed-inoculum/inoculum (%)
$VS_{deg}(t)$	VS degradation of a feedstock (%)
w_i	Akaike weight
x	Composition of methane in the biogas (%)
$Y(t)$	Cumulative methane yield at a time t ($NL.kgVS^{-1}$)
Y_{VFA}	Net VFA yield at a time t ($gCOD.gVS^{-1}$)
Y_i	Experimental methane yield ($NL.kgVS^{-1}$)
Y_{pred}	Predicted methane yield ($NL.kgVS^{-1}$)
z_i	Seed-inoculum composition (% VS)
$m_{control}(t)$	Mass of inoculum in control-bottles at a time t (gVS)
$m_{digestate}(t)$	Mass of digestate at a time t (gVS)

$m_g(t)$	Mass of silage at a time t (gVS)
$m_i(t)$	Mass of inoculum/seed-inoculum at a time t (gVS)
$m_{sample}(t)$	Mass of substrate plus inoculum at a time t (gVS)
$m_s(t)$	Mass of substrate at a time t (gVS)
M	Number of model parameters
N	Number of data points
RMSE	Root mean squared error
TBMP	Theoretical methane potential ($L.kgVS^{-1}$)
ThCOD	Theoretical chemical oxygen demand ($gCOD$ or $kgCOD$)
COD_s	Solids' COD ($mgO_2.L^{-1}$)
C:N ratio	Carbon-to-nitrogen ratio
sCOD	Soluble COD concentration ($gCOD.L^{-1}$)

Chapter 1: Introduction

The looming climate crisis has moved authorities to action in the past years, with many attempts to mitigate climate change and preserve environmental health¹⁻³. Recently, ‘The Green Deal’ set a target of complete neutrality in terms of net greenhouse gas (GHG) emissions in Europe by 2050³, focusing on ‘biodiversity, farming, energy and circular economy’⁴. This is because 75% of the GHG emissions in Europe comes from the transport and energy sector⁴, followed by agriculture (11.4%). In Ireland, the agricultural sector is responsible for most of the GHG emissions (38.4%)⁵. Moreover, Ireland has struggled to reduce its GHG emissions, failing to meet the 16% reduction quota by 2020 and facing a challenging reduction of 51% by 2030⁴. Reducing GHG emissions is crucial as anthropogenic actions have been connected to the increase in natural disasters throughout the world, such as floods, tsunamis and wildfires¹. This year, a modelling study predicted the forthcoming collapse of the Atlantic meridional overturning circulation (AOMC) between 2025-2095⁶. This calls for immediate measures to reduce GHG emissions to prevent losing an important component that regulates our climate system. Therefore, it is imperative to develop processes that lead to a more sustainable economy attaining the UN Sustainable Development Goals for 2030².

The need to mitigate the climate crisis associated with the energy crisis as a consequence of the COVID-19 pandemic and the Russo-Ukrainian war⁷ exposed even more the need to shift towards a more sustainable energy system and chemical production. In this way, the advent of biofuels from lignocellulosic biomass is a key point in the shift from fossil-fuel derived energy to a more sustainable economy. In a green biorefinery⁸, lignocellulosic biomass and agricultural wastes can be used to produce proteins, bioenergy (e.g., biohydrogen, biomethane and biogas), fertiliser, organic acids (e.g., volatile fatty acids, VFAs), alcohols (e.g., ethanol), and bioplastics (e.g., polyhydroxyalkanoates, PHAs)^{8,9}. However, the use of lignocellulosic resources related to food production (e.g., sugarcane, maize) raises an ethical question when the competition with energy production is stimulated by profit. This concern led to the use of agricultural residual biomass to produce second-generation biofuels and chemicals, improving resource recovery from the original lignocellulosic biomass. Agricultural residual biomass are crop and plant residues, vegetable waste, forest residues, grass and livestock manure, which are rich feedstocks that can be converted to bioenergy and biochemicals¹⁰.

Among these lignocellulosic biomasses, permanent grasslands are an abundant, renewable and cheap source of feedstock¹¹ that can be used for the sustainable production of biogas and volatile fatty acids (VFAs) using anaerobic digestion (AD) technology. Permanent grasslands are complex ecosystems consisting of different species of graminoids (e.g., grasses) and forbs (e.g., legumes and herbs), with forbs acting as an important factor to conserve the biodiversity and functionality of grasslands¹². These grasslands are crucial ecosystems for food production with an important role in maintaining soil quality, balancing the ecosystem biodiversity, and sequestering carbon from the atmosphere^{13,14}. However, most of the grassland fields used for food production are intensively managed monocultures, which depend on high supplementation of mineral fertiliser to achieve high forage yields¹⁵ at the expense of the ecosystem’s health (e.g., lower soil quality, contamination of water bodies, air

pollution, and loss of biodiversity)^{15,16}. Alternatively, studies have shown that using multiple species of forbs and legumes associated with grasses can increase forage yield^{17–20} using a lower nitrogen fertiliser input, but better nitrogen efficiency intake (e.g., when mixing legumes and grass)^{21,22} and lower N₂O emissions¹⁴.

In this way, using the biodiversity of grassland ecosystems can result in the sustainable production of forages with a better nutrient balance due to the combination of different species. This has been a major issue in the anaerobic mono-digestion of grass species, as the poor nutrient availability in those species in terms of trace-elements^{23,24} and C:N ratio^{25,26} leads to process failure²⁷. Despite this unbalance in nutrients, grass has been used consistently as a feedstock in AD for the past 20 years²⁸. In fact, only recently few studies have considered the co-digestion of grass and forbs, such as clovers and herbs^{25,29} or the mono-digestion of forbs^{25,29,30}. Clovers have a higher protein content due to their ability to fixate atmospheric N₂³¹, and some herbs such as chicory have a higher quantity of micro-nutrients due to its deep-roots^{25,29,30}. Therefore, clovers and herbs are considered more nutritious than grasses, which improve the nutrient availability for the microbial community leading to better product yields. However, a systematic study from field to digester at mesophilic conditions is still needed, especially considering the possible interaction effects that co-digesting different species of grassland biomass can have on product yield.

Although biogas is indeed the main product of AD, increased interest has been directed to acidogenic fermentation (AF) in the past 25 years since the capital cost for AD is usually high due to long operational times and high reactor volumes³². To focus on the AF, the process can be operated at acidic pH or at high organic loading rates (OLR), which leads to pH drop as a result of VFA accumulation³³. The higher-market value of VFAs⁹ makes its accumulation more attractive compared to biogas/biomethane, especially using an abundant and cheap feedstock such as permanent grassland biomass. However, minimal research has been published focusing on the production of VFAs from grasses^{34–37}, especially focusing in selectively producing higher-chain VFAs such as butyric and caproic acids^{38,39}. Additionally, the potential of clovers or grass-clover mixtures for VFA production has not been studied yet. Butyric acid is an important chemical for many industries, such as food, cosmetics, pharmaceutical and chemical, and butyric acid is mainly obtained through the chemical synthesis of fossil-fuel-derived materials⁴⁰. Despite some existing biological routes, the butyric acid production from the AF of grasses is not established yet, and most studies have reported acetic acid as the highest produced VFA from grass^{34–37}, or caproic acid under specific conditions^{38,39}. Moreover, despite the AF being a microbial-mediated process, the microbial community dynamics in the AF of grass is poorly explored, and very little is known about the influence of grasses' microbial community to the fermentation.

1.1 Thesis Scope

Therefore, this Ph.D. investigates the use of AD technology in the valorisation of permanent grasslands, evaluating biomethane production and the production of VFAs, focusing on the selective ac-

cumulation of butyric acid. This work also aims to elucidate the microbial community dynamics in the fermentation of grassland biomass for VFA production. For that, the following hypotheses were made:

- (i) different grassland forages with different chemical compositions can impact the desired end-product yield and microbial activity;
- (ii) pH can be a determining factor that influences butyric acid production, VFA production, and microbial community dynamics; and
- (iii) different sources of inoculum can lead to different VFA and butyric acid production in terms of yield and profile.

To test these hypotheses, the thesis was structured in five chapters, including this introduction (first chapter). In the second chapter, a critical review published in the special issue ‘Anaerobic Fermentation’ – *A Biological Route Towards Achieving Net Neutrality* (Fermentation, August 2022) is presented in its original form. The review explored the potential for resource recovery from food waste, agricultural and animal residues and some of the recent advances in the production of VFAs from these substrates. Important notes on chemical parameters, state-of-art systems, and applications were provided. The main drawback in VFA production, VFA recovery, was also discussed, highlighting a range of challenges and opportunities, which are the current drivers in the field.

In the third chapter, a study was designed to evaluate the methane potential of six grassland species adapted to temperate climate: *Lolium perenne*, *Phleum pratense*, *Trifolium pratense*, *Trifolium repens*, *Cichorium intybus*, and *Plantago lanceolata*. The influence of nitrogen fertilisation rates in the methane production was also investigated using plots of *L. perenne* supplied with two levels of nitrogen fertiliser. A biomethane potential assay was performed to elucidate the species identity effects and interspecific interaction effects of mono-digesting those species and co-digestion two or six of those species. Those effects were evaluated using a diversity-interaction model, an approach commonly used to evaluate grassland ecosystems but proposed for the first time in the AD field.

In the fourth chapter, two fermentation assays were designed to investigate the production of VFAs from *L. perenne* (two doses of nitrogen fertiliser), *T. pratense* and *T. repens*. The co-fermentation of *L. perenne* and *T. repens* was also evaluated. Leachate and digestate from a pilot-scale leach-bed reactor producing VFAs from grass silage and cattle slurry were used as inoculum. Here, we aimed to understand how VFA production, especially butyric acid, was affected by **i**) fermenting different species of grassland biomass; **ii**) fermenting the same species of grassland biomass with different doses of nitrogen fertiliser; and **iii**) a pre-fermentation step where the grassland biomass indigenous community was used before an acclimatised inoculum was provided.

In the fifth chapter, the microbial community dynamics in the fermentation of grass silage and the influence of silage pH were investigated using three leach-bed reactors operated under pH control. Each reactor was inoculated with a seed-inoculum based on their potential for silage degradation: rumen fluid, rumen solid and granular sludge (reactor 1); cattle slurry and granular sludge (reactor

2); and granular sludge (reactor 3). Silages with pH levels from acid to basic were tested. After the reactor trial, a small batch was performed to investigate the influence of using digestate, leachate or a mixture of both as inoculum in the semi-continuous fermentation of silage. Here, we aimed to **i)** select an inoculum capable of degrading silage while producing VFAs. We also tested **ii)** the effect of silage in the resulting VFA production and profile. Lastly, we aimed to **iii)** elucidate the microbial dynamics in the fermentation of grass and the effect of substrate's microbial community in reactor performance. In the sixth and final chapter, concluding remarks are presented in the form of a final discussion and suggestions for future work.

1.2 References

1. Intergovernmental Panel on Climate Change. *Climate Change 2014: Synthesis Report; Chapter Observed Changes and their Causes* 151 (2014).
2. United Nations. *Transformin our world: the 2030 Agenda for Sustainable Development* tech. rep. A/Res/70/1 (United Nation, New York, 2015), 1–35.
3. European comission. *A European Green Deal - Striving to be the first climate-neutral continent* Dec. 2019. <https://ec.europa.eu/newsroom/know4pol/items/664852>.
4. Ravindran, R. *et al.* Biogas, Biomethane and Digestate Potential of By-Products from Green Biorefinery Systems. *Clean Technologies* **4**, 35–50 (Jan. 2022).
5. EPA - Environmental Protection Agency. *Latest emissions data July 2023*. <https://www.epa.ie/our-services/monitoring--assessment/climate-change/ghg/latest-emissions-data/>.
6. Ditlevsen, P. & Ditlevsen, S. Warning of a forthcoming collapse of the Atlantic meridional overturning circulation. *Nature Communications* **14**, 4254. <https://www.nature.com/articles/s41467-023-39810-w> (July 2023).
7. IEA. *Global Energy Crisis* <https://www.iea.org/topics/global-energy-crisis>.
8. Cherubini, F. *et al.* Toward a common classification approach for biorefinery systems. *Biofuels, Bioproducts and Biorefining* **3**, 534–546 (Sept. 2009).
9. Nzeteu, C., Coelho, F., Davis, E., Trego, A. & O'flaherty, V. Current Trends in Biological Valorization of Waste-Derived Biomass: The Critical Role of VFAs to Fuel a Biorefinery. **8**, 445 (2022).
10. Paudel, S. R. *et al.* Pretreatment of agricultural biomass for anaerobic digestion: Current state and challenges. *Bioresource Technology* **245**, 1194–1205 (2017).
11. Murphy, J. D. *et al.* *The Potential for Grass Biomethane as a Biofuel: Compressed Biomethane Generated from Grass , Utilised as a Transport Biofuel* tech. rep. (Environmental Research Institute, 2011), 1–69.

12. Bråthen, K. A., Pugnaire, F. I. & Bardgett, R. D. The paradox of forbs in grasslands and the legacy of the mammoth steppe. *Frontiers in Ecology and the Environment* **19**, 584–592 (Dec. 2021).
13. Lee, M., Manning, P., Rist, J., Power, S. A. & Marsh, C. A global comparison of grassland biomass responses to CO₂ and nitrogen enrichment. *Philosophical Transactions of the Royal Society B: Biological Sciences* **365**, 2047–2056 (2010).
14. Rahman, M. M. *et al.* in *Advances in Legumes for Sustainable Intensification* (eds Meena, R. S. & Kumar, S.) 381–402 (Academic Press, 2022).
15. Suter, M., Huguenin-Elie, O. & Lüscher, A. Multispecies for multifunctions: combining four complementary species enhances multifunctionality of sown grassland. *Scientific Reports* **11** (Dec. 2021).
16. Salaheen, S. & Biswas, D. in *Safety and Practice for Organic Food* (eds Biswas, D. & Micallef, S. A.) 23–32 (Academic Press, 2019).
17. Finn, J. A. *et al.* Ecosystem function enhanced by combining four functional types of plant species in intensively managed grassland mixtures: a 3-year continental-scale field experiment. *Journal of Applied Ecology* **50** (ed Wilsey, B.) 365–375 (Apr. 2013).
18. Grange, G., Finn, J. A. & Brophy, C. Plant diversity enhanced yield and mitigated drought impacts in intensively managed grassland communities. *Journal of Applied Ecology*, 1365–2664 (June 2021).
19. Cong, W.-F., Suter, M., Lüscher, A. & Eriksen, J. Species interactions between forbs and grass-clover contribute to yield gains and weed suppression in forage grassland mixtures. *Agriculture, Ecosystems & Environment* **268**, 154–161 (Dec. 2018).
20. Grange, G., Brophy, C. & Finn, J. A. Grassland legacy effects on yield of a follow-on crop in rotation strongly influenced by legume proportion and moderately by drought. *European Journal of Agronomy* **138**, 126531 (2022).
21. Connolly, J. *et al.* Weed suppression greatly increased by plant diversity in intensively managed grasslands: A continental-scale experiment. *Journal of Applied Ecology* **55** (ed Inderjit) 852–862 (Mar. 2018).
22. De Neergaard, A., Hauggaard-Nielsen, H., Stoumann Jensen, L. & Magid, J. Decomposition of white clover (*Trifolium repens*) and ryegrass (*Lolium perenne*) components: C and N dynamics simulated with the DAISY soil organic matter submodel. *European Journal of Agronomy* **16**, 43–55 (Jan. 2002).
23. Myszograj, S., Stadnik, A. & Płuciennik-Koropczuk, E. The Influence of Trace Elements on Anaerobic Digestion Process. *Civil and Environmental Engineering Reports* **28**, 105–115 (Dec. 2018).

24. Wall, D. M., Allen, E., Straccialini, B., Kiely, P. O. & Murphy, J. D. The effect of trace element addition to mono-digestion of grass silage at high organic loading rates. *Bioresource Technology* **172**, 349–355 (2014).
25. Cong, W.-F., Moset, V., Feng, L., Møller, H. B. & Eriksen, J. Anaerobic co-digestion of grass and forbs – Influence of cattle manure or grass based inoculum. *Biomass and Bioenergy* **119**, 90–96 (Dec. 2018).
26. Himanshu, H., Murphy, J., Grant, J. & O’Kiely, P. Synergies from co-digesting grass or clover silages with cattle slurry in in vitro batch anaerobic digestion. *Renewable Energy* **127**, 474–480 (Nov. 2018).
27. Thamsiroj, T., Nizami, A. S. & Murphy, J. D. Why does mono-digestion of grass silage fail in long term operation? *Applied Energy* **95**, 64–76 (2012).
28. Prochnow, A. *et al.* Bioenergy from permanent grassland - A review: 1. Biogas. *Bioresource Technology* **100**, 4931–4944 (2009).
29. Wahid, R., Ward, A. J., Møller, H. B., Søgaard, K. & Eriksen, J. Biogas potential from forbs and grass-clover mixture with the application of near infrared spectroscopy. *Bioresource Technology* **198**, 124–132 (2015).
30. Wahid, R. *et al.* Anaerobic mono-digestion of lucerne, grass and forbs – Influence of species and cutting frequency. *Biomass and Bioenergy* **109**, 199–208 (Feb. 2018).
31. Suter, M. *et al.* Nitrogen yield advantage from grass-legume mixtures is robust over a wide range of legume proportions and environmental conditions. *Global Change Biology* **21**, 2424–2438 (June 2015).
32. Ramos-Suarez, M., Zhang, Y. & Outram, V. Current perspectives on acidogenic fermentation to produce volatile fatty acids from waste. *Reviews in Environmental Science and Bio/Technology* **20**, 439–478 (2021).
33. Magdalena, J. A., Greses, S. & González-Fernández, C. Impact of Organic Loading Rate in Volatile Fatty Acids Production and Population Dynamics Using Microalgae Biomass as Substrate. *Scientific Reports* **9**, 18374 (Dec. 2019).
34. Kullavanijaya, P. & Chavalparit, O. The production of volatile fatty acids from Napier grass via an anaerobic leach bed process: The influence of leachate dilution, inoculum, recirculation, and buffering agent addition. *Journal of Environmental Chemical Engineering* **7**, 103458 (Dec. 2019).
35. Jones, R. J., Massanet-Nicolau, J., Fernandez-Feito, R., Dinsdale, R. M. & Guwy, A. J. Recovery and enhanced yields of volatile fatty acids from a grass fermentation via in-situ solids separation and electrodialysis. *Journal of cleaner production* **296**, 126430 (2021).

-
36. Jones, R. J., Massanet-Nicolau, J., Fernandez-Feito, R., Dinsdale, R. M. & Guwy, A. J. Fermentative volatile fatty acid production and recovery from grass using a novel combination of solids separation, pervaporation, and electrodialysis technologies. *Bioresource technology* **342**, 125926 (2021).
 37. Xie, S., Lawlor, P. G., Frost, J. P., Wu, G. & Zhan, X. Hydrolysis and acidification of grass silage in leaching bed reactors. *Bioresource Technology* **114**, 406–413 (2012).
 38. Khor, W. C., Andersen, S., Vervaeren, H. & Rabaey, K. Electricity-assisted production of caproic acid from grass. *Biotechnology for Biofuels* **10**, 1–11 (Dec. 2017).
 39. Sakarika, M., Regueira, A., Rabaey, K. & Ganigué, R. Thermophilic caproic acid production from grass juice by sugar-based chain elongation. *Science of the Total Environment* **860** (Feb. 2023).
 40. Liberato, V. *et al.* Clostridium sp. as Bio-Catalyst for Fuels and Chemicals Production in a Biorefinery Context. *Catalysts* **9**, 962 (Nov. 2019).

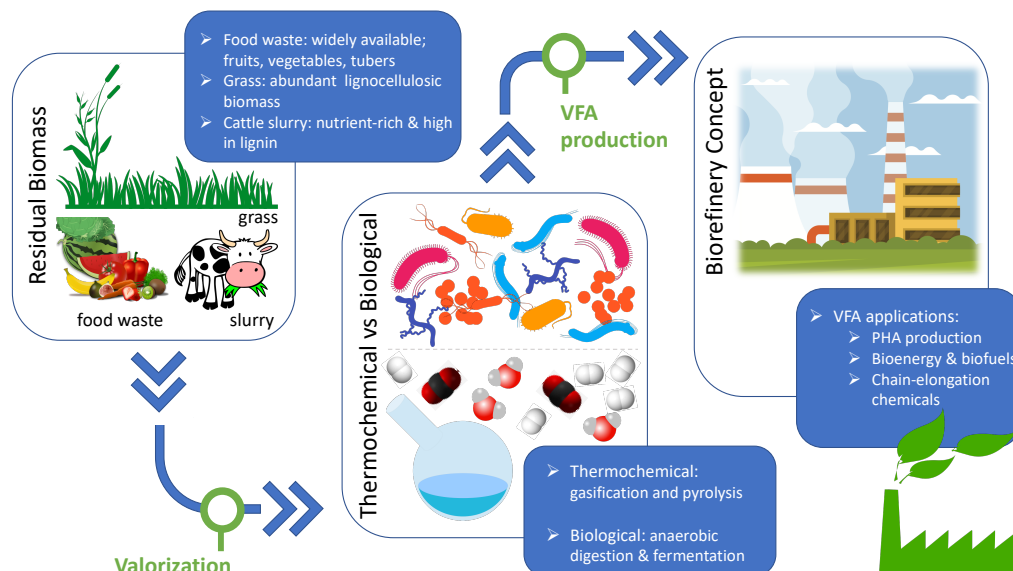
Chapter 2: Current Trends in Biological Valorisation of Waste-Derived Biomass: The Critical Role of VFAs to Fuel a Biorefinery

This work was accepted for publication on August 2022 in the special issue 'Anaerobic Fermentation' – A Biological Route Towards Achieving Net Neutrality from the journal Fermentation. A list of author's contribution can be found at the end of this chapter.

Abstract

The looming climate and energy crises, exacerbated by increased waste generation, are driving research and development of sustainable resource management systems. Research suggests that organic materials such as food waste, grass, and manure, have potential for biotransformation into a range of products, including: high-value volatile fatty acids (VFAs); various carboxylic acids; bioenergy; and bioplastics. Valorising these organic residues would additionally reduce the increasing burden on waste management systems. Here we review the valorisation potential of various feedstocks, particularly, food wastes and agricultural and animal residues. Additionally, we touch on the technologies that are being developed for this purpose; in particular we provide a synthesis of VFA recovery techniques, which remains a significant technological barrier. Furthermore, we highlight a range of challenges and opportunities which will continue to drive research and discovery within the field. Analysis of the literature reveals growing interest in the development of a circular bioeconomy, built upon a biorefinery framework, which utilises biogenic VFAs for chemical, material, and energy applications.

keywords: Anaerobic digestion; biorefinery; fermentation; VFAs; biomass valorization



2.1 Introduction

As both climate change and the global energy crisis escalate, it becomes ever more critical to implement sustainable resource management strategies such as biorefineries and resource recovery systems. These systems typically utilise innovative resource recovery technologies and novel renewable materials. The valorisation of biomass can play a foundational role within these systems, supporting the generation of energy (biofuel) as well as a wide range of biobased products through the biorefinery concept¹⁻⁴. Biomass can be broadly classified as either an energy crop or residue. Energy crops are specifically cultivated for energy generation. These crops are typically cultivated using intensive farming practices. And since they are often edible, using them for energy generation means less food and land that could be otherwise used for human consumption. In contrast biomass residues are non-edible and generally composed of waste products or agro-industrial side streams.

Among biomass residues, food waste and agricultural waste have demonstrated their promising potential for biorefinery applications^{2,3,5-7}. In Europe, these biomasses are valorised using biological, chemical, and thermochemical methods. However, variability in the quantity and composition of biomass limits the technological and economic viability of these valorisation methods. Therefore, these highly variable biomass resources are better suited for processes such as anaerobic digestion (AD), which is able to convert a wide range of organics into products such as volatile fatty acids (VFAs), biohydrogen, polyhydroxyalkanoates (PHAs) and bioenergy. AD can serve as a sustainable and economically attractive biological pre-treatment for lignocellulosic biomass, facilitating its conversion into biobased products by exposing lignin and undigested fibres for further valorisation.

The ultimate purpose of an AD-based biorefinery system is to optimise resource-use efficiency while minimising waste; this is typically accomplished by maximising energy/biogas production. The generation of alternative valuable by-products, in addition to biogas, represents a new opportunity to enhance resource recovery (Figure 2.1). An important value-added by-product, VFAs, are produced during the initial phases of AD in a process known as acidogenic fermentation. VFAs have a wide range of potential applications in the biorefinery industry, where they can be used as feedstock for various biobased products. For instance, VFAs are considered a potential platform for the production of biodegradable PHA polymers⁸. Currently, synthetically produced VFAs are used in the food and beverage industries, as well as in pharmaceutical and synthetic chemistry. The ratios of the specific volatile fatty acids that are produced via acidogenic fermentation are dependent on the feedstock biomass' composition, the extent of hydrolysis, operational conditions, reactor design, and the structure of the microbial community. Research investigating these parameters is being carried out and promises to greatly improve the efficiency and stability of the acid-forming stage.

This review elucidates the potential for low-value biomass to be used as feedstock for VFA generation within a biorefinery model. Specifically, we discuss various techniques and system designs which optimise energy use and product yield. Finally, we discuss current trends and challenges for a biorefinery concept, and the outstanding research necessary to support a functioning bioeconomy.

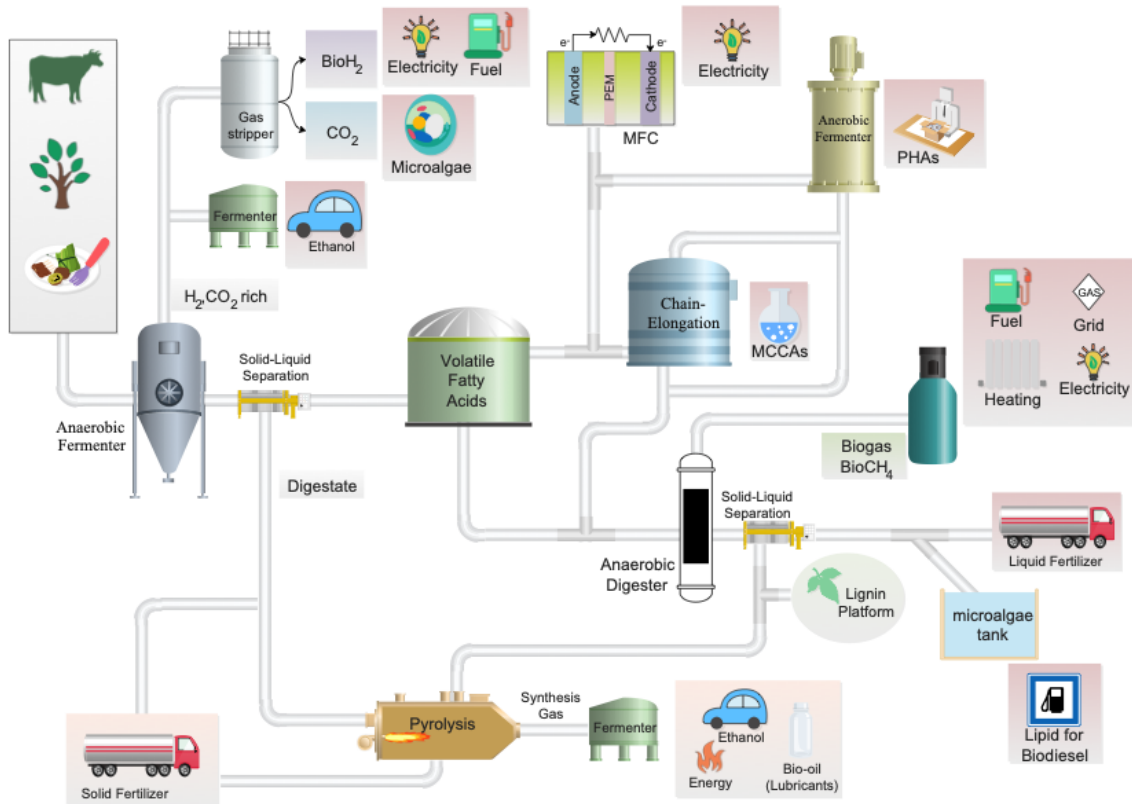


Figure 2.1: Potential biorefinery process focusing on maximising VFA production. The process begins with the valorisation of residual feedstocks and culminates in the potential production of various high-value end-products (highlighted in pink).

2.2 Methods of Valorising Low-value Feedstocks

Biomass valorisation has gained popularity and traction in recent years given its potential to sustainably meet regulatory requirements in terms of energy, chemicals, and materials. Research suggests that within the biorefinery concept, biomass valorisation – where all fractions are processed selectively towards a variety of products – is generally achieved using two strategies: thermochemical and/or biological conversion⁹. While this review focuses on biological processes, we will also briefly mention trends in thermochemical techniques.

2.2.1 Thermochemical approach

Among the thermochemical conversion processes, gasification and pyrolysis are commonly used to produce heat, biochar, and syngas from lignocellulosic biomass. Conventional gasification technologies include fixed beds, fluidised beds, and entrained flow reactors¹⁰. However, these technologies still struggle with process inefficiencies related to biomass moisture content and tar production. Recently, efforts have been made to mitigate these factors^{11–15}. Unlike gasification, pyrolysis is a technology that converts biomass into bio-oil, syngas and biochar in the absence of oxygen¹⁶. Pyrolysis can be used to valorise different types of recalcitrant biomass, such as agricultural residues and wood wastes. The resulting syngas can then be converted by anaerobic bacteria into biochemicals and bio-

fuels independent of the original biomass composition; a process known as hybrid thermochemical-biochemical¹⁷. However, the high cost and safety risk of the pyrolysis process make it unviable for large scale applications¹⁶.

2.2.2 Biological approach

Biological conversion processes encompass both AD and fermentation and are commonly used to valorise biomass such as food waste, agricultural residues, organic fraction of the municipal solid waste (OFMSW) and energy crops. Unlike the thermochemical conversion method, where the primary product is biofuel, the biological conversion of biomass can produce biofuel and chemicals. Due to the high moisture content of most biomass, direct valorisation using thermochemical technologies is challenging. Therefore, biological conversion technologies are reported to be more ecofriendly and appropriate for waste biomass with high moisture content¹⁸.

AD is a well-established process for the sustainable management of solid organic feedstock¹⁸. AD can be used to convert various organic substrates into methane-rich gas destined for energy generation. In this context, organic residues are conveniently used to meet global energy demand while reducing the burden of fuel consumption and waste disposal. In Europe, the success of AD is witnessed by its dynamic ascent with a total of 18,202 biogas installations, producing 11,082 MW, and 63,511 GWh worth of biogas as recorded in 2018^{19,20}. Despite this continued growth, AD technology is still economically unfeasible in terms of biogas production without fiscal incentives. This is due to high costs associated with biogas production, whereas natural gas is available at lower cost worldwide. Therefore, increasing the efficiency of AD processes is critical to improving its economic attractiveness. To this end, feedstock pre-treatment, reactor configuration, and feedstock co-digestion have been studied as potential means of improving resource recovery^{21,22}.

2.2.3 Valorisation - selecting a method

The selection of a particular valorisation method is highly dependent on the biomass characteristics and composition. For instance, biological approaches are suitable for readily degradable, high-moisture content biomass such as food waste. Thermochemical methods are more commonly used for recalcitrant feedstocks such as lignocellulosic biomass. While both treatment options entail installation and operation costs, research and application suggest that the biological approach may be more flexible, in terms of feedstock and products. Moreover, AD and fermentative processes result in fewer undesirable effects such as tar production.

2.3 Sustainable Feedstock Types

2.3.1 Food waste

Food waste makes up a significant portion of anthropogenically derived organic waste and constitutes an environmental burden where landfill disposal is employed. One third of all food produced for

human consumption goes to waste²³, with 14% of food waste occurring during production processes alone²⁴. While post-consumer waste can be minimised through prevention campaigns, production wastage (peelings, damaged or diseased matter, inedible plant parts) is likely to remain at similar or increasing values. Generally, food waste is composed of fruits, vegetables and tubers²⁴. These materials all have relatively high moisture and energy contents and therefore qualify as high value feedstock for AD²⁵. Through AD, this waste stream can be converted into a renewable resource while simultaneously reducing waste related challenges in the long term²⁶.

Food waste composition varies greatly, but is fundamentally a mix of carbohydrates, proteins, and lipids. The ratio of these three biomolecules largely determines the material's energy generation potential. Lipids have higher energy content than carbohydrates and proteins, however they have been reported to be difficult to breakdown in AD bioreactors, even destabilising digesters at high concentrations^{27–29}. Most food waste is primarily composed of complex carbohydrates, including lignocellulosic and/or hemicellulosic compounds (25 – 30 % of total solids (TS))^{30,31}. These carbohydrates originate from plant matter and are challenging to hydrolyse. Indeed, hydrolysis is frequently reported as the rate limiting step in AD³². Efforts to facilitate hydrolysis have been made, primarily the investigation of various pre-treatment methods including alkaline^{21,33}, thermal³⁴, acid²¹ and enzymatic pre-treatments³⁵. However, these treatments all increase operational costs. Whereas biological strategies, such as tailoring operational conditions to promote the growth and persistence of key microbial hydrolysers within AD bioreactors, represent a promising alternative³¹.

2.3.2 Agricultural residues

Agricultural residual biomasses comprise crop and plant residues, vegetable waste, forest residues, grass, and livestock manure³⁶. These are largely composed of lignocellulose, which can be converted via AD and fermentation to bioenergy and biochemicals. The efficiency of these conversions is determined by specific lignocellulosic characteristics such as lignin content, degree of polymerisation, hemicellulose structure, cellulose crystallinity, porosity, and specific area^{37,38}.

Many studies in the literature review the use of pre-treatments that would decrease the recalcitrance of this biomass by improving the accessibility of cellulose to cellulases. This is achieved either by decreasing the hemicellulose content (e.g., dilute acids and bases) or by applying physical treatment (e.g., high temperature and pressure) to disrupt the lignin matrix^{36,38}. Of course, all pre-treatment processes entail a trade-off between the cost of pre-treatment and desired end-product yield increase³⁸. While ionic liquids and deep-eutectic solvents have been recently investigated, full-scale biorefineries generally employ steam explosion, organosolv, or dilute acids^{38,39}. The use of these pre-treatment technologies may negatively impact the indigenous microbiome of the feedstock, which can be critical to the fermentative process.

The use of lignocellulosic waste as feedstock for biogas production through AD is well established. However, the potential of lignocellulosic waste for VFA production has been garnering increased attention⁴⁰. In a biorefinery context, carboxylic acids are a desirable product with high market

value^{41–44}. Among lignocellulosic wastes, grass is an abundant, renewable, and cheap feedstock that has been largely employed to produce biogas in AD⁴⁵. Relatedly, silage is grass which has been fermented to facilitate preservation during storage. During fermentation, lactic acid bacteria use soluble carbohydrates present on the surface of grass in the production of lactic acid, causing a decrease in pH, which allows the feedstock to be preserved for animal feed without risk of spoilage⁴⁶.

While grass is considered a sustainable feedstock due to its carbon sequestering capacity, co-digestion with other agricultural residues, such as cattle slurry, may further enhance the sustainability of the process⁴⁵. Cattle slurry is an abundant agricultural waste and is cheaper and richer in nutrients than grassland feedstocks. Furthermore, by co-digesting this waste stream with grass, greenhouse gas (GHG) emissions from slurry are reduced⁴⁵. The co-digestion of different grassland forages with grass could also improve AD yields due to an improvement in nutrient availability for the microbial community⁴⁷. Moreover, the combined growth of multi-species grassland mixtures (herbs, legumes and grass) in intensively managed grassland may enhance yield while mitigating disturbances such as drought and environmental impact when compared to monocultures⁴⁸.

2.3.3 Animal residues

Animal manure is a primary contributor to environmental pollution in rural areas. This is usually due to emissions from land-spreading and manure storage facilities, which release harmful substances to the soil, water, and atmosphere. Animal manure/slurry has high concentrations of nutrients (such as nitrogen and phosphorus) and metals (such as copper, zinc, arsenic, and cadmium). Leaching of these metals into the surrounding environment increases phytotoxicity, reduces soil fertility and productivity, and increases toxicity of crops and food products grown on the contaminated soil⁴⁹. Meanwhile, leaching of nutrients contributes to water quality degradation and eutrophication. Moreover, the storage and land-spreading of animal manure/slurry can release GHG, such as methane, nitrous oxide and ammonia in the air contributing to climate change^{50,51}.

To mitigate the environmental burden of the manure/slurry, researchers have engaged in developing techniques for its sustainable treatment. Although composting, incineration, pyrolysis, and gasification have been evaluated, AD is outstanding in its capacity to reduce pollution while generating valuable by-products such as fertilisers and renewable energy⁴⁹. However, there are some factors at play which limit the use of slurry/manure fed AD: **(i)** slurry biomethane potential is low due to high moisture and low organic content⁵⁰; **(ii)** a large volume of feedstock, usually collected from multiple sites, is required for efficiencies of scale⁴⁹; and **(iii)** slurry has a low C:N ratio, which tends to inhibit methane production.

These issues can be mitigated or avoided entirely by employing co-digestion, specifically, by making a mixed feedstock composed of slurry with other organic wastes/residues/energy crops that have a high C:N ratio. Several researchers have reported that co-digestions improved biogas production^{52–54} or VFA production^{55,56}. Although the co-digestion of manure/slurry with other feedstock provides a means to increase economic feasibility, the nutrient and metal-rich liquid digestate remains an issue

in an AD-based facility. Therefore, complete valorisation of the manure/slurry within an AD-based biorefinery concept could result in a more desirable digestate product.

2.4 State-of-the-art System Designs

2.4.1 Single-stage system design and application

Anaerobic bioreactors may be designed to optimise the processing of a selected biomass, and for the production of a specific desired product. Many bioreactor types have the capacity to produce VFAs, hydrogen associated with VFA as a by-product, or biogas. Several reactors, including the continuous stirred tank reactor (CSTR), the packed bed biofilm column reactor, leach-bed reactor (LBR), two-stage anaerobic bioreactor, and continuous flow fermentation reactors have been used to produce VFAs (Table 2.2). Studies using solid feedstocks generally use CSTRs or LBRs, and have generated promising results. The CSTR is perhaps the most widely used single-stage wet AD design⁵⁷. CSTRs are suitable for materials with solids content up to 10%⁵⁸ and work by mixing feedstock and microbes thoroughly in the presence of suspended solids⁵⁹. Previous studies have reported successful production of VFAs from food waste and OFMSW using the CSTR configuration (Table 2.1). However, this reactor design has significant inherent inefficiencies including (i) a tendency for biomass washout, (ii) the need for size reduction of the substrates, (iii) energy input required for continuous stirring (iv) the low solids content (<10%) requirement^{60,61}. In an attempt to overcome these limitations, a novel CSTR design consisting of a solid-liquid separator was proposed to retain undigested biomass with the active community in the system⁶⁰. This approach addresses the issue of biomass washout, but not the limitations for feedstock processing (size reduction, low solids) or energy consumption.

LBRs are a promising alternative to the CSTR for VFA production from high-solid waste such as food waste, OFMSW and vegetable waste, and grass (Table 2.1). Compared to CSTRs, these reactors have been reported to permit higher loads and high VFA production^{31,62}. In LBRs, solid material is loaded into the reactor and irrigated with water, which is recycled through the system continuously. Hydrolysis occurs in the solid bed, while fermentation occurs in the liquid phase, thus decoupling the hydrolysis and fermentation processes. The recirculation mechanism allows for the dilution of inhibitory compounds and increases the moisture in the solid bed which facilitates microorganism growth and activity, all with a relatively low water requirement^{63,64}.

Compared to CSTRs, LBRs have several financial advantages – less instrumentation, maintenance and investment are required, making it an attractively low-cost, high-solids AD reactor⁶⁵. However, since LBRs process solid feedstock which is not stirred, VFA product accumulation can occur. And high levels of VFA can inhibit microorganisms involved in the hydrolysis and fermentation stages^{66–68}. In-line VFA separation, which could remove VFA product from the LBR leachate, is currently being investigated^{69,70}. However, there is currently no consensus or single outstanding technology being used to recover VFA from fermentation liquor. Therefore, researchers have focused on developing two-stage systems in which VFAs generated in LBRs are removed and valorised through processes such as chain elongation (CE), PHA production or even biogas production.

Table 2.1: Chemical characteristics of feedstocks and inoculum sources used for VFA production.

Ref.	Raw Material	TS (%ww)	VS (%ww)	COD/TOC (gO ₂ .kgVS ⁻¹)	Lignocellulosic (% TS)	Observation
<i>Feedstock:</i>						
[3]	Cattle manure Ryegrass silage	5.0 - 9.5 35 - 40	7.0 - 7.3 31.3 - 36.0	44 - 54 312 - 360	n/r n/r	TKN: 1.9 - 3.6 TKN: 4.7 - 5.9
[71]	Napier grass	15.1 g.L ⁻¹	12.7 g.L ⁻¹	0.9 g.g ⁻¹	Cel: 36.8%, Hem: 26.2%, Lig: 8.3%	
[72]	Ryegrass silage*	25.5	24.1	n/a	Cel: 34.3%, Hem: 29.6%, Lig: 8.6%	*Data based on fresh ryegrass before ensiling
[73]	Food waste	42.5±0.78	38.5±1.9	53.0±2.3% ^a	n/a	TKN: 2.1±0.2%
[74]	Dried farmland grass	83.6±0.6	72.8±1.1	n/a	n/a	
[75]	OFMSW	12±1.4	10.7±0.7	102.8±13.0	n/a	Mix of feed, inoculum and tap water to a TS of 7 - 8 %ww. TKN: 3.12±0.51
[76]	OFMSW	28.1±4.0	26.0±2.3	312.6±120.8	n/a	A mix of OFMSW and water was used as inoculum after it was acclimatised to 55 °C. TKN: 8.2±1.8
[31]	Food waste	28.2±2.3	26.0±2.1	376.4±51.3 ^b , 28.6±2.3 ^c	Cel: 2.8±1.0%, Hem: 32.6±4.5%	Lipids: 27.5±1.5% ww, Protein: 20.7±1.2% ww
[77]	Food waste	17.8	17.1	320 gO ₂ .L ^{-1,b} , 95 gO ₂ .L ^{-1,c}	n/a	Lipids: 0.6% ww, Protein: 3.8% ww
[78]	Food waste	16.5±0.2	15.5±0.7	264±27 gO ₂ .L ^{-1,b}	n/a	Sludge inoculum acclimatised for 5 days at 37 °C. Inoculum was treated with BES to inhibit methanogenesis
[79]	Kitchen waste	128.9±2.3 g.L ⁻¹	115.9±2.8 g.L ⁻¹	n/a	n/a	
<i>Inoculum:</i>						
[71]	Cow manure	16.8 g.L ⁻¹	11.8 g.L ⁻¹	0.2 g.g ⁻¹	Cel: 18.3%, Hem: 9.1%, Lig: 11.8%	
[72]	Liquid digestate from the co-digestion of pig manure and grass silage	2.3%	1.6%	0.6 gO ₂ .L ^{-1,c}	n/a	Stored at 35 °C until CH ₄ production was minimal
[73]	Cow manure	18.2±0.8	16.3±0.8	50.8±3.0% ^a	n/a	TKN: 1.4±0.0%
	Anaerobic digested food waste	3.0±0.0	2.7±0.0	34.8±1.0% ^a	n/a	TKN: 2.0±0.0%
[31]	Anaerobic granular sludge	9.0±0.1	7.9±0.0	n/a	n/a	
[78]	Anaerobic digestion sludge	0.4±0.1	0.3±0.1	10.5±1.2 gO ₂ .L ^{-1,b} , 5.1±0.8 gO ₂ .L ^{-1,c}	n/a	
[79]	Anaerobic digestion sludge	31.3±0.5 g.L ⁻¹	19.7±0.4 g.L ⁻¹	n/a	n/a	Pre-treated with heat-shock at 70 °C for 30 min

Note: Acronyms: TS - total solids, VS - volatile solids, COD - chemical oxygen demand, TOC - total organic carbon, TKN - total kjendahl nitrogen (in gN.kg⁻¹ww), Cel - cellulose, Hem - hemicellulose, Lig - lignin, BES - 2-bromoethane sulfonic, n/r - not reported. **Notes:** a - TOC, b - Total COD, c - Soluble COD.

2.4.2 Multi-stage system design and application

A multi-stage bioreactor is, broadly, any system with two or more bioreactors. This design facilitates the segregation of different microbial processes into separate reactors, allowing the environment of each reactor to be optimised for a specific functional microbiome. Such systems are capable of efficiently treating organic waste in terms of degradation yield and biogas production⁸⁰, and of

producing valuable products such as VFA, lactic acid, alcohols and medium-chain carboxylic acids (MCCAs)^{81–83}. In a multi-stage system, hydrolysis and acidification stages occur in one reactor, while CE, PHA production and methanogenesis occur in a separate reactor. In this way, the inhibition of the methanogens is avoided in the first reactor and different operating conditions can be used in each stage to maximise yields. This approach has been found to be more stable than single-stage systems in treating organic waste with high solid content^{84,85}. The observed enhanced performance is reportedly due to the flexibility in process control offered by two-stage systems^{8,86}.

The number of multi-stage systems throughout Europe was expected to rise due to their ability to handle higher loading rates, and improved process stability and flexibility. However, less than 10% of AD capacity in Europe are multi-stage systems^{87,88}. This discrepancy is likely due to the complexity and cost of building and operating such systems. Nevertheless, the versatility and potential of multi-stage systems to improve process performance has encouraged ongoing research, especially within the biorefinery context.

2.5 Process optimisation for Carboxylic Acid Production

2.5.1 Producing carboxylic acids

Carboxylic acids could serve as the foundation for a circular bioeconomy; here we focus especially on lactic acid and VFAs. Lactic acid can be used by the cosmetic, dairy and pharmaceutical industries. It is also a precursor for the synthesis of bioplastics (polylactic acid) and MCCAs^{74,89}. VFAs are aliphatic organic acids with less than six carbons that likewise have applications in the pharmaceutical, dairy, food, animal food, textile, and cosmetic industries⁸⁹. However, the commercialisation of biogenic, mixed VFAs is still challenging, as a commercially feasible technology to recover and purify individual VFAs is still needed⁹⁰. Alternatively, many studies have proposed the use of mixed VFAs as building blocks in a biorefinery to produce MCCAs, polyesters, PHAs, bioenergy and electricity^{90,91}.

The fermentative process for VFA production requires further development. As compared to established chemical routes, the process has lower productivity and yield with higher production costs⁹². Of course, the chemical synthesis and petrochemical route produce more GHG emissions and consume non-renewable energy sources⁹⁰. Our review of the literature indicates that VFA production costs could be minimised by valorising low-cost residual biomass, such as food waste, grass, and manure. Moreover, productivity yields and concentration can be improved by optimising operational parameters such as inoculum, feedstock, temperature, pH, organic loading rate and leachate dilution (Tables 2.1 and 2.2). Therefore, it seems that from a sustainability standpoint, the biological production of VFA is the most promising option.

2.5.2 Inoculum - providing an appropriate microbial community

Fermentative processes are carried out by microbial communities, and their composition and activities are directly related to reactor operational conditions. VFAs can be produced through fermentation

employing either pure cultures or mixed cultures as inoculum. The use of pure culture fermentation, however, requires synthetic media, pure substrates, and media sterilisation, increasing production costs⁹³. Alternatively, the use of residual biomass feedstocks during mixed-culture AD does not require energy for sterilisation or pure substrate supplementation, thus providing greater cost-efficiency⁹¹.

AD is catalysed by a microbial consortium composed of different hydrolytic and fermentative bacteria, and methanogenic archaea⁹⁴. VFAs are produced in the second step (acidogenesis) of the AD process, alongside lactic acid, CO₂ and H₂. However, complete mineralisation involves the consumption of VFAs by methanogenic archaea producing acetic acid, CO₂ and H₂ and, ultimately biogas⁴⁵. Therefore, to optimise VFA production, methanogenic archaea must be inhibited using chemical (e.g., BES)⁷⁷ or physical (e.g., heat-shock)⁷⁹ pre-treatments, or by manipulating operational conditions (e.g., pH)⁹⁵. Balancing the trade-off between VFA productivity and the cost of these pre-treatments is necessary to ensure process feasibility.

The use and choice of inoculum is another crucial consideration in VFA production. The absence of inoculum in grass fermentation led to very low biomass degradation and VFA production (Table 2.2)^{71,72}. The use of cow manure as inoculum increased VFA production as well as the degradation of grass. The quantity of inoculum was also shown to be in important consideration; adding more than 20% of cow manure to the solid fraction proved to negatively impact the process due to the high solid content inside the reactor⁷¹. The digestate from an anaerobic co-digestion of pig manure and silage was responsible for increasing VFA production from grass silage, enhancing biomass degradation⁷². Additionally, rumen bacteria from cow manure caused a shift in the profile of VFAs obtained from food waste, leading to increased propionic, butyric acid and ethanol concentrations⁷³.

2.5.3 Two-stage design for optimised carboxylic acid production

As discussed previously, two-stage systems are preferable for the accumulation of VFAs in AD since the optimal operational conditions of acidogenesis and methanogenesis are drastically different. Moreover, a second stage reactor can also be used to further convert VFAs into MCCAs, PHAs and other valuable products. A two-stage strategy for the AD of grass was found to increase hydrolysis of grass silage and biogas productivity⁴⁵. Additionally, a two-stage AD of OFMSW using a mesophilic CSTR produced 24.4 gCOD.L⁻¹ of VFA while maximising acidification⁷⁵. While this study was designed to optimise biogas production in the second stage, the observed accumulation of propionic and valeric acids in the first stage highlight the potential for PHA production. Another two-stage study recorded grass fermentation and subsequent microbial CE of the lactic acid produced⁷⁴. The native microorganisms on the surface of the grass were responsible for the lactic acid production (9.36 g.L⁻¹) at low pH, while caproic acid, acetic acid and butyric were obtained in a CE reactor. Caproic acid has very low solubility in water and is immiscible at concentrations above 11 g.L⁻¹ (20 °C). Therefore, optimising the operational conditions to obtain caproic acid above this concentration would be beneficial for the process, not only due to its high market value, but to decrease costs

associated with product recovery.

Table 2.2: Summary of the operational conditions for VFA production using the raw materials described in Table 2.1.

Ref.	Reactor operation	Leachate dilution	Recirculation (L.h ⁻¹)	pH	Biomass degradation (%VS)	VFA total (gCOD.L ⁻¹)	VFA profile (%)				
							<i>Ace</i>	<i>Prop</i>	<i>But</i>	<i>Val</i>	<i>Cap</i>
[3]	AF ^a , loading 18 kgCOD m ⁻³ day ⁻¹ for 120 days at 35 °C	n/r	n/r	5.5	25.9-37.0	6.4 10.3	77.6 71.1	11.3 12	6.3 7.3	1.9 2.0	0.5 1.2
[71]	LBR, for 28 days at 28±3 °C	No dilution 2x, 3-day interval 2x, 3-day interval	4.0 4.0 4.0	6.6±1.2 6.2±0.8 6.0±0.5	≈55 ≈65 ≈35	22.8 g 46.9 g 25.9 g	35.6 54.2 36.3	15.5 14.0 28.7	32.1 20.4 20.2	16.8 11.5 14.9	n/r n/r n/r
[72]	LBR, loading 0.5-1.0 kg m ⁻³ day ⁻¹ for 24 - 32 days at 28±3 °C	2x, 6-day interval	0.2	6.5 ^b	62.1-66.3	0.3-0.4 ^c	38-41	27-31	25-28	3-5	n/r
[73]	LBR, loading 12.8 kg m ⁻³ day ⁻¹ for 17 days at 35 °C	2x, every sampling	n/r	6.0 ^d	68.05±2.14	5.8	22.6	11.3	66.0	n/r	n/r
[74]	CE ^a , loading 25 mL for 30 days at 32 °C	n/r	n/r	5.5-6.3 ^e	n/r	12 g.L ⁻¹	33.4	2.1	7.5	20.9	34.1
[75]	CSTR, loading 14-15 kgVS m ⁻³ day ⁻¹ for 180 days at 37 °C	n/r	n/r	6.6±0.2	42	24.4±0.2	14.4	28.6	15.4	27.2	n/r
[76]	CSTR, loading 17 kgVS m ⁻³ day ⁻¹ for 100 days at 55 °C	n/r	n/r	5.3±0.1	83	13.9±0.5	n/r	n/r	n/r	n/r	n/r
[31]	CSTR, loading 80 gVS L ⁻¹ for 7 days at 37 °C	15x ^f	0.05	7.0 ^f	68-76	73.5±1.9	28.4	12.1	24.8	0	29.7
[77]	CSTR, loading 40 gVS L ⁻¹ for 12 days at 37 °C	n/r	n/r	6 ^h	55	48 g	≈37	≈13	≈17	≈9	≈21
[78]	LBR, loading 21.7 gVS.L ⁻¹ for 14 days at 22 °C	n/r	4.4	6 7 8	81 84 87	24±0.2 ⁱ 28±0.6 ⁱ 27±0.2 ⁱ	29.2 39.3 51.9	4.2 7.1 18.5	66.7 50.0 29.6	n/r n/r n/r	n/r n/r n/r
[79]	CSTR, loading 5 gVS.L ⁻¹ .day ⁻¹ for 30 days at 37 °C	n/r	n/r	7.0±0.3	n/r	19.6-24.8 g.L ⁻¹	35-48	12-21	24-30	3-13	2-17

Note: Acronyms: AF - acidogenic fermentation, CE - chain elongation, COD - chemical oxygen demand, LBR - leach-bed reactor, CSTR - continuous stirred tank reactors, n/r - not reported. **Notes:** a- reactor configuration was not disclosed, b- adjusted every 6 days, c- VFA in gCOD gsCOD⁻¹., d- adjusted every sampling, e- not adjusted, f- at the beginning of each cycle, g- at the beginning, h- controlled every 2 days, i- VFA production reported in terms of acetic, propionic and butyric acids.

2.5.4 Leachate dilution in LBRs affects VFA production

A recent study demonstrated that diluting LBR's leachate resulted in increased VFA production and grass solubilisation⁷¹. Reactors with undiluted leachate had lower VFA production; the degradation of grass was also limited, represented by the low soluble COD produced (51.5 g). Meanwhile leachate dilution led to a higher production of VFAs – observed as an accumulation of acetic acid (54.2%). The accumulation of higher chain VFAs (e.g., butyric) can have inhibitory effects on microorganisms, negatively impacting overall acid production and feedstock degradation^{71,72}. As an alternative to leachate dilution, in-line selective VFA extraction may remove higher-chain VFAs with a higher

market value to produce PHAs and MCCAs, while separating and concentrating the acetic acid for biomethane production in a high-rate reactor^{3,89,90,96,97}.

2.5.5 pH directly affects biomass degradability and VFA profile

In fermentative processes, it has been found that the pH directly affects the microbial community, as well as biomass degradability⁷³. Further, pH is directly correlated with VFA and H₂ production in the fermentation of food waste⁷⁶. Low pH (below 6.5) effectively inhibits methanogenesis, but may also inhibit hydrolysis when lower than 4^{72,73,95}. Recently, high VFA production during fermentation of OFMSW was attributed to an operational pH of 6.6, which may have been high enough to avoid the inhibitory effects of acidic environments⁷⁵. Moreover, studies showed that pH values ranging from 6 to 7 improved food waste hydrolysis and maize silage solubilisation while increasing VFA accumulation^{98,99}. In the fermentation of grass silage, slightly lower pH levels were responsible for higher VFA yield with stable operational conditions and suppressed methane generation¹⁰⁰. In the fermentation of grass pellets, controlling the pH levels at 5.50 using 6 M sodium hydroxide led to an efficient degradation of grass to produce 4.5 g.L⁻¹ of VFAs⁹⁷. In two stage systems, the recycling of anaerobic leachate from a second reactor can eliminate the need for external buffering agents to control the pH in a first stage LBR – resulting in overall reductions in operational costs, downstream processing, and environmental impacts⁴⁵.

2.5.6 Temperature implications for VFA accumulation

Temperature is also an important factor when considering the digestion of high-solid biomass for the production of VFAs. Although it does not affect the VFA profile as significantly as pH, temperature can affect the microbial community dynamics⁹³. Lower temperatures, in particular, are reported to reduce the hydrolysis of grass, but may have a positive effect on VFA accumulation⁴². Mesophilic temperatures (37 °C) during the fermentation of OFMSW prevented sudden drops in pH, which consequently prevented inhibition of VFA production⁷⁵. Conversely, thermophilic temperatures (55 °C) during the fermentation of food waste in a similar CSTR reactor with no inoculum addition led to a 43% reduction in VFA production^{76,99}. A final consideration when deciding upon an operational temperature is the cost of heating the system – additional heating can add significantly to the operational costs of the treatment. In light of these considerations, low-temperature operational conditions may be ideal for VFA generation.

2.5.7 Organic loading rate and hydraulic retention time

Organic loading rate (OLR) and hydraulic retention time (HRT) are also important parameters in the production of VFAs. At higher HRTs microorganisms are retained in the bioreactor for longer periods, leading to more thorough conversion of the biomass. Although, a high HRT will also increase operational costs⁹³. OLR is an important parameter in VFA production^{101,102} – a higher OLR

translates into increased overall substrate availability and may also cause a decrease in pH, inhibiting methanogenesis⁹⁵. Indeed, increasing the OLR has been shown to successfully inhibit the methane production without the aid of additional methanogen inhibitors⁷⁷. This inhibition and nutrient availability lead to a higher accumulation of VFAs – e.g., in the fermentation of OFMSW in plug-flows, doubling the OLR led to an increase in 150% in VFA production and 30% decrease in specific biogas production¹⁰². On the other hand, the pH decrease that comes with a high OLR may also function to hinder hydrolysis⁷². It was also observed that increasing the OLR at pH levels lower than 5 led to a predominance of ethanol production instead of VFAs in the fermentation of food waste in leach-bed reactors¹⁰¹. Therefore, an optimal pH range associated with a balanced and appropriate OLR are both necessary to support optimal production.

2.5.8 Feedstock choice influences VFA profile

As discussed in Section 2.2.2 (page 11), feedstock has a direct impact on VFA production (Table 2.1), similar to OLR. Characteristics such as ammonia, COD, pH, and micro-nutrient availability could affect the microbial conversion of the biomass to the desired acids⁹³. Notably, the hydrolysis of biomasses that have higher total COD than soluble COD is directly impaired due to degradation of particulate compounds. Feedstock type is also known to affect the profile of VFAs produced due to its characteristics and/or indigenous microbial community^{74,93,99}. For example, propionic and valeric acids were the main VFAs obtained in the fermentation of food waste at 5-day HRT, 14-15 kgVS.m⁻³.day⁻¹⁷⁵, while butyric and acetic acids were the main VFAs produced from fermentation of grass and grass silage (Table 2.2)⁷¹.

2.5.9 The challenge: VFA recovery and concentration

The choice of which operational conditions to employ in VFA generation must be informed by the intended purpose of those VFAs. For example, when designing a second stage to produce biomethane or electricity using microbial fuel cells, conditions should maximise the accumulation of acetic acid⁹³. However, if the primary function is to produce PHAs in a second reactor, conditions should support the accumulation of butyric acid or propionic and valeric acids. In this way, optimising the operational conditions to produce VFAs is extremely important. Although focus has been placed on VFA production and optimisation, the separation of individual VFAs remains a substantial challenge⁸⁹.

The separation of individual VFAs is inherently challenging due to **(i)** the similar physical properties of VFAs, **(ii)** their potential to form azeotropes with water, and **(iii)** their oftentimes low concentrations in fermentation media⁹¹. In one recent study attempting to isolate caproic acid, a VFA-rich stream was treated via electrochemical extraction. It successfully concentrated caproic acid above its solubility concentration in water, which resulted in the formation of a hydrophobic layer making the separation feasible with 70%wt purity⁷⁴. However, scaled application would require external electricity supplementation. In a recent study, two techniques were investigated: a combination of ultrafiltration and reverse osmosis membrane and liquid-liquid extraction with diethyl ether and

methyl-isobutyl-ketone⁸⁹. Another combination of techniques using solid screening, microfiltration, pervaporation and electro dialysis was successful in recovering 4.5 g.L⁻¹ of VFAs from a 80 L reactor fermenting grass while separating the solids⁹⁷. However, to date, the selective separation of individual acids is still unavailable, which directly impacts the commercial feasibility of isolating specific VFAs to sell as individual products^{90,91}.

Moreover, VFA separation from complex media such as fermentation liquor is primarily limited to lab-scale investigations which implement a wide variety of technologies. Analysing trends in this work may facilitate consensus building, and eventual pilot-scale and real-world applications. Current trends suggest that separation methods often consist of multiple steps and technologies, making up process cascades (Figure 2.2). Most required one or more media preparation steps, such as pH correction or solids removal. These steps each require equipment and operational input, and greatly influence the overall efficiency of the pipeline. For instance, approximately 75% of these processes used a solid removal method (Figure 2.2). Most used centrifugation or filtration as opposed to more efficient, passive solids removal technologies such as tank separation. Additionally, while pH correction was implemented in most fermentation systems, it was only considered a step in the VFA separation process if, **(i)** it was corrected to a very high or very low pH^{103,104}, **(ii)** the pH was specifically referenced as facilitating separation¹⁰⁵, or **(iii)** if the fermentation broth was pH-corrected after collection from reactor¹⁰⁶.

CE was used in only 10% of these treatments. Generally, CE alone is not generally sufficient to accomplish VFA separation. Also referred to as a secondary fermentation, it is a microbially mediated process that lengthens the carbon chains of fatty acids, making them more hydrophobic and easier to separate from an aqueous solution. Often CE requires electron donor supplementation (e.g., ethanol). However, one study instead relied on donors produced during primary fermentation⁷⁴. Because fermentation liquors have significant levels of electron donors (e.g. lactic acid) they may be well suited for use as feedstock for CE processes.

In VFA separation processes, research suggests that the last step is the most intensive and effective. Roughly 30% of treatments terminated with the use of electro dialysis or membrane electrolysis, 20% with membrane contractors/membrane based solvent extraction/membrane-based reactant extraction, 14% used leachate absorption and 14% used liquid extraction (Figure 2.2). Only 14% of the terminal treatments were classified as ‘other’ technologies which were used two or fewer times (e.g. distillation, pervaporation). Each separation technology generally entails a trade-off between cost and productivity⁸⁹. The cost of using membranes with electricity is dependent upon the price of the membrane material. Meanwhile, the use of organic solvents is controversial in terms of sustainability since most of these solvents are fossil-fuel derived chemicals. The use of distillation to recover these solvents and VFAs could be feasible, provided a low-cost energy source is available. As mentioned previously, some studies have avoided separation altogether by converting mixed VFAs into desired products directly from the fermentation liquor^{91,93,107–109}. However, more work needs to be done in this area to maximise productivity and improve commercial feasibility.

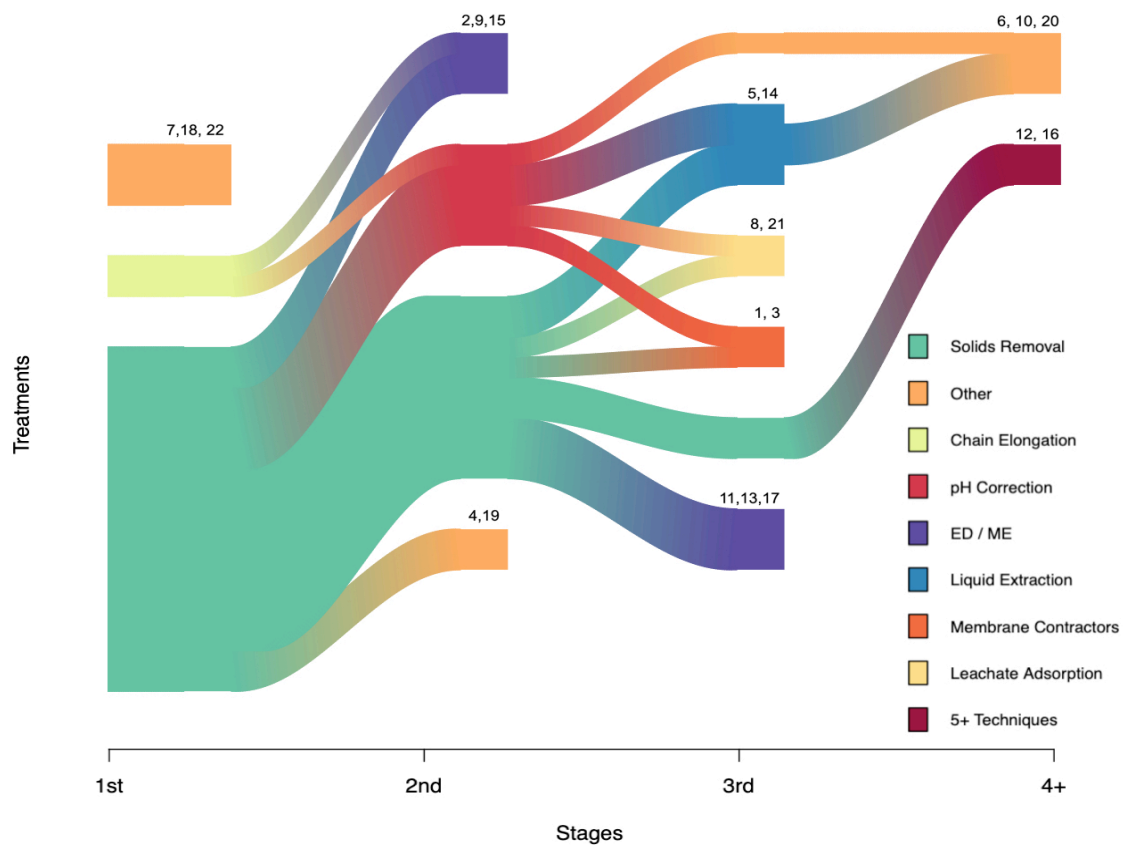


Figure 2.2: Processes used to separate VFAs from fermentation liquors. Sankey plot showing the variety of VFA harvesting processes as a flow of stages (1st, 2nd, 3rd and 4+). Technologies using similar principles and materials were grouped together; for example, electrodialysis and membrane electrolysis were grouped together since they both use membranes and current driven separation of solutes. Technologies were classified as ‘other’ if they were used by only a single study at any given stage. References: 1 - [110]; 2 - [69]; 3 - [106]; 4 - [111]; 5 - [112]; 6 - [41]; 7 - [105]; 8 - [113]; 9 - [114]; 10 - [89]; 11 - [115]; 12 - [97]; 13 - [116]; 14 - [82]; 15 - [74]; 16 - [117]; 17 - [118]; 18 - [119]; 19 - [120]; 20 - [104]; 21 - [103]; 22 - [121].

2.6 Innovative VFA Applications

2.6.1 VFAs for bioplastic production

PHAs are biodegradable thermoplastic polymers synthesised by microorganisms from VFAs (Figure 2.1) and, therefore, are considered an environmentally friendly substitution to fossil fuel-derived plastics^{93,108,122}. The characteristics of the final bioplastic are directly related to the polymer chain-length and the monomers and co-monomers used in its formation^{108,122,123}. Although PHAs are already commercially produced, high operational costs still hinder large-scale production of these bioplastics¹²². Most commercial productions are performed by pure or genetically modified cultures, consequently resulting in high operational costs due to downstream processing (separation, filtration, and centrifugation), energy input (media and reactor sterilisation), substrate formulation (pure VFAs), and equipment cost^{93,122}. However, many studies have shifted focus to the development of processes using mixed cultures and low-cost biomass, thereby improving economic feasibility^{93,108,109,123,124}.

The profitability of PHA production seems to be associated with selecting (i) low-cost feedstocks and (ii) specialised mixed cultures (as opposed to pure cultures) to decrease operational costs. Optimising the conditions for PHA production would also decrease the costs associated with product recovery⁹³.

2.6.2 VFAs for chain elongation chemicals

MCCAs are aliphatic and straight carboxylic acids composed of 6-12 atoms of carbon¹⁰⁷. MCCAs are produced from the biological CE of ethanol and/or short-chain carboxylic acids (SCCAs) through the reverse β -oxidation pathway by anaerobic bacteria¹²⁵. The MCCAs have longer carbon chains and are hydrophobic as compared to SCCAs. Thus, the recovery of MCCAs from liquid media is easier, translating into lower downstream separation costs for higher-market-value compounds¹⁰⁷. As with PHA production, the use of mixed-species cultures rather than pure cultures would increase commercial feasibility. Therefore, many studies on optimising the production of MCCAs from low-cost feedstock and VFA-rich streams have been conducted^{31,74,107,110,126-130}. Challenges remain in terms of optimising operational conditions to selectively produce the MCCAs of interest and concentrate them to a solubility level that would facilitate separation from the liquid media. Moreover, the development of effective and cheap separation processes would also increase the competitiveness of MCCAs.

2.6.3 VFAs for bioenergy and biofuel

Biogenic VFAs can also be converted into bioenergy and biofuels such as biogas, biomethane, biohydrogen and electricity (Figure 2.1). Although not as profitable an application as the synthesis of PHAs and MCCAs, bioenergy is essential to the function of a biorefinery. In order to support chemical platforms of the biorefinery, VFAs can be converted to energy and used to sustainably maintain the biorefinery processes. Surplus energy could be sold to the grid, while biogas can be used as a source of heat, for combined heat and power (CHP) plants¹³¹, or upgraded to biomethane¹³². Biohydrogen has also attracted attention as a fossil-fuel substitute for transport due to its clean combustion (generating water) and high energetic value¹³³. VFAs can be used to generate biohydrogen through photo-fermentation and microbial electrolysis cell^{93,134,135}. Alternatively, VFAs can also be used to produce electricity from microbial fuel cells⁹³. These processes, however, have not yet achieved a commercial state and are highly dependent upon an acetic acid rich VFA stream to maximise efficiency.

2.7 Fermentative Microbial Communities

2.7.1 Microbial communities – why bother?

Microbiology provides a validation that communities develop and adapt to conditions inside engineered systems^{31,136-138}. Understanding their responses and ongoing development can give us confidence around applications of new technologies. Understanding that there are degradative processes that can be linked to biological processes and further linked to design^{139,140}, is critical for the future of the field. Furthermore, understanding how microbial communities develop under these conditions and

underpin efficient conversions, supports the application of biotechnologies under conditions which were previously considered unsuitable. Gaining a deeper understanding of the interactions, ongoing development and functions of built-ecosystem microbiomes will move us one step further into harnessing their transformative metabolisms at a full capacity - resulting in more efficient systems, and a wider range of bioproducts at higher yields.

2.7.2 Key fermentative groups

The structure and function of a bioreactor's microbial consortium directly depend upon the applied operating conditions; thus, community profiles vary from study to study. For example, operational choices such as pre-treatment¹⁴¹, temperature¹⁴², inoculum¹⁴³ and even digester design¹³⁹ all induce shifts in microbial community structure and function. However, while fermentative systems support a diverse range of community profiles, several common trends, and notable findings reoccur. Namely, *Clostridia* are consistently cited for efficient production of VFA across a wide range of studies with differing operational conditions^{31,43,141,144}. Other important players in terms of efficient VFA production are *Sporanaerobacter*, *Tissierella*, *Bacillus*, and *Firmicutes*^{143,144}. Interestingly however, one study noted that *Chloroflexi* were negatively associated with increased VFA yields¹⁴³.

2.8 Future Perspectives: Biorefinery Concept, Application, and Challenges

Most existing AD plants generate biofuel and/or biochemicals in single production chains, generating low-value products or residues which are treated as waste or land spread. In contrast, AD plants can function within a biorefinery as part of a zero-waste strategy, resulting in the complete conversion of wastes into valuable products. The biorefinery concept is parallel to the refinery process in the oil industry, where crude oil is taken in and separated into a myriad of petrochemical products including fuels, lubricants, waxes, asphalt, and polymer production chemicals. Similarly, a biorefinery is a facility that takes in biogenic feedstock to produce biofuels, power, and biochemicals¹⁴⁵.

However, unlike an oil refinery, biorefineries must cope with an extensive variability of feedstock in terms of carbohydrate composition, recalcitrance, ash content, etc. In order to optimally produce zero-waste end-products the biorefinery must integrate physical, chemical, biological and thermochemical processes to convert each fraction into product^{2,7}. Via process integration, these systems convert heterogenous biogenic and waste streams into a multitude of value-added products. AD has great potential as a valuable core technology within the biorefinery concept (Figure 2.1) due to its diverse functionality. It can carry out waste remediation, bioenergy production, bio-based product synthesis, and biological pre-treatment of lignocellulosic biomass^{2,3,7}.

AD is a proven process that generally produces energy-rich biogas as the main attractive product. However, biogas production is usually not stable in digester systems dealing with heterogeneous feedstock (e.g., food waste, grass, and slurry). Therefore, the yield of biogas is reduced, further reducing its already low economical added value. An alternative approach is to bioengineer the AD

process for the production of carboxylic acids alongside biogas and other products thereby converting biogas plants into biorefineries.

Carboxylic acids such as lactic, succinic and VFAs have been successfully generated from the initial anaerobic fermentation of food waste, agricultural waste (silage and cattle liquid manure) and OFMSW (Table 2.1). These carboxylic acids are valuable products when separated from the fermentation broth. However, due to their high solubility in water, the recovery has proven difficult and economically unattractive^{120,146}. These carboxylic acids may be further processed into biogas or converted through biological and chemical process into alcohol-based fuels (e.g., ethanol and butanol) or other value-added products (e.g., PHAs and MCCAs), or they can be used directly to generate electricity in microbial fuel cells^{3,7,147}. In addition to organic acids, gaseous molecular hydrogen and carbon dioxide are normally produced during the anaerobic fermentation of organic substrates. These can be biologically converted to methane¹⁴⁸ or chemically processed into methanol¹⁴⁹.

The solid residue obtained in the anaerobic treatment of biomass, known as digestate, has been viewed as a low-value product, conventionally managed as a fertiliser or animal bedding. However, recent studies have proposed innovative concepts and techniques for its valorisation to biogas and bio-based products^{2,3,150,151}. The digestate, together with a low VFA-liquor and biogas, can be processed to a methane-rich biogas, which in turn can be used to supply heat and electricity for facility operation. Furthermore, studies have demonstrated that AD can act as a biological pre-treatment for lignocellulosic feedstock as it degrades hemicellulose faster than cellulose, thereby facilitating the subsequent enzymatic hydrolysis of cellulose in downstream processes^{152,153}. Following the cellulose extraction, the lignin-rich residue can be thermochemically processed to biofuel or other valuable products.

Interestingly, a significant opportunity exists to valorise the nutrient-rich liquor from the digester for macro- and microalgae production. This approach not only allows for the production of algal biomass, which can be further processed into biofuels and bio-based products, but also accomplishes nutrient-removal from AD effluents, which can then be recycled back as process-water into the AD plant^{7,154}. Despite the potential value offered by biomass biorefineries, technological, spatial, and logistical barriers impact its economic viability, thus hindering widespread application¹⁵⁵. Notably, the technological barrier seems to be the most pressing challenge, as it directly affects production yield. To maximise product yield from biomass, various pre-treatment methods and enzymatic hydrolysis techniques have been used within the AD-based biorefinery. However, these techniques present many limitations (e.g., low efficiency and high cost). Apart from the technological barriers, challenges such as the recovery of products from effluent, the transportation of the fuel and feedstock also impact the success of AD-based biorefinery (Figure 2.3).

Addressing these challenges by developing novel, sustainable, and economically viable technologies will contribute towards the development of an economically attractive biomass biorefinery. For instance, some studies have pointed out potential nanotechnology applications in pre-treatment methods¹⁵⁶. The enzymatic hydrolysis pre-treatment method could be improved by using magnetic nanoparticles to immobilize hydrolytic enzymes, thus allowing them to be re-used in multiple cycles

of hydrolysis¹⁵⁷. Novel nanotechnological solutions should be further investigated, with an aim to improve product yield and process efficiency.

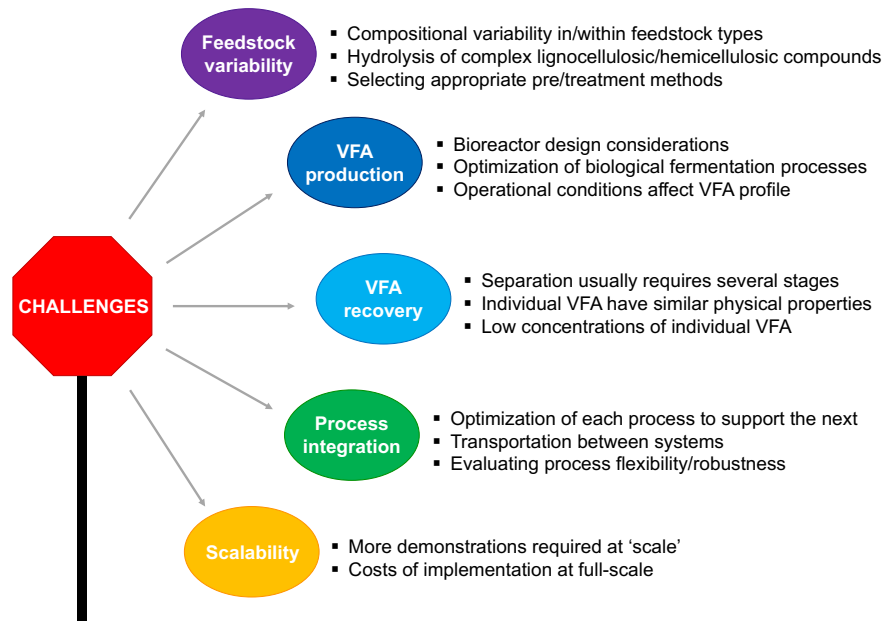


Figure 2.3: Challenges and opportunities for future research. The promise of a biorefinery-based bioeconomy will rely on innovative and interdisciplinary solutions. The literature suggests that key challenges with respect to feedstock variability, VFA production and recovery, process integration and scalability all need to be tackled.

2.9 Conclusions

Although there is clearly room for technological advancements and for closing research gaps, literature suggests that the use of residual biomass within the biorefinery framework is paving the way for a closed-loop bioeconomy. Within such a framework, VFA production could serve as the core platform to produce both energy and a range of bio-based products. This would propel us towards a functioning circular economy that minimises waste and maximises production.

2.10 Acknowledgement and contributions

This work was financially supported by grants from the Higher Education Authority (HEA) of Ireland through: the Programme for Research at Third Level Institutions, Cycle 5 (PRTL-5), co-funded by the European Regional Development Fund (ERDF); the Enterprise Ireland Technology Centres Programme (TC/2014/0016) and Science Foundation Ireland (14/IA/2371 and 16/RC/3889).

This review was designed by Corine Nzeteu (CN), Fabiana Coelho (FC), Emily Davis (ED), Anna Trego (ACT), and Vincent O’Flaherty (VOF). CN, FC, ED, and ACT reviewed the literature and drafted the manuscript and VOF revised the document. All authors approve the paper and agree for

accountability of the work therein. Tables 2.1-2.2 and Figure 2.1 were made by FC. Figure 2.2 was made by ED. Figure 2.3 was made by CN and AT.

2.11 References

1. Badgujar, K. C. & Bhanage, B. M. in *Waste Biorefinery* (eds Bhaskar, T., Pandey, A., Mohan, S. V., Lee, D.-J. & Khanal, S. K.) 3–38 (Elsevier, 2018).
2. Coma, M. *et al.* Organic waste as a sustainable feedstock for platform chemicals. *Faraday Discussions* **202**, 175–195 (2017).
3. Righetti, E., Nortilli, S., Fatone, F., Frison, N. & Bolzonella, D. A Multiproduct Biorefinery Approach for the Production of Hydrogen, Methane and Volatile Fatty Acids from Agricultural Waste. *Waste and Biomass Valorization* **11**, 5239–5246 (Oct. 2020).
4. Wainaina, S., Lukitawesa, Kumar Awasthi, M. & Taherzadeh, M. J. Bioengineering of anaerobic digestion for volatile fatty acids, hydrogen or methane production: A critical review. *Bioengineered* **10**, 437–458 (Jan. 2019).
5. Lytras, G., Lytras, C., Mathioudakis, D., Papadopoulou, K. & Lyberatos, G. Food Waste Valorization Based on Anaerobic Digestion. *Waste and Biomass Valorization* **12**, 1677–1697 (2021).
6. Michalopoulos, I. *et al.* Hydrogen and Methane Production from Food Residue Biomass Product (FORBI). *Waste and Biomass Valorization* **11**, 1647–1655 (2020).
7. Surendra, K. C., Sawatdeenarunat, C., Shrestha, S., Sung, S. & Khanal, S. K. *Anaerobic digestion-based biorefinery for bioenergy and biobased products* Apr. 2015.
8. Demirer, G. N. & Chen, S. Two-phase anaerobic digestion of unscreened dairy manure. *Process Biochemistry* **40**, 3542–3549 (2005).
9. Ning, P. *et al.* Recent advances in the valorization of plant biomass. *Biotechnology for Biofuels* **14**, 102 (2021).
10. Farzad, S., Mandegari, M. A. & Görgens, J. F. A critical review on biomass gasification, co-gasification, and their environmental assessments. en. *Biofuel Research Journal* **3**, 483–495 (2016).
11. Bonilla, J., Gordillo, G. & Cantor, C. Experimental Gasification of Coffee Husk Using Pure Oxygen-Steam Blends. *Frontiers in Energy Research* **7** (2019).
12. Guo, Y., Wang, S., Huelsman, C. M. & Savage, P. E. Products, pathways, and kinetics for reactions of indole under supercritical water gasification conditions. *The Journal of Supercritical Fluids* **73**, 161–170 (2013).
13. Heidenreich, S. & Foscolo, P. U. New concepts in biomass gasification. *Progress in Energy and Combustion Science* **46**, 72–95 (2015).

14. Kalinci, Y., Hepbasli, A. & Dincer, I. Exergoeconomic analysis and performance assessment of hydrogen and power production using different gasification systems. *Fuel* **102**, 187–198 (2012).
15. Sikarwar, V. S. *et al.* An overview of advances in biomass gasification. *Energy & Environmental Science* **9**, 2939–2977 (2016).
16. Hu, X. & Gholizadeh, M. Biomass pyrolysis: A review of the process development and challenges from initial researches up to the commercialisation stage. *Journal of Energy Chemistry* **39**, 109–143 (2019).
17. Latif, H., Zeidan, A. A., Nielsen, A. T. & Zengler, K. Trash to treasure: production of bio-fuels and commodity chemicals via syngas fermenting microorganisms. *Current Opinion in Biotechnology* **27**, 79–87 (June 2014).
18. Sevillano, C. A., Pesantes, A. A., Peña Carpio, E., Martínez, E. J. & Gómez, X. Anaerobic Digestion for Producing Renewable Energy—The Evolution of This Technology in a New Uncertain Scenario. *Entropy* **23**, 145 (Jan. 2021).
19. Cesaro, A. The valorization of the anaerobic digestate from the organic fractions of municipal solid waste: Challenges and perspectives. *Journal of Environmental Management* **280**, 111742 (2021).
20. EBA. *European Biogas Association Annual Report 2020* tech. rep. (2020), 1–38.
21. Cheah, Y.-K., Vidal-Antich, C., Dosta, J. & Mata-Álvarez, J. Volatile fatty acid production from mesophilic acidogenic fermentation of organic fraction of municipal solid waste and food waste under acidic and alkaline pH. *Environmental Science and Pollution Research* **26**, 35509–35522 (2019).
22. Menzel, T., Neubauer, P. & Junne, S. Role of Microbial Hydrolysis in Anaerobic Digestion. *Energies* **13**, 5555 (Oct. 2020).
23. Food and Agriculture Organization of the United Nations. *Global Food Losses and Food waste : extent, causes and prevention* tech. rep. (2011), 1–37.
24. Food and Agriculture Organization of the United Nations. *The state of food and agriculture 2019. Moving forward on food loss and waste reduction* tech. rep. (2019), 1–182.
25. Matharu, A. S., de Melo, E. M. & Houghton, J. A. Opportunity for high value-added chemicals from food supply chain wastes. *Bioresource Technology* **215**, 123–130 (2016).
26. Morales-Polo, C., del Mar Cledera-Castro, M. & Moratilla Soria, B. Y. Reviewing the Anaerobic Digestion of Food Waste: From Waste Generation and Anaerobic Process to Its Perspectives. *Applied Sciences* **8**, 1804 (Oct. 2018).
27. Fernández, A., Sánchez, A. & Font, X. Anaerobic co-digestion of a simulated organic fraction of municipal solid wastes and fats of animal and vegetable origin. *Biochemical Engineering Journal* **26**, 22–28 (2005).

28. Girault, R. *et al.* Anaerobic co-digestion of waste activated sludge and greasy sludge from flotation process: Batch versus CSTR experiments to investigate optimal design. *Bioresource Technology* **105**, 1–8 (2012).
29. Neves, L., Gonçalo, E., Oliveira, R. & Alves, M. M. Influence of composition on the biomethanation potential of restaurant waste at mesophilic temperatures. *Waste Management* **28**, 965–972 (2008).
30. Fisgativa, H., Tremier, A. & Dabert, P. Characterizing the variability of food waste quality: A need for efficient valorisation through anaerobic digestion. *Waste Management* **50**, 264–274 (2016).
31. Nzeteu, C. O., Trego, A. C., Abram, F. & O’Flaherty, V. Reproducible, high-yielding, biological caproate production from food waste using a single-phase anaerobic reactor system. *Biotechnology for Biofuels* **11**, 1–14 (Dec. 2018).
32. Ma, J. *et al.* A simple methodology for rate-limiting step determination for anaerobic digestion of complex substrates and effect of microbial community ratio. *Bioresource Technology* **134**, 391–395 (2013).
33. Fang, Q. *et al.* Impact of Alkaline Pretreatment to Enhance Volatile Fatty Acids (VFAs) Production from Rice Husk. *Biochemistry Research International* **2019** (ed Linhardt, R. J.) 8489747 (2019).
34. Zhang, D. *et al.* Effect of thermal hydrolysis pretreatment on volatile fatty acids production in sludge acidification and subsequent polyhydroxyalkanoates production. *Bioresource Technology* **279**, 92–100 (2019).
35. Kim, J. K., Oh, B. R., Chun, Y. N. & Kim, S. W. Effects of temperature and hydraulic retention time on anaerobic digestion of food waste. *Journal of Bioscience and Bioengineering* **102**, 328–332 (Oct. 2006).
36. Paudel, S. R. *et al.* Pretreatment of agricultural biomass for anaerobic digestion: Current state and challenges. *Bioresource Technology* **245**, 1194–1205 (2017).
37. Bhatia, S. K. *et al.* Recent developments in pretreatment technologies on lignocellulosic biomass: Effect of key parameters, technological improvements, and challenges. *Bioresource Technology* **300**, 122724 (2020).
38. Zoghalmi, A. & Paës, G. Lignocellulosic Biomass: Understanding Recalcitrance and Predicting Hydrolysis. *Frontiers in Chemistry* **7**, 874 (Dec. 2019).
39. Baruah, J. *et al.* *Recent Trends in the Pretreatment of Lignocellulosic Biomass for Value-Added Products* 2018.
40. Sun, J., Zhang, L. & Loh, K. C. *Review and perspectives of enhanced volatile fatty acids production from acidogenic fermentation of lignocellulosic biomass wastes* Dec. 2021.

41. Cerrone, F. *et al.* Medium chain length polyhydroxyalkanoate (mcl-PHA) production from volatile fatty acids derived from the anaerobic digestion of grass. *Applied Microbiology and Biotechnology* **98**, 611–620 (2014).
42. Cysneiros, D. *et al.* Temperature effects on the trophic stages of perennial rye grass anaerobic digestion. *Water Science and Technology* **64**, 70–76 (2011).
43. Joyce, A. *et al.* Linking microbial community structure and function during the acidified anaerobic digestion of grass. *Frontiers in Microbiology* **9**, 1–13 (2018).
44. Tilman, D., Hill, J. & Lehman, C. Supportin online material for: Carbon-negative biofuels from low-input high-diversity grassland biomass. *Science (New York, N.Y.)* **314**, 1598–600 (2006).
45. Murphy, J. D. *et al.* *The Potential for Grass Biomethane as a Biofuel: Compressed Biomethane Generated from Grass , Utilised as a Transport Biofuel* tech. rep. (Environmental Research Institute, 2011), 1–69.
46. Kung Jr, L., Shaver, R. D., Grant, R. J. & Schmidt, R. J. Silage review: Interpretation of chemical, microbial, and organoleptic components of silages. *Journal of Dairy Science* **101**, 4020–4033 (2018).
47. Cong, W.-F., Moset, V., Feng, L., Møller, H. B. & Eriksen, J. Anaerobic co-digestion of grass and forbs – Influence of cattle manure or grass based inoculum. *Biomass and Bioenergy* **119**, 90–96 (Dec. 2018).
48. Grange, G., Finn, J. A. & Brophy, C. Plant diversity enhanced yield and mitigated drought impacts in intensively managed grassland communities. *Journal of Applied Ecology*, 1365–2664 (June 2021).
49. Díaz-Vázquez, D. *et al.* Evaluation of biogas potential from livestock manures and multicriteria site selection for centralized anaerobic digester systems: The case of Jalisco, Mexico. *Sustainability (Switzerland)* **12** (May 2020).
50. Nolan, S. *et al.* Landspreading with co-digested cattle slurry, with or without pasteurisation, as a mitigation strategy against pathogen, nutrient and metal contamination associated with untreated slurry. *Science of The Total Environment* **744**, 140841 (2020).
51. Wolter, M., Prayitno, S. & Schuchardt, F. Greenhouse gas emission during storage of pig manure on a pilot scale. *Bioresource Technology* **95**, 235–244 (2004).
52. Clemens, J., Trimborn, M., Weiland, P. & Amon, B. Mitigation of greenhouse gas emissions by anaerobic digestion of cattle slurry. *Agriculture, Ecosystems & Environment* **112**, 171–177 (2006).
53. Kougias, P. G., Kotsopoulos, T. A. & Martzopoulos, G. G. Effect of feedstock composition and organic loading rate during the mesophilic co-digestion of olive mill wastewater and swine manure. *Renewable Energy* **69**, 202–207 (2014).

54. Orive, M., Cebrián, M. & Zufía, J. Techno-economic anaerobic co-digestion feasibility study for two-phase olive oil mill pomace and pig slurry. *Renewable Energy* **97**, 532–540 (2016).
55. Tampio, E. A., Blasco, L., Vainio, M. M., Kahala, M. M. & Rasi, S. E. Volatile fatty acids (VFAs) and methane from food waste and cow slurry: Comparison of biogas and VFA fermentation processes. *GCB Bioenergy* **11**, 72–84 (Jan. 2019).
56. Yin, D.-m., Mahboubi, A., Wainaina, S., Qiao, W. & Taherzadeh, M. J. The effect of mono- and multiple fermentation parameters on volatile fatty acids (VFAs) production from chicken manure via anaerobic digestion. *Bioresource Technology* **330**, 124992 (2021).
57. Seán Moran. *An Applied Guide to Process and Plant Design* (Elsevier, 2019).
58. Van, D. P., Fujiwara, T., Leu Tho, B., Song Toan, P. P. & Hoang Minh, G. A review of anaerobic digestion systems for biodegradable waste: Configurations, operating parameters, and current trends. *Environmental Engineering Research* **25**, 1–17 (Mar. 2019).
59. Pastor-Poquet, V. *et al.* High-solids anaerobic digestion model for homogenized reactors. *Water Research* **142**, 501–511 (2018).
60. Kariyama, I. D., Zhai, X. & Wu, B. Influence of mixing on anaerobic digestion efficiency in stirred tank digesters: A review. *Water Research* **143**, 503–517 (2018).
61. Lindmark, J., Thorin, E., Bel Fdhila, R. & Dahlquist, E. Effects of mixing on the result of anaerobic digestion: Review. *Renewable and Sustainable Energy Reviews* **40**, 1030–1047 (2014).
62. Doğan, E. & Demirer, G. N. Volatile Fatty Acid Production from Organic Fraction of Municipal Solid Waste Through Anaerobic Acidogenic Digestion. *Environmental Engineering Science* **26**, 1443–1450 (Sept. 2009).
63. Pommier, S., Chenu, D., Quintard, M. & Lefebvre, X. A logistic model for the prediction of the influence of water on the solid waste methanization in landfills. *Biotechnology and Bioengineering* **97**, 473–482 (June 2007).
64. Sanphoti, N., Towprayoon, S., Chairasert, P. & Nopharatana, A. The effects of leachate recirculation with supplemental water addition on methane production and waste decomposition in a simulated tropical landfill. *Journal of Environmental Management* **81**, 27–35 (2006).
65. Degueurce, A., Trémier, A. & Peu, P. Dynamic effect of leachate recirculation on batch mode solid state anaerobic digestion: Influence of recirculated volume, leachate to substrate ratio and recirculation periodicity. *Bioresource Technology* **216**, 553–561 (2016).
66. Cadavid-Rodríguez, L. S. & Horan, N. J. Production of volatile fatty acids from wastewater screenings using a leach-bed reactor. *Water Research* **60**, 242–249 (2014).
67. Dahiya, S., Sarkar, O., Swamy, Y. V. & Venkata Mohan, S. Acidogenic fermentation of food waste for volatile fatty acid production with co-generation of biohydrogen. *Bioresource Technology* **182**, 103–113 (2015).

68. Hussain, A., Filiatrault, M. & Guiot, S. R. Acidogenic digestion of food waste in a thermophilic leach bed reactor: Effect of pH and leachate recirculation rate on hydrolysis and volatile fatty acid production. *Bioresource Technology* **245**, 1–9 (2017).
69. Arslan, D. *et al.* In-situ carboxylate recovery and simultaneous pH control with tailor-configured bipolar membrane electrodialysis during continuous mixed culture fermentation. *Separation and Purification Technology* **175**, 27–35 (2017).
70. Roume, H., Arends, J. B., Ameril, C. P., Patil, S. A. & Rabaey, K. Enhanced product recovery from glycerol fermentation into 3-carbon compounds in a bioelectrochemical system combined with in situ extraction. *Frontiers in Bioengineering and Biotechnology* **4** (Sept. 2016).
71. Kullavanijaya, P. & Chavalparit, O. The production of volatile fatty acids from Napier grass via an anaerobic leach bed process: The influence of leachate dilution, inoculum, recirculation, and buffering agent addition. *Journal of Environmental Chemical Engineering* **7**, 103458 (Dec. 2019).
72. Xie, S., Lawlor, P. G., Frost, J. P., Wu, G. & Zhan, X. Hydrolysis and acidification of grass silage in leaching bed reactors. *Bioresource Technology* **114**, 406–413 (2012).
73. Yan, B. H., Selvam, A. & Wong, J. W. C. Application of rumen microbes to enhance food waste hydrolysis in acidogenic leach-bed reactors. *eng. Bioresource technology* **168**, 64–71 (Sept. 2014).
74. Khor, W. C., Andersen, S., Vervaeren, H. & Rabaey, K. Electricity-assisted production of caproic acid from grass. *Biotechnology for Biofuels* **10**, 1–11 (Dec. 2017).
75. Valentino, F. *et al.* Enhancing volatile fatty acids (VFA) production from food waste in a two-phases pilot-scale anaerobic digestion process. *Journal of Environmental Chemical Engineering* **9**, 106062 (2021).
76. Gottardo, M., Micolucci, F., Bolzonella, D., Uellendahl, H. & Pavan, P. Pilot scale fermentation coupled with anaerobic digestion of food waste - Effect of dynamic digestate recirculation. *Renewable Energy* **114**, 455–463 (2017).
77. Lukitawesa, R. J. P., Millati, R., Sárvári-horváth, I. & Taherzadeh, M. J. Factors influencing volatile fatty acids production from food wastes via anaerobic digestion production. *Bioengineered* **11**, 39–52 (2020).
78. Xiong, Z., Hussain, A., Lee, J. & Lee, H.-s. Food waste fermentation in a leach bed reactor: Reactor performance, and microbial ecology and dynamics. *Bioresource Technology* **274**, 153–161 (Feb. 2019).
79. Swiatkiewicz, J., Slezak, R., Krzystek, L. & Ledakowicz, S. Production of Volatile Fatty Acids in a Semi-Continuous Dark Fermentation of Kitchen Waste: Impact of Organic Loading Rate and Hydraulic Retention Time. *Energies* **14**, 2993 (May 2021).

80. Pohland, F. G. & Ghosh, S. Developments in Anaerobic Stabilization of Organic Wastes - The Two-Phase Concept. *Environmental Letters* **1**, 255–266 (Jan. 1971).
81. Grootsholten, T., Strik, D., Steinbusch, K., Buisman, C. & Hamelers, H. Two-stage medium chain fatty acid (MCFA) production from municipal solid waste and ethanol. *Applied Energy* **116**, 223–229 (Mar. 2014).
82. Kannengiesser, J., Sakaguchi-Söder, K., Mrukwia, T., Jager, J. & Schebek, L. Extraction of medium chain fatty acids from organic municipal waste and subsequent production of bio-based fuels. *Waste Management* **47**, 78–83 (2016).
83. Xu, J. *et al.* Temperature-Phased Conversion of Acid Whey Waste Into Medium-Chain Carboxylic Acids via Lactic Acid: No External e-Donor. *Joule* **3**, 885–888 (Mar. 2018).
84. Fezzani, B. & Ben Cheikh, R. Two-phase anaerobic co-digestion of olive mill wastes in semi-continuous digesters at mesophilic temperature. *Bioresource Technology* **101**, 1628–1634 (Mar. 2010).
85. Khalid, A., Arshad, M., Anjum, M., Mahmood, T. & Dawson, L. The anaerobic digestion of solid organic waste. *Waste Management* **31**, 1737–1744 (Aug. 2011).
86. Cho, J. K., Park, S. C. & Chang, H. N. Biochemical methane potential and solid state anaerobic digestion of Korean food wastes. *Bioresource Technology* **52**, 245–253 (Jan. 1995).
87. De Baere, L. & Mattheeuws, B. *Anaerobic Digestion of the Organic Fraction of Municipal Solid Waste in Europe-Status, Experience and Prospects* in *ISTANBUL3WCONGRESS 2013* (2013), 517–526.
88. Rapport, J. *et al.* *California Integrated Waste Management Board Current Anaerobic Digestion Technologies Used for Treatment of Municipal Organic Solid Waste* *S T A T E O F C A L I F O R N I A INTEGRATED WASTE MANAGEMENT BOARD* tech. rep. (2008).
89. Jänisch, T. *et al.* Separation of volatile fatty acids from biogas plant hydrolysates. *Separation and Purification Technology* **223**, 264–273 (2019).
90. Atasoy, M., Owusu-Agyeman, I., Plaza, E. & Cetecioglu, Z. Bio-based volatile fatty acid production and recovery from waste streams: Current status and future challenges. *Bioresource Technology* **268**, 773–786 (2018).
91. Ramos-Suarez, M., Zhang, Y. & Outram, V. Current perspectives on acidogenic fermentation to produce volatile fatty acids from waste. *Reviews in Environmental Science and Bio/Technology* **20**, 439–478 (2021).
92. Luo, H. *et al.* Recent advances and strategies in process and strain engineering for the production of butyric acid by microbial fermentation. *Bioresource Technology* **253**, 343–354 (Apr. 2018).

93. Lee, W. S., Chua, A. S. M., Yeoh, H. K. & Ngoh, G. C. A review of the production and applications of waste-derived volatile fatty acids. *Chemical Engineering Journal* **235**, 83–99 (2014).
94. Biosantech, T. A. S., Rutz, D., Janssen, R. & Drosch, B. in *The Biogas Handbook* (eds Wellinger, A., Murphy, J. & Baxter, D.) 19–51 (Elsevier, 2013).
95. Magdalena, J. A., Greses, S. & González-Fernández, C. Impact of Organic Loading Rate in Volatile Fatty Acids Production and Population Dynamics Using Microalgae Biomass as Substrate. *Scientific Reports* **9**, 18374 (Dec. 2019).
96. Vartoukian, S. R., Palmer, R. M. & Wade, W. G. The division “Synergistes”. *Anaerobe* **13**, 99–106 (2007).
97. Jones, R. J., Massanet-Nicolau, J., Fernandez-Feito, R., Dinsdale, R. M. & Guwy, A. J. Fermentative volatile fatty acid production and recovery from grass using a novel combination of solids separation, pervaporation, and electrodialysis technologies. *Bioresource technology* **342**, 125926 (2021).
98. Cysneiros, D., Banks, C. J., Heaven, S. & Karatzas, K.-A. G. The effect of pH control and ‘hydraulic flush’ on hydrolysis and Volatile Fatty Acids (VFA) production and profile in anaerobic leach bed reactors digesting a high solids content substrate. *Bioresource Technology* **123**, 263–271 (Nov. 2012).
99. Moza, A., Ram, N. R., Srivastava, N. & Nikhil, G. Bioprocessing of low-value food waste to high value volatile fatty acids for applications in energy and materials: A review on process-flow. *Bioresource Technology Reports* **19**, 101123 (Sept. 2022).
100. Steinbrenner, J., Oskina, A., Müller, J. & Oechsner, H. pH-dependent flushing in an automatized batch leach bed reactor system for volatile fatty acid production. *Bioresource Technology* **360**, 127611 (2022).
101. Campuzano, R., Trejo-Aguilar, G. M., Cuetero-Martínez, Y., Ramírez-Vives, F. & Monroy, O. Acidogenesis of food wastes at variable inlet and operational conditions. *Environmental Technology & Innovation* **25**, 102162 (2022).
102. Rossi, E., Pecorini, I., Paoli, P. & Iannelli, R. Plug-flow reactor for volatile fatty acid production from the organic fraction of municipal solid waste: Influence of organic loading rate. *Journal of Environmental Chemical Engineering* **10**, 106963 (2022).
103. Yousuf, A., Bonk, F., Bastidas-Oyanedel, J.-R. & Schmidt, J. E. Recovery of carboxylic acids produced during dark fermentation of food waste by adsorption on Amberlite IRA-67 and activated carbon. *Bioresource Technology* **217**, 137–140 (Oct. 2016).
104. Yin, J. *et al.* Improving production of volatile fatty acids from food waste fermentation by hydrothermal pretreatment. *Bioresource Technology* **171**, 323–329 (2014).

105. Dessì, P. *et al.* Fermentative hydrogen production from cheese whey with in-line, concentration gradient-driven butyric acid extraction. *International Journal of Hydrogen Energy* **45**, 24453–24466 (Sept. 2020).
106. Aydin, S., Yesil, H. & Tugtas, A. E. Recovery of mixed volatile fatty acids from anaerobically fermented organic wastes by vapor permeation membrane contactors. *Bioresource Technology* **250**, 548–555 (Feb. 2018).
107. De Groof, V., Coma, M., Arnot, T., Leak, D. J. & Lanham, A. B. Medium Chain Carboxylic Acids from Complex Organic Feedstocks by Mixed Culture Fermentation. *Molecules* **24**, 398 (Jan. 2019).
108. Mannina, G., Presti, D., Montiel-Jarillo, G., Carrera, J. & Suárez-Ojeda, M. E. Recovery of polyhydroxyalkanoates (PHAs) from wastewater: A review. *Bioresource Technology* **297**, 122478 (2020).
109. Pagliano, G., Galletti, P., Samorì, C., Zaghini, A. & Torri, C. Recovery of Polyhydroxyalkanoates From Single and Mixed Microbial Cultures: A Review. *Frontiers in Bioengineering and Biotechnology* **9** (2021).
110. Agler, M. T., Spirito, C. M., Usack, J. G., Werner, J. J. & Angenent, L. T. Chain elongation with reactor microbiomes: upgrading dilute ethanol to medium-chain carboxylates. *Energy & Environmental Science* **5**, 8189 (2012).
111. Bak, C., Yun, Y.-M., Kim, J.-H. & Kang, S. Electrodialytic separation of volatile fatty acids from hydrogen fermented food wastes. *International Journal of Hydrogen Energy* **44**, 3356–3362 (Feb. 2019).
112. Braune, M. *et al.* A Downstream Processing Cascade for Separation of Caproic and Caprylic Acid from Maize Silage-Based Fermentation Broth. *Frontiers in Bioengineering and Biotechnology* **9** (2021).
113. Fernando-Foncillas, C., Cabrera-Rodríguez, C. I., Caparrós-Salvador, F., Varrone, C. & Straathof, A. J. Highly selective recovery of medium chain carboxylates from co-fermented organic wastes using anion exchange with carbon dioxide expanded methanol desorption. *Bioresource Technology* **319**, 124178 (Jan. 2021).
114. Hassan, G. K. *et al.* Increasing 2 -Bio- (H₂ and CH₄) production from food waste by combining two-stage anaerobic digestion and electrodialysis for continuous volatile fatty acids removal. *Waste Management* **129**, 20–25 (June 2021).
115. Jones, R. J., Fernández-Feito, R., Massanet-Nicolau, J., Dinsdale, R. & Guwy, A. Continuous recovery and enhanced yields of volatile fatty acids from a continually-fed 100L food waste bioreactor by filtration and electrodialysis. *Waste Management* **122**, 81–88 (Mar. 2021).

116. Jones, R. J., Massanet-Nicolau, J., Fernandez-Feito, R., Dinsdale, R. M. & Guwy, A. J. Recovery and enhanced yields of volatile fatty acids from a grass fermentation via in-situ solids separation and electro dialysis. *Journal of cleaner production* **296**, 126430 (2021).
117. Kucek, L. A., Xu, J., Nguyen, M. & Angenent, L. T. Waste Conversion into n-Caprylate and n-Caproate: Resource Recovery from Wine Lees Using Anaerobic Reactor Microbiomes and In-line Extraction. *Frontiers in Microbiology* **7**, 1892 (Nov. 2016).
118. Tao, B. *et al.* Recovery and concentration of thermally hydrolysed waste activated sludge derived volatile fatty acids and nutrients by microfiltration, electro dialysis and struvite precipitation for polyhydroxyalkanoates production. *Chemical Engineering Journal* **295**, 11–19 (July 2016).
119. Yesil, H., Calli, B. & Tugtas, A. E. A hybrid dry-fermentation and membrane contactor system: Enhanced volatile fatty acid (VFA) production and recovery from organic solid wastes. *Water Research* **192** (Mar. 2021).
120. Yesil, H., Tugtas, A. E., Bayrakdar, A. & Calli, B. Anaerobic fermentation of organic solid wastes: volatile fatty acid production and separation. *eng. Water Science and Technology* **69**, 2132–2138 (May 2014).
121. Zhang, Y. & Angelidaki, I. Bioelectrochemical recovery of waste-derived volatile fatty acids and production of hydrogen and alkali. *Water Research* **81**, 188–195 (2015).
122. Sabapathy, P. C. *et al.* Recent developments in Polyhydroxyalkanoates (PHAs) production – A review. *Bioresource Technology* **306**, 123132 (2020).
123. Zhang, W. *et al.* Value-Added Products Derived from Waste Activated Sludge: A Biorefinery Perspective. *Water* **10**, 545 (Apr. 2018).
124. Costa, S. S., Miranda, A. L., de Morais, M. G., Costa, J. A. V. & Druzian, J. I. Microalgae as source of polyhydroxyalkanoates (PHAs) — A review. *International Journal of Biological Macromolecules* **131**, 536–547 (2019).
125. Angenent, L. T. *et al.* Chain Elongation with Reactor Microbiomes: Open-Culture Biotechnology To Produce Biochemicals. *Environmental Science & Technology* **50**, 2796–2810 (Mar. 2016).
126. Reddy, M. V., Mohan, S. V. & Chang, Y.-C. Medium-Chain Fatty Acids (MCFA) Production Through Anaerobic Fermentation Using *Clostridium kluyveri*: Effect of Ethanol and Acetate. *Applied Biochemistry and Biotechnology* **185**, 594–605 (2018).
127. Roghair, M. *et al.* Controlling Ethanol Use in Chain Elongation by CO₂ Loading Rate. *Environmental Science & Technology* **52**, 1496–1505 (Feb. 2018).
128. Roghair, M. *et al.* Effect of n-Caproate Concentration on Chain Elongation and Competing Processes. *ACS Sustainable Chemistry & Engineering* **6**, 7499–7506 (June 2018).

129. Steinbusch, K. J. J., Hamelers, H. V. M., Plugge, C. M. & Buisman, C. J. N. Biological formation of caproate and caprylate from acetate: fuel and chemical production from low grade biomass. *Energy Environ. Sci.* **4**, 216–224 (2011).
130. Nzeteu, C. o. *et al.* Development of an enhanced chain elongation process for caproic acid production from waste-derived lactic acid and butyric acid. *Journal of Cleaner Production* **338**, 130655 (Mar. 2022).
131. O’Flaherty, V., Collins, G. & Mahony, T. in *Environmental Microbiology* (eds Mitchell, R. & Gu, J.-D.) Second. April 2018, 265–287 (John Wiley & Sons, Inc., Hoboken, NJ, USA, June 2010).
132. Angelidaki, I. *et al.* Biogas upgrading and utilization: Current status and perspectives. *Biotechnology Advances* **36**, 452–466 (2018).
133. Toledo-Alarcón, J. *et al.* in *Bioreactors for Microbial Biomass and Energy Conversion* (eds Liao, Q., Chang, J.-s., Herrmann, C. & Xia, A.) 199–220 (Springer Singapore, Singapore, 2018).
134. Kadier, A. *et al.* Recent advances and emerging challenges in microbial electrolysis cells (MECs) for microbial production of hydrogen and value-added chemicals. *Renewable and Sustainable Energy Reviews* **61**, 501–525 (2016).
135. Reungsang, A. *et al.* in *Bioreactors for Microbial Biomass and Energy Conversion* (eds Liao, Q., Chang, J.-s., Herrmann, C. & Xia, A.) 221–317 (Springer Singapore, Singapore, 2018).
136. Keating, C. *et al.* Cold adaptation and replicable microbial community development during long-term low-temperature anaerobic digestion treatment of synthetic sewage. *FEMS Microbiology Ecology* **94**, fiy095 (July 2018).
137. Trego, A. C. *et al.* Combined Stochastic and Deterministic Processes Drive Community Assembly of Anaerobic Microbiomes During Granule Flotation. *Frontiers in Microbiology* **12** (2021).
138. Trego, A. C. *et al.* Growth and Break-Up of Methanogenic Granules Suggests Mechanisms for Biofilm and Community Development. *Frontiers in Microbiology* **11** (2020).
139. McAteer, P. G. *et al.* Reactor configuration influences microbial community structure during high-rate, low-temperature anaerobic treatment of dairy wastewater. *Bioresource Technology* **307**, 123221 (2020).
140. Trego, A. C. *et al.* First proof of concept for full-scale, direct, low-temperature anaerobic treatment of municipal wastewater. *Bioresource Technology* **341**, 125786 (2021).
141. Yang, G. & Wang, J. Kinetics and microbial community analysis for hydrogen production using raw grass inoculated with different pretreated mixed culture. *Bioresource Technology* **247**, 954–962 (2018).

142. Yuan, Y. *et al.* Short-chain fatty acids production and microbial community in sludge alkaline fermentation: Long-term effect of temperature. *Bioresource Technology* **211**, 685–690 (2016).
143. Atasoy, M., Eyice, O., Schnürer, A. & Cetecioglu, Z. Volatile fatty acids production via mixed culture fermentation: Revealing the link between pH, inoculum type and bacterial composition. *Bioresource Technology* **292**, 121889 (2019).
144. Wu, Q.-L. *et al.* Enhancement of volatile fatty acid production by co-fermentation of food waste and excess sludge without pH control: The mechanism and microbial community analyses. *Bioresource Technology* **216**, 653–660 (2016).
145. Cherubini, F. The biorefinery concept: Using biomass instead of oil for producing energy and chemicals. *Energy Conversion and Management* **51**, 1412–1421 (July 2010).
146. Li, Q. *et al.* One step recovery of succinic acid from fermentation broths by crystallization. *Separation and Purification Technology* **72**, 294–300. <https://www.sciencedirect.com/science/article/pii/S138358661000081X> (2010).
147. Chen, H., Meng, H., Nie, Z. & Zhang, M. Polyhydroxyalkanoate production from fermented volatile fatty acids: Effect of pH and feeding regimes. *Bioresource Technology* **128**, 533–538 (2013).
148. Leonzio, G. Upgrading of biogas to bio-methane with chemical absorption process: simulation and environmental impact. *Journal of Cleaner Production* **131**, 364–375 (2016).
149. Yao, Y., Sempuga, B. C., Liu, X. & Hildebrandt, D. Production of Fuels and Chemicals from a CO₂/H₂ Mixture. *Reactions* **1**, 130–146 (Nov. 2020).
150. Budzianowski, W. M. High-value low-volume bioproducts coupled to bioenergies with potential to enhance business development of sustainable biorefineries. *Renewable and Sustainable Energy Reviews* **70**, 793–804. <https://linkinghub.elsevier.com/retrieve/pii/S1364032116310425> (Apr. 2017).
151. Khoshnevisan, B., Tsapekos, P., Zhang, Y., Valverde-Pérez, B. & Angelidaki, I. Urban biowaste valorization by coupling anaerobic digestion and single cell protein production. *Bioresource Technology* **290**, 121743 (Oct. 2019).
152. MacLellan, J. *et al.* Anaerobic treatment of lignocellulosic material to co-produce methane and digested fiber for ethanol biorefining. *Bioresource Technology* **130**, 418–423 (Feb. 2013).
153. Yue, Z., Teater, C., MacLellan, J., Liu, Y. & Liao, W. Development of a new bioethanol feedstock – Anaerobically digested fiber from confined dairy operations using different digestion configurations. *Biomass and Bioenergy* **35**, 1946–1953 (2011).
154. Rajagopal, R., Mousavi, S. E., Goyette, B. & Adhikary, S. Coupling of Microalgae Cultivation with Anaerobic Digestion of Poultry Wastes: Toward Sustainable Value Added Bioproducts. *Bioengineering* **8**, 57 (May 2021).

155. Philippini, R. R. *et al.* Agroindustrial Byproducts for the Generation of Biobased Products: Alternatives for Sustainable Biorefineries. *Frontiers in Energy Research* **8** (2020).
156. Ingle, A. P., Philippini, R. R. & Silvério da Silva, S. Pretreatment of sugarcane bagasse using two different acid-functionalized magnetic nanoparticles: A novel approach for high sugar recovery. *Renewable Energy* **150**, 957–964 (2020).
157. Rai, M. *et al.* Emerging role of nanobiocatalysts in hydrolysis of lignocellulosic biomass leading to sustainable bioethanol production. *Catalysis Reviews* **61**, 1–26 (Jan. 2019).

Chapter 3: Synergistic and antagonistic effects in the anaerobic digestion of permanent grassland biomass species

Abstract

Grasses have been extensively evaluated as a potential feedstock for anaerobic digestion (AD) due to their sustainability and abundance, but other permanent grassland biomass, such as legumes and herbs, have been overlooked despite their higher nutritional value. The present work evaluates the methane potential of three functional groups of permanent grassland biomass – grasses (*L. perenne* and *P. pratense*), legumes (*T. pratense* and *T. repens*), and herbs (*C. intybus* and *P. lanceolata*) – as mono-substrates and co-substrates. The effect of nitrogen fertilisation rate in the mono-digestion of *L. perenne* was also evaluated by digesting *L. perenne* supplied with two doses of nitrogen fertiliser (150 and 300 kgN.ha⁻¹.yr⁻¹). A biomethane potential assay was performed based on a simplex design composed of those species – in total, 33 substrates were tested. The results were analysed based on the First order kinetics model, which was selected out of four models as it better explained the methane production from grassland biomass. Moreover, the interspecific interactions from digesting different species of grassland biomass, as well the effect of species identity, were investigated using the Diversity-interaction model framework. Synergistic effects were observed in the co-digestion of both *T. repens* and *C. intybus*, and *L. perenne* and *T. pratense*. Antagonistic effects, though, were observed in the co-digestion of grass species. Improved substrate-specific methane yield was observed in the mono-digestion of *L. perenne* with a higher dose of nitrogen fertiliser. However, a comparable area-specific methane yield was reached in the co-digestion of an equi-proportional mixture of six grassland species.

3.1 Introduction

Permanent grassland fields are complex ecosystems consisting of different species of graminoids (e.g., grasses) and forbs (e.g., legumes and herbs), with forbs acting as an important factor to conserve the biodiversity and functionality of grasslands¹. These grasslands are crucial ecosystems for food production with an important role in maintaining soil quality, balancing the ecosystem biodiversity, and sequestering carbon from the atmosphere^{2,3}. These benefits, however, are affected by field management strategies⁴. Intensively managed monocultures are common practice in food production, but they rely on the same species over multiple years as well as the supplementation of high quantities of inorganic fertiliser to achieve high forage yields⁵. This comes at the expense of the ecosystem's health, e.g., lower soil quality, contamination of water bodies, and loss of biodiversity^{5,6}. Alternatively, improving diversity in grassland fields has proved to be as valuable to forage yield as fertilisation rates or harvesting strategies⁷. Studies have shown that mixed-species swards and crop-rotation can

sustainably improve forage yield^{8–11} with lower nitrogen fertiliser input, but better nitrogen efficiency intake (e.g., when mixing legumes and grass)^{12,13} and lower N₂O emissions³.

A sustainable production of grassland biomass is also important to secure an energy feedstock that can contribute to neutralise the greenhouse gas (GHG) emissions in Europe by 2050¹⁴. Moreover, as the energy sector substantially contributes to GHG emissions¹⁵, anaerobic digestion (AD) is an important process to reach the ‘The Green Deal’ target by generating cleaner energy products such as biomethane and electricity. As grass is considered one of AD’s main sustainable feedstocks^{16,17}, the higher forage yield resulting from the grassland’s biodiversity and sustainable field management may improve biogas yield and digestate quality. In the past 20 years, the potential of grasses in AD has been extensively investigated, especially the digestion of perennial ryegrass, grass silage, residue grass and timothy^{17–30}. However, the poor nutrient availability of grasses is a disadvantage for the mono-digestion of this grassland biomass in the long run^{29,31}. Studies have shown that co-digestion with animal residues^{20,31,32}, and forbs^{31,33–35} could further improve the sustainability of a grass-based AD²⁰ with a more balanced nutrition for the microbial community. The co-digestion of grass with animal slurry, however, was less favourable to the production of methane compared to the mono-digestion of grass despite its higher nutrition^{29,32}. On the other hand, mixing legumes and herbs with ryegrass resulted in improved C:N ratio and fibre composition, thus improving the production of methane^{33,34}. Despite this potential for methane production, few studies have focused on the mono-digestion^{33–35} of clovers and herbs or its co-digestion with grass³³.

Most studies evaluate the methane potential from a feedstock by performing a biomethane potential assay (BMP) assay, and many empirical models have been proposed over the years to fit experimental data and to predict the production of methane^{36,37}. One of the main challenges with BMP assays and predictive models is the standardisation of the methodology^{38,39}, which is influenced by operational conditions, experimental setup and inoculum source^{36,40,41}. For that reason, care must be taken when comparing and exploring the limits between the methane potential and kinetic constants across different feedstock and experiments. Although the use of empirical kinetic modelling is powerful to understand other important aspects of the methane production, there is no universal model that represents all feedstocks or operational conditions⁴⁰. Each kinetic model has its constraints, discontinuities and mathematical formulas in light of the experimental observations. Particularly in the digestion of grassland biomass, the cumulative production of methane has been investigated using different non-linear empirical models, such as first order kinetics (FOK)^{31–33,38,40–44}, modified gompertz (MG)^{31–34,40,42–44}, corrected modified gompertz (CMG)^{37,40}, and CONE⁴⁵. Generally, the FOK model is a simple and good fit to the experimental data in most studies and, therefore, most commonly applied. The MG model has been frequently used, as well, to predict the maximum methane yield and specific methane production rate. However, the MG model does not predict a null methane yield at the start of the experiment, which led to a correction in the form of the CMG model^{37,40}. Similarly to the FOK model, the CONE model also considers the initial methane yield as zero, before the lag phase, but incorporates more parameters (the shape factor, *n*).

It is established that empirical kinetic models are important to predict the production of methane,

but these models do not elucidate the effects of mixing grassland species as co-substrates. Synergistic (positive) and antagonistic (negative) effects in the co-digestion of silage and slurry were explained by Himanshu *et al.*^{31,32} using Scheffè polynomials and a non-linear blending method. Synergistic and antagonistic effects were also evaluated by Cong *et al.*³³ in the co-digestion of grass, legumes and herbs by computing the difference in methane yield obtained using two linear models that resembled diversity–interaction (DI) models. DI models are modelling frameworks that estimate the effect of species identity, community composition, richness and interspecific interactions to a response variable⁴⁶. Previously, DI models were used with permanent grassland species to predict and understand how those effects contribute to forage yield^{8–10}, weed suppression¹², nitrogen yield¹⁰, and N₂O emissions⁴⁷. The parameters estimated from the DI models can be used to understand how species identity and interspecific interactions contribute to methane production, improving the understanding regarding grassland species as co-substrates.

Therefore, the present work was designed to evaluate the methane potential of six grassland species that are common to temperate climate. These six species were received from monocultures and mixed-species swards of an existing pilot-scale field in Ireland. The study was designed to evaluate the species identity effects and interspecific interaction effects of mono-digesting those species and co-digestion two or six of those species by using the results from a BMP assay to estimate the coefficients from DI models. Moreover, the effect of nitrogen fertiliser supplementation in the methane yield was investigated by digesting *Lolium perenne* in two different doses of nitrogen supplementation. To the best of our knowledge, this is the first study to consider the co-digestion of six species of grassland biomass for the production of methane, directly from the field. Moreover, it is the first attempt to use a diversity–interaction model to understand the interaction between six grassland species in the production of methane.

3.2 Materials and Methods

3.2.1 Substrate

Perennial forages were selected in June 2019 from a pilot–scale field experiment at Johnstown Castle, Wexford, in the south-east of Ireland (52°17'57.8"N, 6°30'23.3"W, 71 m a.s.l)¹⁰. The field received natural water supply and was established on a field previously grass-dominated with sandy-loam soil with pH 5.7, total carbon of 12.2 g/kg of soil, and total nitrogen of 2.45 g/kg of soil⁹. In this field, six species from three FG of grassland were cultivated as monocultures, and mixtures from two to six species of grass (*Lolium perenne*, *Phleum pratense*), legume (*Trifolium pratense*, *Trifolium repens*), and herb (*Cichorium intybus*, *Plantago lanceolata*). The forages were supplied with nitrogen (150 kg.ha⁻¹.yr⁻¹), phosphorus (60 kg.ha⁻¹.yr⁻¹), and potassium (300 kg.ha⁻¹.yr⁻¹). Plots of *L. perenne* fertilised with a double dose of nitrogen (300 kg.ha⁻¹.yr⁻¹) were also cultivated.

For the purposes of this study, the substrates were selected from field plots consisting of monocultures, mixtures of two grassland species, and mixtures of six grassland species. Each monoculture had two plots as replicates, while three plots were selected for the mix of six species and for *L. per-*

enne supplied with 300 kg.ha⁻¹.yr⁻¹ of nitrogen fertiliser. In total, the study evaluated 33 substrates, comprising seven monocultures (one with a higher dose of nitrogen), 15 mixtures of two species, and one mixture of six species. Each substrate represented a field sample from a respective plot. The intended species from each plot were manually separated from unsown species, cut to approximately 2 cm and stored in sample bags at -20 °C. For *P. lanceolata*, both leaves and stems were separated. For mixed-species plots, each of the intended species were manually separated and stored in different bags until the experiment. Each species and the *L. perenne* supplied with a double dose of nitrogen fertiliser were characterised in terms of total (TS) and volatile (VS) solids (Table 3.1).

Table 3.1: Summary of the total and volatile solids for each species.

Grassland species	Nitrogen fertiliser (kgN.ha ⁻¹ .yr ⁻¹)	Total solids (%FW)	Volatile solids (%FW)
<i>L. perenne</i>	150	31.2 (2.5)	28.9 (2.3)
<i>L. perenne</i>	300	21.4 (1.3)	19.7 (1.2)
<i>P. pratense</i>	150	22.8 (0.4)	21.2 (0.4)
<i>T. pratense</i>	150	17.0 (0.2)	15.1 (0.1)
<i>T. repens</i>	150	16.0 (1.3)	14.1 (1.0)
<i>C. intybus</i>	150	18.9 (1.8)	16.4 (1.6)
<i>P. lanceolata</i>	150	19.4 (0.5)	17.3 (0.4)

Note: average values with standard deviation (in brackets).

3.2.2 Inoculum

Granular sludge from a full-scale expanded granular sludge bed (EGSB) reactor applied to treat dairy wastewater from Arrabawn Dairies Co. in Kilconnell, Ireland, was used as inoculum. The granular sludge was harvested in November 2020 and stored with its leachate at 4 °C. The inoculum TS and VS were 12.7 (0.1)% and 9.6 (0.0)%, respectively. Prior to the experiment, the granular sludge was filtered using a metal sieve and a cloth, washed with tap water and drained. The inoculum was prepared by mixing intact and crushed granules (50-50% in VS); the granules were crushed using a mortar and a pestle. The inoculum was acclimatised in sodium bicarbonate buffer (10 g.L⁻¹, 250 mL) at 37 °C and 100 rpm for 5 days. Anaerobic conditions were provided by flushing N₂/CO₂ for 5 minutes.

3.2.3 Biomethane potential experimental setup

The methane potential of 33 substrates composed of grasses and forbs (legumes and herbs) were evaluated using a modified BMP assay. The setup consisted of 500 mL plastic bottles with Fisherbrand™ solid rubber stoppers and 1 L Tedlar gas bags attached using a needle and a tap. Methane production was monitored for 21 days at 37 °C and constant agitation (100 rpm). The digestion time was determined based on previous BMP experiments, in which it was observed that the methane accumulation was constant after 21 days of digestion. Inoculum-acclimatised bottles were prepared with an

inoculum loading of 10 gVS.L⁻¹, and substrate loading based on a substrate-to-inoculum ratio of 1:1. Substrate composition followed a simplex design⁴⁸ considering species' composition of 100% VS (monocultures), 50% VS of each species (two species mixture), and 16.7% VS of each species for the six-species centroid (Table 3.2, each line represents a field plot). The mixture of species were manually assembled based on the VS content of each species (Table 3.1) and the intended composition (Table 3.2). Inoculum-acclimatised bottles were used as a negative control to monitor the production of methane from any residual substrate available in the inoculum. Anaerobic conditions were provided by flushing N₂/CO₂ (80-20%) for 5 minutes, and 0.42 mL of a trace elements solution was supplied⁴⁹. The experiment was performed in triplicate, with biological replicates from different plots (e.g., two different field plots of *L. perenne* – *Lp*₁ and *Lp*₂). Biogas volume was monitored at regular intervals (0, 2, 4, 8, 15, 18 and 21 days) or when the gas bags were full to limit disturbances in gas production. Biomass consumption was determined as VS degradation, where VS values measured at the beginning and after 21 days of digestion.

Table 3.2: Grassland species composition for each substrate based on its volatile solids content.

Substrate	Species composition (%VS)					
	<i>L. perenne</i> , Lp	<i>P. pratense</i> , Pp	<i>T. pratense</i> , Tp	<i>T. repens</i>	<i>C. intybus</i> , Ci	<i>P. lanceolata</i> , Pl
Lp ₁	100%					
Lp ₂	100%					
Pp ₁		100%				
Pp ₂		100%				
Tp ₁			100%			
Tp ₂			100%			
Tr ₁				100%		
Tr ₂				100%		
Ci ₁					100%	
Ci ₂					100%	
Pl ₁						100%
Pl ₂						100%
Lp* ₁	100%					
Lp* ₂	100%					
Lp* ₃	100%					
Lp:Pp	50%	50%				
Lp:Tp	50%		50%			
Lp:Tr	50%			50%		
Lp:Ci	50%				50%	
Lp:Pl	50%					50%
Pp:Tp		50%		50%		
Pp:Tr		50%			50%	
Pp:Ci		50%				50%
Pp:Pl		50%				50%
Tp:Tr			50%	50%		
Tp:Ci			50%		50%	
Tp:Pl			50%			50%
Tr:Ci				50%	50%	
Tr:Pl				50%		50%
Ci:Pl					50%	50%
6-species ₁	16.7%	16.7%	16.7%	16.7%	16.7%	16.7%
6-species ₂	16.7%	16.7%	16.7%	16.7%	16.7%	16.7%
6-species ₃	16.7%	16.7%	16.7%	16.7%	16.7%	16.7%

Note: *higher dose of nitrogen fertiliser.

3.2.4 Analytical methods

Substrate, liquid digestate and solid digestate were analysed in terms of TS, VS and pH according to standard methods⁵⁰. pH was measured at the beginning and end of the digestion. Substrate samples

were also characterised in terms of elemental carbon (C), nitrogen (N), oxygen (O), hydrogen (H), and sulphur (S) by Celnis Analytical (Limerick, Ireland) as described in the European Standard EN 15104:2011 – the elemental data was analysed in duplicate and reported in terms of dry matter. The amount of C, N, O, H, and S was used to estimate the theoretical chemical oxygen demand (ThCOD)⁵¹, the theoretical BMP TBMP⁵², and the C:N ratio. The crude protein content was calculated by multiplying the %N by 6.25⁵³. Data related to the fibre content of the grassland biomass was provided by Teagasc in dry weight as neutral detergent fibre (NDF) and acid detergent fibre (ADF) – fibre content was determined using near-infrared spectroscopy (NIRS) technology and following the procedure described by Lorenz *et al.*⁵⁴. Hemicellulose content was calculated as the difference between NDF and ADF; and ADF was used as a proxy for the cellulose and lignin content^{33,55}. Biogas volume was measured using the water displacement method⁵⁶. Methane composition was determined using gas chromatography (Varian CP-3800, Varian Inc., Walnut Creek, CA USA) equipped with a thermal conductivity detector (TCD), and a hydrogen generator (WhatmanTM). Total ammonia nitrogen (TAN) values were calculated from ammonium results obtained using a colorimetric method based on the reaction of ammonia with hypochlorite ions generated by the alkaline hydrolysis of sodium dichloroisocyanurate to monochloramine (GalleryTM Plus Discrete Analyzer, Thermo Fisher Scientific). Ammonia measurements were performed in one replicate of selected substrates, based on the BMP performance and C:N ratio – *L. perenne* (Lp₁ and Lp*₁), *P. pratense* (Pp₁), *T. repens* (Tr₁), six species mixture (6-species₁), the mixture of *L. perenne* with *P. pratense* (Lp:Pp), and the mixture of *T. repens* with *C. intybus* (Tr:Ci).

3.3 Chemical Parameters and Modelling

3.3.1 Volatile solids degradation

Substrate conversion was defined as the ultimate consumption of the biomass' biodegradable materials after the digestion under optimum methanogenic conditions, which are favourable to maximise the degradation of the feedstock. Substrate conversion is represented by the VS degradation, which can be expressed mathematically (Equations 1). Previously, this Equation was also referred to as VS destruction⁴⁴. Volatile solids of liquid phase and solid phase were considered to calculate the VS of inoculum and substrate. As the conditions provided in both sample-bottles and control-bottles were similar, the VS of the control-bottles were approximated as the VS of the inoculum itself (Equation 1c).

$$VS_{deg}(t) = 1 - \frac{m_s(t)}{m_s(0)} \quad (1a)$$

$$m_{sample}(t) = m_s(t) + m_i(t) \quad (1b)$$

$$m_{control}(t) = m_i(t), \quad (1c)$$

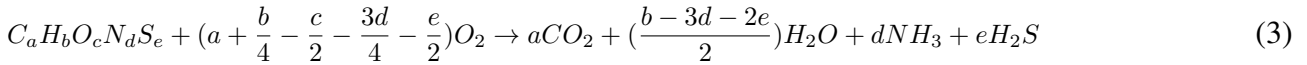
Where: t is the digestion time; $m_{sample}(t)$ is the mass of substrate, $m_s(t)$, plus the mass of inoculum, $m_i(t)$; $m_{control}(t)$ is the mass of inoculum in control-bottles, $m_s(0)$ is the mass of substrate at $t = 0$; and $VS_{deg}(t)$ represents the VS degradation of a substrate after the digestion (in %VS). Mass is expressed in gVS .

3.3.2 Theoretical chemical oxygen demand

The ThCOD of each substrate was calculated based on the elemental composition of the dried biomass and its minimal formula ($C_aH_bO_cN_dS_e$, Equation 2)⁵⁷. The amount of oxygen needed to oxidise the biomass is calculated based on the chemical oxidation of the biomass (Equation 3), considering that the nitrogen of amines is eliminated as ammonia⁵¹, and the sulphur is eliminated as hydrogen sulphide⁵⁸. In this study, sulphur was not considered in the minimal formula, as the amount of sulphur was below 1%.

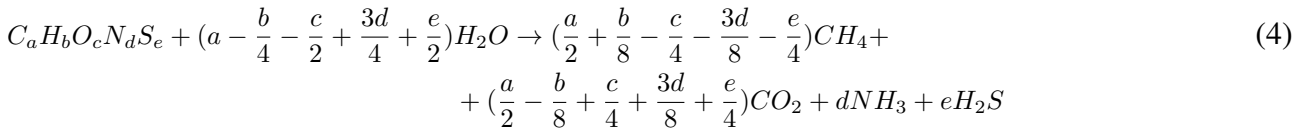
$$\text{ThCOD} = \frac{32(a + \frac{b}{4} - \frac{c}{2} - \frac{3d}{4} - \frac{e}{2})}{12a + b + 16c + 14d + 32e}, \quad (2)$$

Where: ThCOD is the theoretical COD in terms of gO_2 per $gC_aH_bO_cN_dS_e$ (volatile solids). The indexes a , b , c , d and e represent, respectively, the number of atoms of carbon, hydrogen, oxygen, nitrogen and sulphur in the minimal formula.



3.3.3 Theoretical methane potential and biodegradability index

The TBMP was calculated based on Buswell's stoichiometric equation^{52,58} under standard conditions ($0^\circ C$, 1 atm), considering the elemental composition of the biomass (Equations 4-5). In this study, sulphur was not considered in the minimal formula, as the amount of sulphur was below 1%. The biodegradability index (Equation 7) of each substrate was determined as the ratio of the measured (BMP) and the theoretical (TBMP) methane potential.



$$\text{TBMP} = \frac{(\frac{a}{2} + \frac{b}{8} - \frac{c}{4} - \frac{3d}{8} - \frac{e}{4}) \cdot 22.4 \cdot 10000}{12a + b + 16c + 14d + 32e}, \quad (5)$$

$$(6)$$

$$B_d = \frac{BMP}{TBMP}, \quad (7)$$

Where: TBMP is the theoretical methane potential (L per $kgC_aH_bO_cN_dS_e$), B_d is the biodegradability index (%). The indexes a , b , c , d and e represent, respectively, the number of atoms of carbon, hydrogen, oxygen, nitrogen and sulphur in the minimal formula.

3.3.4 Biomethane production

The volume of biogas and biomethane was normalised to standard conditions (101.3 kPa, 273 K) using Equation 8⁵⁹. The cumulative biogas production was calculated considering the headspace volume ($v^h = 213.27$ NL), and the volume collected from the gas bags (v^b) at each sampling point (Equation 9a). The cumulative production of methane considered the composition of methane in the biogas at each sampling point (Equation 9b)⁴⁰. As the bottles were not vented between measurements, a correction for the methane composition in the headspace from a previous sampling point was added in Equation 9b. The volumetric yield for methane and biogas was calculated in terms of volatile solids of substrate fed to the digestion (Equation 9c). The production of methane and biogas from each substrate was corrected by subtracting the volume produced in the control-bottles.

$$v = v_{dry} = \frac{v_{wet} \cdot (P - P_w) \cdot T_o}{p_o \cdot T}, \quad (8)$$

Where: v_{dry} is the volume of dry gas in standard conditions (NL), v_{wet} is the volume of wet gas (L), P and T are the operational pressure and temperature (101.3 kPa and 310 K), respectively; P_w is the vapour pressure of water at 25°C (3.169 kPa), p_o and T_o are the standard temperature and pressure, respectively.

$$V_{biogas} = v_h + \sum_{i=1}^n v_{b_i} \quad (9a)$$

$$V_{CH_4} = \sum_{i=1}^n (v_{b_i} \cdot x_i) + \sum_{\substack{i,j=1 \\ i>j}}^n (x_i - x_j) \cdot v_h \quad (9b)$$

$$Y_{biogas/CH_4} = \frac{V_{biogas/CH_4}}{m_s(0)}, \quad (9c)$$

Where: V is the cumulative production of biogas or methane, v_b is the volume of gas sampled from gas bags, v_h is the volume of the headspace (213.27 NL), n is the number of sampling points, x is the composition of methane in the biogas, Y is the volumetric yield of gas in terms of mass of substrate added, $m_s(0)$.

3.3.5 Empirical kinetic models

The cumulative production of methane for the different species of grassland biomass was modelled using four empirical kinetic models³⁷. The mathematical models for FOK (Equation 10a), MG (Equation 10b), CMG (Equation 10c), and CONE (Equation 10d) were selected based on the number of citations and relevance to the studies cited in the present work. The parameter λ (lag phase) was considered in the first-order kinetics to evaluate its relevance to the estimation.

$$Y(t) = \begin{cases} B_o[1 - e^{-k \cdot (t-\lambda)}], & t > \lambda \\ 0, & t \leq \lambda \end{cases} \quad (10a)$$

$$Y(t) = B_o \cdot e^{-e^{-\frac{\mu_{max}}{B_o} \cdot (t-\lambda)+1}} \quad (10b)$$

$$Y(t) = B_o \cdot (e^{-e^{-\frac{\mu_{max}}{B_o} \cdot (t-\lambda)+1}} - e^{-e^{-\frac{\mu_{max}}{B_o} \cdot \lambda+1}}) \quad (10c)$$

$$Y(t) = \begin{cases} \frac{B_o}{1+[k \cdot (t-\lambda)]^{-n}}, & t > \lambda \\ 0, & t \leq \lambda, \end{cases} \quad (10d)$$

Where: $Y(t)$ is the cumulative methane yield (NL.kgVS⁻¹) at a time t (days), B_o is the maximum methane yield, k is the hydrolysis constant rate (days⁻¹), λ is the lag phase time (days), μ_{max} is the maximum methane production rate (NL.kgVS⁻¹.day⁻¹), n is the shape factor for the CONE model, and e is the Euler's number. In this work, B_o was expressed both as substrate-specific maximum methane yield ($B_{o_{sub}}$, in NL.kgVS⁻¹) and as area-specific maximum methane yield ($B_{o_{area}}$, in Nm³.ha⁻¹.yr⁻¹). The $B_{o_{area}}$ was obtained based on an estimation of the forage yield (Section 3.3.6).

The non-linear model parameters were estimated by minimising the residual sum of squares (RSS) using the sequential quadratic programming (SQP) estimation algorithm in IBM® SPSS® Statistics version 28.0.0.0 (190). For this estimation, the bounds for the parameters were set as $B_o > 0$, $\lambda \geq 0$, $k \geq 0$, $\mu_{max} > 0$, and $n > 0$. To determine the model with the best fit, statistical indicators such as the confidence interval of B_o , the root mean squared error (RMSE) (Equation 11a), the akaike information criterion (AIC) (Equations 11c-11g)⁶⁰, and bayesian information criterion (BIC) (Equation 11i)⁶¹ were analysed.

$$RMSE = \sqrt{\frac{RSS}{N - M - 1}} = \sqrt{\frac{\sum_i^N (Y_i - Y_{pred})^2}{N - M - 1}} \quad (11a)$$

$$(11b)$$

$$AIC = \begin{cases} N \cdot \ln\left(\frac{RSS}{N}\right) + 2M + \frac{2M(M+1)}{N-M-1}, & \frac{N}{M} < 40 \\ N \cdot \ln\left(\frac{RSS}{N}\right) + 2M, & \frac{N}{M} \geq 40 \end{cases} \quad (11c)$$

$$(11d)$$

$$\Delta_i(AIC) = AIC_i - \min AIC \quad (11e)$$

$$(11f)$$

$$w_i(AIC) = \frac{\exp\{-\frac{1}{2}\Delta_i(AIC)\}}{\sum_{k=1}^K \exp\{-\frac{1}{2}\Delta_k(AIC)\}} \quad (11g)$$

$$(11h)$$

$$BIC = N \cdot \ln\left(\frac{RSS}{N}\right) + M \cdot \ln(N), \quad (11i)$$

Where: N is the number of data points, M is the number of parameters in the model, y_i is the experimental methane yield, y_{pred} is the methane yield predicted by the model, w_i is the Akaike weight and K is the number of models evaluated.

3.3.6 DI model

The generalised diversity-interaction framework⁴⁶ was used to investigate possible effects from species identity, richness, and interspecific interactions to the production of methane from different grasslands. A multiple regression analysis was performed in Rstudio (2022.12.0, R version 4.2.1) using the DImodels package⁶². Substrate-specific maximum methane yield (Bo_{sub}) and area-specific maximum methane yield (Bo_{area}) were used as response variables. The best diversity-interaction model for maximum methane yield was selected from four DI models using the automatic model selection function (*autoDI*), and the F-test as a selection criteria⁶³.

The four DI models tested were the species identity (ID) model, the evenness or average interactions (AV) model, the functional group effects (FG) model, and the separate pairwise interactions (FULL) model. The equations for these models are described in detail by Moral *et al.*⁴⁶ and Kirwan *et al.*⁶³. In brief, the response variable is modelled by a linear equation that considers both species identity effects and diversity effects (Equation 12). The ID model assumes that the interaction between species does not affect the production of methane, only the identity of each species. The AV model assumes that the interactions can be considered equal for all species, while the FG model assumes that the interaction between different functional groups may have a stronger impact in the production. The FULL model assumes that the synergistic or antagonistic effects from the unique interaction between species impact the production of methane⁴⁶.

$$y = \sum_i^6 \beta_i p_i + \beta_{Lp^*} p_{Lp^*} + \sum_{\substack{i,j=1 \\ i < j}}^6 \delta_{i,j} (p_i p_j) + \epsilon, \quad (12)$$

Where: y is the response variable (Bo), p_i and p_j are the proportion of species in the mixture (Table 3.2) – *L. perenne* (1), *P. pratense* (2), *T. pratense* (3), *T. repens* (4), *C. intybus* (5), and *P. lanceolata* (6). The sum of proportions is always 1. The coefficient β_i represents the identity effects of each species (i) while β_{Lp^*} and p_{Lp^*} represents, respectively, the identity effects and proportion of *L. perenne* supplied with a double dose of nitrogen fertiliser (in this case, $p_{Lp^*} = 1$). The coefficient $\delta_{i,j}$ represents the interspecific interaction effects of a pair of species (i and j). The error ϵ was considered normally distributed with a mean of zero and a variance of σ^2 .

Diversity-interaction modelling was also used to estimate the annual forage yield for each substrate tested in this study. The annual forage yield was estimated using the FG model and used to calculate the area-specific maximum methane yield (Bo_{sub} , in $Nm^3 \cdot ha^{-1} \cdot yr^{-1}$) of each substrate. The DI model coefficients for identity and interaction effects were based on Grange *et al.*⁹, considering similar grassland managing conditions (e.g., rainfed, nitrogen fertilisation rate).

3.4 Results

3.4.1 A similar VS degradation was observed in the digestion of all monocultures and mixtures, regardless of chemical composition

Overall, different levels of carbon, nitrogen and fibre content were observed when mixing functional groups (grasses, legumes and herbs), and species. The highest C:N ratio and lowest crude protein content was observed with *L. perenne* (supplied with a lower dose of nitrogen fertiliser, Lp). Moreover, monocultures of grass presented a higher difference in C:N ratio when comparing species within the same functional group (FG). While forbs had a maximum C:N ratio difference of 4% TS, the difference in C:N ratio between grasses was 14.9% TS. Supplying more nitrogen to *L. perenne* (Lp*) or mixing *L. perenne* with *P. pratense* (Lp:Pp) led to a 27-28% decrease in C:N ratio and a 36-38% increase in crude protein. Mixing six grassland species or adding legumes to two-species mixtures resulted in substrates with lower C:N ratios and higher crude protein levels, when compared to monocultures of herbs and grasses. *T. repens* presented the highest crude protein level (29.3% TS on average), and levels above 26% TS were observed when mixing clovers (*T. repens* with *T. pratense*), and mixing clover and grass (*T. repens* with *P. pratense*). Fibre content values varied between 47.6-59.9% VS (NDF) and 18.7-32.6% VS (ADF). The highest values of NDF content was observed for *P. pratense* monoculture (59.0% VS), and two-species mixtures with *P. pratense* (e.g., with *P. lanceolata*: 59.9% VS). On average, *L. perenne* presented low values of ADF as a monoculture (Lp: 18.9% VS, Lp*: 20.0% VS) and when mixed with *P. pratense* (19.5% VS).

Despite those differences in chemical composition, an average biomass degradation of 80% in terms of volatile solids degradation was observed for most substrates (Figure 3.1). The lowest degradation was observed when digesting one of the field replicates of *T. repens* (Tp₁, 66.0±7.5% VS). The digestion of *L. perenne* resulted in similar VS degradation levels despite the difference in nitrogen fertilisation rate. On average, the VS degradation levels of monocultures supplied with 150 kgN.ha⁻¹.yr⁻¹ was 78.3 ± 6.6%, while the digestion of 300 kgN.ha⁻¹.yr⁻¹ *L. perenne* reached 82.2 ± 1.7%. Considering the mixtures, a digestion of two species of grassland biomass resulted in an average VS degradation of 78.6 ± 4.7%, while the digestion of six-species mixtures resulted in a VS degradation of 80.3 ± 3.1%.

3.4.2 First order kinetics selected to model the methane production from grassland species

The kinetic model with the best fit for methane production was selected based on the experimental data acquired in the digestion of two substrates – *L. perenne* (Lp₁, field plot 40), and the mixture of *L. perenne* and *T. pratense* (Lp:Tp). The selected model will be later used to compare the different grassland species studied in this work. The four kinetic models presented a similar fit to the experimental data, but CONE and FOK presented a better prediction for the end of the exponential phase (Figure 3.2). Although there is no clear difference between models and the values of RMSE are similar (Table 3.4), the confidence interval values for the maximum methane yield estimated with the CONE model

Table 3.3: Field yield and chemical characteristics for substrates used in this experiment. Substrates were labelled according to Table 3.2.

Substrate	Forage yield (tDW.ha ⁻¹ .yr ⁻¹)	C:N (% TS)	Cr. PTN (% TS)	Ash (% TS)	VS/TS (%)	NDF (% VS)	ADF (% VS)	Hemicellulose (% VS)	ThCOD (kgCOD.kgVS ⁻¹)
Lp ₁	9.2	40.3	7.1	8.0	92.0	48.4	19.4	29.0	1.46
Lp ₂	9.2	37.2	7.7	5.1	94.9	47.7	18.3	29.4	1.38
Pp ₁	10.7	23.8	12.3	7.4	92.6	60.0	28.5	31.5	1.45
Pp ₂	10.7	23.9	12.3	8.0	92.0	58.0	25.5	32.5	1.43
Tp ₁	10.0	11.7	25.3	8.4	91.6	52.7	28.4	24.3	1.44
Tp ₂	10.0	14.6	19.6	12.4	87.6	57.0	31.2	25.8	1.46
Tr ₁	10.0	9.8	31.0	8.6	91.4	51.9	25.6	26.3	1.47
Tr ₂	10.0	10.5	27.6	11.3	88.7	53.7	25.5	28.2	1.50
Ci ₁	8.5	19.5	14.9	14.0	86.0	55.7	23.6	32.1	1.56
Ci ₂	8.5	20.6	14.0	14.1	85.9	58.1	32.0	26.0	1.56
Pl ₁	10.6	24.3	11.7	11.8	88.2	54.4	28.9	25.5	1.53
Pl ₂	10.6	24.3	11.9	10.3	89.7	55.1	25.3	29.8	1.51
Lp* ₁	10.5	31.9	8.8	8.5	91.5	48.8	19.3	29.5	1.41
Lp* ₂	10.5	25.5	11.1	8.6	91.4	51.9	20.0	31.9	1.43
Lp* ₃	10.5	27.9	10.3	7.4	92.6	53.2	20.8	32.4	1.45
Lp:Pp	10.3	27.7	10.3	6.4	93.6	50.1	19.5	30.6	1.38
Lp:Tp	11.2	15.0	18.6	12.8	87.2	57.1	28.5	28.6	1.44
Lp:Tr	11.2	14.4	20.4	10.9	89.1	55.4	25.6	29.8	1.51
Lp:Pi	9.8	29.9	9.6	6.9	93.1	47.6	18.7	28.9	1.36
Lp:Pl	10.8	29.5	9.9	7.9	92.1	50.1	21.5	28.5	1.40
Pp:Tp	12.0	13.8	21.2	9.9	90.1	57.8	32.6	25.2	1.45
Pp:Tr	12.0	11.0	26.8	10.1	89.9	58.1	29.1	29.0	1.52
Pp:Pi	10.5	23.5	11.9	11.0	89.0	51.1	21.7	29.5	1.42
Pp:Pl	11.6	22.8	12.7	8.9	91.1	59.9	27.2	32.6	1.45
Tr:Tp	10.7	10.9	26.7	9.9	90.1	53.0	26.4	26.6	1.43
Tr:Pi	11.1	13.0	22.1	11.1	88.9	55.8	27.7	28.1	1.45
Tr:Pl	12.1	16.0	18.1	8.6	91.4	52.8	26.1	26.7	1.43
Tr:Tr	11.1	12.8	22.0	9.7	90.3	56.6	28.6	28.0	1.40
Tr:Pl	12.1	13.6	21.0	8.9	91.1	52.2	25.8	26.5	1.41
Ci:Pl	9.3	22.7	12.3	11.4	88.6	51.1	23.2	27.8	1.41
6-species ₁	11.9	19.1	14.8	10.0	90.0	55.7	25.9	29.8	1.40
6-species ₂	11.9	16.6	17.3	12.1	87.9	58.0	31.2	26.8	1.46
6-species ₃	11.9	15.6	18.3	9.7	90.3	54.9	28.7	26.2	1.32

Note: *higher dose of nitrogen fertiliser. Standard deviations are summarised in Table A.2.

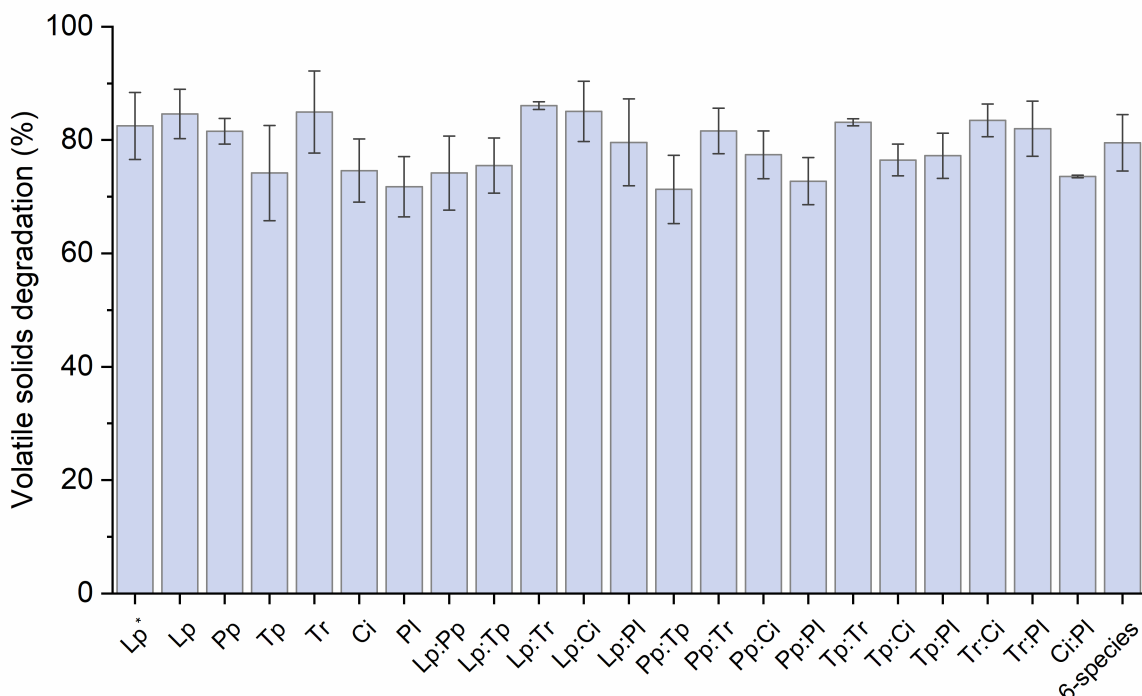


Figure 3.1: Average volatile solids degradation reached in the digestion of monocultures and mixtures of grassland species. Substrates were labelled according to Table 3.2. The degradation of each plot of grassland species is represented in Figure A.1.

and the CMG model were considerably higher when compared to the FOK model and the MG model.

The AIC (Equation 11c) and BIC (Equation 11i) values were used as an information criteria to select the best model, as they add a penalty based on the number of parameters (M) and are often used to avoid model over-fitting³⁷. As a rule of thumb, differences in BIC values above 2 show evidence to support the model with the smaller BIC⁶⁴, and the Akaike weight (Equations 11e-11g) shows the probability of a model being the best fit⁶⁰. The FOK model presented the lowest BIC value and the highest Akaike weight, with strong evidence of difference when compared to the MG model. Therefore, the FOK model was selected as the kinetic model with the best fit to the experimental data.

Table 3.4: Information criteria to select the model with the best fit to the experimental data.

Model	M	RMSE	Maximum methane yield (NL.kgVS ⁻¹)	AIC test		BIC test	
				AIC	Akaike weight	BIC	Difference
FOK	3	12.834	276.15 ± 10.70	156.89	0.80	160.17	0.000
MG	3	14.483	269.38 ± 8.36	164.14	0.02	167.42	7.25
CGM	3	13.914	287.94 ± 30.72	161.74	0.07	165.02	4.85
Cone	4	13.101	288.96 ± 36.54	160.80	0.11	164.81	4.64

Note: Data based on the digestion of *L. perenne* + *T. pratense* (N=30).

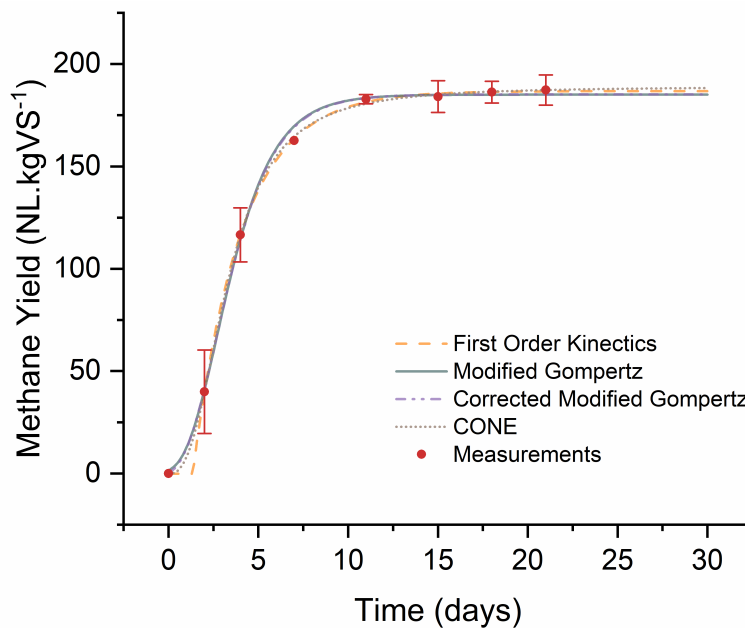


Figure 3.2: Model prediction based on the digestion of *L. perenne* (plot 40). An average of the experimental observations (red dots) are presented with its standard deviation.

3.4.3 Grassland species varied in methane potential with similar lag phase times and hydrolysis constant rates

The first order kinetics model was used to estimate the kinetic parameters for all the substrates – hydrolysis constant rate (k), lag phase time (λ), the substrate-specific (Bo_{sub}) and area-specific (Bo_{area})

maximum methane yield per field area (Tables 3.5 and A.3). The Bo_{area} was calculated considering the estimated values of forage yield using the model developed by Grange et al.⁹ (Table 3.3). The highest gap between TBMP values and Bo_{sub} values (biodegradability index) were observed for both mixtures of *P. lanceolata* with clover species (Tp:Pl and Tr:Pl). The highest biodegradability index was observed for *P. pratense* monocultures and the mixture of *T. repens* with *C. intybus*.

Table 3.5: Theoretical BMP (TBMP), biodegradability index (B_d), area-specific maximum methane yield (Bo_{area}), substrate-specific maximum methane yield (Bo_{sub}), hydrolysis constant rate (k) and lag phase time (λ) observed in the digestion of permanent grasslands.

Substrate	TBMP (NL.kgVS ⁻¹)	B_d (%)	Bo_{area} (Nm ³ .ha ⁻¹ .yr ⁻¹)	Bo_{sub} (NL.kgVS ⁻¹)	k (days ⁻¹)	λ (days)
Lp ₁	510.7	36.6	1617.9	186.8 ± 7.6	0.4 ± 0.1	1.3 ± 0.4
Lp ₂	481.1	46.5	1927.1	223.5 ± 33.6	0.2 ± 0.2	0.8 ± 1.7
Pp ₁	508.4	60.3	3073.4	306.6 ± 9.7	0.2 ± 0.1	0.0 ± 0.6
Pp ₂	499.4	61.8	3076.2	308.5 ± 33.0	0.2 ± 0.1	0.0 ± 1.7
Tp ₁	504.2	40.3	1723.6	203.4 ± 20.0	0.3 ± 0.2	0.6 ± 1.4
Tp ₂	508.1	51.2	2158.6	260.0 ± 51.8	0.2 ± 0.3	0.7 ± 2.4
Tr ₁	513.3	58.6	2501.5	300.9 ± 29.0	0.3 ± 0.1	1.3 ± 0.8
Tr ₂	521.3	42.9	1840.8	223.6 ± 17.3	0.4 ± 0.2	1.4 ± 0.6
Ci ₁	543.2	42.1	1633.1	228.9 ± 21.7	0.5 ± 0.4	1.2 ± 1.0
Ci ₂	546.0	39.8	1478.5	217.1 ± 49.2	0.3 ± 0.6	0.7 ± 3.4
Pl ₁	533.1	49.7	2391.8	265.1 ± 11.6	0.3 ± 0.1	0.6 ± 0.6
Pl ₂	528.7	40.3	2048.2	212.8 ± 28.7	0.6 ± 1.0	0.8 ± 2.3
Lp* ₁	493.7	58.0	2789.8	286.4 ± 18.6	0.3 ± 0.1	0.0 ± 1.2
Lp* ₂	498.8	52.3	2496.7	261.0 ± 6.3	0.3 ± 0.1	0.0 ± 0.6
Lp* ₃	503.6	47.1	2310.4	237.2 ± 16.5	0.3 ± 0.1	0.0 ± 0.9
Lp:Pp	483.0	28.3	1265.8	136.6 ± 9.0	0.4 ± 0.2	0.3 ± 1.3
Lp:Tp	502.1	55.0	2625.8	276.2 ± 10.7	0.3 ± 0.1	0.7 ± 0.5
Lp:Tr	528.4	44.2	2370.1	233.3 ± 45.7	0.3 ± 0.3	0.4 ± 2.0
Lp:Ci	473.3	40.4	1677.0	191.1 ± 10.6	0.5 ± 0.3	0.0 ± 0.9
Lp:Pl	490.0	40.5	1912.2	198.4 ± 14.0	0.5 ± 0.3	0.0 ± 1.1
Pp:Tp	505.5	44.3	2375.3	224.1 ± 7.8	0.3 ± 0.1	0.0 ± 0.5
Pp:Tr	530.2	45.6	2572.2	241.6 ± 7.2	0.3 ± 0.1	0.3 ± 0.4
Pp:Ci	497.2	46.0	2096.4	228.9 ± 30.4	0.2 ± 0.2	0.0 ± 1.6
Pp:Pl	505.4	47.6	2572.6	240.6 ± 18.4	0.2 ± 0.1	0.4 ± 0.9
Tp:Tr	498.9	52.8	2392.1	263.6 ± 19.1	0.4 ± 0.3	0.9 ± 0.9
Tp:Ci	505.7	52.5	2450.9	265.5 ± 13.3	0.5 ± 0.4	1.0 ± 0.9
Tp:Pl	498.8	32.1	1641.4	159.9 ± 18.2	0.3 ± 0.2	1.2 ± 0.9
Tr:Ci	489.3	70.4	3070.0	344.5 ± 20.4	0.5 ± 0.4	1.0 ± 0.9
Tr:Pl	492.0	38.2	1864.8	188.0 ± 15.0	0.8 ± 1.4	0.8 ± 2.2
Ci:Pl	491.4	47.8	1806.5	234.7 ± 15.7	0.4 ± 0.2	0.3 ± 1.3
6-species ₁	488.4	49.7	2427.2	242.5 ± 18.9	0.3 ± 0.2	0.7 ± 1.0
6-species ₂	505.8	45.2	2402.8	228.6 ± 84.8	0.2 ± 0.4	0.0 ± 4.8
6-species ₃	455.5	52.8	2470.8	240.6 ± 16.8	0.3 ± 0.2	0.7 ± 1.0

Note: The '±' symbol represents the parameter's confidence interval (95% confidence level); *higher dose of nitrogen fertiliser. Substrates were labelled according to Table 3.2.

The hydrolysis constant rate (k) was similar for all substrates digested, with k values varying around 0.4 days⁻¹ and the 95% confidence interval overlapping. Moreover, most substrates had an estimated lag phase time (λ) of zero as a mean value or considering the parameter's confidence interval. The exceptions were monocultures of *L. perenne* (Lp₁), *T. repens* (Tr₁ and Tr₂), and *C. intybus* (Ci₁), as well as three mixtures with *T. pratense* (Lp:Tp, Tp:Ci, and Tp:Pl), and the mixture of *T. repens* with *C. intybus* (Tr:Ci) – which were not significantly different from each other. It it

important to emphasise that the production of methane started within a day for some of the substrates, not necessarily filling the gas bags, which were collected when full. Therefore, more sampling points would be required within the first day to properly estimated values for the lag phase.

In terms of methane, a similar substrate-specific maximum methane yield (Bo_{sub}) was reached when digesting most monocultures and mixtures of two grassland species. The lowest value of Bo_{sub} was observed in the co-digestion of grasses (Lp:Pp, 136.6 ± 9.0 NL.kgVS⁻¹), and the co-digestion of *T. pratense* with *P. lanceolata* (Tp:Pl, 159.9 ± 18.2 NL.kgVS⁻¹). Substrate-specific maximum methane yields above 300 NL.kgVS⁻¹ were observed for both monocultures of *P. pratense* (Pp₁ and Pp₂), a plot of *T. pratense* (Tp₁), and the mixture of *T. repens* with *C. intybus* (Tr:Ci). A parallel trend was observed for the area-specific maximum methane yield (Bo_{area}), with the lowest value obtained from the co-digestion of *L. perenne* with *P. pratense* (Lp:Pp), and the highest values observed for *P. pratense* monocultures (Pp₁ and Pp₂), and the mixture of *T. repens* with *C. intybus* (Tr:Ci).

When analysing the effect of nitrogen fertilisation rate on methane yield, higher values of Bo_{area} and Bo_{sub} were observed for the *L. perenne* supplied with a higher dose of nitrogen fertiliser (Lp*). Moreover, the area-specific maximum methane yield from the digestion of *L. perenne* supplied with a higher dose of nitrogen fertiliser were equivalent to the area-specific maximum methane yield obtained from the digestion of the six species mixture. Mixing different species of herbs with clovers resulted in different maximum methane yields – clover mixtures with *C. intybus* (Tp:Ci and Tr:Ci) presented a higher methane yield when compared to clover mixtures with *P. lanceolata* (Tp:Pl and Tr:Pl). The same was not observed when mixing different species of herbs and grasses.

3.4.4 Antagonistic and synergistic effects identified with the Diversity-interaction models

The best diversity-interaction model was identified using the *autoDI* function, following the steps discussed in detail by Moral *et al.*⁶³ considering both substrate-specific and area-specific maximum methane yield data (Table A.5). The ‘FULL’ model (Equation 12) was selected for modelling the species identity effects and interspecific interaction effects on both the substrate-specific Bo , Bo_{sub} (comparing the FG model with the FULL model yielded $F_{9,11} = 3.399$, $p = 0.030$), and area-specific Bo , Bo_{area} (comparing the FG model with the FULL model yielded $F_{9,11} = 4.017$, $p = 0.017$).

Considering a confidence level of 95%, the identity effects (β) of all species were significant ($p < 0.001$) to the production of methane per substrate, Bo_{sub} , and per field area, Bo_{area} (Table 3.6). Some interspecific interaction effects (δ) were not significant for the maximum methane yield, meaning the maximum methane yield from that substrate was mainly affected by species identity effects (Table 3.6). From the results it can be observed that the mixture of grasses had a significant antagonistic effect on the production of methane (Bo_{sub} : -113.9 NL.kgVS⁻¹, $p < 0.01$; Bo_{area} : -1093.1 Nm³.ha⁻¹.yr⁻¹, $p < 0.05$, Figure 3.3). On the other hand, the mixture of *L. perenne* with *T. pratense* had a significant synergistic effect in the production of methane, especially for the area-specific (Bo_{area} : 833.8 Nm³.ha⁻¹.yr⁻¹, $p < 0.05$). The highest maximum methane yield contribution was observed with the synergistic mixture of *T. repens* with *C. intybus* (Bo_{sub} : 107.8 NL.kgVS⁻¹,

$p < 0.01$; Bo_{area} : $1271.3 \text{ Nm}^3 \cdot \text{ha}^{-1} \cdot \text{yr}^{-1}$, $p < 0.001$). Although the mixture of six species presented antagonistic effects to the maximum methane yield per substrate ($-17.4 \text{ NL} \cdot \text{kgVS}^{-1}$), when considering the forage yield, synergistic effects were observed ($202.9 \text{ Nm}^3 \cdot \text{ha}^{-1} \cdot \text{yr}^{-1}$).

Table 3.6: Estimated values for species identity effects and interspecific interaction effects using the pairwise interaction (FULL) DI model.

Substrate	Coefficients ($\text{NL} \cdot \text{kgVS}^{-1}$)	SE	Pr(> t)	Coefficients ($\text{Nm}^3 \cdot \text{ha}^{-1} \cdot \text{yr}^{-1}$)	SE	Pr(> t)
<i>Species identity (β)</i>						
Lp ^{*,a}	261.53	16.26	5.5E-09	2532.31	138.70	1.42E-09
Lp ^a	203.19	19.80	5.7E-07	1750.89	168.92	5.16E-07
Pp ^a	305.60	19.80	8.4E-09	3053.23	168.92	1.58E-09
Tp ^a	229.74	19.80	1.6E-07	1919.50	168.92	2.03E-07
Tr ^a	260.27	19.80	4.5E-08	2149.59	168.92	6.35E-08
Ci ^a	221.00	19.80	2.4E-07	1534.21	168.92	1.92E-06
Pl ^a	236.99	19.80	1.2E-07	2198.39	168.92	5.03E-08
<i>Pairwise interspecific interaction (δ)</i>						
Lp:Pp ^b	-455.65	123.39	0.004	-4372.21	1052.65	0.002
Lp:Tp ^{d,b}	254.42	123.39	0.064	3335.09	1052.65	0.009
Lp:Tr	22.00	123.39	0.862	1852.08	1052.65	0.106
Lp:Ci	-68.33	123.39	0.591	310.48	1052.65	0.773
Lp:Pl	-71.12	123.39	0.576	-76.76	1052.65	0.943
Pp:Tp	-158.47	123.39	0.225	-271.32	1052.65	0.801
Pp:Tr	-149.49	123.39	0.251	56.17	1052.65	0.958
Pp:Ci	-121.86	123.39	0.345	-616.47	1052.65	0.570
Pp:Pl	-106.97	123.39	0.404	-39.95	1052.65	0.970
Tp:Tr	89.94	123.39	0.481	1603.11	1052.65	0.156
Tp:Ci ^{-c}	176.17	123.39	0.181	3069.17	1052.65	0.014
Tp:Pl ^{c,-}	-278.30	123.39	0.045	-1497.15	1052.65	0.182
Tr:Ci ^{b,a}	431.11	123.39	0.005	5085.17	1052.65	0.000
Tr:Pl ^{d,-}	-226.80	123.39	0.093	-1063.95	1052.65	0.334
Ci:Pl	38.59	123.39	0.760	-66.39	1052.65	0.951

Note: a: $p \leq 0.001$, b: $p \leq 0.01$, c: $p \leq 0.05$, and d: $p \leq 0.1$. In the same row, one letter indicates that both area-specific and substrate-specific Bo values were significant at that level. The mark '-' in a row indicates that only one of the Bo values were is significant. SE stands for 'standard error'. Substrates were labelled according to Table 3.2.

As some of the interspecific interaction effects were not significant, a comparison between two FULL DI models were performed – a FULL model considering all the interspecific interaction coefficients (FULL₁) and a FULL model considering only the significant coefficients (FULL₀). No significant difference was observed (Table A.6) in the prediction of both models considering the substrate-specific Bo ($F_{10,10} = 0.925$, $p = 0.548$) and the area-specific Bo ($F_{11,10} = 0.891$, $p = 0.576$). Therefore, to represent the diversity of these grassland systems, the model FULL₁ was selected to predict the maximum methane yield at substrate level and field-area level considering diversity-interaction effects (Figure 3.4, Table A.7).

A higher maximum methane yield was observed when *L. perenne* was supplied with a double dose of nitrogen fertiliser, especially in terms of area-specific Bo (Lp: 1750.9 ± 168.9 compared to Lp*: $2532.3 \pm 138.7 \text{ Nm}^3 \cdot \text{ha}^{-1} \cdot \text{yr}^{-1}$). Considering monocultures, values of substrate-specific and area-specific maximum methane yield for *P. pratense* were the highest observed (Bo_{sub} : 305.6 ± 19.8

NL.kgVS⁻¹, Bo_{area}: 3053.2±168.9 Nm³.ha⁻¹.yr⁻¹).

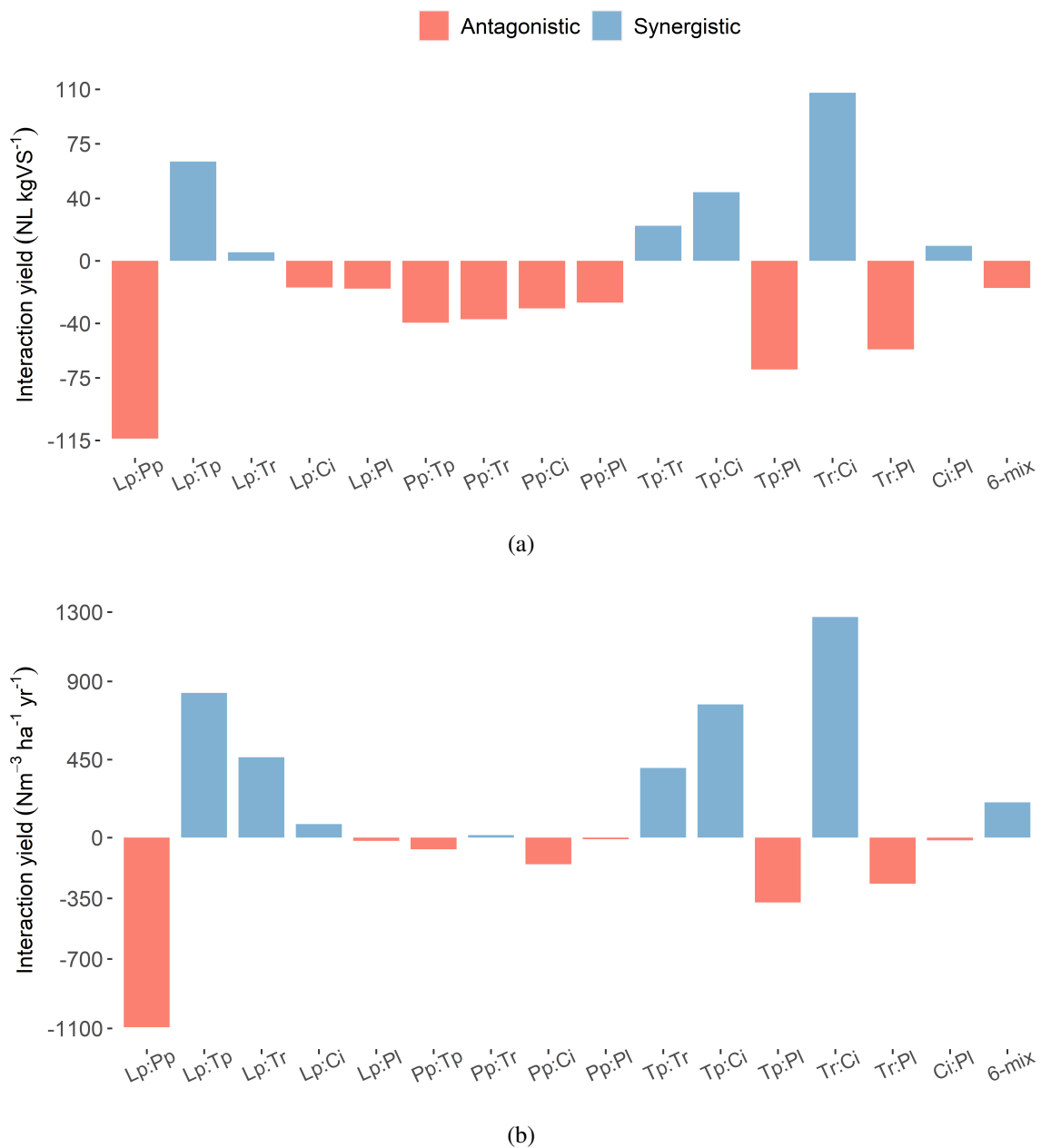
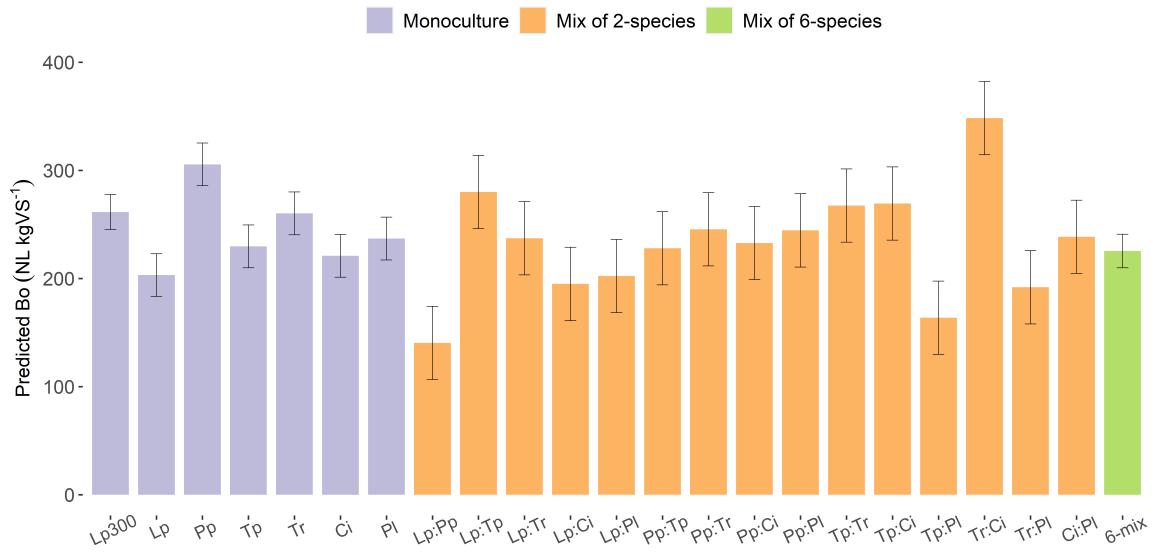


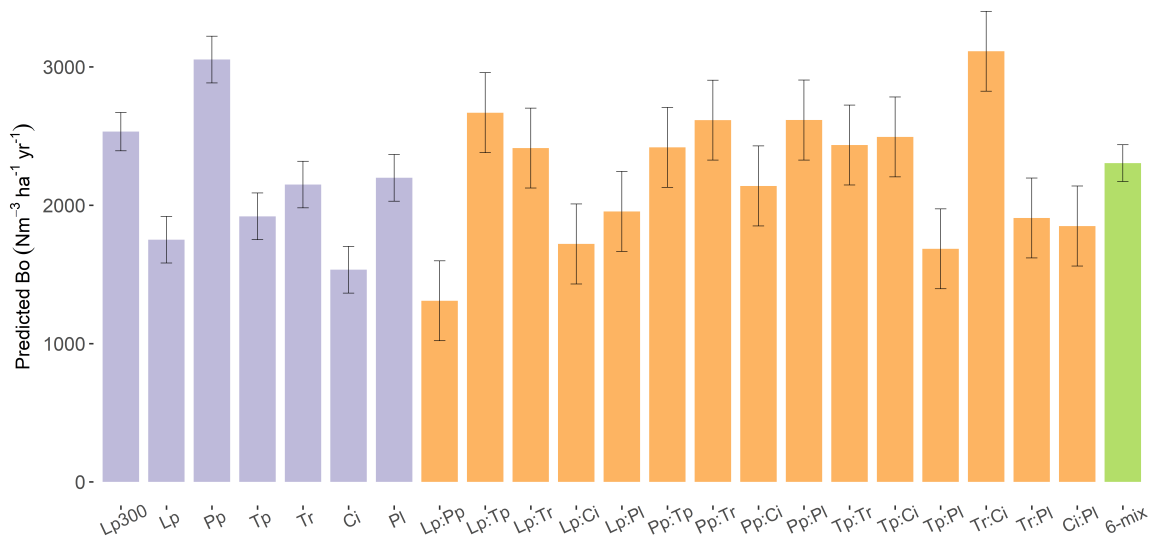
Figure 3.3: Interspecific contribution to the substrate-specific (a) and area-specific (b) maximum methane yield. Error bars presented as standard error, and substrates were labelled according to Table 3.2.

Mixing *L. perenne* with clovers improved both maximum methane yields when compared to mixing *L. perenne* with *P. pratense*. The effect of mixing herbs and legumes were different depending on the choice of herb – mixtures with *C. intybus* resulted in higher maximum methane yields when compared to *P. lanceolata*. In fact, the highest substrate-specific and area-specific Bo was observed when mixing *T. repens* with *C. intybus* (Bo_{sub}: 348.4±33.9 NL.kgVS⁻¹, Bo_{area}: 3113.2±289.0 Nm³.ha⁻¹.yr⁻¹) – this was comparable to other substrates such as *P. pratense*, and mixing *L. perenne* with *T. pratense*. Considering the production of methane per forage area, synergistic effects in the

combination of six species of grassland biomass led to a similar maximum methane yield ($2304.4 \pm 132.6 \text{ Nm}^3 \cdot \text{ha}^{-1} \cdot \text{yr}^{-1}$) when compared to *L. perenne* supplied with a higher dose of nitrogen fertiliser ($2532.3 \pm 138.7 \text{ Nm}^3 \cdot \text{ha}^{-1} \cdot \text{yr}^{-1}$).



(a)



(b)

Figure 3.4: Substrate-specific (a) and area-specific (b) maximum methane yield based on the coefficients predicted for the FULL DI model 3.6. Error bars are presented as standard error, and substrates were labelled according to Table 3.2. Lp300 is equivalent to Lp*.

3.5 Discussion

3.5.1 Biodegradability and methane yield varied between and within species, indicating the biomass heterogeneity

Theoretical BMP values varied slightly between plots of the same species (e.g., *L. perenne*: 510.7 compared to 481.1 NL.kgVS⁻¹), indicating the variability in chemical composition between plots of the same species and, therefore, the heterogeneity of the grassland biomass. This has been observed previously, for example, with methane yields for ryegrass varying from 198 to 360 NL.kgTS⁻¹ considering different varieties of *L. perenne*¹⁷.

As expected, TBMP values were higher than substrate-specific maximum methane yield, Bo_{sub} (Table 3.5). Different from the Bo_{sub} , the TBMP calculation is based on the biomass composition in terms of carbon, hydrogen, oxygen, nitrogen and sulphur⁵², thus accounting for both biodegradable and non-biodegradable materials^{42,43}. As the lignocellulosic biomass is not only composed of fermentable sugars (water soluble carbohydrates) or components that can be hydrolysed to fermentable sugars (hemicellulose and cellulose), but also other materials that are not metabolised into methane, such as lignin and chlorophyll^{57,65,66}, Bo_{sub} yields are commonly lower than TBMP values. Moreover, as the TBMP accounts for the entirety of the biomass while the Bo_{sub} accounts for the biodegradable part of the biomass, the ratio between the two (B_d) represents the biodegradability of the substrate.

Most of the substrates presented a biodegradability index between 42.2 and 51.4%. Biodegradability levels in the co-digestion of clovers with herbs seemed to be affected by the species of herb that was added to the mix. Biodegradability levels were lower when mixing *P. lanceolata* with *T. repens* (Tr:Pl, 38.2%) and *T. pratense* (Tp:Pl, 32.1%), when compared to mixing *C. intybus* with clovers (Tr:Ci, 70.4%; Tp:Ci, 52.8%). In fact, this lower biodegradability can be a result of adding *P. lanceolata* to the mixture, as lignin levels in *P. lanceolata* are three times higher than *C. intybus* and twice higher than *T. repens*³³. These biodegradability levels show that, despite reaching an average VS degradation of 80% for all substrates, the digestion of grassland species may result in different methane yields due to differences in the chemical characteristics of each substrate, such as fibre content, C:N ratio and availability of biodegradable materials.

3.5.2 Improved methane yield in monocultures species resulted from balanced C:N ratio and fibre content

L. perenne is one of the most studied grassland species as a feedstock for AD¹⁷⁻³⁰, mostly at mesophilic temperatures^{17,28,31,67} but recently at thermophilic conditions³³. However, the effect of nitrogen fertilisation to the digestion of grassland biomass and methane yield has yet to be explored. The results from this work shows that doubling the supplementation of nitrogen fertiliser to *L. perenne* led to a 29% increase in the substrate-specific maximum methane yield (Figure 3.4, a). This increase was even higher when considering the forage yield – as the annual forage yield increased 14% with a higher nitrogen fertilisation, the average Bo_{area} increased 45% (Figure 3.4,b; Table A.7, Lp*:

2532.3±138.7 compared to Lp: 1750.9±168.9).

Differences in methane production observed in this study can be correlated to the chemical characteristics of the substrates, such as fibre content and C:N ratio (Table 3.3). For example, that gap in the methane production when considering *L. perenne* with different doses of nitrogen fertiliser can be explained by the difference in the C:N ratio when comparing these substrates – *L. perenne* supplied with 150 kgN.ha⁻¹.yr⁻¹ had a C:N ratio of approximately 38.8% while the C:N ratio for *L. perenne* supplied with 300 kgN.ha⁻¹.yr⁻¹ was 28.4% on average.

The C:N ratio can be a critical factor in AD, with optimum values proposed between 20 and 30%⁶⁸. As acidogenic bacteria consume nitrogen faster than methanogenic archaea, high values of C:N ratio lead to pH drop due to the rapid accumulation of acids^{68,69}. On the other hand, low values of C:N ratio decrease the acid production resulting in an increased pH due to a higher total ammonia nitrogen release^{68,69}. In the present study, the TAN levels (Table A.4) were below the inhibitory range of 1.7 to 14 g.L⁻¹⁷⁰, even for the substrate with the lowest C:N ratio, *T. repens* (Tr₁, Table 3.3); the digestion of *T. repens* (Tr₁) resulted in a substrate-specific maximum methane yield of 306.92±29.0 NL.kgVS⁻¹. This has been observed for *T. repens* previously, when the thermophilic monodigestion of a *T. repens* with a C:N ratio of 10.5% reached a methane yield of 340 NL.kgVS⁻¹ without ammonia inhibition³³.

Comparing monocultures, only the grass functional group presented a significant difference between species when comparing substrate-specific maximum methane yields. Considering the Bo_{sub} predicted using the DI model, similar yields were observed for species of clovers (Tp: 229.7±19.8, and Tr: 260.3±19.8 NL.kgVS⁻¹) and herbs (Ci: 221±19.8, and Tr: 237.0±19.8 NL.kgVS⁻¹). On the other hand, the methane yield obtained in the digestion of *P. pratense* (305.6±19.8 NL.kgVS⁻¹) was higher than the methane yield observed for *L. perenne* (203.2±19.8 NL.kgVS⁻¹), when both monocultures supplied with 150 kgN.ha⁻¹.yr⁻¹. The 50% increase in methane yield can be explained by the lower C:N ratio of *P. pratense* (Pp: 23.9%, Lp: 38.8% on average) as well as its higher fibre content when compared to *L. perenne* (Table 3.3).

Hemicellulose (NDF-ADF), cellulose (ADF-ADL) and lignin are important components of the lignocellulosic biomass cell wall – cellulose and hemicellulose are hydrolysed to C6 and C5 sugars⁷¹, which are converted to methane. Therefore, a higher content of fibres, such as NDF and ADF, can lead to a higher production of methane depending on lignin levels³⁴. NDF and ADF values of *P. pratense* are higher than the values presented for *L. perenne*, leading to a higher hemicellulose content (Pp: 32.0%VS, Lp: 29.2%VS). Despite the higher ADF values for *P. pratense* (Pp: 27.0%VS, Lp: 18.9%VS), the lack of measurements for ADL hinders the calculation of lignin for the substrates used in this work. However, assuming lignin values as reported in the literature for *L. perenne* (2%VS)³³ and for *P. pratense* (2.5-4.6%VS)⁷², sugar content in terms of cellulose would be higher for *P. pratense*. Therefore, the higher production of methane from *P. pratense* could be correlated to both the C:N ratio and the fibre content of the substrate.

3.5.3 Synergistic/antagonistic effects were dependent on species, not functional groups

Using the diversity interaction modelling framework to predict the production of methane from grassland species was crucial to understanding the synergistic and antagonistic effects of mixing two or more species of grassland biomass. Overall, the identity effects of each grassland species had a significant impact on the production of methane (Table 3.6), but mixing certain species led to antagonistic (e.g., *L. perenne* with *P. pratense*) and synergistic (e.g., *T. repens* with *C. intybus*) effects on the methane production (Figure 3.3, Table A.7).

Despite mixing *L. perenne* with the monoculture that yielded the highest methane production (*P. pratense*), antagonistic effects had a significant impact on the production of methane. The resulting yield from the interaction of grasses decreased the maximum methane yield in 113.9 NL.kgVS⁻¹ and 1093.1 Nm³.ha⁻¹.yr⁻¹, resulting in a final maximum methane yield of 140.5±33.9 NL.kgVS⁻¹ and 1309.0±289.0 Nm³.ha⁻¹.yr⁻¹. When comparing the chemical characteristics of these substrates (Table 3.3), the mixture of grasses had a similar NDF and ADF fibre content compared to the monoculture of *L. perenne*, but a more balanced C:N ratio. On the other hand, all mixtures with *P. pratense* presented antagonistic effects, although not significant to the production of methane.

Antagonistic effects can be a result not only of an unbalanced C:N ratio, but also deficiency in trace elements, ammonia toxicity or high concentration of VFA³². pH levels were maintained between 7.5 and 8.0 in the digestion of all substrates, indicating that an inhibition due to an accumulations of VFAs was unlikely. Unbalanced micro-nutrient levels could explain the antagonistic effect observed with *P. pratense* mixtures. Despite the same trace elements solution being supplied during the digestion of all substrates, each species mixture may have a specific deficiency in individual trace elements that would require extra supplementation. However, the micro-nutrients composition of each substrate was not characterised in this work. Despite the wide range of C:N ratios in the present study, no ammonia inhibition was observed, with TAN values varying between 0.16 g.L⁻¹ and 0.83 g.L⁻¹ (Table A.4) and, therefore, below the inhibitory range⁷⁰.

Synergistic effects occur when balancing micro-nutrients and macro-nutrients such as nitrogen, trace elements, surface sugars, and fibre content leading to an improvement in methane production³². These synergistic effects were observed especially when mixing *C. intybus* with both clovers, resulting in one of the highest maximum methane yields obtained from two-species in this work – *T. repens* with *C. intybus*: 348.4±33.9 NL.kgVS⁻¹ and 3113.2±289.0 Nm³.ha⁻¹.yr⁻¹ (Figures 3.3-3.4). On the other hand, mixing another species of herb, *P. lanceolata*, with clovers had the opposite effect, leading to a lower production of methane due to antagonistic effects (Figure 3.3, Tr:Pl – 191.9±33.9 NL.kgVS⁻¹, 1908.0±289.0 Nm³.ha⁻¹.yr⁻¹). *C. intybus* are a deep-root herbs, which make this forbs richer in micro-nutrients when compared to other species³³⁻³⁵. This, associated with a balanced C:N ratio due to the higher nitrogen of clovers can aid to explain the better performance in producing methane of clover mixtures with *C. intybus*. Also, as explained before in this work, the mixture of clovers with *P. lanceolata* presented a low biodegradability due to its higher lignin content, indicating recalcitrance this mixture.

3.5.4 A comparable area-specific methane yield was observed when digesting *L. perenne*, the six-species mixture, and *L. perenne* mixed with *T. pratense*

Synergistic effects in the production of methane were also observed when *L. perenne* was mixed with *T. pratense* (Figures 3.3-3.4). This synergistic contribution resulted in a 38% higher predicted Bo_{sub} when compared to *L. perenne* supplied with $150 \text{ kgN} \cdot \text{ha}^{-1} \cdot \text{yr}^{-1}$; in terms of predicted Bo_{area} , the increase reached 52%. Moreover, the predicted substrate- and area-specific maximum methane yield reached when digesting the mixture of *L. perenne* and *T. pratense* was comparable to the digestion of *L. perenne* supplied with a double dose of nitrogen fertiliser. The association of clovers with grass increased the nitrogen content in the substrate (Table 3.3), without the need for additional nitrogen fertiliser due to the legumes' ability to fixate atmospheric N_2 ⁷³. Therefore, the mixture resulted in a substrate with an improved nutrient availability when compared to both *L. perenne* monocultures (lower C:N ratio), and, therefore, a better nutrient balance to the micro-organisms and improved methane production.

The combination of six grassland species also resulted in a substrate with a more balanced fibre content and C:N ratio when compared to *L. perenne* supplied with $150 \text{ kgN} \cdot \text{ha}^{-1} \cdot \text{yr}^{-1}$. Despite the antagonistic effects (Figure 3.3), the predicted substrate-specific maximum methane yield of the six grassland species ($225.4 \pm 15.5 \text{ NL} \cdot \text{kgVS}^{-1}$) was similar to the yield observed with *L. perenne* supplied with a lower dose of nitrogen fertiliser ($203.2 \pm 19.8 \text{ NL} \cdot \text{kgVS}^{-1}$), higher than the mixture of grasses ($140.5 \pm 33.9 \text{ NL} \cdot \text{kgVS}^{-1}$), but lower than the yield obtained with a higher supplementation of nitrogen to *L. perenne* ($261.5 \pm 16.3 \text{ NL} \cdot \text{kgVS}^{-1}$).

On the other hand, when considering the area-specific maximum methane yield, synergistic effects from mixtures that had a higher forage yield play an important role in improving the methane yield obtained from the digestion of six grassland species. Considering the Bo_{area} , the maximum methane yield obtained with the six species ($2304.4 \pm 132.6 \text{ Nm}^3 \cdot \text{ha}^{-1} \cdot \text{yr}^{-1}$) is comparable to the maximum methane yield obtained from the digestion of *L. perenne* supplied with a higher dose of nitrogen fertiliser ($2532.3 \pm 138.7 \text{ Nm}^3 \cdot \text{ha}^{-1} \cdot \text{yr}^{-1}$). Therefore, these results show that the maximum methane yield that can be obtained per field area when digesting *L. perenne* supplied with a higher dose of nitrogen fertiliser is comparable to the digestion of *L. perenne* mixed with *T. pratense* and the digestion of the six-species mixture. Moreover, in light of the synergistic effects between clovers and *C. intybus*, improving the proportion of these species in the mixture of six species may be beneficial for the production of methane.

3.6 Conclusions

The present work aimed to study the six grassland species most common to the Irish soil and climate to improve the understanding of the AD of grassland species and to propose a more sustainable grassland-based AD. To the best of our knowledge, this was the first attempt in digesting a mixture of six grassland species with equi-proportional composition. Moreover, it is the first attempt in testing the effect of nitrogen fertilisation to the digestion of *L. perenne* and the first time a pairwise-interaction

DI model was used to predict the production of methane and the contribution of identity effects and interspecific interaction effects to the production of methane. The results of this work are a powerful indication that mixing six grassland species can yield a similar or higher maximum methane yield, when compared to *L. perenne* supplied with 150 or 300 kgN.ha⁻¹.yr⁻¹. Moreover, strong synergistic effects were observed when digesting mixtures of *T. repens* with *C. intybus* and *L. perenne* with *T. pratense*. Antagonistic effects were observed when co-digesting clovers with *P. lanceolata*, and *L. perenne* with *P. pratense*. In terms of monocultures, the highest maximum methane yield was observed with *P. pratense*, which was similar to the yields obtained in the synergistic mixtures. The synergistic effects observed when mixing *T. repens* and *C. intybus* as well as the antagonistic effects observed when mixing grass species, can be an indication that better results for methane yield can be obtained by mixing the six species in different proportions. It is the authors' belief that multi-species swards are the way forward to secure food production but also to improve the sustainability of grassland-based AD; this work adds one more argument towards this.

3.7 Acknowledgement and contributions

This work was financially supported by Science Foundation Ireland (SFI), grant number 16/RC/3889. The authors would like to acknowledge the BiOrbic (Bioeconomy SFI Research Centre) for the technical and financial support, and Arrabawn Dairies for the inoculum supply. Forages were supplied by Teagasc Johnstown (Dr. Guylain Grange). This work was possible due to the technical support of Sandra O'Connor and Andrew Bartle. The study was conceptualised in collaboration with Dr. Corine Nzeteu, Prof. Caroline Brophy, Dr. John Finn and Prof. Vincent O'Flaherty. Prof. Caroline Brophy and Dr. John Finn assisted in the statistical analysis. Dr. Anna Trego, Dr. Corine Nzeteu and Prof. Vincent O'Flaherty revised this manuscript.

3.8 References

1. Bråthen, K. A., Pugnaire, F. I. & Bardgett, R. D. The paradox of forbs in grasslands and the legacy of the mammoth steppe. *Frontiers in Ecology and the Environment* **19**, 584–592 (Dec. 2021).
2. Lee, M., Manning, P., Rist, J., Power, S. A. & Marsh, C. A global comparison of grassland biomass responses to CO₂ and nitrogen enrichment. *Philosophical Transactions of the Royal Society B: Biological Sciences* **365**, 2047–2056 (2010).
3. Rahman, M. M. *et al.* in *Advances in Legumes for Sustainable Intensification* (eds Meena, R. S. & Kumar, S.) 381–402 (Academic Press, 2022).
4. Huber, R., Le'Clec'h, S., Buchmann, N. & Finger, R. Economic value of three grassland ecosystem services when managed at the regional and farm scale. *Scientific Reports* **12**, 4194 (Mar. 2022).

5. Suter, M., Huguenin-Elie, O. & Lüscher, A. Multispecies for multifunctions: combining four complementary species enhances multifunctionality of sown grassland. *Scientific Reports* **11** (Dec. 2021).
6. Salaheen, S. & Biswas, D. in *Safety and Practice for Organic Food* (eds Biswas, D. & Micallef, S. A.) 23–32 (Academic Press, 2019).
7. Schaub, S. *et al.* Plant diversity effects on forage quality, yield and revenues of semi-natural grasslands. *Nature Communications* **11**, 768 (2020).
8. Finn, J. A. *et al.* Ecosystem function enhanced by combining four functional types of plant species in intensively managed grassland mixtures: a 3-year continental-scale field experiment. *Journal of Applied Ecology* **50** (ed Wilsey, B.) 365–375 (Apr. 2013).
9. Grange, G., Finn, J. A. & Brophy, C. Plant diversity enhanced yield and mitigated drought impacts in intensively managed grassland communities. *Journal of Applied Ecology*, 1365–2664 (June 2021).
10. Grange, G., Brophy, C. & Finn, J. A. Grassland legacy effects on yield of a follow-on crop in rotation strongly influenced by legume proportion and moderately by drought. *European Journal of Agronomy* **138**, 126531 (2022).
11. Cong, W.-F., Suter, M., Lüscher, A. & Eriksen, J. Species interactions between forbs and grass-clover contribute to yield gains and weed suppression in forage grassland mixtures. *Agriculture, Ecosystems & Environment* **268**, 154–161 (Dec. 2018).
12. Connolly, J. *et al.* Weed suppression greatly increased by plant diversity in intensively managed grasslands: A continental-scale experiment. *Journal of Applied Ecology* **55** (ed Inderjit) 852–862 (Mar. 2018).
13. De Neergaard, A., Hauggaard-Nielsen, H., Stoumann Jensen, L. & Magid, J. Decomposition of white clover (*Trifolium repens*) and ryegrass (*Lolium perenne*) components: C and N dynamics simulated with the DAISY soil organic matter submodel. *European Journal of Agronomy* **16**, 43–55 (Jan. 2002).
14. European commission. *A European Green Deal - Striving to be the first climate-neutral continent* Dec. 2019. <https://ec.europa.eu/newsroom/know4pol/items/664852>.
15. Ravindran, R. *et al.* Biogas, Biomethane and Digestate Potential of By-Products from Green Biorefinery Systems. *Clean Technologies* **4**, 35–50 (Jan. 2022).
16. Auer, A. *et al.* Agricultural anaerobic digestion power plants in Ireland and Germany: policy and practice. *Journal of the Science of Food and Agriculture* **97**, 719–723 (Feb. 2017).
17. Prochnow, A. *et al.* Bioenergy from permanent grassland - A review: 1. Biogas. *Bioresource Technology* **100**, 4931–4944 (2009).
18. Chiumenti, A., Boscaro, D., Da Borso, F., Sartori, L. & Pezzuolo, A. Biogas from fresh spring and summer grass: Effect of the harvesting period. *Energies* **11** (2018).

19. Korres, N. E., Singh, A., Nizami, A.-S. & Murphy, J. D. Is grass biomethane a sustainable transport biofuel? *Biofuels, Bioproducts and Biorefining* **4**, 310–325 (May 2010).
20. Murphy, J. D. *et al.* *The Potential for Grass Biomethane as a Biofuel: Compressed Biomethane Generated from Grass , Utilised as a Transport Biofuel* tech. rep. (Environmental Research Institute, 2011), 1–69.
21. Bedoić, R. *et al.* Green biomass to biogas – A study on anaerobic digestion of residue grass. *Journal of Cleaner Production* **213**, 700–709 (2019).
22. Wall, D. M., Allen, E., Straccialini, B., O’Kiely, P. & Murphy, J. D. Optimisation of digester performance with increasing organic loading rate for mono- and co-digestion of grass silage and dairy slurry. *Bioresource Technology* **173**, 422–428 (2014).
23. McEniry, J. *et al.* How much grassland biomass is available in Ireland in excess of livestock requirements ? *Irish Journal of Agricultural and Food Research* **52**, 67–80 (2013).
24. Nizami, A.-S., Korres, N. E. & Murphy, J. D. Review of the Integrated Process for the Production of Grass Biomethane. *Environmental Science & Technology* **43**, 8496–8508 (Nov. 2009).
25. Nimmanterdwong, P., Chalermisinsuwan, B., Østergård, H. & Piumsomboon, P. Environmental performance assessment of Napier grass for bioenergy production. *Journal of Cleaner Production* **165**, 645–655 (2017).
26. Mattioli, A. *et al.* Biogas from Residual Grass : A Territorial Approach for Sustainable Bioenergy Production. *Waste and Biomass Valorization* **8**, 2747–2756 (2017).
27. Wall, D. M., Allen, E., Shea, R. O., Kiely, P. O. & Murphy, J. D. Investigating two-phase digestion of grass silage for demand-driven biogas applications: Effect of particle size and rumen fluid addition. *Renewable Energy* **86**, 1215–1223 (2016).
28. Nizami, A.-S. & Murphy, J. D. Optimizing the Operation of a Two-Phase Anaerobic Digestion System Digesting Grass Silage. *Environmental Science & Technology* **45**, 7561–7569 (Sept. 2011).
29. Wall, D. M., O’Kiely, P. & Murphy, J. D. The potential for biomethane from grass and slurry to satisfy renewable energy targets. *Bioresource Technology* **149**, 425–431 (Dec. 2013).
30. McEniry, J., Allen, E., Murphy, J. D. & Kiely, P. O. Grass for biogas production: The impact of silage fermentation characteristics on methane yield in two contrasting biomethane potential test systems. *Renewable Energy* **63**, 524–530 (2014).
31. Himanshu, H., Murphy, J., Grant, J. & O’Kiely, P. Synergies from co-digesting grass or clover silages with cattle slurry in in vitro batch anaerobic digestion. *Renewable Energy* **127**, 474–480 (Nov. 2018).
32. Himanshu, H., Murphy, J., Grant, J. & O’Kiely, P. Antagonistic effects on biogas and methane output when co-digesting cattle and pig slurries with grass silage in in vitro batch anaerobic digestion. *Biomass and Bioenergy* **109**, 190–198 (Feb. 2018).

33. Cong, W.-F., Moset, V., Feng, L., Møller, H. B. & Eriksen, J. Anaerobic co-digestion of grass and forbs – Influence of cattle manure or grass based inoculum. *Biomass and Bioenergy* **119**, 90–96 (Dec. 2018).
34. Wahid, R., Ward, A. J., Møller, H. B., Sjøgaard, K. & Eriksen, J. Biogas potential from forbs and grass-clover mixture with the application of near infrared spectroscopy. *Bioresource Technology* **198**, 124–132 (2015).
35. Wahid, R. *et al.* Anaerobic mono-digestion of lucerne, grass and forbs – Influence of species and cutting frequency. *Biomass and Bioenergy* **109**, 199–208 (Feb. 2018).
36. Raposo, F., Borja, R. & Ibelli-Bianco, C. Predictive regression models for biochemical methane potential tests of biomass samples: Pitfalls and challenges of laboratory measurements. *Renewable and Sustainable Energy Reviews* **127**, 109890 (2020).
37. Pererva, Y., Miller, C. D. & Sims, R. C. Existing Empirical Kinetic Models in Biochemical Methane Potential (BMP) Testing, Their Selection and Numerical Solution. *Water* **12**, 1831 (June 2020).
38. Angelidaki, I. *et al.* Defining the biomethane potential (BMP) of solid organic wastes and energy crops: a proposed protocol for batch assays. *Water Science and Technology* **59**, 927–934 (Mar. 2009).
39. Jingura, R. M. & Kamusoko, R. Methods for determination of biomethane potential of feedstocks: a review. *Biofuel Research Journal* **4**, 573–586 (June 2017).
40. Filer, J., Ding, H. H. & Chang, S. Biochemical Methane Potential (BMP) Assay Method for Anaerobic Digestion Research. *Water* **11**, 921 (May 2019).
41. Moset, V., Al-zohairi, N. & Møller, H. B. The impact of inoculum source, inoculum to substrate ratio and sample preservation on methane potential from different substrates. *Biomass and Bioenergy* **83**, 474–482 (2015).
42. Nguyen, D. D. *et al.* Thermophilic anaerobic digestion of model organic wastes: Evaluation of biomethane production and multiple kinetic models analysis. *Bioresource Technology* **280**, 269–276 (May 2019).
43. Kafle, G. K. & Chen, L. Comparison on batch anaerobic digestion of five different livestock manures and prediction of biochemical methane potential (BMP) using different statistical models. *Waste Management* **48**, 492–502 (Feb. 2016).
44. Browne, J. D., Allen, E. & Murphy, J. D. Assessing the variability in biomethane production from the organic fraction of municipal solid waste in batch and continuous operation. *Applied Energy* **128**, 307–314 (Sept. 2014).
45. Zahan, Z., Othman, M. Z. & Muster, T. H. Anaerobic digestion/co-digestion kinetic potentials of different agro-industrial wastes: A comparative batch study for C/N optimisation. *Waste Management* **71**, 663–674 (Jan. 2018).

46. Kirwan, L., Connolly, J., Finn, J. A., Brophy, C. & Nyfeler, D. *Diversity-interaction modeling: estimating contributions of species identities and interactions to ecosystem function* tech. rep. 8 (2009), 2032–2038.
47. Cummins, S. *et al.* Beneficial effects of multi-species mixtures on N₂O emissions from intensively managed grassland swards. *Science of The Total Environment* **792**, 148163 (2021).
48. Cornell, J. A. in *A Primer on Experiments with Mixtures* 23–94 (John Wiley & Sons, Incorporated, Hoboken, UNITED STATES, 2011).
49. Zehnder, A. J. B., Huser, B. A., Brock, T. D. & Wuhrmann, K. Characterization of an acetate-decarboxylating, non-hydrogen-oxidizing methane bacterium. *Archives of Microbiology* **124**, 1–11 (Jan. 1980).
50. APHA. *Standard Methods for the Examination of Water and Wastewater* 20th ed. (eds Eaton, A. D., Clesceri, L. S., Franson, M. A. H. F., Rice, E. W. & Greenberg, A. E.) *Standard Methods for the Examination of Water and Wastewater v. 21* (American Public Health Association, 2005).
51. Gerike, P. The biodegradability testing of poorly water soluble compounds. *Chemosphere* **13**, 169–190 (Jan. 1984).
52. Buswell, A. M. & Neave, S. L. *Laboratory studies of sludge digestion* tech. rep. (Department of registration and education. Division of the state Water survey, Urbana, Illinois, 1930).
53. Hames, B., Scalata, C. & Sluiter, A. *Determination of protein content in biomass* (eds Sluiter, A., Scarlata, C. & (U.S.), N. R. E. L.) (National Renewable Energy Laboratory, Golden, Colo, 2005).
54. Lorenz, H., Reinsch, T., Kluß, C., Taube, F. & Loges, R. Does the admixture of forage herbs affect the yield performance, yield stability and forage quality of a grass clover ley? *Sustainability (Switzerland)* **12** (July 2020).
55. Van Soest, P., Robertson, J. & Lewis, B. Methods for Dietary Fiber, Neutral Detergent Fiber, and Nonstarch Polysaccharides in Relation to Animal Nutrition. *Journal of Dairy Science* **74**, 3583–3597 (Oct. 1991).
56. Selvankumar, T. *et al.* Process optimization of biogas energy production from cow dung with alkali pre-treated coffee pulp. *3 Biotech* **7** (Aug. 2017).
57. Koch, K., Lübken, M., Gehring, T., Wichern, M. & Horn, H. Biogas from grass silage – Measurements and modeling with ADM1. *Bioresource Technology* **101**, 8158–8165 (2010).
58. Alice, M., Corigliano, O. & Fragiaco, P. Energetic-Environmental Enhancement of Waste and Agricultural Biomass by Anaerobic Digestion Process. *Energy Technology & Policy* **1**, 59–69 (Jan. 2014).

59. Pham, C. H., Triolo, J. M., Cu, T. T., Pedersen, L. & Sommer, S. G. Validation and recommendation of methods to measure biogas production potential of animal manure. *Asian-Australasian Journal of Animal Sciences* **26**, 864–873 (2013).
60. Wagenmakers, E.-J. & Farrell, S. AIC model selection using Akaike weights. *Psychonomic Bulletin & Review* **11**, 192–196 (Feb. 2004).
61. Schwarz, G. Estimating the Dimension of a Model. *The Annals of statistics* **6**, 461–464 (1978).
62. Moral, R. d. A., Connolly, J., Vishwakarma, R. & Brophy, C. *DImodels: Diversity-Interactions (DI) Models* 2022. <https://cran.r-project.org/web/packages/DImodels/index.html>.
63. Moral, R. A. *et al.* Going beyond richness: Modelling the BEF relationship using species identity, evenness, richness and species interactions via the DImodels R package, and a comparison with traditional approaches (Dec. 2022).
64. Bauldry, S. in *International Encyclopedia of the Social & Behavioral Sciences* 615–620 (Elsevier, Mar. 2015).
65. Hendriks, A. T. & Zeeman, G. Pretreatments to enhance the digestibility of lignocellulosic biomass. *Bioresource Technology* **100**, 10–18 (2009).
66. Sluiter, A., Ruiz, R. O., Scarlata, C., Sluiter, J. & Templeton, D. *Determination of Extractives in Biomass* tech. rep. July (Golden, Colo., National Renewable Energy Laboratory./, 2005), 1–9.
67. Nizami, A.-S., Singh, A. & Murphy, J. D. Design, Commissioning, and Start-Up of a Sequentially Fed Leach Bed Reactor Complete with an Upflow Anaerobic Sludge Blanket Digesting Grass Silage. *Energy & Fuels* **25**, 823–834 (Feb. 2011).
68. Yan, Z. *et al.* The effects of initial substrate concentration, C/N ratio, and temperature on solid-state anaerobic digestion from composting rice straw. *Bioresource Technology* **177**, 266–273 (2015).
69. Choi, Y., Ryu, J. & Lee, S. R. Influence of carbon type and carbon to nitrogen ratio on the biochemical methane potential, pH, and ammonia nitrogen in anaerobic digestion. *Journal of Animal Science and Technology* **62**, 74–83 (Jan. 2020).
70. Chen, Y., Cheng, J. J. & Creamer, K. S. Inhibition of anaerobic digestion process: A review. *Bioresource technology* **99**, 4044–4064 (2008).
71. Bhatia, S. K. *et al.* Recent developments in pretreatment technologies on lignocellulosic biomass: Effect of key parameters, technological improvements, and challenges. *Bioresource Technology* **300**, 122724 (2020).
72. Mathiesen, S. D. & Aagnes Utsi, T. H. The quality of the forage eaten by Norwegian reindeer on South Georgia in summer. *Rangifer* **20**, 17 (Mar. 2000).

73. Suter, M. *et al.* Nitrogen yield advantage from grass-legume mixtures is robust over a wide range of legume proportions and environmental conditions. *Global Change Biology* **21**, 2424–2438 (June 2015).

A.1 Appendices

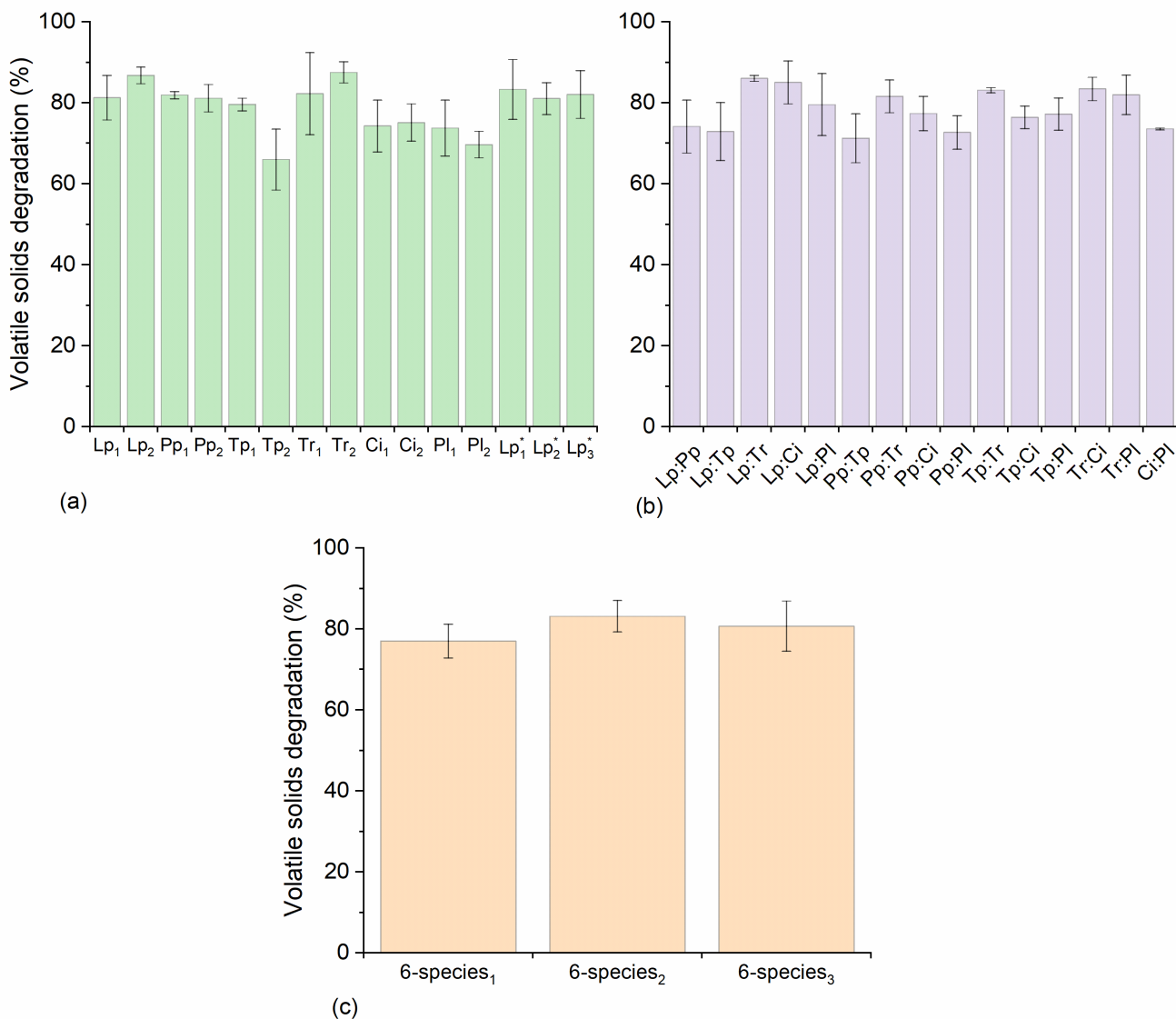


Figure A.1: Volatile solids degradation of monocultures (green bars, a), and mixtures of two species (purple bars, b) and six species (orange bars, c). Substrates were labelled according to Table 3.2.

Table A.1: Results of the elemental analysis (in %TS) for each substrate. Data is reported in average (and standard deviation) of duplicate measurements.

Substrate	Field plot	C	H	O	N	S	Ash
Lp ₁	40	46.0 (0.2)	6.6 (0.1)	38.4 (0.1)	1.1 (0.1)	0.0 (0.0)	8.0 (0.1)
Lp ₂	42	45.7 (0.2)	6.6 (0.0)	41.4 (0.3)	1.2 (0.0)	0.0 (0.0)	5.1 (0.3)
Pp ₁	2	46.6 (0.2)	6.5 (0.0)	37.6 (0.2)	2.0 (0.0)	0.0 (0.0)	7.4 (0.4)
Pp ₂	11	46.9 (0.4)	5.9 (0.2)	37.1 (0.7)	2.0 (0.1)	0.1 (0.0)	8.1 (0.0)
Tp ₁	53	47.6 (0.6)	5.8 (0.0)	34.0 (0.7)	4.1 (0.1)	0.2 (0.1)	8.4 (0.3)
Tp ₂	8	45.8 (0.1)	5.7 (0.1)	33.4 (0.2)	3.1 (0.0)	0.1 (0.0)	12.4 (0.0)
Tr ₁	52	48.5 (0.2)	5.7 (0.3)	32.1 (0.6)	5.0 (0.0)	0.1 (0.1)	8.6 (0.4)
Tr ₂	39	46.4 (0.8)	6.0 (0.2)	31.5 (0.9)	4.4 (0.1)	0.3 (0.1)	11.4 (0.2)
Ci ₁	38	46.3 (0.6)	5.7 (0.1)	31.4 (0.6)	2.4 (0.0)	0.2 (0.0)	14.0 (0.3)
Ci ₂	55	46.1 (0.4)	5.9 (0.2)	31.5 (0.6)	2.2 (0.1)	0.2 (0.0)	14.1 (0.1)
Pl ₁	34	45.5 (0.2)	6.4 (0.1)	34.3 (0.3)	1.9 (0.1)	0.1 (0.0)	11.8 (0.1)
Pl ₂	43	46.3 (0.0)	6.3 (0.2)	35.0 (0.2)	1.9 (0.0)	0.1 (0.0)	10.4 (0.3)
Lp ₁ [*]	10	44.9 (0.4)	6.4 (0.3)	38.8 (0.3)	1.4 (0.2)	0.0 (0.0)	8.5 (0.1)
Lp ₂ [*]	25	45.2 (0.3)	6.4 (0.1)	37.8 (0.5)	1.8 (0.0)	0.3 (0.0)	8.6 (0.1)
Lp ₃ [*]	3	46.0 (0.5)	6.5 (0.1)	37.9 (0.5)	1.7 (0.0)	0.5 (0.1)	7.5 (0.3)
Lp:Pp	9	45.5 (0.8)	6.4 (0.3)	40.0 (0.7)	1.6 (0.2)	0.0 (0.0)	6.5 (0.3)
Lp:Tp	45	44.5 (0.1)	5.7 (0.1)	33.8 (0.3)	3.0 (0.2)	0.2 (0.0)	12.8 (0.0)
Lp:Tr	4	47.2 (0.0)	5.9 (0.2)	32.5 (0.1)	3.3 (0.2)	0.2 (0.1)	11.0 (0.5)
Lp:Ci	24	46.1 (0.0)	5.7 (0.2)	39.6 (0.2)	1.5 (0.0)	0.2 (0.0)	6.9 (0.3)
Lp:Pl	36	46.6 (0.6)	5.8 (0.2)	38.0 (0.7)	1.6 (0.0)	0.2 (0.0)	7.9 (0.4)
Pp:Tp	61	46.7 (0.5)	5.8 (0.4)	34.1 (0.9)	3.4 (0.0)	0.1 (0.0)	9.9 (0.3)
Pp:Tr	59	47.2 (0.4)	6.3 (0.0)	32.0 (0.5)	4.3 (0.1)	0.1 (0.0)	10.1 (0.2)
Pp:Ci	54	44.8 (0.2)	5.9 (0.1)	36.3 (0.2)	1.9 (0.0)	0.1 (0.0)	11.0 (0.2)
Pp:Pl	21	46.2 (0.0)	6.1 (0.0)	36.5 (0.1)	2.0 (0.0)	0.2 (0.0)	8.9 (0.4)
Tp:Tr	41	46.4 (0.1)	5.8 (0.0)	33.5 (0.3)	4.3 (0.2)	0.2 (0.0)	9.9 (0.1)
Tp:Ci	31	45.8 (0.3)	5.8 (0.1)	33.5 (0.3)	3.5 (0.1)	0.2 (0.0)	11.1 (0.7)
Tp:Pl	63	46.3 (0.1)	6.0 (0.1)	36.0 (0.1)	2.9 (0.1)	0.2 (0.0)	8.6 (0.2)
Tr:Ci	26	45.1 (0.4)	6.0 (0.0)	35.5 (0.6)	3.5 (0.2)	0.2 (0.0)	9.7 (0.2)
Tr:Pl	16	45.8 (0.0)	6.0 (0.0)	35.7 (0.1)	3.4 (0.1)	0.2 (0.0)	8.9 (0.4)
Ci:Pl	65	44.7 (0.2)	5.6 (0.0)	36.0 (0.2)	2.0 (0.0)	0.2 (0.0)	11.4 (0.4)
6-species ₁	12	45.0 (0.1)	5.9 (0.1)	36.5 (0.2)	2.4 (0.1)	0.3 (0.0)	10.0 (0.0)
6-species ₂	44	45.8 (0.3)	5.4 (0.1)	33.1 (0.3)	2.8 (0.0)	0.8 (0.0)	12.2 (0.2)
6-species ₃	56	45.7 (0.1)	4.7 (0.1)	36.1 (0.2)	2.9 (0.0)	0.9 (0.1)	9.7 (0.4)

Note: ^{*}higher dose of nitrogen fertiliser. Substrates were labelled according to Table 3.2.

Table A.2: Standard deviations for the mean values of C:N ratio, ash and crude protein displayed in Table 3.3.

Substrate (%TS)	C:N ratio (%TS)	Ash (%TS)	Cr. PTN
Lp ₁	1.8	0.3	0.05
Lp ₂	0.6	0.1	0.30
Pp ₁	0.2	0.1	0.42
Pp ₂	0.8	0.4	0.00
Tp ₁	0.4	0.9	0.33
Tp ₂	0.1	0.1	0.01
Tr ₁	0.1	0.3	0.37
Tr ₂	0.3	0.5	0.16
Ci ₁	0.4	0.3	0.29
Ci ₂	0.6	0.4	0.07
Pl ₁	0.9	0.4	0.06
Pl ₂	0.1	0.1	0.25
Lp ₁ [*]	3.4	0.9	0.11
Lp ₂ [*]	0.2	0.1	0.05
Lp ₃ [*]	0.3	0.0	0.34
Lp:Pp	2.6	0.9	0.32
Lp:Tp	1.1	1.4	0.04
Lp:Tr	0.8	1.2	0.51
Lp:Ci	0.2	0.1	0.31
Lp:Pl	0.7	0.2	0.39
Pp:Tp	0.2	0.1	0.32
Pp:Tr	0.3	0.6	0.16
Pp:Ci	0.1	0.1	0.20
Pp:Pl	0.4	0.3	0.40
Tp:Tr	0.4	1.1	0.07
Tp:Ci	0.3	0.6	0.66
Tp:Pl	0.6	0.6	0.17
Tr:Ci	0.8	1.4	0.15
Tr:Pl	0.4	0.6	0.42
Ci:Pl	0.4	0.2	0.35
6-species ₁	1.1	0.9	0.02
6-species ₂	0.1	0.1	0.15
6-species ₃	0.1	0.1	0.36

Note: *higher dose of nitrogen fertiliser. Substrates were labelled according to Table 3.2

Table A.3: Statistics for the First order kinetics model fitting the experimental data present at Table 3.5.

Substrate	Difference¹	Adj. R²	rMSE	AIC	BIC
Lp ₁	0.0%	0.99	7.9	66.75	66.69
Lp ₂	2.0%	0.90	27.8	111.09	111.41
Pp ₁	0.7%	1.00	7.3	64.32	64.27
Pp ₂	1.9%	0.96	22.2	97.77	97.71
Tp ₁	0.8%	0.95	17.4	90.56	90.50
Tp ₂	5.0%	0.83	42.2	124.47	124.79
Tr ₁	2.2%	0.95	25.9	108.85	109.17
Tr ₂	0.0%	0.96	17.3	84.91	84.42
Ci ₁	1.6%	0.92	24.6	100.88	100.82
Ci ₂	0.2%	0.74	45.3	126.72	127.04
Pl ₁	0.8%	0.99	9.7	72.88	72.82
Pl ₂	0.2%	0.83	33.8	110.45	110.39
Lp ₁ [*]	1.9%	0.95	22.7	191.01	194.29
Lp ₂ [*]	1.8%	0.99	9.3	67.40	66.92
Lp ₃ [*]	3.2%	0.97	15.3	92.00	92.32
Lp:Pp	0.7%	0.94	12.1	123.48	125.82
Lp:Tp	1.1%	0.98	12.8	156.89	160.17
Lp:Tr	6.7%	0.81	41.8	124.14	124.45
Lp:Ci	7.5%	0.96	13.0	86.73	87.05
Lp:Pl	0.2%	0.94	16.7	94.84	95.16
Pp:Tp	0.8%	0.99	7.9	70.65	70.97
Pp:Tr	0.8%	0.99	8.1	95.91	97.85
Pp:Ci	3.9%	0.92	24.6	107.22	107.53
Pp:Pl	2.4%	0.97	14.7	127.63	129.78
Tp:Tr	1.2%	0.97	17.8	85.70	85.22
Tp:Ci	3.9%	0.98	15.4	86.83	86.77
Tp:Pl	1.4%	0.91	19.3	122.74	124.23
Tr:Ci	1.3%	0.96	27.5	143.34	145.06
Tr:Pl	3.2%	0.95	17.1	95.45	95.77
Ci:Pl	1.1%	0.97	14.0	78.97	78.49
6-species ₁	1.6%	0.94	22.3	153.10	155.44
6-species ₂	3.2%	0.71	52.4	139.15	139.80
6-species ₃	1.2%	0.95	19.5	128.98	130.70

Note: 1- relative difference between the maximum methane yield (Bo) predicted and measured (absolute). Substrates were labelled according to Table 3.2.

Table A.4: Total ammonia nitrogen, C:N ratio, pH and substrate-specific maximum methane yield (Bo_{sub}) for selected substrates in the digestion of grassland species.

Substrate	Total ammonia nitrogen ($g.L^{-1}$)	C:N (% TS)	pH	Bo_{sub} ($NL.kgVS^{-1}$)
Lp ₁	0.19	40.3	8.0	186.8 ± 7.6
Pp ₁	0.16	23.8	7.7	306.6 ± 9.7
Tr ₁	0.83	9.8	8.0	300.9 ± 29.0
Lp* ₁	0.69	31.9	8.0	286.4 ± 18.6
Lp:Pp	0.16	27.7	8.1	136.6 ± 9.0
Tr:Ci	0.69	12.8	8.0	344.5 ± 20.4
6-species ₁	0.77	19.1	8.0	242.5 ± 18.9

Note: *higher dose of nitrogen fertiliser. Substrates labelled according to Table 3.2.

Table A.5: Comparison between DI models when investigating *interactions* using the *autoDI* function. DI models compared: STR (structures), ID (species identity), AV (average interactions), FG (functional group effects), and FULL (pairwise interactions).

DI model	Residual df	RSS	RSME	df	SS	F	Pr(> F)
<i>Substrate-specific maximum methane yield - Bo_{sub}</i>							
'STR'	31	58632.4	1891.4				
'ID'	26	44928.8	1728.0	5	13703.65	3.457	0.040
'AV'	25	43844.6	1753.8	1	1084.21	1.367	0.267
'FG'	20	32976.1	1648.8	5	10868.51	2.741	0.076
'FULL'	11	8722.1	792.9	9	24253.96	3.399	0.030
<i>Area-specific maximum methane yield - Bo_{area}</i>							
'STR'	31	6761678.6	218118.7				
'ID'	26	4460275.3	171549.1	5	171549.1	7.976	0.002
'AV'	25	4311960.4	172478.4	1	148314.9	2.570	0.137
'FG'	20	2721316.4	136065.8	5	1590644.0	5.512	0.009
'FULL'	11	634830.2	57711.8	9	2086486.2	4.017	0.017

Note: STR model is an intercept only model. 'df' represents the degrees of freedom, RSS represents the residual sum of squares, RMSE represents the root-mean squared error, SS represents the sum of squares, and F is the F-value (ratio of variances)

Table A.6: Comparison between DI models when investigating *interactions* using the *autoDI* function. DI models compared: STR (structures), ID (species identity), AV (average interactions), FG (functional group effects), and FULL (pairwise interactions).

DI model	Using all δ	Residual df	RSS	RSME	df	SS	F	Pr(> F)
<i>Substrate-specific maximum methane yield - Bo_{sub}</i>								
'FULL ₀ '	FALSE	20	16790.8	28.97				
'FULL ₁ '	TRUE	10	8722.8	29.53	10	8068.02	0.925	0.548
<i>Area-specific maximum methane yield - Bo_{area}</i>								
'FULL ₀ '	FALSE	21	1256169.0	244.58				
'FULL ₁ '	TRUE	10	634487.9	251.89	11	621681.13	0.891	0.576

Note: Model considering all the δ coefficients ('FULL₁') or only the significant δ coefficients ('FULL₀'); 'df' represents the degrees of freedom, RSS represents the residual sum of squares, RMSE represents the root-mean squared error, SS represents the sum of squares, and F is the F-value (ratio of variances)

Table A.7: Predictions for maximum methane yield (Predicted Bo_{sub} and Predicted Bo_{area}), and for the contribution of species interaction to maximum methane yield (Interactions) using the pairwise-interaction DI model

Substrate	Predicted Bo_{sub} (NL.kgVS ⁻¹)	Interactions	Predicted Bo_{area} (Nm ³ .ha ⁻¹ .yr ⁻¹)	Interactions
Lp*	261.5 (16.3)	NA	2532.3 (138.7)	NA
Lp	203.2 (19.8)	NA	1750.9 (168.9)	NA
Pp	305.6 (19.8)	NA	3053.2 (168.9)	NA
Tp	229.7 (19.8)	NA	1919.5 (168.9)	NA
Tr	260.3 (19.8)	NA	2149.6 (168.9)	NA
Ci	221.0 (19.8)	NA	1534.2 (168.9)	NA
Pl	237.0 (19.8)	NA	2198.4 (168.9)	NA
Lp:Pp	140.5 (33.9)	-113.9	1309.0 (289.0)	-1093.1
Lp:Tp	280.1 (33.9)	63.6	2669.0 (289.0)	833.8
Lp:Tr	237.2 (33.9)	5.5	2413.3 (289.0)	463.0
Lp:Ci	195.0 (33.9)	-17.1	1720.2 (289.0)	77.6
Lp:Pl	202.3 (33.9)	-17.8	1955.5 (289.0)	-19.2
Pp:Tp	228.1 (33.9)	-39.6	2418.5 (289.0)	-67.8
Pp:Tr	245.6 (33.9)	-37.4	2615.5 (289.0)	14.0
Pp:Ci	232.8 (33.9)	-30.5	2139.6 (289.0)	-154.1
Pp:Pl	244.6 (33.9)	-26.7	2615.8 (289.0)	-10.0
Tp:Tr	267.5 (33.9)	22.5	2435.3 (289.0)	400.8
Tp:Ci	269.4 (33.9)	44.0	2494.1 (289.0)	767.3
Tp:Pl	163.8 (33.9)	-69.6	1684.7 (289.0)	-374.3
Tr:Ci	348.4 (33.9)	107.8	3113.2 (289.0)	1271.3
Tr:Pl	191.9 (33.9)	-56.7	1908.0 (289.0)	-266.0
Ci:Pl	238.6 (33.9)	9.6	1849.7 (289.0)	-16.6
6-species	225.4 (15.5)	-17.4	2304.4 (132.6)	202.9

Note: This data is represented graphically in Figures 3.3 and 3.4. *higher dose of nitrogen fertiliser. Values for standard error are represented in brackets. Substrates were labelled according to Table 3.2.

Chapter 4: Producing butyric acid and VFAs from permanent grassland monocultures: the potential of *Lolium perenne*, *Trifolium pratense* and *Trifolium repens*

Abstract

The co-digestion of grass and clovers in anaerobic digestion can improve the nutrient availability to micro-organisms, and consequently methane yields. Here, we investigate the use of grass (*Lolium perenne*) and clovers (*Trifolium repens*, *Trifolium pratense*) for the production of volatile fatty acids (VFAs), as substrates and co-substrates (*L. perenne* and *T. repens*). The effect of mineral nitrogen fertiliser in VFA yield was also evaluated by testing a *L. perenne* supplied with 150 and 300 kgN.ha⁻¹.yr⁻¹. For that, a one-stage fermentation and a two-stage fermentation were designed at 37 °C using an inoculum from the co-fermentation of cattle slurry and grass silage at similar conditions to our study. In the one-stage fermentation, all substrates were fermented for 7 days, while 150 kgN.ha⁻¹.yr⁻¹ *L. perenne* was fermented for extra 7 days to evaluate the impact of a longer solid retention time to biomass degradation and VFA production. In the two-stage fermentation, *L. perenne*, *T. repens* and the mixture of *L. perenne* and *T. repens* were fermented in water with no inoculum addition for 7 days. Afterwards, liquid and solid fraction from the first-stage were separated and inoculated similarly to the one-stage fermentation. We observed that the buffering capacity of clovers was important for biomass degradation, but favoured the accumulation of methane instead of VFAs. Doubling the dose of nitrogen fertiliser did not improve the production of VFAs or butyric acid from *L. perenne*, but improved the total product yield due to a higher accumulation of methane. No difference in VFA production was observed between the one-stage fermentation and the two-stage fermentation. However, the lactic acid produced in the first-stage was responsible for the sharp drop in pH and correlated to the production of butyric acid in the second-stage fermentation *L. perenne*. The lowest production of VFAs was observed from the one-stage fermentation of *T. repens* (218.6±23.2 mg.mgVS⁻¹). The highest VFA yield was obtained in the fermentation of 300 kgN.ha⁻¹.yr⁻¹ *L. perenne*, 316.4±10.4 mg.mgVS⁻¹, which was significantly higher than most substrates but the 150 kgN.ha⁻¹.yr⁻¹ *L. perenne* (after 7 and 14 days). The best performance in terms of butyric acid was observed in the one-stage fermentation of the 150 kgN.ha⁻¹.yr⁻¹ *L. perenne* (1.4±0.1 g.L⁻¹; 106.0±11.1 mg.gVS⁻¹; 7 days) or its mixture with *T. repens* (1.1±0.1 g.L⁻¹; 102.6±7.2 mg.gVS⁻¹). Our work demonstrates the benefit of co-fermenting grasses and clovers and a lower mineral fertilise rate for butyric acid and VFA production, paving the way for potential developments that associate sustainable forage production with VFA production.

4.1 Introduction

In 2019, the European Commission released ‘The Green Deal’, which aims to reduce greenhouse gases (GHG) emissions in Europe by 50% until 2030, reaching complete neutrality by 2050¹. Permanent grassland fields are an abundant and renewable feedstock in temperate regions², representing an asset to aid Europe in ‘The Green Deal’. Permanent grasslands are composed of graminoids (e.g., grasses - *L. perenne*) and forbs (e.g., clovers - *T. repens* and *T. pratense*)³, and are crucial ecosystems for food production while maintaining soil quality, balancing the ecosystem biodiversity, and sequestering carbon from the atmosphere^{4,5}. Especially due to conservation strategies, grassland forage yields have been improved by mixing forbs and grasses^{6–9} leading to a more sustainable feedstock with better nutrient intake efficiency at a lower quantity of mineral fertiliser^{10,11} and lower N₂O emissions^{5,12}. Moreover, grassland fields that are managed for biodiversity preservation can result in a biogas production that is 160% higher in ton per dry matter than other cereals and crop waste¹³.

Permanent grassland biomass can be used as feedstock in a green biorefinery¹⁴, combining grasses, forbs and possibly agricultural wastes to produce proteins, bioenergy (e.g., biomethane and biogas), fertiliser, and organic acids, such as volatile fatty acids (VFAs), medium-chain carboxylic acids (MCCAs) and bioplastics (polyhydroxyalkanoate (PHAs))¹⁵. In this biorefinery, the anaerobic digestion (AD) technology can be used as a core process, as it can be an efficient strategy for resource recovery by minimising waste while maximising conversion in terms of biogas/biomethane production¹⁵. In fact, the production of biogas and biomethane has been the aim of most studies in grass-based AD, with *L. perenne* and *L. perenne* silage as the most studied feedstock at mesophilic^{2,16–24} and thermophilic conditions²⁵. However, the anaerobic mono-digestion of grass tends to fail in the long run²⁶ due to an unbalance in nutrient availability (e.g., lack of trace elements such as cobalt and selenium, and poor C:N ratio)^{25–27}. Failures in grass-based AD are also associated with operational setbacks due to the blockage of pipes with grass fibres, and to lactic acid accumulation²⁸. A strategy to increase the nutrient content in grasses is its cultivation with legumes (clovers), which can result in a forage with a higher protein content using less mineral nitrogen fertiliser due to clovers’ ability to fixate atmospheric N₂²⁹. Besides an improvement in sustainability and forage yield from grassland fields, the association of forbs and grasses has resulted in a substrate with improved C:N ratio and fibre composition and, consequently, a higher production of methane^{25,30}.

Although biogas and biomethane are the main products of AD, increased interest has been directed to acidogenic fermentation (AF) in the past 25 years since the capital cost for AD is usually high due to long operational times and high reactor volumes³¹. Moreover, due to methane being a more harmful and potent GHG compared to carbon dioxide, fugitive emissions can have a negative impact to the environment. Therefore, centring the process in VFA accumulation can be beneficial for AD by maximising feedstock conversion while decreasing capital expense, as VFAs have a higher-market value^{15,32} compared to biogas/biomethane. To focus on the AF, the AD process can be tailored for the accumulation of VFAs if methanogenic archaea are inhibited by adjusting the pH or even by increasing the organic loading rate (OLR), thus leading to a pH decrease due to the accumulation

of VFAs³³. Despite the interest in VFA production and feedstock abundance, minimal research has published focusing on the production of VFAs from grasses^{34–37}, especially focusing in selectively producing higher-chain VFAs such as butyric and caproic acids^{38,39}. Additionally, the potential of clovers or grass-clover mixtures for VFA production has not been studied yet. Butyric acid is an important chemical for many industries, such as food, cosmetics, pharmaceutical and chemical with global market demand of 80,000 tons per year⁴⁰. Also, butyric acid is still mainly produced through the chemical synthesis of fossil-fuel-derived materials. Its production from the acidogenic fermentation of grasses is not established yet, as most works have reported acetic acid as the highest produced VFA^{34–37}, or caproic acid under specific conditions^{38,39}.

One of the main challenges in the fermentation of lignocellulosic biomass, such as grasses, is its recalcitrance, which negatively impacts product yield and biomass degradation efficiency⁴¹. Lignin content, cellulose crystallinity and hemicellulose structure have been highlighted as important factors that increase biomass recalcitrance⁴². Chemical and physical treatments have been proposed over the years to reduce lignocellulosic recalcitrance^{42,43} at the expense of increasing operational costs, which could be justified depending on the VFA yield³² or feedstock price. Some studies have proposed alternative ways to improve grass conversion to VFAs bypassing its recalcitrance by mechanically separating the grass juice and pressed cake³⁹. Sakarika *et al.*³⁹ achieved a caproic acid concentration of 7.2 g.L⁻¹ (32% selectivity) by fermenting the grass juice with glucose supplementation at 50°C and pH 6.0, using an acclimatised inoculum for caproic acid production. Steinbrenner *et al.*⁴⁴ combined lime carbonated and low dry matter content in the ensiling process of maize to increase butyric acid concentrations up to 75.06 g.kg⁻¹TS. The same ensiling technique was used to obtain a grass juice with 20.1 g.kg⁻¹TS of butyric acid after 90 days at mesophilic conditions – the pressed cake was assessed for theoretical methane production⁴⁵. Additionally, it is the authors' understanding that chemical and physical pre-treatments may disturb the biomass' indigenous community, which has been linked to the production of lactic acid⁴⁶, butyric acid and acetic acid⁴⁴. Lactic acid is an important fermentation intermediate, which can be further used by bacteria to produce butyric acid⁴⁷ and caproic acid^{38,47}. From grass, Khor *et al.*³⁸ has demonstrated the accumulation of lactic acid (9.4±1.0 g.L⁻¹) in a semi-continuous fermentation after 33 days at 32°C, without adding any extra source of inoculum and using water as media. Furthermore, this lactic acid was elongated to caproic acid in a second-stage fermenter at pH 5.5-6.2, 32°C and using an inoculum acclimatised for caproic acid.

In this work, we investigated the potential of grass and clovers for the production of VFAs, focusing in the selective production of butyric acid. Moreover, the effect of nitrogen fertiliser dosage was investigated using a *L. perenne* substrate supplied with 150 kgN.ha⁻¹.yr⁻¹ and 300 kgN.ha⁻¹.yr⁻¹. Due to the lack of information regarding grassland species and VFA production, a biomethane potential assay (BMP) assay was performed to establish a baseline in terms of product conversion and biodegradability. Subsequently, VFA production and butyric acid accumulation was evaluated in a one-stage fermentation and a two-stage fermentation – both using an acclimatised inoculum for VFA production from grass. The two-stage fermentation was designed to evaluate if a fermentation of grass and clovers in water with no inoculum addition as a first-stage would increase the production

of butyric acid in a subsequent second-stage with an acclimatised inoculum.

4.2 Materials and Methods

4.2.1 Substrates

Perennial forages common to temperate grasslands were selected in June 2019 from a pilot-scale field experiment at Johnstown Castle, Wexford, in the south-east of Ireland (52°17'57.8"N, 6°30'23.3"W, 71 m a.s.l.)⁸. The field received natural water supply and was established on a field previously grass-dominated with sandy-loam soil with pH 5.7, total carbon of 12.2 g/kg of soil, and total nitrogen of 2.45 g/kg of soil⁷. The same forages from the Teagasc field were previously used (see Chapter 3). In this study (Chapter 4), the selected grassland forages were *Lolium perenne* (perennial ryegrass), *Trifolium repens* (white clover), *Trifolium pratense* (red clover) and a mixture of *L. perenne* and *T. repens* (Table 4.1).

Table 4.1: Chemical parameters for the grassland biomass used in this study.

Parameters	<i>Lolium perenne</i> (Lp)	<i>Lolium perenne</i> (Lp*)	<i>Trifolium pratense</i> (Tp)	<i>Trifolium repens</i> (Tr)	<i>L. perenne</i> + <i>T. repens</i> (Lp+Tr)
Composition	Lp: 92%	Lp: 97%	Tp: 70%	Tr: 51%	Lp: 46%, Tr: 42%
Unsown sps. ¹	8%	3%	30%	49%	12%
Total Solids (%FW)	24.4 (0.0)	20.5 (0.4)	17.6 (0.3)	17.0 (0.7)	19.8 (1.0)
Volatile Solids (%FW)	22.8 (0.2)	19.2 (0.4)	15.9 (0.3)	15.1 (0.6)	17.9 (0.9)
Ash (%FW)	1.6 (0.0)	1.7 (0.1)	1.7 (0.0)	1.6 (0.1)	1.9 (0.2)
pH	6.7	6.4	6.4	6.2	6.4
ThCOD (gCOD.g ⁻¹ VS)	1.42	1.41	1.46	1.48	1.40
C/N (%)	26.5 (0.1)	27.7 (0.7)	14.6 (0.1)	11.3 (0.1)	15.0 (0.1)
Cr. Protein (%)	10.8 (0.0)	10.3 (0.2)	19.6 (0.1)	25.1 (0.2)	17.1 (0.1)
NDF (%TS)	45.8	48.6	49.9	49.4	52.5
ADF (%TS)	24.3	26.4	27.3	20.6	26.1
Hemicellulose (%TS)	21.6	22.1	22.6	28.8	26.4

Note: *Supplied with 300 kgN.ha⁻¹.yr⁻¹. ¹Unsown species are popularly known as weeds, and represent the intrusion of species that were not seeded in the field.

With the exception of *T. pratense*, the forages used in this study were harvested from the same field as the previous study (see Chapter 3), but from a different plot. In total, five forages were used as substrates – four of them were supplied with 150 kgN.ha⁻¹.yr⁻¹, and one perennial ryegrass supplied with 300 kgN.ha⁻¹.yr⁻¹ (Lp*). All five forages were also supplied with phosphorus (60 kg.ha⁻¹.yr⁻¹) and potassium (300 kg.ha⁻¹.yr⁻¹). The forages were conserved at -20 °C in plastic bags as received from the field. After thawed, forages were used as they were received from the field, without separating the intended species from the unsown species (weeds), as performed in the previous study (see Chapter 3). For the fermentation assays, each substrate was collected from a plot bag and cut to approximately 2 cm before feeding to the bottles. For the BMP assay, each substrate was fed directly to the bottles after thawing – thus, no size reduction was performed.

4.2.2 Biomethane potential assay

The methane potential and biodegradability of the selected grassland forages were evaluated using a modified BMP assay. The setup consisted of 500 mL plastic bottles with Fisherbrand™ solid

rubber stoppers and 1 L Tedlar gas bags attached using a needle and a tap. Methane production was monitored for 28 days at 37 °C and constant agitation (100 rpm). Granular sludge from a full-scale expanded granular sludge bed (EGSB) reactor applied to treat dairy wastewater from Arrabawn Dairies Co. in Kilconnell, Ireland, was used as inoculum. The granular sludge was harvested in August 2020 and stored with its leachate at 4 °C. The inoculum total (TS) and volatile (VS) solids were 10.3 (0.4)% and 8.5 (0.3)%, respectively.

Prior to the experiment, the granular sludge was filtered using a metal sieve and a cloth, washed with tap water and drained. The inoculum was prepared by mixing intact and crushed granules (50-50% in VS); the granules were crushed using a mortar and a pestle. The inoculum was acclimatised in sodium bicarbonate buffer (10 g.L⁻¹, 250 mL) at 37 °C and 100 rpm for 5 days. Then, inoculum-acclimatised bottles were fed with substrate loading based on a substrate-to-inoculum ratio of 1:1, a concentration of 10 gVS.L⁻¹. Anaerobic conditions were provided by flushing N₂/CO₂ (80-20%) for 5 minutes, and 0.42 mL of a trace elements solution was supplied⁴⁸. Biogas volume was monitored at regular intervals (0, 2, 4, 8, 14, 21 and 28 days) or when the gas bags were full to limit disturbances in gas production. Substrate consumption was determined as VS degradation, where VS values measured at the beginning and after 28 days of digestion.

4.2.3 One-stage fermentation assay

The potential of grassland biomass for VFA production was tested in a one-stage fermentation assay (Figure 4.1). The setup consisted of 500 mL plastic bottles with Fisherbrand™ solid rubber stoppers and 1 L Tedlar gas bags attached using a needle and a tap. The acidogenic fermentation was performed in batch-mode for 7 days at 37 °C and 100 rpm for all substrates selected from the Teagasc field. The fermentation of *L. perenne* (supplied with 150 kgN.ha⁻¹.yr⁻¹) was performed for a further 7 days (in total 14 days) to evaluate the effect of prolonged fermentation time in biomass degradation and VFA production. An OLR of 2 gVS.L⁻¹.day⁻¹ was applied as well as an inoculum loading of 2.4 gVS.L⁻¹.day⁻¹.

The inoculum used was composed of a solid digestate and liquid leachate, both sourced from an acidogenic fermenter (LBR) producing VFAs from silage grass and cattle slurry. Leachate was diluted (11x) with tap water before it was fed to the bottles alongside 0.42 mL of a trace elements⁴⁹ solution – this liquid mix had a volume of 275 mL, and the final working volume was 300 mL. Sodium bicarbonate was added at the beginning of the batch to correct the starting pH to approximately 6.0, but pH was left to fluctuate during the fermentation. The experiment was performed in triplicate, and control bottles were prepared without the addition of any substrate.

Liquid samples were collected at days 0-3 and 5-7 to monitor VFA production, COD profile, ammonia levels, and pH profile. Solid samples were collected at the beginning and end of the fermentation to measure the VS degradation. The gas production was monitored constantly – gas volumes were measured both when the gas bags were full, and by the end of each batch; gas samples were collected for methane composition.

4.2.4 Two-stage fermentation assay

A fermentation assay was designed in two stages to investigate the effects of pre-fermenting the grassland biomass on the accumulation of VFAs. The same set-up from the one-stage fermentation assay was used in this design. Three substrates were tested in this assay – *L. perenne*, *T. repens*, and the mixture of *L. perenne* with *T. repens*. In the first stage of the assay, 4.2 gVS of each substrate was placed in 275 mL of water without an external source of inoculum for 7 days at 37 °C and 100 rpm (Figure 4.2). After 7 days, the liquid fraction and the solid fraction from the first stage fermentation of each substrate were separated in different bottles and inoculated with an inoculum loading of 2.4 gVS.L⁻¹.day⁻¹.

The inoculum was composed of a solid digestate and liquid leachate, both sourced from an acidogenic fermenter (LBR) producing VFAs from silage grass and cattle slurry. In the bottles fed with the liquid fraction, the leachate was diluted 11 times in that liquid fraction. In the bottles fed with the solid digestate, the leachate was diluted (11x) with tap water. Both bottles received 0.42 mL of a trace elements⁴⁹ and the final working volume in the first and second stages was set at 300 mL. Sodium bicarbonate was added at the beginning of the batch to correct the starting pH to approximately 6.5, but pH was left to fluctuate during the fermentation. The second stage of fermentation was performed for 7 days at 37 °C and 100 rpm; the experiment was performed in triplicate for 14 days in total.

Liquid samples were collected at days 0-2, 6-9, 12, and 14 to monitor VFA production, lactic acid accumulation, COD profile, ammonia levels, and pH profile. Solid samples were collected at the beginning and end of each stage of fermentation to estimate the VS degradation. The gas production was monitored constantly – gas volumes were measured as the gas bags were full and by the end of each batch; gas samples were collected for methane composition.

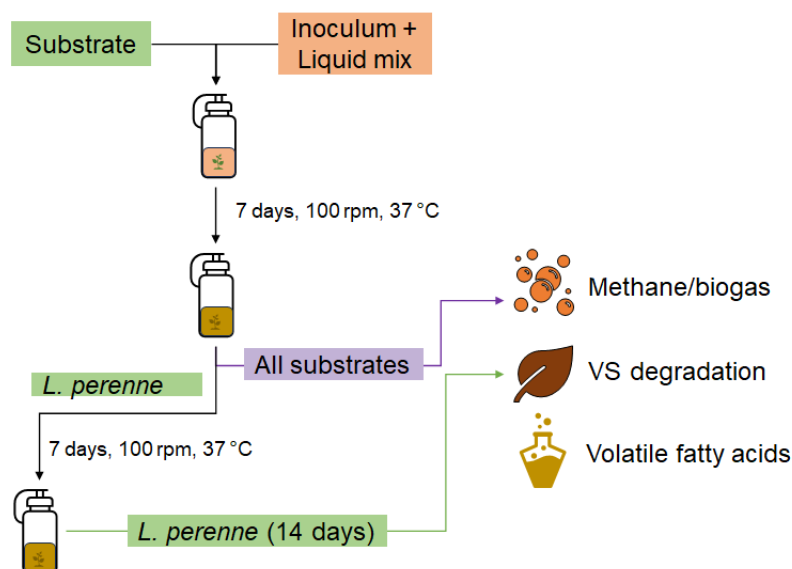


Figure 4.1: Setup for the one-stage fermentation assay.

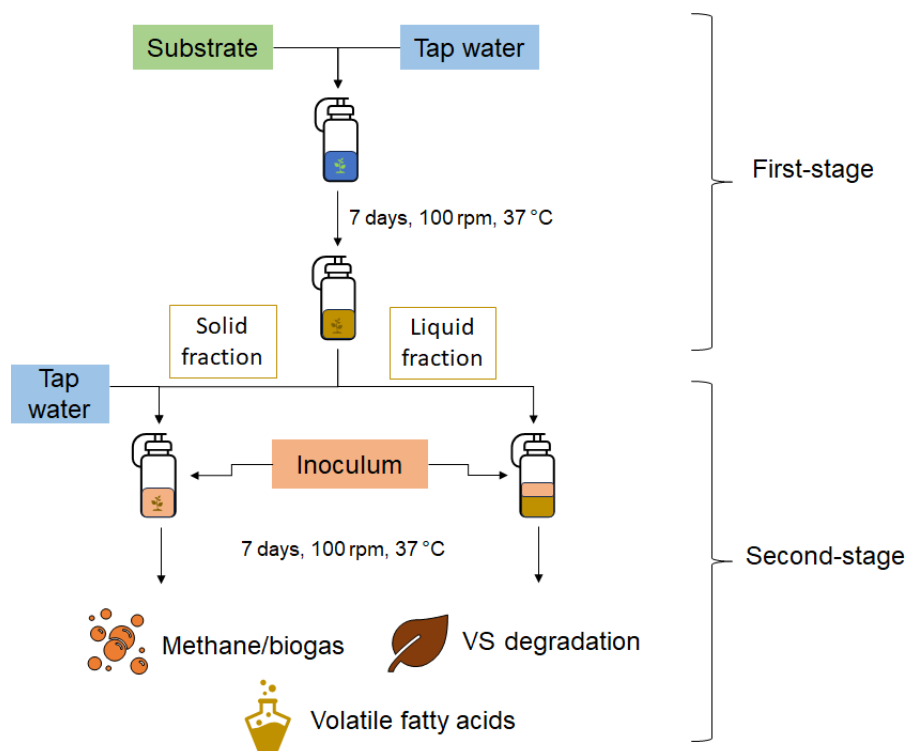


Figure 4.2: Setup for the two-stage fermentation assay.

4.2.5 Analytical methods

Substrate and solid digestate samples were analysed in terms of total (TS) and volatile (VS) solids, while liquid samples were analysed in terms of total (TSS), (VSS) suspended solids and pH according to standard methods⁵⁰. Samples were preserved at -20 °C after sampling until further analysis were performed.

Besides TS and VS, substrate samples were characterised in terms of elemental carbon (C), nitrogen (N), oxygen (O), hydrogen (H), and sulphur (S) by Celnigis Analytical (Limerick, Ireland) as described in the European Standard EN 15104:2011 – the elemental data was analysed in duplicate and reported in terms of dry matter. The amount of C N, O, H, and S was used to estimate the theoretical chemical oxygen demand (ThCOD)⁵¹ (Chapter 3), the theoretical BMP (TBMP)⁵² (Chapter 3), and the C:N ratio. The crude protein content was calculated by multiplying the %N by 6.25⁵³. Data related to the fibre content of the grassland biomass was provided by Teagasc in dry weight as neutral detergent fibre (NDF) and acid detergent fibre (ADF) – fibre content was determined using near-infrared spectroscopy (NIRS) technology and following the procedure described by Lorenz *et al.*⁵⁴. Hemicellulose content was calculated as the difference between NDF and ADF; and ADF was used as a proxy for the cellulose and lignin content^{25,55}. Gas volume was measured using the water displacement method⁵⁶. Methane composition was determined using gas chromatography (Varian CP-3800, Varian Inc., Walnut Creek, CA USA) equipped with a thermal conductivity detector (TCD), and a hydrogen generator (WhatmanTM).

Liquid samples were thawed to room temperature, centrifuged at 16×1000 *g* for 10 min, and

filtered (pore size of 0.2 μm). These filtered samples were used to determine soluble COD, VFAs, lactic acid, and ammonia. Soluble COD was measured using photometric kits (0-1500 $\text{mg}\cdot\text{L}^{-1}$, Reagecon[®], Reagecon Diagnostics Ltd., Ireland) and readings were performed in UV/Vis Spectrophotometer (DR3900, Hach[®], EUA). TAN values were calculated from ammonium results obtained using a colorimetric method based on the reaction of ammonia with hypochlorite ions generated by the alkaline hydrolysis of sodium dichloroisocyanurate to monochloramine (Gallery[™] Plus Discrete Analyzer, Thermo Fisher Scientific). D-Lactic acid and L-lactic acid concentrations were measured using a photometric method based on the enzymatic reaction of D-lactic acid and L-lactic acid with D-Lactate-Dehydrogenase and L-Lactate-Dehydrogenase, respectively, at 37 °C (Gallery[™] Plus Discrete Analyzer, Thermo Fisher Scientific). The concentration of lactic acid reported here consists of a combination of D- and L-lactic acid. VFAs were analysed using gas chromatography (7890 GC System, Agilent Technology) equipped with a flame ionisation detector (FID), and a hydrogen generator (Whatman[™]). Helium was used as carrier gas and acid separation was performed using a capillarity column BP21, FFAP (SGE Analytical Science) with 0.25 μm of film thickness, 30 m of length and 0.25 mm of internal diameter. VFA samples were diluted with distilled water (when appropriate), and an internal standard solution (100 μL , fixed volume) prepared with orthophosphoric acid and ethyl-butyric acid. The calibration curve was prepared for the following acids: acetic, propionic, butyric, iso-butyric, valeric, iso-valeric, and caproic. The COD equivalent for VFAs and lactic acid was calculated based on its complete oxidation to CO_2 and H_2O – 1.067 (acetic and lactic), 1.514 (propionic), 1.818 (iso/butyric), 2.039 (iso/valeric), and 2.207 (caproic). In this work, results for lactic acid and VFA are mainly expressed in $\text{gCOD}\cdot\text{L}^{-1}$; VFA results are also expressed in terms of grassland biomass added ($\text{gCOD}\cdot\text{gVS}^{-1}$). Significant analysis was performed when applicable ($n \geq 3$) to compare the difference between means in IBM[®] SPSS[®] Statistics version 28.0.0.0 (190) using a Welch's t-test, considering a confidence level of 95%.

4.3 Chemical Parameters

4.3.1 Volatile solids degradation

Substrate conversion was defined as the consumption of the biomass' biodegradable materials and is represented by the VS degradation of each substrate. The VS degradation for the BMP experiment was described previously in Chapter 3 (page 45). For both fermentation assays, the VS degradation also considered the VS measured in both liquid phase and solid phase at the beginning and end of each fermentation trial. Moreover, it was assumed that only the substrate was consumed over the course of the fermentation, meaning that the solid digestate did not degrade over time and had a constant VS of $m_{digestate}(0)$ (Equation 13)⁵⁷.

$$m_{sample}(t) = m_s(t) + m_{digestate}(0) \quad (13)$$

$$VS_{deg}(t) = 1 - \frac{m_s(t)}{m_s(0)} \quad (14)$$

Where: t is the digestion time, $m_{sample}(t)$ is the mass of substrate plus inoculum at a time t ; $m_s(t)$ is the mass of substrate; $m_i(0)$ is the mass of inoculum at the beginning of the fermentation; and $VS_{deg}(t)$ represents the VS degradation of a substrate after the digestion (in %VS). Mass is expressed in gVS .

4.3.2 Biomethane production

The volume of biogas and biomethane was normalised to standard conditions (101.3 kPa, 273 K) for all experiments proposed in this study (Equation 8, Section 3.3.4, page 47)⁵⁸. The cumulative biogas production was calculated considering the headspace volume ($v^h = 213.27$ NL for bottles), and the volume collected from the gas bags (v^b) at each sampling point (Equation 9a, Section 3.3.4, page 47). The cumulative production of methane considered the composition of methane in the biogas at each sampling point (Equation 9b, Section 3.3.4)⁵⁹. As the bottles were not vented between measurements, a correction for the methane composition in the headspace from a previous sampling point was considered (Equation 9b, Section 3.3.4). The volumetric yield for methane and biogas was calculated in terms of volatile solids of grassland biomass silage fed to the digestion (Equation 9c, Section 3.3.4). For the BMP assay, the production of methane and biogas from each substrate was corrected by subtracting the volume produced in the control-bottles. For fermentation assays, no correction was applied to the production observed from the sample-bottles.

4.3.3 Acidification yield and VFA production

VFA production was evaluated in terms of acidification, VFA concentration, and VFA net production (yield). The acidification yield was calculated based on the accumulation of VFAs and soluble COD in the leachate at the end of the fermentation (Equation 15)³⁷. The net production of VFAs was calculated by discounting the amount of VFAs in the leachate at the beginning of the batch (Equation 16), and the yield was obtained by dividing the net production of VFAs by the initial quantity of substrate supplied (Equation 17).

$$\chi = \frac{VFA_t}{sCOD}, \quad (15)$$

Where, χ represents the acidification yield (%), VFA_t represents the concentration of VFAs (in total) at the end of each batch ($gCOD.L^{-1}$), and $sCOD$ represents the amount of soluble COD at the end of each batch ($gCOD.L^{-1}$).

$$VFA_{net}(t) = VFA(t) - VFA(0), \quad (16)$$

Where, VFA_{net} is the net concentration of VFAs (or any specific acid) at a time t , $VFA(t)$ is the VFA concentration in the leachate at a time t , and $VFA(0)$ is the VFA concentration in the leachate at the

beginning of each batch. All concentrations are represented here in gCOD.L⁻¹.

$$Y_{VFA} = \frac{VFA_{net}(t)}{m_g(0)}, \quad (17)$$

Where, Y_{VFA} is the yield of VFAs produced at a time t (gCOD.gVS⁻¹) based on the VFA net concentration (VFA_{net}) at that time t , and the mass of silage fed to the bottles or reactor ($m_g(0)$, in gVS).

To incorporate the methane production observed in the one-stage fermentation assay to the total product yield, methane volumes in STP were converted to chemical oxygen demand (COD) using the theoretical conversion $1gCOD = 350mLCH_4$. Methane yield was calculated by dividing the gCOD of methane by the gVS of silage added. The total production yield was obtained by summing the VFA yield and methane yield.

4.4 Results and Discussion

4.4.1 Clover's buffering capacity can be associated with its higher volatile solids degradation under fermentation conditions

The main objective of this study was to investigate the potential of fresh grassland biomass (such as grasses and clovers) as feedstock for AD, focusing on the production of VFAs, especially butyric acid. Moreover, the effect of nitrogen fertilisation on substrate conversion and degradation was also evaluated. For that, as a first step, the degradation of each substrate (Table 4.2) was determined in two different settings – under methanogenic conditions (BMP assay) and under fermentation conditions (one- and two-stage fermentation assays). The lack of studies focusing on the fermentation of fresh grassland biomass (e.g., clovers) to VFAs for butyric acid production motivated the design of this BMP assay. In this way, the results for degradation and conversion under methanogenic conditions were used to establish a baseline of comparison for the substrates tested.

Table 4.2: Volatile solids degradation for each experiment: in the one-stage fermentation (after 7 and 14 days); in each stage of the two-stage fermentation (6 and 14 days); and in the biomethane potential assay (after 28 days).

Substrate	One-stage fermentation		Two-stage fermentation		BMP (28 days)
	(7 days)	(14 days)	(6 days)	(14 days)	
<i>L. perenne</i> , Lp	62.8 (4.8)	63.3 (1.5)	37.8 (3.8)	70.9 (6.8)	83.2 (7.3)
<i>L. perenne</i> *, Lp*	69.1 (8.0)		n/a	n/a	88.7 (0.6)
<i>T. pratense</i> , Tp	73.1 (18.7)		n/a	n/a	73.5 (4.0)
<i>T. repens</i> , Tr	84.0 (6.3)		13.3 (3.2)	76.1 (7.2)	72.8 (2.9)
<i>L. perenne</i> + <i>T. repens</i> , Lp+Tp	64.2 (13.7)		19.7 (2.5)	62.4 (8.1)	75.6 (4.7)

Note: *Supplied with 300 kgN.ha⁻¹.yr⁻¹. In the two-stage fermentation, 7 days is equivalent to the end of the first-stage. All VS degradation levels are compared to the starting VS of substrate added to the bottles.

Overall, the VS degradation observed in the BMP assay varied between 72.8±2.8% (*T. repens*) to 88.7±0.6% (300 kgN.ha⁻¹.yr⁻¹ *L. perenne*). Moreover, no difference in degradation was observed when comparing *L. perenne* supplied with 150 kgN.ha⁻¹.yr⁻¹ and 300 kgN.ha⁻¹.yr⁻¹ (p-value =

0.247), indicating that a higher dose of nitrogen fertiliser had no effect in substrate degradation. Although the same pattern was observed in the previous study (see Chapter 3), where VS degradation levels varied around 80%, it is important to highlight that the substrate addition to the bottles was different in both studies.

In the present study, each substrate was added to the digestion bottles as they were received from the field, with the intended species (e.g., *T. pratense*, 70% of species composition) mixed with the unsown species (e.g., 30% of species proportion). Consequently, no manual separation between intended and unsown species was performed, as in the previous study. However, a difference in species composition was observed between monocultures, with the proportion of intended species in monocultures of clovers particularly lower compared to *L. perenne* monocultures (Table 4.1). The presence of unsown species in monoculture grassland fields has been associated with lower forage quality and yield, reducing animal feed production at higher operational costs and higher usage of chemical weed control¹⁰. However, the impact of unsown species in the digestion of *T. repens* and *T. pratense* was not representative in terms of VS degradation, when comparing the VS degradation values from the previous study (see Chapter 3, substrate sorting and separation) and this study (no separation). Therefore, manually separating the unsown species from the intended species did not seem to affect the degradation of the substrate.

Another important factor investigated with the BMP assay was the rate of degradation of each substrate (Figure B.1). Methanogenic conditions favour biomass degradation as a consequence of the neutral to basic pH levels and constant conversion of acids to methane^{32,60}. Therefore, digesting these substrates at methanogenic conditions made it possible to establish a biodegradability threshold. In our study, no difference was observed in the profile of VS degradation between *T. pratense* and *T. repens*. No difference was also observed in the profile of VS degradation between *L. perenne* supplied with 150 and 300 kgN.ha⁻¹.yr⁻¹. Results showed that the VS degradation profile was the same for species of the same functional group. Moreover, a sharper and faster decrease in VS content was observed for both *L. perenne* substrates compared to *T. pratense* and *T. repens*, especially for the *L. perenne* supplied with 300 kgN.ha⁻¹.yr⁻¹. After 2 days of digestion, the VS degradation rate of *L. perenne* (150 kgN.ha⁻¹.yr⁻¹) was 55% and 94% higher than the degradation rate of *T. pratense* and *T. repens*, respectively.

When considering the VS degradation rate of *L. perenne* (300 kgN.ha⁻¹.yr⁻¹), it was 2.4-fold higher compared to clovers. Therefore, despite starting with the same amount of VS, the degradation of clovers was slower than the degradation of grasses. Clovers are richer in nitrogen than other grassland biomass (Table 4.1) due to its ability to fixating atmospheric N₂²⁹. The degradation of clovers led to a higher accumulation of ammonia⁶¹, which can negatively impact the biomass degradation⁶⁰, slowing the process. On the other hand, a slower degradation of the biomass could be beneficial for the process, as it will result in a slower accumulation of acids, decreasing possible inhibitory effects of a fast acid accumulation³³. Irrespective of the substrate used, most of the biomass degradation was reached by 14 days of digestion – afterwards, the VS content was constant. Therefore, it was observed that the maximum degradation for all substrates was reached by 14 days, with a maximum degrada-

tion rate between 2 to 7 days. This maximum degradation, at this work’s operational conditions, was considered as the biodegradability threshold for these substrates. Moreover, this threshold was used as a baseline to design the fermentation assays.

Alternatively, substrate degradation levels were different in the one-stage fermentation depending on the grassland biomass fermented. In the one-stage fermentation of *L. perenne*, lower VS degradation levels were observed compared to the BMP assay, irrespective of the nitrogen fertiliser dose that was supplied to the grass. On the other hand, VS degradation levels for both clovers (*T. pratense*, *T. repens*), and the mixture of two species (*L. perenne* with *T. repens*) were closer to the degradation levels reached in the BMP assay. This discrepancy for grasses and the similarity for clovers may be a result of the pH profile observed during the one-stage fermentation (Figure 4.3).

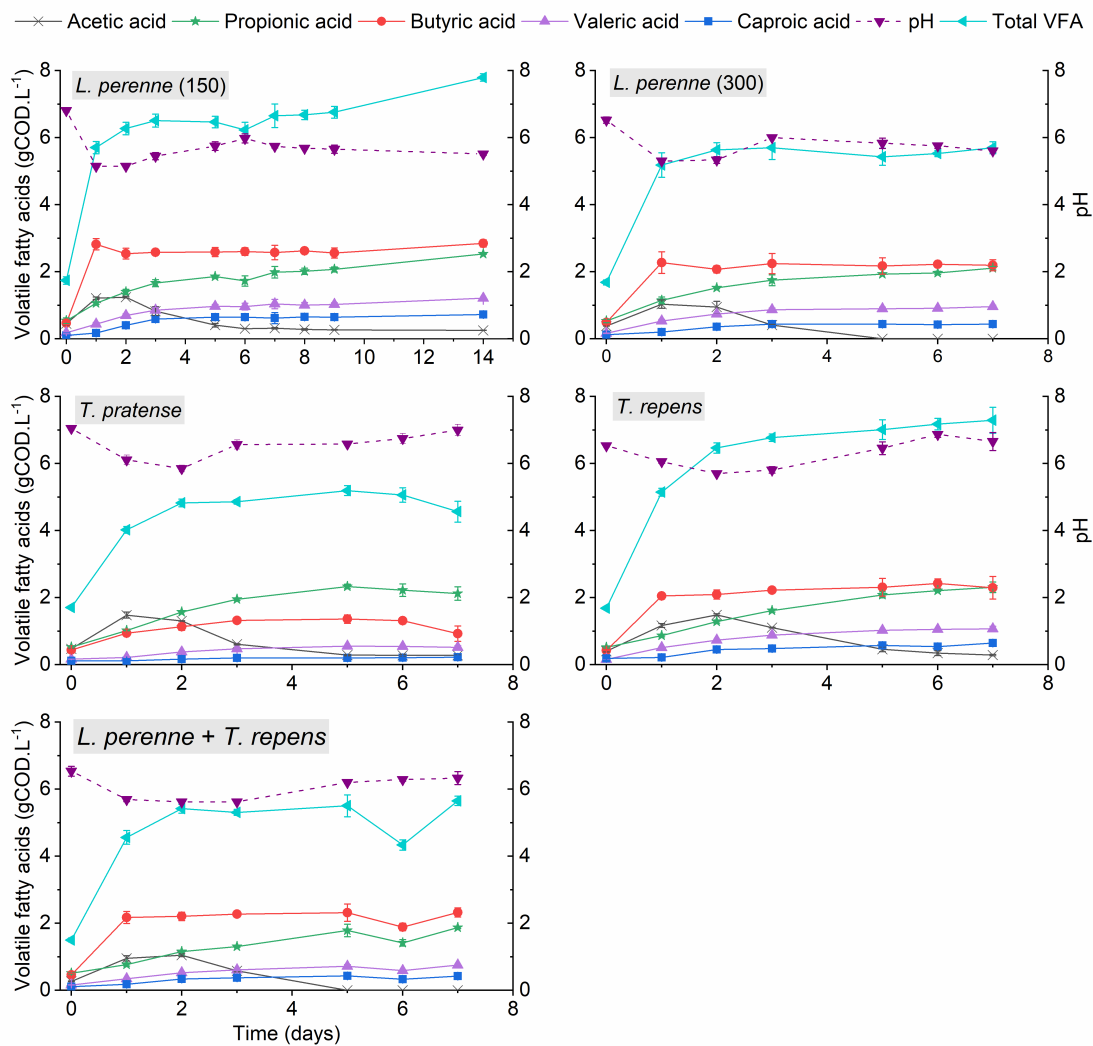


Figure 4.3: pH profile and volatile fatty acids production in the one-stage fermentation of *L. perenne* (150, 150 kgN.ha⁻¹.yr⁻¹), *L. perenne* (300, 300 kgN.ha⁻¹.yr⁻¹), *T. pratense*, *T. repens*, and a mixture of *L. perenne* and *T. repens*. Results for the inoculum (negative control) are also displayed.

It is known that the hydrolysis of biomass can be hindered at acidic pH levels³², with neutral to basic ranges considered ideal to maximise the biomass hydrolysis^{37,62}. In the BMP assay, these neutral

to basic pH levels (7.5-8.0) were constantly maintained. On the other hand, in the fermentation of both *L. perenne* substrates, pH levels started at 6.5-6.8, reaching 5.2-5.3 after two days, and 5.6-5.7 after 7 days. Even increasing the fermentation time to 14 days for *L. perenne* did not improve the substrate degradation, and the final pH level was still acidic (5.5 ± 0.0). In the fermentation of clovers, however, pH levels were consistently above 5.7, with lower pH levels reached after two days of fermentation (5.7-5.9), and mildly-acidic to neutral levels reached by the end of the fermentation (6.7-7.0). The same pattern from clovers was observed when the mixture of *L. perenne* and *T. repens* was fermented. This was associated with the higher nitrogen content of clovers and the release of ammonia from its degradation, as explained before. For example, in the fermentation of *T. repens*, TAN levels reached values 11x higher compared to the fermentation of *L. perenne* after 7 days. For *T. pratense*, TAN levels were 6x higher compared to *L. perenne*. As a consequence of this ammonia release, the degradation of clovers contributed to buffering the pH of the fermentation. Therefore, pH levels reached favourable ranges for biomass degradation in the fermentation of clovers compared to the fermentation of grasses.

Operating the fermentation of *L. perenne* ($150 \text{ kgN} \cdot \text{ha}^{-1} \cdot \text{yr}^{-1}$), *T. repens*, and *L. perenne* with *T. repens* in two stages did not improve substrate degradation compared to the one-stage fermentation. In fact, in the pre-treatment first-stage (first stage, SRT=7 days), when no inoculum was added to the bottles, VS degradation levels were lower compared to the one-stage fermentation. However, the fact that no inoculum was added at the first 7 days of fermentation does not necessarily mean the absence of a microbial community. In fact, pH levels started around 6.0 and decreased to 4.0 after two days, reaching levels of 3.5-4.0 by the end of the first-stage. As these substrates were not sterilised before the experiment, this pH decrease could be a result of the substrate indigenous microbial community, which can fermenting the water soluble carbohydrates from the surface of the substrate to produce lactic acid⁶³ (Figure 4.4). This has been applied previously as a strategy to accumulate lactic acid in leach-bed reactors (LBRs) from fresh grass over a 33-day trial ($9.4 \pm 0.9 \text{ g} \cdot \text{L}^{-1}$)³⁸.

Despite reaching pH levels that hindered degradation³⁷, a significant difference was observed between *L. perenne* and the other two substrates (p -value <0.01) at this first-stage. This could be associated with the production rate of lactic acid, which was faster at the first two days of pre-treatment for *T. repens* and the mixture of *L. perenne* with *T. repens*. When thawing the substrate prior to the fermentation assays, a rich-liquor with approximately $40 \text{ gCOD} \cdot \text{L}^{-1}$ leached from the *T. repens* substrate when it was pressed quickly by hand. From this liquor's COD, 47.6% was composed of total reducing sugars. Applying the same technique to *L. perenne*, however, did not result in a liquor, and COD measurements were only possible when *L. perenne* was immersed in water ($0.9 \text{ gCOD} \cdot \text{L}^{-1}$). Therefore, this rich-liquor from *T. repens* could have provided the necessary nutrition for the lactic-acid producing bacteria on the surface of *T. repens*, resulting in a faster production of lactic acid and a lower degradation of the substrate as consequence. This rich-liquor opens the possibility for other processes that may be designed to further valorise *T. repens*, starting from a recovery step to extract this liquor efficiently and the conversion of its sugars to VFAs and lactic acid.

As mentioned previously, VS degradation levels were numerically the same when comparing the

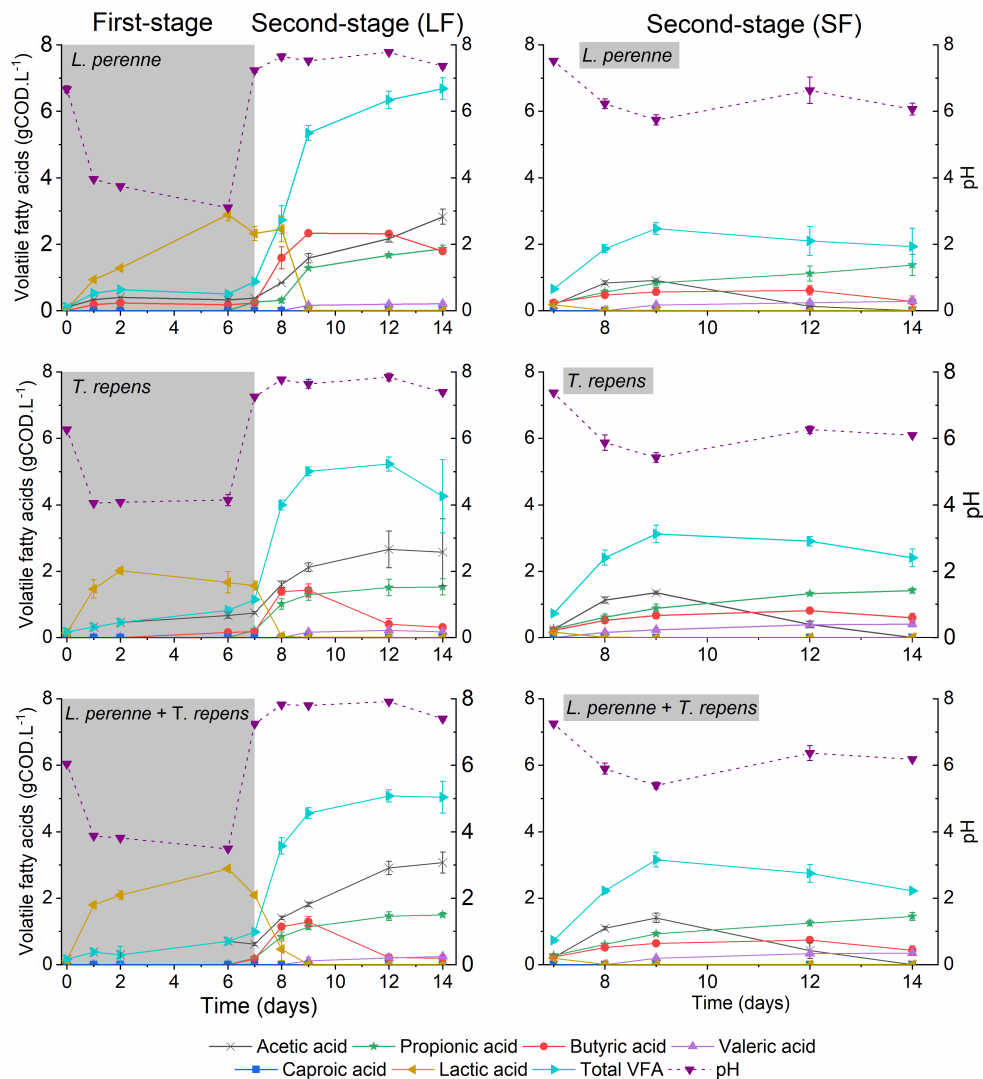


Figure 4.4: Profile of pH, lactic acid and volatile fatty acids in the two-stage fermentation of *L. perenne*, *T. repens*, and a mixture of *L. perenne* and *T. repens*. LF stands for liquid fraction and SF stands for solid fraction.

one-stage and the two-stage fermentation. The VS degradation of the two-stage fermentation was measured considering the degradation in both first-stage and second-stage, in comparison to the fresh substrate added to the bottles. At the beginning of the second-stage, pH levels were also corrected to neutral levels (Figure 4.4) to balance the lower pH from the first-stage. After inoculation, pH levels were mildly acidic (around 6.0) as the solid fraction from the first-stage was fermented further. The inoculum used in the one-stage fermentation and the two-stage fermentation consisted of the leachate and solid digestate from a stable LBR for the production of VFAs from ryegrass (*L. perenne*) silage and cattle slurry. Therefore, it was an acclimatised inoculum not only to produce VFAs, but also to degrade lignocellulosic biomass. Considering only the second stage of the two-stage fermentation, VS degradation levels reached $55.0 \pm 5.2\%$ (Lp), $77.9 \pm 3.6\%$ (Tr), and $57.3 \pm 13.2\%$ (Lp+Tr), which are higher values compared to the first-stage. Therefore, an acclimatised inoculum was crucial for increasing degradation levels, indicating the importance of selecting an appropriate inoculum source

not only for the production of VFAs, but also for substrate degradation.

4.4.2 A balanced C:N ratio for *L. perenne* as effective as a higher nitrogen fertilisation rate

BMP assays have been thoroughly applied to determine the potential of a wide-range of feedstocks for AD purposes. However, comparing the same feedstock with different studies has been discouraged as important operational conditions in the AD process such as temperature, digestion time, vessel configuration and inoculum have a great impact in the methane production and are usually not the same across studies^{59,64,65}. In our study, some grassland species harvested from the same field as in the previous study (see Chapter 3), but not the same plots, were tested – *L. perenne*, *T. pratense*, *T. repens*, and a mixture of *L. perenne* and *T. repens*. Moreover, the same inoculum was used in both studies. The main difference was how substrates were prepared - for this study, intended species were not manually separated from unsown species and the size of the substrate was not reduced. Therefore, as the grassland biomass was received from the field it was directly fed to the bottles. However, the decision to avoid cutting the substrate led to failures in our system. Gas bubbles were trapped in the biomass bed, which was pushed up as more gas was produced, blocking and clogging the needles that connected gas bags to the bottles. Consequently, some bottles opened, decreasing the amount of replicates in the BMP assay, which hindered an appropriate statistical analysis for most substrates tested. It is recommended to observe these results as a screening for further experiments, which should be performed to draw more specific conclusions.

One of the first aspects tested in our study was the effect of nitrogen fertilisation rate to methane and VFA yields. Higher doses of nitrogen fertiliser are commonly supplied to forages to achieve high forage yields⁶⁶. However, this practice leads to higher land management and environmental costs⁶⁶ at a lower nitrogen efficiency¹⁰, and its gains to methane or VFA production are still unknown. Therefore, the efficiency of using a higher fertilisation rate in feedstocks for methane or VFA production should be evaluated. In our study, no significant difference in methane yield was observed from the digestion of *L. perenne*, irrespective of the nitrogen fertiliser dose applied to the forage in the field (Figure 4.5). This indicates that applying a higher dose of nitrogen fertiliser did not improve methane yield at substrate-level. Numerically, the methane yield obtained using the 150 kgN.ha⁻¹.yr⁻¹ *L. perenne* was 18% higher than the methane yield obtained from digesting the 300 kgN.ha⁻¹.yr⁻¹ *L. perenne* after 21 days. The difference in methane yield between *L. perenne* substrates decreased from 18% to 10% after 28 days. In comparison, an opposite trend was observed in the previous study (see Chapter 3), where a higher dose of nitrogen fertiliser led to a 29% higher methane yield at substrate-level compared to a *L. perenne* supplied with 150 kgN.ha⁻¹.yr⁻¹ after 21 days of digestion.

The lower methane production from the 150 kgN.ha⁻¹.yr⁻¹ *L. perenne* in the previous study (see Chapter 3) was associated with its higher C:N ratio, which was also outside the optimum range for AD⁶⁷. In this work, however, the C:N ratio of both *L. perenne* substrates was the same irrespective of the nitrogen fertiliser dose supplied to each forage, and within the optimum range for methane production (Table 4.1). Moreover, the C:N ratio of the 150 kgN.ha⁻¹.yr⁻¹ *L. perenne* used in this

study was approximately 30% lower compared to the same forage (from another plot) used in the previous study (see Chapter 3). Therefore, nitrogen fertiliser dose to *L. perenne* fields does not affect the production of methane as long as a balance C:N ratio is achieved for the forage. However, it is also worth noting that these comparisons are considering the production of methane at substrate-level. As shown in the previous study (see Chapter 3), a higher dose of nitrogen fertiliser improved the forage yield of *L. perenne*, which directly affected the prediction of methane yield per field area. The higher forage yield represented an increase of 44% in area-specific methane yield when comparing both *L. perenne* substrates. Therefore, it is safe to assume that the same impact in area-specific methane yield would be observed in the results of this study's BMP assay.

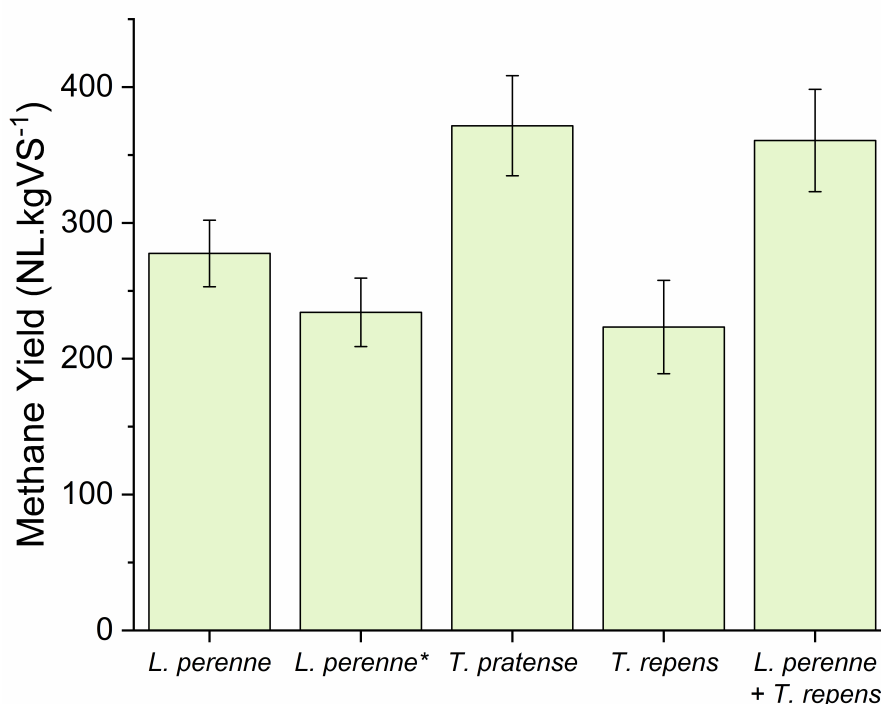


Figure 4.5: Maximum methane yield observed from *L. perenne* (150 kgN.ha⁻¹.yr⁻¹), *L. perenne* (300 kgN.ha⁻¹.yr⁻¹), *T. pratense*, *T. repens*, and a mixture of *L. perenne* and *T. repens* after 28 days.

4.4.3 Weed intrusion as factor hindering the accumulation of methane from clover fields

Despite *L. perenne* being vastly studied as a substrate, alternatives to the mono-digestion of *L. perenne* have been proposed due to the substrate low and unbalance nutrient content²⁵, which can lead to process failure over an extended period of time²⁸. Clovers, lucerne and herbs have been proposed as substrate^{68,69} or co-substrates^{25,30} in AD due to its higher nutrient availability, which can improve substrate digestibility and conversion.

In our study, the highest methane yield was reached in the mono-digestion of *T. pratense* (371.5 ±36.9 NL.kgVS⁻¹) and the co-digestion of *L. perenne* and *T. repens* (360.6 ±37.6 NL.kgVS⁻¹). These results are aligned with some observations from the literature and what has been discussed

previously in the previous study (see Chapter 3). Higher methane production from *T. repens* has been observed at thermophilic conditions using a manure-based inoculum compared to *L. perenne* digested with the same inoculum²⁵. Under mesophilic conditions, the mono-digestion of *T. pratense* led to methane yields between 306-328 NL.kgVS⁻¹ after 90 days, while the co-digestion of *L. perenne*, *T. pratense*, and *T. repens* resulted in methane yields between 342-352 NL.kgVS⁻¹³⁰. Moreover, synergistic effects were observed from associating *L. perenne* with clovers and herbs²⁵, at both substrate-level and field-level (see Chapter 3) due to the higher nitrogen content from *T. repens*^{25,70}.

However, in the present work, a high numerical difference in methane yield was observed when mono-digesting *T. pratense* (371.5 ± 36.9 NL.kgVS⁻¹) and *T. repens* (223.4 ± 34.4 NL.kgVS⁻¹). This difference may be associated with the weed intrusion in the *T. repens* field plot (Table 4.1). As highlighted in the previous study (see Chapter 3), not necessarily co-digesting different grassland species will prove beneficial for methane accumulation, as mixing some species would result in antagonistic effects – e.g., the co-digestion of *T. repens* or *T. pratense* with *Phleum pratense* (another species of grass) or *Plantago lanceolata* (a common herb in temperate grasslands). Moreover, it is likely that the unsown grassland species that composed the *T. repens* substrate is not only composed of *L. perenne* as the methane yield observed for the co-digestion of *L. perenne* and *T. repens* was higher than *T. repens* (Figure 4.5).

In reality, despite cultivated in the same field and under the same conditions, each field plot of the same species of grassland biomass may have a different species composition due to weed intrusion, which contributes to the heterogeneity of the feedstock. For example, from five bags of *L. perenne* supplied with 150 kgN.ha⁻¹.yr⁻¹ received from five different field plots, the quantity of *L. perenne* species in those bags varied between 80% to 92%. For *L. perenne* supplied with a double dose of nitrogen fertiliser, the intrusion of weed was lower, and *L. perenne* represented 87% to 97%. On the other hand, the intrusion of weed in clover field plots was higher compared to grasses – *T. pratense* represented 53% and 70% of the species composition in a plot, while *T. repens* represented 37%, 48%, and 78% of the species composition. However, even if not manual separation was performed, the bags containing the higher amount of the intended species were selected as substrate for the BMP assay and fermentation assays.

Despite understanding that the methane production from *T. repens* in this study does not represent the potential of the species itself (as shown in Chapter 3), it is unlikely that manual separation will be performed for *T. repens* in a large-scale AD plant. Therefore, the experimental design for fermentation in this study did not include manual separation of species – but further studies are encouraged to understand the potential of each species in VFA production. Moreover, both the previous study (see Chapter 3) and this study presented evidence that digesting the same species from the same field may not necessarily translate into the same product yield due to a variability in chemical composition when considering different plots of the same species, in same field and at the same time/season. This would affect designing forage fields for biomass production and AD plants, as this heterogeneity affects nutrient availability of crops, leading to AD failure in the long run^{26,28,71}.

4.4.4 Selective production of butyric acid mainly obtained from the fermentation of *L. perenne*

The main goal of the one-stage fermentation assay was to evaluate the potential of grassland biomass for VFA accumulation, focusing in selectively producing butyric acid. In this way, VFA and butyric acid production was monitored in batch-mode for 7-14 days using *L. perenne* (150 and 300 kgN.ha⁻¹.yr⁻¹), *T. pratense*, *T. repens*, and a mixture of *L. perenne* and *T. repens* as substrates. The experiment was designed based on a stable pilot-scale reactor for VFA production from grass silage and cattle slurry. The inoculum used in our study was sourced from this pilot-scale reactor to establish a minimal efficiency in the fermentation, as the inoculum was acclimatised to produce VFAs from lignocellulosic biomass. Moreover, pH levels were corrected at the beginning of the fermentation using a sodium bicarbonate buffer to prevent acidic levels from the start. This was performed because a sharp drop in pH has been previously observed during the fermentation of these feedstocks – which, associated with the further decrease due to the production of VFAs, could hinder substrate degradation and product yield^{62,67}.

The highest production of VFAs in our study was observed when fermenting *L. perenne* substrates, irrespective of the fertilisation dose supplied to these forages. In fact, no significant difference (Figure 4.6, p-value = 0.137) was observed when comparing the VFA yield resulting from the fermentation of 300 kgN.ha⁻¹.yr⁻¹ (558.4±18.5 mg O₂.gVS⁻¹) and 150 kgN.ha⁻¹.yr⁻¹ *L. perenne* (473.1±63.7 mg O₂.gVS⁻¹). Moreover, no significant difference was observed in terms of butyric acid yield (p-value = 0.442), with butyric acid accounting for approximately 40% *g.L⁻¹ of the VFA yield for both substrates. This indicates that a double dose of nitrogen fertiliser did not improve the production of butyric acid or VFAs. However, a significant difference was observed in terms of total product yield, which considered both the production of VFAs and methane. The fermentation of 300 kgN.ha⁻¹.yr⁻¹ resulted in a total product yield 37% higher (p-value < 0.05) compared to 150 kgN.ha⁻¹.yr⁻¹ – which was attributed to the 67% higher methane accumulation in the 300 kgN.ha⁻¹.yr⁻¹ (Figure 4.6). The difference in methane accumulation for both *L. perenne* substrates may be a result of the pH profile, as pH levels reached 6.0 after three days of fermentation using the 300 kgN.ha⁻¹.yr⁻¹ *L. perenne*. This increase in pH coincided with an increase in the accumulation of methane, leading to a higher methane yield after 7 days of fermentation.

The pH profile in the fermentation of *T. pratense* was also correlated to the substrate's production profile, leading to a higher methane accumulation and lower VFA production. In fact, the VFA yield observed from *T. pratense* was significantly lower compared to 150 kgN.ha⁻¹.yr⁻¹ *L. perenne* (p-value < 0.05) and the other substrates (p-value < 0.01). The lowest pH reached in the fermentation of *T. pratense* was 5.8 (after two days), but levels were consistently above 6.6, which favoured the production of methane⁷². This pH profile was correlated to the release of ammonia in the fermentation liquid, as discussed previously, with TAN values reaching 224.2±14.0 mg.L⁻¹ after 7 days. The same pH profile was observed in the fermentation of *T. repens*, with a pH of 6.7 and TAN levels of 384.3±28.0 mg.L⁻¹ after 7 days (Figure 4.3). However, despite having a similar production of methane, the production of VFAs from the fermentation of *T. repens* was significantly higher compared

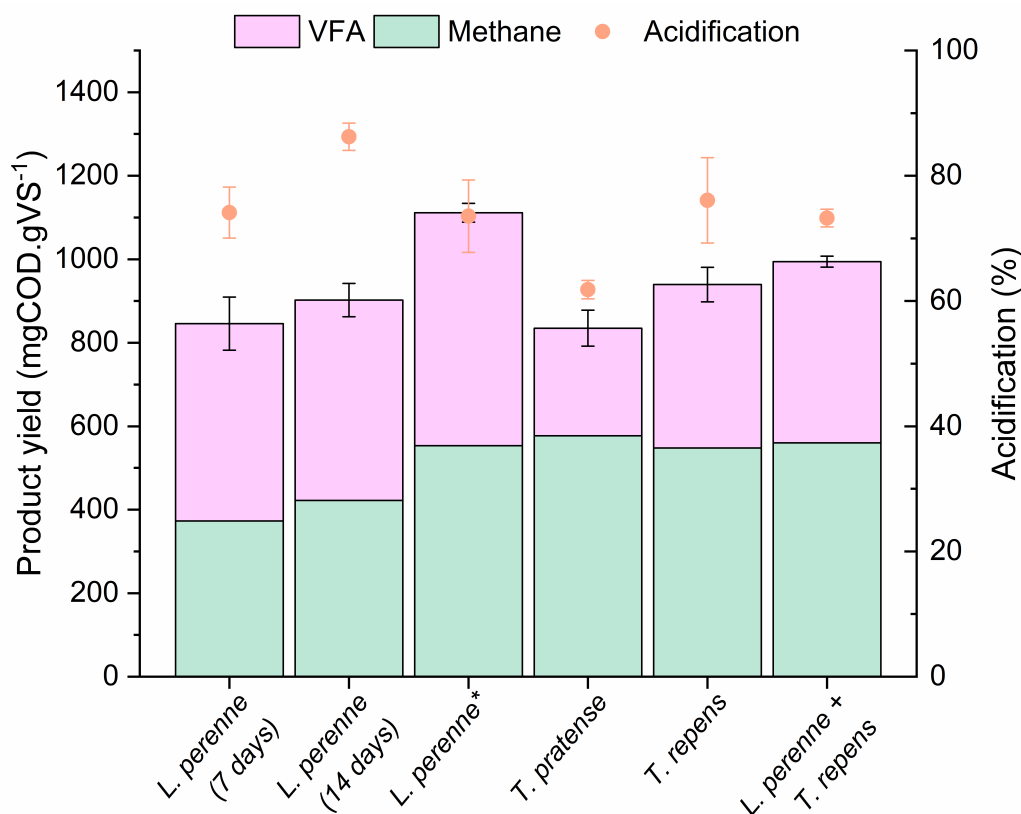


Figure 4.6: Acidification (orange dot) and total product yield – as VFA (pink bar) and methane (green bar) – in the one-stage fermentation of *L. perenne* (150 kgN.ha⁻¹.yr⁻¹) after 7 and 14 days); and *L. perenne** (300 kgN.ha⁻¹.yr⁻¹), *T. pratense*, *T. repens*, and a mixture of *L. perenne* and *T. repens* (after 7 days).

to the fermentation of *T. pratense*. This may be associated to unsown species that intruded the *T. repens* field. The presence of these species may have favoured the production of VFAs, especially butyric acid, possibly indicating interspecific effects that should be further investigated. On the other hand, even with this higher production of VFAs from *T. repens*, the total product yield of both clover substrates was the same. The total product yield of clovers was only significantly different from the total product yield of 300 kgN.ha⁻¹.yr⁻¹ *L. perenne* (28%, p-value < 0.01) due to a combination of VFA and methane accumulation (Figure 4.6).

Table 4.3: Net production of Volatile fatty acids (VFAs) in the one-stage fermentation of grassland biomass.

Substrate	VFAs (g.L ⁻¹)	Acetic (%)	Propionic (%)	Butyric (%)	Valeric (%)	Caproic (%)	VFA yield ^c (gCOD.gCOD ⁻¹)
<i>L. perenne</i> ^a	2.8 (0.4)	0.0	31.6	40.3	18.1	10.0	0.32 (0.04)
<i>L. perenne</i> ^b	3.3 (0.2)	0.0	35.8	37.3	17.2	9.7	0.37 (0.03)
<i>L. perenne</i> ^{*,a}	2.7 (0.1)	0.0	39.4	35.9	17.4	7.3	0.36 (0.01)
<i>T. pratense</i> ^a	2.1 (0.3)	0.0	52.5	18.1	12.3	5.0	0.16 (0.03)
<i>T. repens</i> ^a	3.4 (0.4)	0.0	35.2	30.3	15.4	8.6	0.26 (0.03)
<i>L. perenne</i> + <i>T. repens</i> ^a	2.5 (0.1)	0.0	36.0	41.8	14.5	7.6	0.31 (0.01)

Note: ^aSupplied with 300 kgN.ha⁻¹.yr⁻¹; ^asubstrates fermented for 7 days; ^bsubstrates fermented for 14 days; ^cin terms of substrate theoretical COD.

pH is a very important parameter in the production of VFAs not only because it affects biomass

hydrolysis¹⁵ and VFA yield⁷², but also the VFA profile^{15,32}. In our study, the fermentation of *T. pratense* resulted in a different VFA profile when compared to the fermentation of *L. perenne* and the co-fermentation of *L. perenne* and *T. repens*. In the fermentation of *T. pratense*, a predominance of propionic acid can be observed over the seven days of fermentation (Figure 4.3), representing 52.5% of the VFA mix while butyric acid represented 18.1% (in g.L⁻¹, Table 4.3). For *L. perenne* (150 kgN.ha⁻¹.yr⁻¹), the highest accumulated VFA was butyric acid (40.3% in g.L⁻¹), followed by propionic acid (31.6% in g.L⁻¹). Even after 14 days, the production of butyric acid (37.3% in g.L⁻¹) was slightly higher than the production of propionic acid (35.8% in g.L⁻¹).

Propionic acid also dominated the VFA mix in the fermentation of 300 kgN.ha⁻¹.yr⁻¹ *L. perenne* and *T. repens*. A predominance of propionic acid compared to acetic acid and butyric acid has been observed in the fermentation of cheese whey at pH 6.0 using a continuous chemostat⁷³. At neutral pH, propionic was also predominant in the VFA mix obtained from the sequencing batch fermentation of cheese whey, while an equiproportional mixture of acetic acid, propionic acid, butyric acid, and valeric acid was obtained at pH 5.0⁷⁴. In our study, the increase in pH levels over time was attributed to the accumulation of ammonia (especially in clover mixtures) and the consumption of acetic acid (Figure 4.3) – and both contributed to the accumulation of methane. For clovers, approximately 54% of the COD produced was directed to methane production, which could have been transformed to VFAs. Moreover, it can be seen that the pH adjustment with sodium bicarbonate at the beginning of the fermentation led to pH levels above 6.5. Although this may not have affected the production of VFAs from *L. perenne*, as seen in the rapid acid accumulation (Figure 4.3), the same cannot be said about the fermentation of clovers. Therefore, this system would benefit from a pH control system especially for clovers, which could maintain the pH at mildly acidic levels (e.g., 5.5) potentially leading to a higher accumulation of VFAs.

Overall, no difference was observed in terms of VFA production in the fermentation of 150 kgN.ha⁻¹.yr⁻¹ *L. perenne*, *T. repens*, and the mixture of *L. perenne* and *T. repens*. Also, the acidification yield was the same for the three substrates. The main difference between *L. perenne* and *T. repens*, however, was observed in terms of butyric acid yield (p-value < 0.01). In fact, numerically, the highest production of butyric acid in our study was observed when fermenting the *L. perenne* with lower nitrogen fertiliser – 1.4±0.1 g.L⁻¹. Extending the fermentation of *L. perenne* for more 7 days neither increase significantly the production of VFAs/butyric acid nor *L. perenne*'s degradation (Table 4.2). Moreover, the fermentation of *L. perenne* after 14 days resulted in an acidification level of 86.2±2.2%, which was the highest observed when comparing all substrates. The VFA production from *L. perenne* in our study (2.8±0.4 g.L⁻¹, 0.32±0.04 gCOD.gCOD⁻¹) was comparable to other grass fermentation studies^{34,37}. In the fermentation of Napier grass using LBRs at mesophilic temperatures and pH 6.0-6.5 for 28 days, a VFA concentration of 1.6 g.L⁻¹ was reached, with butyric acid representing 32.1% of the VFA mix³⁴. The same was observed in comparison to the fermentation of ryegrass silage in LBRs for 24 days at mesophilic temperatures and pH 6.5 (0.3-0.4 gCOD.gCOD⁻¹)³⁷. However, it is important to highlight that the hydrodynamics of our study and the studies with LBRs are different, as an important parameter such as recirculation¹⁵ was not assessed in

our study. Moreover, other operational regimes may improve the accumulation of VFAs, as observed in the fermentation of grass pellets in continuous mode with in-line recovery of VFAs^{35,36}.

4.4.5 Sharp pH drop in the two-stage fermentation of all substrates was associated to lactic acid, but two-stage and one-stage fermentation had the same VFA yield

The two-stage fermentation assay was designed to evaluate how a setup consisting of two different fermentation stages could benefit the production of VFAs from *L. perenne* (150 kgN.ha⁻¹.yr⁻¹), *T. repens*, and a mixture of *L. perenne* and *T. repens*. The goal was to separate the conversion of the substrate's soluble materials from the conversion of the lignocellulosic fibre, without employing any addition process for mechanical or chemical pre-treatment of the biomass. In this way, the two-stage fermentation consisted of a first-stage in which substrates were placed in water with no inoculum addition, and a second-stage where an external inoculum acclimatised to the production of VFAs from lignocellulosic wastes was used.

Our previous studies have shown that placing grassland biomass in water for 7 days led to a pH below 4.0 (150 and 300 kgN.ha⁻¹.yr⁻¹ *L. perenne*: 3.3±0.0; *T. pratense*: 4.7±0.2; *T. repens*: 3.7±0.0; *L. perenne* + *T. repens*: 3.6±0.0). At that point, an hypothesis was made that the drop in pH was due to the production of lactic acid, which could have been a result of fermenting the surface sugars from grasses and clovers⁶³. In fact, the accumulation of lactic acid from grass in water has been demonstrated (9.4±1.0 g.L⁻¹) in a 33-day semi-continuous process, with no inoculum addition³⁸. Moreover, in the ensiling of grass, lactic acid bacteria (LAB) are responsible for fermenting the available surface sugars to lactic acid, preventing the lignocellulosic matrix from spoilage⁷⁵. Therefore, the sharp decrease in pH observed in previous studies was attributed to the accumulation of lactic acid. These preliminary results motivated the design of the two-stage fermentation assay, specifically focusing on the accumulation of butyric acid from lactic acid.

Results from the first-stage showed that lactic acid accumulated in the liquid phase irrespective of the substrate tested, but at different rates (Figure 4.4). In the fermentation of *T. repens*, lactic acid was mainly produced after 2 days of fermentation, while lactic acid accumulated towards the end of the first-stage for *L. perenne*. For the co-fermentation of *L. perenne* and *T. repens*, both a fast accumulation of lactic acid followed by an increase towards the end of the first-stage was observed. As observed in our previous studies, pH levels dropped below 4.0 after one day and remained at acidic levels until the end of the first-stage. Therefore, the correlation between acidic pH levels and the accumulation of lactic acid was confirmed in this study for all three substrates tested. This sharp drop in pH was important to show the accumulation of lactic acid, which could be further converted to butyric acid as intended. However, low pH levels are inhibitory for both hydrolytic bacteria⁷⁶ and acidogens⁷³, which explains the low VS degradation in the first-stage as well as the low accumulation of VFAs. Therefore, both liquid and solid fractions from the first-stage were separated and inoculated at a starting pH of approximately 7.25 with the same inoculum used in the one-stage fermentation.

Overall, the VFA yield obtained from fermenting the solid fraction was lower for all substrates

compared to the VFA yield obtained from the liquid fraction (Figure 4.7). On the other hand, the pH of the liquid fraction reached neutral levels despite the production of VFAs, while acidic levels were observed in the fermentation of the solid fraction. No difference in VFA yield was observed between the solid fraction of the three substrates, and the same VFA profile was achieved regardless of the substrate fermented, with propionic acid as the highest produced VFA after 7 days (Figure 4.4).

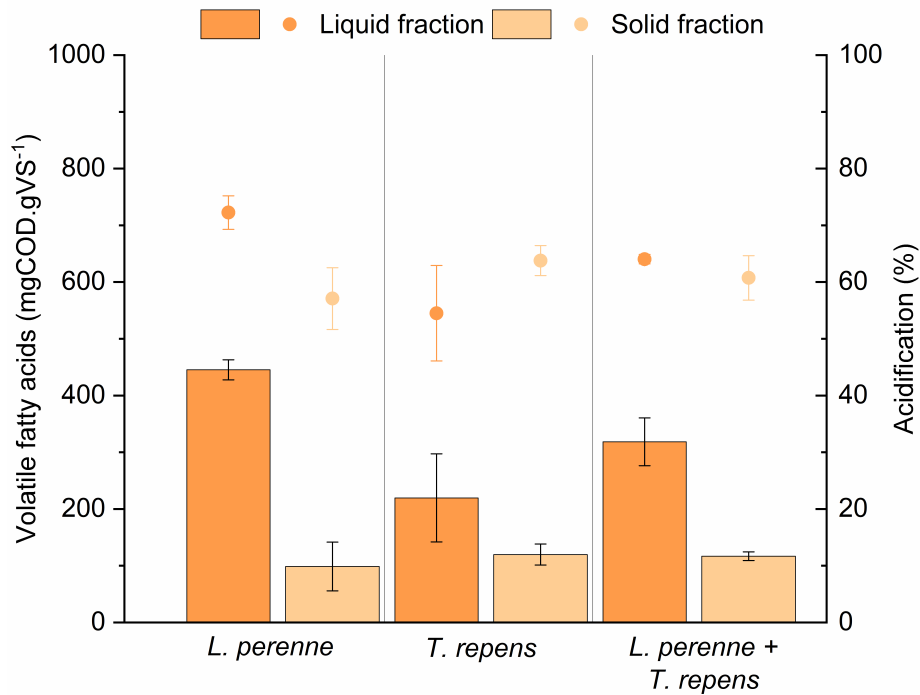


Figure 4.7: VFA yield (bars) and acidification (dots) in the second-stage fermentation of *L. perenne*, *T. repens*, and a mixture of *L. perenne* with *T. repens* – the light orange represents the production from the solid fraction while the darker orange represents the production from the liquid fraction after the pre-treatment.

Despite the higher VFA yield obtained from the fermentation of *L. perenne*'s liquid fraction, no significant difference was observed in terms of VFA yield when comparing the three substrates. In fact, the VFA yield for *L. perenne* was 2-fold higher compared to *T. repens*, but the high variability observed in the fermentation of *T. repens* may have affected the statistical analysis (p -value = 0.062). From the production profile of the liquid fraction (Figure 4.4), it is possible to observe that butyric acid production reached its maximum after two days of fermentation, when lactic acid was completely consumed. At this point, the highest concentration of butyric acid between the three substrates was obtained from the fermentation of *L. perenne*'s liquid fraction (2.3 ± 0.0 gCOD.L⁻¹, 160.0 ± 7.5 mgCOD.gVS⁻¹). Afterwards, VFA production slightly increased (for *L. perenne*) or remained constant (for the other two substrates), with butyric acid consumption for acetic acid production at pH levels above 7.5. By the end of the fermentation, acetic acid was the highest produced VFA followed by propionic acid, as reported previously in the fermentation of grass³⁴⁻³⁷.

The idea of accumulating lactic acid in the first-stage was to provide an important intermediary for the production of butyric acid^{47,77}, which was performed in the subsequent stage. The solid fraction

would also be fermented in the second-stage, resulting in the conversion of the substrate's cell wall components. The hypothesis was that separating liquid and solid fractions could improve VFA and butyric acid accumulation in comparison to the one-stage. However, adding a new stage where the substrate was immersed in water did not improve VFA production (Figure 4.8). In fact, butyric acid production was lower compared to the one-stage fermentation, indicating a decrease in selectivity.

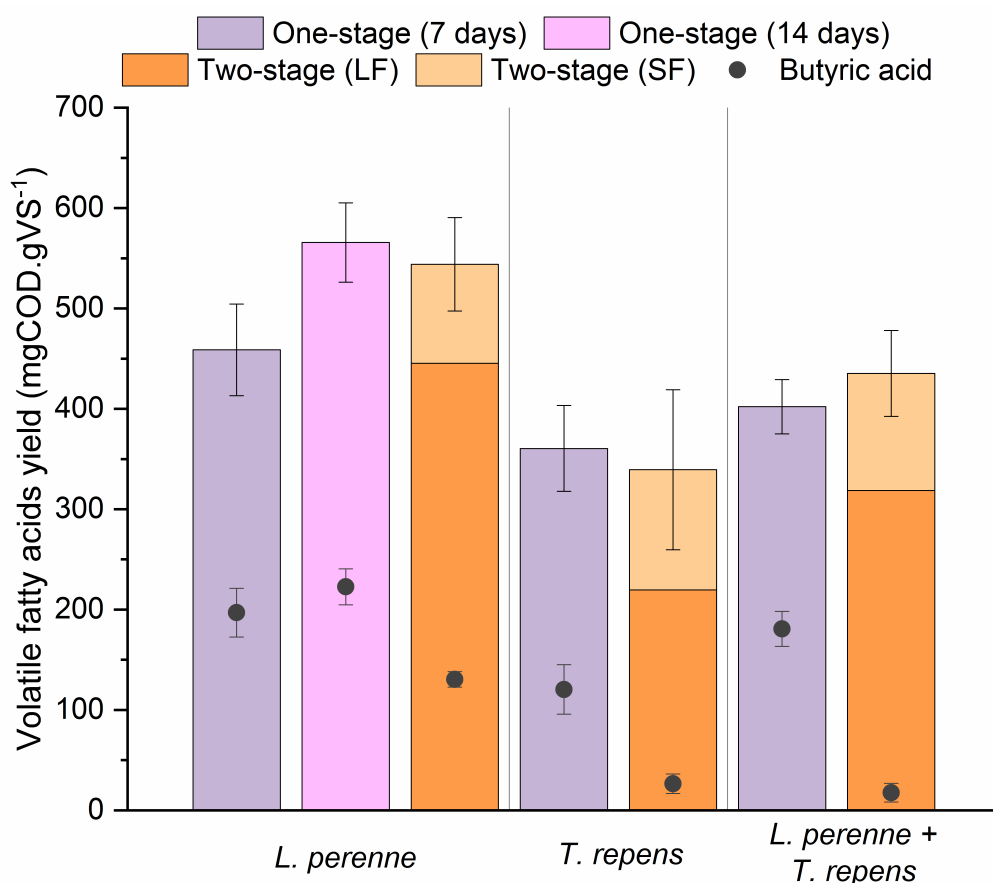


Figure 4.8: Comparison between the one-stage and second-stage fermentation of *L. perenne*, *T. repens*, and a mixture of *L. perenne* with *T. repens* in terms of VFA yield (bars) and butyric acid yield (black dots).

On the other hand, the fact that separating the substrate's soluble materials and its lignocellulosic fibre resulted in a similar yield to the one-stage fermentation shows the importance of all components of the grassland biomass for VFA production. It also important to highlight that operational conditions could be optimised for butyric acid in this study – e.g., a lower pH for the fermentation of the liquid fraction, or a higher solid retention time in the fermentation of the solid fraction. Controlling pH levels below 6.0 seems important to produce butyric acid from precursors such as lactic acid and readily available sugars, as pH levels above 6.0 can lead to a predominant accumulation of propionic^{73,74} and acetic acid³². However, despite our results showing that the conditions provided in the one-stage fermentation were better for butyric acid accumulation – *L. perenne* was still the most suitable grassland biomass for the accumulation of butyric acid with the conditions provided in this study.

4.5 Conclusions

In our study, we evaluated the potential of *L. perenne*, *T. pratense*, and *T. repens* as substrates for the production of VFAs using AD technology. We learned that the buffering capacity of clovers was a great asset for substrate degradation, but product conversion seemed favourable for methane accumulation due to the pH profile. Moreover, we observed that supplying a higher dose of nitrogen fertiliser did not affect the production of VFAs, but resulted in a higher accumulation of methane which was also correlated to the pH profile. No difference was observed in the production of VFAs when the one-stage fermentation and the two-stage fermentation was performed. Data from the two-stage fermentation indicated that butyric acid was mainly produced from the consumption of lactic acid, which was produced from the substrate surface material. The best performance for butyric acid and VFA accumulation was observed from the fermentation of *L. perenne*, as a monoculture or as a mixture with *T. repens*. This is important result for the sustainable production of VFAs in AD, considering the negative environmental impact of monocultures to forage production. However, synergistic and antagonistic effects of species interaction should be further evaluated. To the best of our knowledge, this is the first time clovers are studied for VFA production using an acclimatised inoculum and not for methane production.

4.6 Acknowledgement and contributions

This work was financially supported by Science Foundation Ireland (SFI). The authors would like to acknowledge the BiOrbic (Bioeconomy SFI Research Centre) for the technical and financial support, and Arrabawn Dairies for the inoculum supply. Forages were supplied by Teagasc Johnstown (Guylain Grange). This work was possible due to the technical support of Sandra O'Connor and Andrew Bartle. The study was conceptualised in collaboration with Dr. Corine Nzeteu and Prof. Vincent O'Flaherty. Dr. Corine Nzeteu also assisted in data analysis. Dr. Anna Trego, Dr. Corine Nzeteu and Prof. Vincent O'Flaherty revised this manuscript.

4.7 References

1. European comission. *A European Green Deal - Striving to be the first climate-neutral continent* Dec. 2019. <https://ec.europa.eu/newsroom/know4pol/items/664852>.
2. Murphy, J. D. *et al. The Potential for Grass Biomethane as a Biofuel: Compressed Biomethane Generated from Grass , Utilised as a Transport Biofuel* tech. rep. (Environmental Research Institute, 2011), 1–69.
3. Bråthen, K. A., Pugnaire, F. I. & Bardgett, R. D. The paradox of forbs in grasslands and the legacy of the mammoth steppe. *Frontiers in Ecology and the Environment* **19**, 584–592 (Dec. 2021).

4. Lee, M., Manning, P., Rist, J., Power, S. A. & Marsh, C. A global comparison of grassland biomass responses to CO₂ and nitrogen enrichment. *Philosophical Transactions of the Royal Society B: Biological Sciences* **365**, 2047–2056 (2010).
5. Rahman, M. M. *et al.* in *Advances in Legumes for Sustainable Intensification* (eds Meena, R. S. & Kumar, S.) 381–402 (Academic Press, 2022).
6. Finn, J. A. *et al.* Ecosystem function enhanced by combining four functional types of plant species in intensively managed grassland mixtures: a 3-year continental-scale field experiment. *Journal of Applied Ecology* **50** (ed Wilsey, B.) 365–375 (Apr. 2013).
7. Grange, G., Finn, J. A. & Brophy, C. Plant diversity enhanced yield and mitigated drought impacts in intensively managed grassland communities. *Journal of Applied Ecology*, 1365–2664 (June 2021).
8. Grange, G., Brophy, C. & Finn, J. A. Grassland legacy effects on yield of a follow-on crop in rotation strongly influenced by legume proportion and moderately by drought. *European Journal of Agronomy* **138**, 126531 (2022).
9. Cong, W.-F., Suter, M., Lüscher, A. & Eriksen, J. Species interactions between forbs and grass-clover contribute to yield gains and weed suppression in forage grassland mixtures. *Agriculture, Ecosystems & Environment* **268**, 154–161 (Dec. 2018).
10. Connolly, J. *et al.* Weed suppression greatly increased by plant diversity in intensively managed grasslands: A continental-scale experiment. *Journal of Applied Ecology* **55** (ed Inderjit) 852–862 (Mar. 2018).
11. De Neergaard, A., Hauggaard-Nielsen, H., Stoumann Jensen, L. & Magid, J. Decomposition of white clover (*Trifolium repens*) and ryegrass (*Lolium perenne*) components: C and N dynamics simulated with the DAISY soil organic matter submodel. *European Journal of Agronomy* **16**, 43–55 (Jan. 2002).
12. Cummins, S. *et al.* Beneficial effects of multi-species mixtures on N₂O emissions from intensively managed grassland swards. *Science of The Total Environment* **792**, 148163 (2021).
13. French, K. E. Assessing the bioenergy potential of grassland biomass from conservation areas in England. *Land Use Policy* **82**, 700–708 (Mar. 2019).
14. Cherubini, F. *et al.* Toward a common classification approach for biorefinery systems. *Biofuels, Bioproducts and Biorefining* **3**, 534–546 (Sept. 2009).
15. Nzeteu, C., Coelho, F., Davis, E., Trego, A. & O’flaherty, V. Current Trends in Biological Valorization of Waste-Derived Biomass: The Critical Role of VFAs to Fuel a Biorefinery. **8**, 445 (2022).
16. Korres, N. E., Singh, A., Nizami, A.-S. & Murphy, J. D. Is grass biomethane a sustainable transport biofuel? *Biofuels, Bioproducts and Biorefining* **4**, 310–325 (May 2010).

17. Wall, D. M., Allen, E., Straccialini, B., O’Kiely, P. & Murphy, J. D. Optimisation of digester performance with increasing organic loading rate for mono- and co-digestion of grass silage and dairy slurry. *Bioresource Technology* **173**, 422–428 (2014).
18. McEniry, J. *et al.* How much grassland biomass is available in Ireland in excess of livestock requirements ? *Irish Journal of Agricultural and Food Research* **52**, 67–80 (2013).
19. Prochnow, A. *et al.* Bioenergy from permanent grassland - A review: 1. Biogas. *Bioresource Technology* **100**, 4931–4944 (2009).
20. Nizami, A.-S., Korres, N. E. & Murphy, J. D. Review of the Integrated Process for the Production of Grass Biomethane. *Environmental Science & Technology* **43**, 8496–8508 (Nov. 2009).
21. Nizami, A.-S. & Murphy, J. D. Optimizing the Operation of a Two-Phase Anaerobic Digestion System Digesting Grass Silage. *Environmental Science & Technology* **45**, 7561–7569 (Sept. 2011).
22. Wall, D. M., O’Kiely, P. & Murphy, J. D. The potential for biomethane from grass and slurry to satisfy renewable energy targets. *Bioresource Technology* **149**, 425–431 (Dec. 2013).
23. McEniry, J., Allen, E., Murphy, J. D. & Kiely, P. O. Grass for biogas production: The impact of silage fermentation characteristics on methane yield in two contrasting biomethane potential test systems. *Renewable Energy* **63**, 524–530 (2014).
24. Wall, D. M., Allen, E., Shea, R. O., Kiely, P. O. & Murphy, J. D. Investigating two-phase digestion of grass silage for demand-driven biogas applications: Effect of particle size and rumen fluid addition. *Renewable Energy* **86**, 1215–1223 (2016).
25. Cong, W.-F., Moset, V., Feng, L., Møller, H. B. & Eriksen, J. Anaerobic co-digestion of grass and forbs – Influence of cattle manure or grass based inoculum. *Biomass and Bioenergy* **119**, 90–96 (Dec. 2018).
26. Wall, D. M., Allen, E., Straccialini, B., Kiely, P. O. & Murphy, J. D. The effect of trace element addition to mono-digestion of grass silage at high organic loading rates. *Bioresource Technology* **172**, 349–355 (2014).
27. Myszograj, S., Stadnik, A. & Pluciennik-Koropczuk, E. The Influence of Trace Elements on Anaerobic Digestion Process. *Civil and Environmental Engineering Reports* **28**, 105–115 (Dec. 2018).
28. Thamsiroj, T., Nizami, A. S. & Murphy, J. D. Why does mono-digestion of grass silage fail in long term operation? *Applied Energy* **95**, 64–76 (2012).
29. Suter, M. *et al.* Nitrogen yield advantage from grass-legume mixtures is robust over a wide range of legume proportions and environmental conditions. *Global Change Biology* **21**, 2424–2438 (June 2015).

30. Wahid, R., Ward, A. J., Møller, H. B., Søgaard, K. & Eriksen, J. Biogas potential from forbs and grass-clover mixture with the application of near infrared spectroscopy. *Bioresource Technology* **198**, 124–132 (2015).
31. Ramos-Suarez, M., Zhang, Y. & Outram, V. Current perspectives on acidogenic fermentation to produce volatile fatty acids from waste. *Reviews in Environmental Science and Bio/Technology* **20**, 439–478 (2021).
32. Lee, W. S., Chua, A. S. M., Yeoh, H. K. & Ngoh, G. C. A review of the production and applications of waste-derived volatile fatty acids. *Chemical Engineering Journal* **235**, 83–99 (2014).
33. Magdalena, J. A., Greses, S. & González-Fernández, C. Impact of Organic Loading Rate in Volatile Fatty Acids Production and Population Dynamics Using Microalgae Biomass as Substrate. *Scientific Reports* **9**, 18374 (Dec. 2019).
34. Kullavanijaya, P. & Chavalparit, O. The production of volatile fatty acids from Napier grass via an anaerobic leach bed process: The influence of leachate dilution, inoculum, recirculation, and buffering agent addition. *Journal of Environmental Chemical Engineering* **7**, 103458 (Dec. 2019).
35. Jones, R. J., Massanet-Nicolau, J., Fernandez-Feito, R., Dinsdale, R. M. & Guwy, A. J. Recovery and enhanced yields of volatile fatty acids from a grass fermentation via in-situ solids separation and electrodialysis. *Journal of cleaner production* **296**, 126430 (2021).
36. Jones, R. J., Massanet-Nicolau, J., Fernandez-Feito, R., Dinsdale, R. M. & Guwy, A. J. Fermentative volatile fatty acid production and recovery from grass using a novel combination of solids separation, pervaporation, and electrodialysis technologies. *Bioresource technology* **342**, 125926 (2021).
37. Xie, S., Lawlor, P. G., Frost, J. P., Wu, G. & Zhan, X. Hydrolysis and acidification of grass silage in leaching bed reactors. *Bioresource Technology* **114**, 406–413 (2012).
38. Khor, W. C., Andersen, S., Vervaeren, H. & Rabaey, K. Electricity-assisted production of caproic acid from grass. *Biotechnology for Biofuels* **10**, 1–11 (Dec. 2017).
39. Sakarika, M., Regueira, A., Rabaey, K. & Ganigué, R. Thermophilic caproic acid production from grass juice by sugar-based chain elongation. *Science of the Total Environment* **860** (Feb. 2023).
40. Liberato, V. *et al.* Clostridium sp. as Bio-Catalyst for Fuels and Chemicals Production in a Biorefinery Context. *Catalysts* **9**, 962 (Nov. 2019).
41. Ruiz-Dueñas, F. J. & Martínez, Á. T. Microbial degradation of lignin: how a bulky recalcitrant polymer is efficiently recycled in nature and how we can take advantage of this. *Microbial Biotechnology* **2**, 164–177 (Mar. 2009).

42. Zoghalmi, A. & Paës, G. Lignocellulosic Biomass: Understanding Recalcitrance and Predicting Hydrolysis. *Frontiers in Chemistry* **7**, 874 (Dec. 2019).
43. Paudel, S. R. *et al.* Pretreatment of agricultural biomass for anaerobic digestion: Current state and challenges. *Bioresource Technology* **245**, 1194–1205 (2017).
44. Steinbrenner, J., Nägele, H.-J., Buschmann, A., Hülsemann, B. & Oechsner, H. Testing different ensiling parameters to increase butyric acid concentration for maize silage, followed by silage separation and methane yield potential of separated solids residues. *Bioresource Technology Reports* **7**, 100193 (Sept. 2019).
45. Steinbrenner, J., Mueller, J. & Oechsner, H. Combined Butyric Acid and Methane Production from Grass Silage in a Novel Green Biorefinery Concept. *Waste and Biomass Valorization* **13**, 1873–1884. <https://doi.org/10.1007/s12649-021-01626-4> (2022).
46. Kung Jr, L., Shaver, R. D., Grant, R. J. & Schmidt, R. J. Silage review: Interpretation of chemical, microbial, and organoleptic components of silages. *Journal of Dairy Science* **101**, 4020–4033 (2018).
47. Gao, M. *et al.* Production of medium-chain fatty acid caproate from Chinese liquor distillers' grain using pit mud as the fermentation microbes. *Journal of Hazardous Materials* **417** (Sept. 2021).
48. Zehnder, A. J. B., Huser, B. A., Brock, T. D. & Wuhrmann, K. Characterization of an acetate-decarboxylating, non-hydrogen-oxidizing methane bacterium. *Archives of Microbiology* **124**, 1–11 (Jan. 1980).
49. Zhu, X. *et al.* The synthesis of n-caproate from lactate: a new efficient process for medium-chain carboxylates production. *Scientific Reports* **5**, 1–9 (Nov. 2015).
50. APHA. *Standard Methods for the Examination of Water and Wastewater* 20th ed. (eds Eaton, A. D., CClesceri, L. S., Franson, M. A. H. F., Rice, E. W. & Greenberg, A. E.) *Standard Methods for the Examination of Water and Wastewater* v. **21** (American Public Health Association, 2005).
51. Gerike, P. The biodegradability testing of poorly water soluble compounds. *Chemosphere* **13**, 169–190 (Jan. 1984).
52. Buswell, A. M. & Neave, S. L. *Laboratory studies of sludge digestion* tech. rep. (Department of registration and education. Division of the state Water survey, Urbana, Illinois, 1930).
53. Hames, B., Scalata, C. & Sluiter, A. *Determination of protein content in biomass* (eds Sluiter, A., Scarlata, C. & (U.S.), N. R. E. L.) (National Renewable Energy Laboratory, Golden, Colo, 2005).
54. Lorenz, H., Reinsch, T., Kluß, C., Taube, F. & Loges, R. Does the admixture of forage herbs affect the yield performance, yield stability and forage quality of a grass clover ley? *Sustainability (Switzerland)* **12** (July 2020).

55. Van Soest, P., Robertson, J. & Lewis, B. Methods for Dietary Fiber, Neutral Detergent Fiber, and Nonstarch Polysaccharides in Relation to Animal Nutrition. *Journal of Dairy Science* **74**, 3583–3597 (Oct. 1991).
56. Selvankumar, T. *et al.* Process optimization of biogas energy production from cow dung with alkali pre-treated coffee pulp. *3 Biotech* **7** (Aug. 2017).
57. Browne, J. D., Allen, E. & Murphy, J. D. Assessing the variability in biomethane production from the organic fraction of municipal solid waste in batch and continuous operation. *Applied Energy* **128**, 307–314 (Sept. 2014).
58. Pham, C. H., Triolo, J. M., Cu, T. T., Pedersen, L. & Sommer, S. G. Validation and recommendation of methods to measure biogas production potential of animal manure. *Asian-Australasian Journal of Animal Sciences* **26**, 864–873 (2013).
59. Filer, J., Ding, H. H. & Chang, S. Biochemical Methane Potential (BMP) Assay Method for Anaerobic Digestion Research. *Water* **11**, 921 (May 2019).
60. Fischer, M. A. *et al.* Immediate Effects of Ammonia Shock on Transcription and Composition of a Biogas Reactor Microbiome. *Frontiers in Microbiology* **10** (Sept. 2019).
61. Khanal, S. K., Tirta Nindhia, T. G. & Nitayavardhana, S. in *Sustainable Resource Recovery and Zero Waste Approaches* 165–174 (Elsevier, The Netherlands, 2019).
62. Cysneiros, D. *et al.* Temperature effects on the trophic stages of perennial rye grass anaerobic digestion. *Water Science and Technology* **64**, 70–76 (2011).
63. Han, X., Hong, F., Liu, G. & Bao, J. An Approach of Utilizing Water-Soluble Carbohydrates in Lignocellulose Feedstock for Promotion of Cellulosic α -Lactic Acid Production. *Journal of Agricultural and Food Chemistry* **66**, 10225–10232 (Oct. 2018).
64. Raposo, F., Borja, R. & Ibelli-Bianco, C. Predictive regression models for biochemical methane potential tests of biomass samples: Pitfalls and challenges of laboratory measurements. *Renewable and Sustainable Energy Reviews* **127**, 109890 (2020).
65. Moset, V., Al-zohairi, N. & Møller, H. B. The impact of inoculum source, inoculum to substrate ratio and sample preservation on methane potential from different substrates. *Biomass and Bioenergy* **83**, 474–482 (2015).
66. Suter, M., Huguenin-Elie, O. & Lüscher, A. Multispecies for multifunctions: combining four complementary species enhances multifunctionality of sown grassland. *Scientific Reports* **11** (Dec. 2021).
67. Yan, B. H., Selvam, A. & Wong, J. W. C. Application of rumen microbes to enhance food waste hydrolysis in acidogenic leach-bed reactors. *eng. Bioresource technology* **168**, 64–71 (Sept. 2014).

68. Himanshu, H., Murphy, J., Grant, J. & O’Kiely, P. Synergies from co-digesting grass or clover silages with cattle slurry in in vitro batch anaerobic digestion. *Renewable Energy* **127**, 474–480 (Nov. 2018).
69. Wahid, R. *et al.* Anaerobic mono-digestion of lucerne, grass and forbs – Influence of species and cutting frequency. *Biomass and Bioenergy* **109**, 199–208 (Feb. 2018).
70. Himanshu, H., Murphy, J., Grant, J. & O’Kiely, P. Antagonistic effects on biogas and methane output when co-digesting cattle and pig slurries with grass silage in in vitro batch anaerobic digestion. *Biomass and Bioenergy* **109**, 190–198 (Feb. 2018).
71. Beausang, C., McDonnell, K. & Murphy, F. Assessing the environmental sustainability of grass silage and cattle slurry for biogas production. *Journal of Cleaner Production* **298**, 126838 (May 2021).
72. Nagarajan, S., Jones, R. J., Oram, L., Massanet-Nicolau, J. & Guwy, A. Intensification of Acidogenic Fermentation for the Production of Biohydrogen and Volatile Fatty Acids—A Perspective. *Fermentation* **8**, 325 (July 2022).
73. Bengtsson, S., Hallquist, J., Werker, A. & Welander, T. Acidogenic fermentation of industrial wastewaters: Effects of chemostat retention time and pH on volatile fatty acids production. *Biochemical Engineering Journal* **40**, 492–499 (July 2008).
74. Atasoy, M. & Cetecioglu, Z. The effects of pH on the production of volatile fatty acids and microbial dynamics in long-term reactor operation. *Journal of Environmental Management* **319**, 115700 (Oct. 2022).
75. Pahlow, G., Muck, R. E., Driehuis, F., Elferink, S. J. W. H. O. & Spoelstra, S. F. in *Silage Science and Technology* 31–93 (Jan. 2003).
76. Jiang, J. *et al.* Volatile fatty acids production from food waste: Effects of pH, temperature, and organic loading rate. *Bioresource Technology* **143**, 525–530 (2013).
77. Detman, A. *et al.* Cell factories converting lactate and acetate to butyrate: *Clostridium butyricum* and microbial communities from dark fermentation bioreactors. *Microbial Cell Factories* **18**, 36 (Dec. 2019).

B.1 Appendices

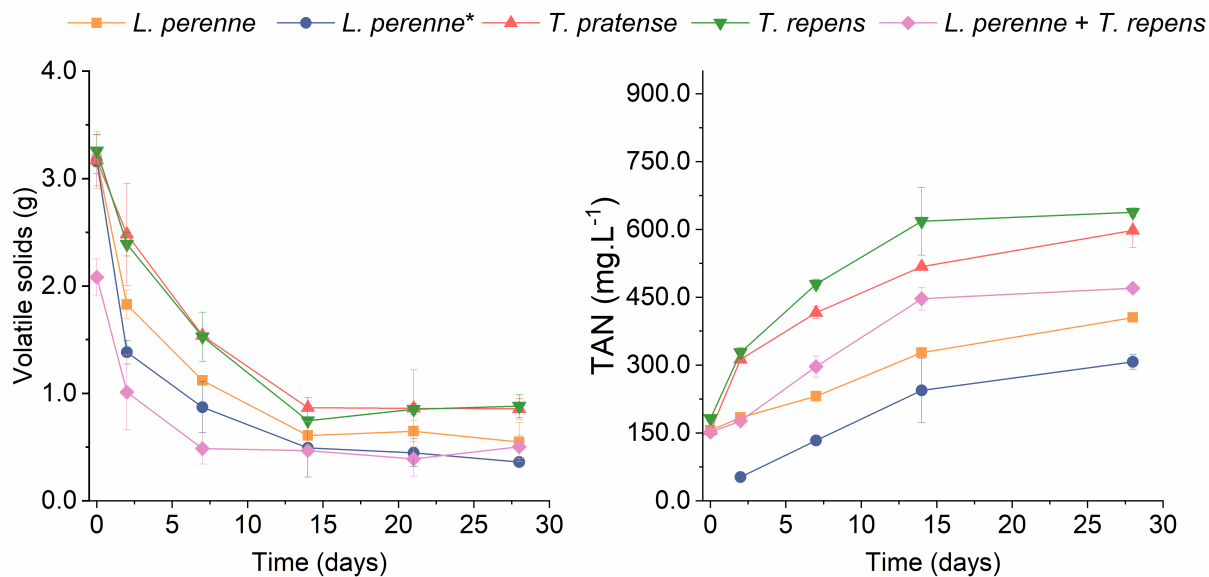


Figure B.1: Profile of volatile solids degradation (on the left) and Total ammonia nitrogen (TAN, on the right) for each substrate during the biomethane potential assay. The * represents the substrate supplied with $300 \text{ kgN} \cdot \text{ha}^{-1} \cdot \text{yr}^{-1}$.

Chapter 5: Silage fermentation for butyric acid production in leach-bed reactors: the impact of silage pH and inoculum source in the fermentation process

Abstract

Ensiled grass has been extensively studied for biomethane production using anaerobic digestion technology. However, its potential for volatile fatty acids (VFAs) is not well explored. Here, we investigate the fermentation of ensiled grass from temperate regions aiming to elucidate the effect of silage pH and inoculum source in the production of VFAs, focusing on the selective accumulation of butyric acid. The work was divided in three stages. In the first stage, the digestion of grass was performed using granular sludge (GS), rumen fluid (RF), rumen solid (RS) and cattle slurry (CS) as inoculum, individually and as a mixture. We observed that mixing GS with RF and RS, and with CS led to a higher VS degradation and methane yield compared to using each inoculum source individually. Therefore, mixtures of GS with the other inoculum sources were used as seed-inoculum in the second stage of experiments, which consisted of a fermentation trial in three leach-bed reactors (LBRs) – Reactor 1 (RF+RS+GS), Reactor 2 (CS+GS), and Reactor 3 (GS). The fermentation was performed for 9 months and divided in six experimental phases (Start Up, Batch 16, and Phases I-V), in which four silages with different pHs were fermented (4.3, Start Up, Phases I-III; 8.1, Batch 16; 6.6, Phase V; and 4.6, Phase V). Our results showed that i) silage degradation levels were the same throughout the fermentation trial, irrespective of the seed-inocula supplied in the Start Up. Moreover, ii) silage pH was responsible for the shift in VFA profile and yield, with a lower pH (4.3 and 4.6) favouring the accumulation of VFAs (Phase I and V) and a high pH leading to a very low concentration of VFAs (Batch 16). Higher concentrations of butyric acid were obtained when lactic acid accumulated in the leachate due to the fermentation of the low pH silage. High-throughput sequencing of the 16S rRNA gene on DNA and cDNA samples extracted from digestate and leachate samples reinforced the hypothesis that silage pH was a driving force in the reactor performance. Moreover, combining seed-inocula and silage was important to compose a richer microbial community. In all reactors, *Prevotella* and *Lactobacillus* were the most abundant genera. The higher presence of *Lactobacillus* associated with the presence of *Caproiciproducens* may explain the accumulation of butyric acid and caproic acid observed in Phase V. After the reactor trial, the influence of inoculum approaches was investigated in the semi-continuous fermentation of silage by using digestate, leachate or a mixture of both. We concluded that the solid digestate was an important inoculum in the degradation of silage, and the combination of leachate and digestate led to a faster VFA production.

5.1 Introduction

The world has been facing drastic consequences of climate change due to the accumulation of residues and the continuous release of harmful compounds to the atmosphere. To mitigate this situation, ‘The Green Deal’ was launched in 2019, aiming to neutralise greenhouse gas (GHG) emissions in Europe by 2050¹, focusing on farming activities, circular economy and energy production². To meet this target, a green biorefinery could be an important process, using grassland biomass and agricultural waste as feedstocks to produce proteins, bioenergy (e.g., biomethane and biogas), fertiliser, organic acids (e.g., volatile fatty acids (VFAs), medium-chain carboxylic acids (MCCAs)), and bioplastics (polyhydroxyalkanoates, PHAs)^{3,4}. Within this biorefinery, the anaerobic digestion (AD) technology can be used as an efficient strategy for resource recovery by minimising waste while maximising conversion to biogas/biomethane³. Moreover, the process can be tailored for the accumulation of VFAs as a potential platform for chain-elongation (e.g., caproic acid, caprylic acid), PHAs production, hydrogen, and electricity³. Over the years, however, the AD of grassland biomass has been centred on biogas and biomethane yields, with most VFA studies optimising acetic acid accumulation for biomethane production in second-stage^{5–10}. Although few works have demonstrated the production of VFAs from grass^{11–14}, none have highlighted butyric acid as the main acid in the VFA mix thus far.

Butyric acid is a high-demand chemical with a global market size of 125 million USD (2020)¹⁵. It is currently used within the plastic, food, and pharmaceutical^{15,16} industries with a market demand of 80,000 tons per year¹⁶. Moreover, butyric acid has recently been proposed as an electron acceptor in the chain-elongation process to caproic acid using lactic acid as electron-donor^{17–20}. The chain-elongation of butyric acid to caproic acid can unfold an even more profitable side of the grass-based AD, due to caproic acid’s market size (75-89 million USD, 2018)¹⁵ and its hydrophobicity, which reduces recovery complexity and costs²¹. Although mainly produced by the chemical synthesis of fossil-fuel-derived materials, butyric acid can also be obtained by the biological conversion of carbohydrates, glycerol, and lactic acid¹⁶ using bacteria from genera *Clostridium*^{16,22}, *Megasphaera*¹⁶, *Roseburia*^{16,23,24}, *Caproiciproducens*^{20,25}, and *Acidaminococcus*²⁶. The production of butyric acid as part of a VFA-mix has been reported during acidogenic fermentation of food waste^{3,27,28}, grass silage^{7,12–14}, dairy waste-water^{22,29}, and manure²⁰; with a VFA-mix dominated by butyric acid when food-waste and dairy wastewater were fermented^{3,22,28}. Dark fermentation has also been employed for the accumulation of VFAs and biohydrogen³⁰, with some studies demonstrating a VFA production dominated by butyric acid when lactate and acetate were used as substrates^{31,32}. Moreover, Detman et al.³² showed the relevance of pH and microbial community in dark fermentation studies, highlighting that butyric acid from lactate and acetate was the main produced VFA when operating at pH 5.0-6.0 with a community composed of *Lactobacillus*, *Prevotella*, *Bifidobacterium*, and *Clostridium*³².

Many process parameters (e.g., feedstock type, temperature, organic loading rate) affect the VFA production in terms of yield, concentration, profile, and microbial community dynamics^{3,33}. Among those parameters, pH has been extensively studied in the literature as one of the crucial parameters in the process³³, with levels from acidic to alkaline proposed for different feedstocks and

configurations^{3,33}. Acidic levels are employed to inhibit methanogenic archaea³⁴, but sometimes at the expense of decreasing biomass hydrolysis efficiency and VFA conversion²⁸, as pH levels below 5 are inhibitory to acidogenic bacteria³⁵. On the other hand, alkaline pH levels add to operational costs³⁵, and may lead to a VFA profile dominated by acetic acid³⁵ or propionic acid²⁹, or butyric acid³⁶ depending on the feedstock used and microbial community dynamics. In the acidification of grassland biomass, pH values between 5.5-6.0 have been applied successfully to obtain VFAs from grass¹²⁻¹⁴. This pH range has also contributed to a constant production of butyric acid from dairy wastewater (pH 5.0)²⁹, and a VFA production dominated by butyric acid from a dairy manure hydrolysate (pH 5.5)²⁰.

As pH can be a predominant factor for VFA production³³, the selection of an appropriate silage can be crucial. Silage is obtained when the soluble carbohydrates available in the grass' surface are fermented, especially by lactic acid bacteria (LAB)³⁷. The production of lactic acid reduces drastically the silage pH, preventing spoilage and further degradation³⁸. However, contamination with soil and manure can lead to the predominance of fungi and other fermentative bacteria that degrade the grass fibre and available sugars, resulting in a silage with higher pH, prone to spoilage and lower quality³⁷. Therefore, choosing a silage with an appropriate pH is important to guarantee the integrity of the feedstock, but also the microbial community that will be incorporated in the process' dynamics.

VFA production using the microbial community from lignocellulosic biomass has been explored before. The fermentation of grass in water with no external inoculum led to the accumulation of lactic acid ($9.36 \pm 0.95 \text{ g.L}^{-1}$) over 33 days of semi-continuous operation, which was later converted to caproic acid ($4.09 \pm 0.54 \text{ g.L}^{-1}$) at pH 5.5-6.2 using an acclimatised inoculum¹¹. Additionally, the recovery of butyric acid during maize ensiling was improved by increasing buffering capacity and by decreasing dry matter content, with no external inoculum addition, resulting in a juice with 75.06 g.kg^{-1} DM of butyric acid at $20 \text{ }^\circ\text{C}$ ³⁹ and $20.1 \pm 4.5 \text{ g.kg}^{-1}$ at $37 \text{ }^\circ\text{C}$ ⁴⁰. Nevertheless, Xie et al.⁷ has shown that the addition of an external inoculum source in association with the feedstock's microbial community was important for VFA accumulation from silage, increasing VFA production in 10-fold and improving degradation⁷.

In this way, equally important as the feedstock's microbial community, selecting an inoculum source with good biodegradability and VFA potential is crucial. Rumen material and cattle manure have been used to enhance the hydrolysis of lignocellulosic biomass in association with other inocula (e.g., granular sludge), thus improving biomethane/VFA yield and biomass degradation^{28,41-43}. The hydrolytic capability of rumen material and cattle manure is a result of its complex microbial community, which is composed of fibrolytic microorganisms responsible for degrading the lignocellulosic material through carbohydrate active enzymes (CAZymes)⁴⁴, such as endocellulases, α - and β -glucosidases, and endoxylanases⁴⁵. In the rumen, these enzymes can be produced by species of *Prevotella*, *Butyrivibrio*, *Ruminococcus*, and *Fibrobacter*^{44,45}, and they are important in breaking down the glycosidic bonds from the lignocellulosic matrix, releasing glucose, xylose and mannose that will be used by acidogenic bacteria during fermentation⁴⁶. In this way, selecting an appropriate inoculum can be as important for VFA accumulation and biomass degradation from grass, especially

considering the substrate's microbial community.

Therefore, the present work investigates the effect of silage pH, organic loading, and seed-inoculum source in the fermentation of ryegrass and multi-species silage for VFA production, focusing on the selective accumulation of butyric acid. The work was divided in three main experimental stages - the first stage was designed for the selection of an appropriate inoculum that could both degrade the grass and convert the silage, using inoculum sources such as granular sludge, rumen fluid, rumen solid and cattle slurry. In the second stage, the fermentation of silage with the selected inoculum source from the first stage was performed in a semi-continuous reactor run. In this stage, microbial community samples were taken to understand the effect of silage pH and inoculum source in the production of VFAs from grass. In the third stage, the influence of using a solid digestate or leachate as inoculum in the production of VFAs from silage was investigated.

5.2 Materials and Methods

5.2.1 Seed-inoculum

Four sources of inocula were assessed as a potential seed-inoculum for VFA accumulation and silage degradation – granular sludge (GS), rumen fluid (RF), rumen solid (RS), and cattle slurry (CS). GS was collected from a full-scale expanded granular sludge bed (EGSB) reactor treating dairy wastewater (Arrabawn Dairies Co., Kilconnell, Ireland) in November 2020, and had a total (TS) and volatile (VS) solids content of 12.68 (0.09)% and 9.63 (0.03)%, respectively. CS was collected from a local farm in Co. Galway (Ireland) in January 2021, with a TS and VS content of 9.29 (0.04)% and 7.11 (0.04)%, respectively, and a pH of 7.8. RF was collected from a local abattoir in Co. Mayo (Ireland), with a solid content of 3.97 (0.01)% TS, 2.99 (0.03)% VS, and 34.4 (0.3) gVS/L (RF^a). Rumen content was also collected from cannulated cattle (Teagasc Grange, Co. Meath, Ireland) in fresh rumen fluid form (RF^b) and solid form (RS). The solid content for RF^b was 1.68 (0.02)%TS, 0.69 (0.02)%VS, and 6.8 (0.4) gVS.L⁻¹ and pH 7.1. The RS had a solid content of 19.90 (0.47)% TS, and 18.20 (0.45)% VS. GS and CS were stored at 4 °C until the beginning of the experiments, while both rumen fluids (RF^a and RF^b), and the rumen solid (RS) were stored at room temperature for a maximum of 12h before inoculation.

5.2.2 Substrate

The influence of the pH from grassland biomass silage in the production of butyric acid, VFAs, and silage degradation was evaluated for four different silages (Table 5.1. Silage PI, Silage B16, and Silage PIV were collected from a local farm in Co. Galway (Ireland) and composed mainly of perennial ryegrass (*Lolium perenne*). Silage PI was collected in January 2022, while Silage B16 and Silage PIV were collected in May 2022. Silage PV was collected from a research centre in Co. Wexford (Teagasc Jonhstown Castle) in July 2022; Silage PV was composed of a mixture of six species of grassland biomass – grasses (*Lolium perenne*, *Phleum pratense*), legumes (*Trifolium*

pratense, *Trifolium repens*), and herbs (*Cichorium intybus*, *Plantago lanceolata*). Silage PI, B16 and PIV were composed mainly of *Lolium perenne*.

Table 5.1: Chemical parameters for the four silages used in this study.

Parameters	Units	Silage PI	Silage B16	Silage PIV	Silage PV
pH		4.6	8.1	6.6	4.3
COD	gCOD.gFW ⁻¹	0.43	0.27 ^a	0.31	0.26
Total solids	%FW	30.7±0.9	21.5±0.3	21.2±2.7	23.4±0.0
Volatile solids	%FW	27.1±0.1	19.6±0.1	19.6±2.5	20.6±0.1
Extractives	%TS	38.8±0.2	18.5±0.4	25.4±0.4	22.1±0.1
Water-extractives	%TS	32.3±0.0	9.9±0.1	21.8±0.5	19.2±1.6
Ethanol-extractives	%TS	6.5±0.1	8.6±0.3	3.6±0.2	2.9±1.5
Ash	%TS	8.1±0.0	9.1±0.2	7.5±0.1	9.2±0.0
Lignocellulose	%TS	62.0±0.3	67.5±0.9	60.4±0.1	70.0±0.4
Cellulose	%TS	29.0±0.2	36.4±0.6	25.8±0.5	30.3±0.3
Hemicellulose	%TS	15.9±0.1	13.0±0.4	14.9±0.0	12.1±0.0
Lignin	%TS	17.1±0.0	18.1±0.0	19.7±0.3	20.6±0.0
C:N ratio	%TS	20.1±0.3	22.1±0.6	16.4±0.9	14.4±0.1
Crude protein	%TS	14.4±0.2	13.1±0.4	13.1±0.5	19.8±0.1

Note: ^aSilage COD was determined based on a wet chemistry oxidative assay, except for Silage B16, which was based on Buswell's equation⁴⁷. FW stands for fresh weight and TS stands for total solids. '±' symbols represents the standard deviation of duplicate to triplicate measurements.

5.2.3 Selecting a seed-inoculum for the reactor trial (First stage)

A batch test was designed (Figure 5.1) to select three sources of seed-inoculum to be used in the fermentation of grassland biomass silage for VFA production in leach-bed reactors (LBRs). Due to difficulties in replicating the fermentation conditions in the LBRs (such as pH control), the batch test focused on maximising the degradation of grassland silage and its conversion to methane.

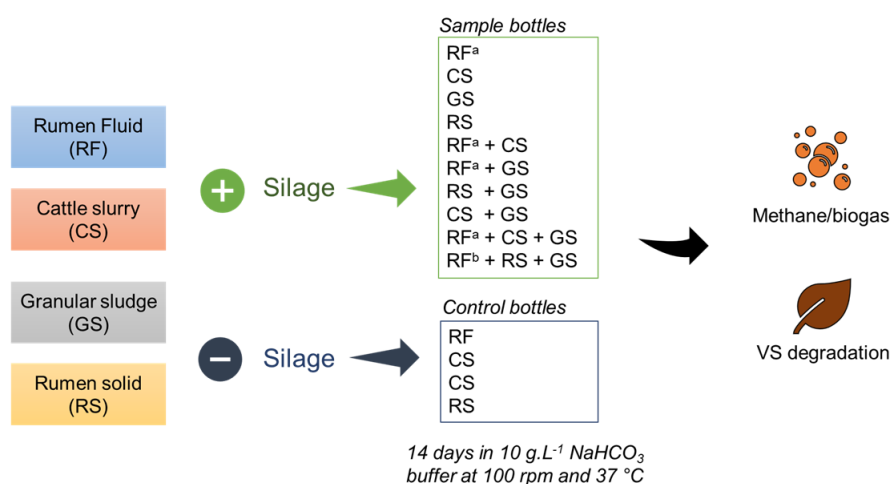


Figure 5.1: Schematic representation of the seed-inoculum selection experiment using rumen fluid (RF), rumen solid (RS), cattle slurry (CS), and granular sludge (GS) as seed-inoculum.

The setup consisted of 500 mL plastic bottles with FisherbrandTM solid rubber stoppers and 1 L Tedlar gas bags attached using a needle and a tap. Inoculum and silage were added in a 1:1 ratio

(10 gVS.L⁻¹) to a 250 mL NaHCO₃ solution (10 g.L⁻¹). The same quantity of silage was added to all bottles (around 2.5 gVS), while the quantity of GS, CS, RF, RS varied depending on the seed-inoculum or mixture of seed-inocula used (Table 5.2). Negative control-bottles were prepared for GS, CS, RS and RF without the addition of silage, and used to monitor the production of methane from the seed-inocula and its degradation over time. Anaerobic conditions were ensured by flushing N₂/CO₂ (80-20%) for 5 minutes, and 0.42 mL of a trace elements solution was supplied⁴⁸. The experiment was performed in triplicate and conducted in batch-mode for 14 days at 100 rpm and 37 °C.

Biogas volume and methane composition was monitored as the gas bags were full to limit disturbances in gas production. Silage consumption was determined as VS degradation; VS values were measured at the beginning and at the end of the batch. The methane production from silage and its VS degradation was obtained by discounting the contribution of the seed-inoculum to methane production and VS degradation. When a mixture of inocula was used (e.g., GS+CS), the proportion of each seed-inoculum in the mixture was considered when accounting for the methane production from silage and the VS degradation (see Section 5.3.1 at page 117 for more details).

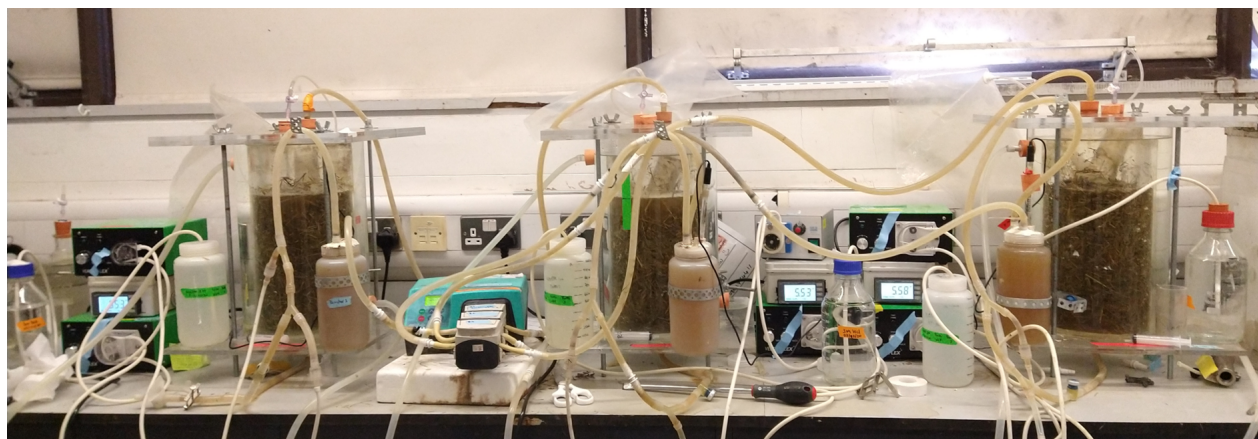
Table 5.2: Seed composition, in %VS, fed to batch bottles in the seed-inoculum selection experiment. RF^a was collected from a local abattoir in Co. Mayo, while RF^b was collected from a cannulated cattle experiment (Teagasc Grange, Co. Meath).

Seed-inoculum	Rumen fluid (RF)	Cattle slurry (CS)	Granular sludge (GS)	Rumen solid (RS)
RF ^a	100%			
CS		100%		
GS			100%	
RS				100%
RF ^a +CS	42%	58%		
RF ^a +GS	42%		58%	
RS + GS			31%	69%
CS + GS		50%	50%	
RF ^a + CS + GS	26%	37%	37%	
RF ^b + RS + GS	6%		30%	54%

Note: The composition presented in this table correspond to the real-loading observed after the commencement of the experiment.

5.2.4 Silage fermentation in leach-bed reactors (Second stage)

The fermentation of grassland silage to selectively produce butyric acid was studied using three 6 L LBRs coupled with an equalisation tank (5 L total working volume, Figure 5.2). The reactor setup was coupled to a pH control system assembled in the laboratory consisting of a pH controller, a pH probe, two pumps, a NaOH solution (1M and 3M, 4 mL.min⁻¹), and a HCl solution (3M, 5 mL.min⁻¹). The pH controller received the signal from the pH probe, compared it to a set-point, and activated one of the pumps depending on the measured pH value. Two set-points were used to maintain acidity levels around 5.5. The high set-point was activated when pH was higher than 5.40±0.05, pumping acid into the line; while the low set-point was activated when pH was lower than 5.30±0.05, injecting base into the line. The pH probe was placed inside an equalisation tank. The pH values observed in the pH controller's monitor was compared to values from a pH-meter, which worked as an indication to calibrate the pH probe.



- 1 Rumen fluid
Rumen solid
Granular sludge
- 2 Cattle slurry
Granular sludge
- 3 Granular sludge

Figure 5.2: Reactor setup for the fermentation of silage using different seed-inoculum.

The fermentation was operated in semi-continuous mode with a solid retention time (SRT) of 6 days and a re-circulation speed of $500 \text{ mL} \cdot \text{min}^{-1}$. During start-up, each reactor received a different seed-inoculum: a combination of rumen fluid, rumen solid and granular sludge (Reactor 1, R1), a combination of cattle slurry and granular sludge (Reactor 2, R2), and granular sludge (Reactor 3, R3). Each subsequent batch was loaded with fresh silage, water, and trace elements⁴⁹. The solid digestate and leachate (diluted 11x) from the immediately previous batch was used as an inoculum for the subsequent batch. The reactor trial was divided in five different phases (Figure C.1), with different conditions and strategies (Table 5.3).

Table 5.3: Summary of the operational conditions per phase in the fermentation of grassland biomass silage – number of batches^a, solid retention time (SRT), organic loading rate OLR.

Phases	Batches ^a	SRT	Ratio silage:digestate	Substrate OLR ($\text{gVS} \cdot \text{L}^{-1} \cdot \text{day}^{-1}$)	Silage
Start up	n=1	13	5.7 : 1.0 (R1) ^a 5.9 : 1.0 (R2) ^a 6.2 : 1.0 (R3) ^a	2.8	PI, pH = 4.6
Batch 1 ^b	n=1	6	1.1 : 1.0	3.7	PI, pH = 4.6
Phase I	n=4	6	1.1 : 1.0	3.7	PI, pH = 4.6
Phase II ^c	n=3	6	1.1 : 1.0	3.7	PI, pH = 4.6
Phase III ^d	n=3	6	1.0 : 1.0	2.8	PI, pH = 4.6
Batch 16	n=1	6	1.1 : 1.0	3.7	B16, pH = 8.1
Phase IV	n=6	6	1.1 : 1.0	3.7	PIV, pH = 6.6
Batch 24 ^b	n=1	6	1.1 : 1.0	3.7	PV, pH = 4.3
Phase V	n=6	6	1.1 : 1.0	3.7	PV, pH = 4.3

Note: ^aRatio was calculated considering the loading of silage and the total loading of seed-inocula.

^bTransient batches between phases, where conditions were stabilising. ^cLeachate with extra dilution at day 0. ^dWashing of solid mixture (digestate and silage) before inoculation.

Batches 1 and 24 were considered transient batches between phases, where operational conditions were stabilising. In Phases I, IV and V, and in Batch 16 the impact of silage pH on VFA production was investigated. In Phase II, the influence of the initial COD on VFA accumulation was tested by

replacing 2 L of leachate with water at the beginning of each batch. In Phase III, a lower OLR was investigated as well as the influence of the silage COD and digestate COD; the latter was evaluated by washing the solid mixture with tap water before adding leachate and trace elements. The pH control system was activated on day 0 approximately one hour after starting the batch, except in Start Up, Batch 1, and Phase I where the pH was left to fluctuate for a day.

Liquid samples were collected at days 0-6 to monitor the VFA production, the lactic acid accumulation, the COD profile, and the pH profile. Solid samples were collected at the end of each batch to estimate the VS degradation, the COD content in the remaining digestate, lignocellulosic composition, and elemental composition. The gas production was monitored constantly – gas volumes were measured as the gas bags were full and by the end of each batch; gas samples were collected for methane composition.

5.2.5 Influence of inoculum approaches in silage fermentation (Third stage)

A batch fermentation was designed to investigate the influence of using digestate or leachate as inoculum in the production of VFAs and the degradation of silage. The setup consisted of 500 mL plastic bottles with Fisherbrand™ solid rubber stoppers and 1 L Tedlar gas bags attached using a needle and a tap. Silage PV was used as substrate, and digestate and leachate harvested from the last batch of each reactor (Phase V, batch 30) were used as inoculum.

The inoculation approach (using solid digestate or leachate) was tested in three different bottles – using digestate only, using leachate only and using a mixture of digestate and leachate. Conditions such as OLR (digestate and silage), and leachate dilution (11x) were the same as provided in Phase V (Table 5.3). The bottles had a working volume of 0.4 L, and the liquid phase consisted of tap water, trace elements and leachate (when applicable). The fermentation was performed in triplicate and conducted in batch-mode for 6 days at 100 rpm and 37 °C. The pH was monitored in the first 3 days of fermentation and corrected to 5.33 ± 0.03 with a 3 M NaOH solution and a 3 M HCl solution on day 1 and day 2 of the fermentation.

The gas production was constantly monitored similarly as it was performed in the reactor trial. Liquid samples were collected at days 0, 1, 2, and 6 to monitor the VFA production, the COD profile, and the pH profile. Solid samples were collected at the end of each batch to estimate the volatile solids degradation.

5.2.6 Analytical methods

Samples of substrate, leachate, and digestate (solid) were analysed in terms of TS and VS according to standard methods⁵⁰. The samples were conserved at -20 °C after sampling until further analysis were performed. pH values were obtained at the time of sampling using a pH-meter (Jenway 3510, Cole-Parmer®, UK) and using the control system assembled in the lab.

Gas samples was collected in gas bags – the volume was measured using the water displacement methodwater displacement method⁵¹. Methane composition was determined using gas chromato-

graphy (Varian CP-3800, Varian Inc., USA) equipped with a thermal conductivity detector (TCD), and a hydrogen generator (Whatman®).

Leachate samples were thawed to room temperature, centrifuged at $16 \times 1000 g$ for 10 min, and filtered (pore size of $0.2 \mu\text{m}$). The filtered samples were used to determine soluble COD, VFAs, lactic acid (reactor trial), and ethanol (reactor trial). Soluble COD was measured using the photometric kits ($0\text{-}15000 \text{ mg}\cdot\text{L}^{-1}$, Reagecon®, Reagecon Diagnostics Ltd., Ireland) and readings were performed in UV/Vis Spectrophotometer (DR3900, Hach®, EUA). Lactic acid and ethanol were measured with high-performance liquid chromatography (HPLC, 1260 Infinity, 237, Agilent Technology, USA). The HPLC was equipped with a refractive index detector (RID) and a Hi-Plex H column. VFAs were analysed using gas chromatography (Varian 450 GC, Agilent Technology) equipped with a flame ionisation detector (FID), and a hydrogen generator (Whatman™). Helium was used as carrier gas and acids' separation was performed using a capillarity column BP21, FFAP (SGE Analytical Science) with $0.25 \mu\text{m}$ of film thickness, 30 m of length and 0.25 mm of internal diameter.

VFA samples were diluted with distilled water (when appropriate), and an internal standard solution ($100 \mu\text{L}$, fixed volume) prepared with orthophosphoric acid and ethyl-butyric acid. The calibration curve was prepared for the following acids: acetic, propionic, butyric, iso-butyric, valeric, iso-valeric, caproic, and iso-caproic. The COD equivalent for VFAs and lactic acid was calculated based on its complete oxidation to CO_2 and H_2O – 1.067 (acetic and lactic), 1.514 (propionic), 1.818 (iso/butyric), 2.039 (iso/valeric), and 2.207 (iso/caproic). In this work, results for lactic acid, ethanol and VFA are mainly expressed in $\text{gCOD}\cdot\text{L}^{-1}$; VFA results are also expressed in terms of silage VS added ($\text{gCOD}\cdot\text{gVS}^{-1}$).

Solid samples of silages and solid digestate from Batches 29 and 30 were characterised in terms of elemental carbon (C), nitrogen (N), oxygen (O), hydrogen (H), and sulphur (S) as described in the European Standard EN 15104:2011. The elemental data was analysed in duplicate and reported in terms of dry matter. This data was used to estimate the C:N ratio and the crude protein content, which was calculated by multiplying the %N by 6.25^{52} . The elemental data was also used to estimate the ThCOD^{53} for Silage B16 (Section 3.3.2, page 46). The COD for other silages and digestates were characterised based in a wet-chemistry assay (Section 5.3.4, page 119).

Silage samples and solid digestate samples from Batch 29 and 30 digestate were also characterised in terms of its lignocellulosic components by Celignis Analytical (Limerick, Ireland). The company uses the protocols developed by the National Renewable Energy Laboratory (NREL, USA). Briefly, after preparing the samples to appropriate moisture content and particle size⁵⁴, the dried samples were placed in a Soxhlet extractor using water and ethanol as solvents to remove the extractives that are soluble to those solvents⁵⁵. The extractives' free biomass was then hydrolysed with strong sulphuric acid (72%) and diluted sulphuric acid (4%), in a two-step hydrolysis to extract the lignocellulosic sugars from the biomass⁵⁶. Lignin is measured from the remaining solid, and acid soluble lignin was measured in the hydrolysed liquid before sugar quantification, at acidic pH.

5.2.7 Microbial community sampling

The microbial community dynamics in the fermentation of silage in LBRs (Section 5.2.4, page 111) was evaluated from samples of silage (Table 5.1 – PI, PIV and PV), seed-inocula, digestate and leachate. The reactor samples were selected from Start Up, Batch 1, Batches 2-4 (Phase I), Batches 19-20 (Phase IV), and Batches 27, 29 and 30 (Phase V). Community samples were collected in triplicate and divided in two categories – liquid samples (20 or 40 mL; leachate and rumen fluid), and solid samples (10 g; silage, digestate, cattle slurry, granular sludge and rumen solid).

Microbial cells from solid samples were detached in 90 mL of PBS (Phosphate Buffered Saline, Fisher[®] Bioreagents, pH 7.2-7.6) using an ultrasonic bath (Sonorex Digiplus DL 102H, Bandelin electronic GmbH & Co.) for 20 min at 100 W (35 kHz). The sonicated liquid and the liquid samples were centrifuged for 30 min at 7,197 *g*, and the pellet was resuspended using 2.0 mL of a resuspension buffer to transfer the content to small centrifuge tubes (2 mL) for storage. Two resuspension buffers were used alternatively – RNAlater[®] (Start up, Batch 1, Phase I and Phase IV Batch 20), and PBS (Phase IV Batch 19, and Phase V). When RNAlater[®] was used, resuspended pellets were incubated at 4 °C, as recommended by the manufacturer. After resuspension (and incubation in the case of RNAlater[®]), the pellet was obtained after 10 min of centrifugation at $8 \times 1,000g$. The pellet was frozen with liquid nitrogen and stored at -80 °C until nucleic acid extraction.

5.2.8 DNA/RNA co-extraction and cDNA synthesis

DNA and RNA were extracted from liquid and solid samples (n=3; for Phase IV, n=4), for a total of n=127 DNA samples and n=18 RNA samples – samples were organised per reactor and/or phase (e.g., leachate samples from Reactor 3 in Phase I were named ‘R3_PI_leachate’; or Silage PI samples were named ‘Silage_PI’).

Before the extraction, replicates from the same reactor and batch were pooled under the flame, and 0.1-0.5 g of wet sample were washed twice with PBS; the pellet was separated by centrifugation at 4° C and $10 \times 1,000g$ for 5 min. The washed samples were then co-extracted using a modified version of the protocol described by Griffiths *et al.*⁵⁷ Briefly, cell lysis was performed with bead-beating for 10 min (IKA Vortex Genius 3) in a CTAB buffer composed of 5% cetyl-trimethylammonium bromide (Sigma-Aldrich[®], USA), 0.35 M NaCl and 120 mM phosphate buffer (pH = 8.0), and 0.75 mL of Phenol:Chloroform:Isoamyl alcohol (25:24:1, Sigma-Aldrich[®], USA). After phase separation (centrifugation), the excess of phenol was removed using 0.5 mL of Chloroform:Isoamyl alcohol (24:1). Following a brief mix, the top aqueous layer was removed and DNA was precipitated on ice using 0.9 mL of a 30% polyethylene glycol solution (PEG600, Sigma-Aldrich[®], USA) and 1 mL of 70% ethanol. Purified nucleic acids were resuspended in nuclease-free water, and nucleic acid concentration was determined using a Qubit fluorometer (Invitrogen[®], USA). The extracted nucleic acid quality was assessed by 1% agarose electrophoresis and NanoDrop[™] spectrophotometer (Thermo Fisher Scientific, Waltham, MA, USA). DNA samples were stored at -20° C and RNA samples were stored at -80° C.

The cDNA synthesis was performed in two steps. In the first step, a DNase treatment was performed using a DNA-free™ kit (AMBION – invitrogen, USA) by following the rigorous DNase treatment according to the manufacturer's recommendations. The absence of residual DNA was confirmed by 2% agarose electrophoresis. In the second step, cDNA was synthesised using the SuperScript® IV Reverse Transcriptase kit (ThermoFisher®, USA) according to the manufacturer's recommendations. The cDNA concentration was determined using a Qubit fluorometer (Invitrogen®, USA), and samples were stored at -20° C.

5.2.9 Sequencing, bioinformatics and statistical analysis

The V4 region of the 16S rRNA gene was amplified on the Illumina MiSeq by Mr.DNA (Molecular Research LP, Texas, USA) using the universal bacterial primer 515F and reverse primer 806R⁵⁸. Abundance tables were generated by constructing ASVs using the QIIME2™ workflow⁵⁹ and the DADA2 denoising algorithm⁶⁰. The bioinformatics steps used in the present work were similar to Batool *et al.*⁶¹ – P=81,237 ASVs were obtained for n=145 samples. Additionally, PICRUSt2 algorithm⁶² was used as a QIIME2 plugin on ASVs to predict the functional abundance of microbial communities by using the weighted NSTI threshold of 2.0 in the software, recovering both KEGG enzymes (P=10,543) and MetaCyc pathways (P=489) for n=145 samples. As a pre-processing step, typical contaminants, such as Mitochondria and Chloroplasts, were removed as well as any ASVs that were unassigned at all levels, as per recommendations given at <https://docs.qiime2.org/2022.8/tutorials/filtering/>. Samples not relevant to this study (or with fewer than 5,000 reads) were also filtered out. The resulting abundance table had n=145 samples x P= 71,636 ASVs (sample-wise read statistics as [Minimum: 26,107; 1st Quartile: 39,623; Median: 48,736; Mean: 49,317; 3rd Quartile: 56,842; and Maximum: 91,865]).

Taxonomic bar plots were generated considering the 25 most abundant microbes at genus level using R's ggplot2 package. The vegan package⁶³ was used for alpha and beta diversity analyses (R version 4.2.1). The measures used for alpha diversity were: (i) Shannon entropy – a commonly used index to measure balance within a community; and (ii) rarefied richness – the estimated number of species/features in a rarefied sample (to minimum library size); and exponential of Shannon entropy. R's *aov()* function was used to calculate the pair-wise analysis of variance (ANOVA) p-values.

Ordination of the ASV table in reduced space (beta diversity) was done using PCoA with two distance measures: (i) Bray-Curtis distance on the ASV abundance table to visualise the compositional changes; and (ii) Hierarchical Meta–Storms (HMS)⁶⁴. HMS is a recent functional beta diversity distance, which takes the observed KOs recovered from the dataset and calculates the functional beta diversity distance in a hierarchical fashion propagating the KEGG Orthologs (KO)s abundances upward to the pathways in a multi-level pathway hierarchy to give a weighted dissimilarity measure. Additionally, the vegan package was also used to perform PERMANOVA analyses to evaluate if the microbial or functional community structures can be explained by different sources of variability. In addition to the above mentioned distance measures, weighted and unweighted UniFrac distances were

employed in the PERMANOVA using R's Phyloseq package⁶⁵.

5.3 Chemical Parameters

Results for chemical parameters are presented in this study as mean values with standard deviation, unless otherwise informed. For the reactor trial, the difference between phases and reactor was evaluated in terms of VS destruction, and the production of butyric acid, caproic acid and total VFAs. This was analysed by computing the difference between means in IBM® SPSS® Statistics version 28.0.0.0 (190) with a Welch's t-test, considering a confidence level of 95%. This test was selected due to differences in sample size. It was also observed that the hypothesis of equal variance was not valid for some samples using a Levene's test.

5.3.1 Volatile solids degradation

Substrate conversion was defined as the consumption of the biomass' biodegradable materials after the digestion/fermentation in batch bottles or the fermentation in LBRs and is represented by the VS degradation of grassland biomass silage (Equation 18)⁶⁶. For the seed-inoculum selection experiment (Section 5.2.3, page 110), the VS of both liquid and solid phases were considered to determine the VS degradation of silage (Equation 20-21). As the same conditions were provided in both sample bottles and control-bottles, the VS of the control-bottles were approximated as the VS of the seed-inoculum itself. Depending on the mixture of seed-inocula used in the experiment, the composition of seed-inoculum (Table 5.2) was incorporated in the calculation as z_i to determine the quantity of silage left in the bottles post digestion (Equation 21). If the VS degradation of an inoculum was higher than 10% in control bottles (Equation 19), this degradation was considered in the VS degradation of the solid and discounted so only the consumption of silage would be evaluated (Equation 21).

$$VS_{deg}(t) = 1 - \frac{m_g(t)}{m_g(0)} \quad (18)$$

$$VS_{deg_i}(t) = 1 - \frac{m_i(t)}{m_i(0)} \quad (19)$$

$$m_{digestate}(t) = m_g(t) + m_i(t) \quad (20)$$

$$m_{digestate}(t) = m_g(t) + \sum_{i=1}^{Seed} (VS_{deg_i} \cdot z_i \cdot m_i(t)) \quad (21)$$

Where: t is the digestion time; $m_g(t)$ is the mass of silage; $m_g(0)$ is the mass of silage at the beginning of the experiment; $m_i(t)$ is the mass of seed-inoculum; $m_i(0)$ is the mass of inoculum at the beginning of the experiment; $VS_{deg}(t)$ is the VS degradation of the silage; $VS_{deg_i}(t)$ is the VS degradation of the seed-inoculum; $m_{digestate}(t)$ is the mass of digestate after the experiment (considering both seed-inoculum and digested grass, if any); and z_i is the seed-inoculum composition fed to the bottles. Mass is expressed in gVS and VS degradation in %.

For the fermentation of silage in LBRs (Section 5.2.4, page 111) and the batch to study the inoculum phase in batch bottles (Section 5.2.5, page 113), only the VS of the solid phase was considered to estimate the VS degradation of silage (Equation 18). Moreover, it was assumed that only the silage fed to the reactor degraded after each batch, meaning that the solid digestate fed at the beginning of each batch did not degrade over time and had a constant VS of $m_{digestate}(0)$ (Equation 22).

$$m_{digestate}(t) = m_g(t) + m_{digestate}(0) \quad (22)$$

Where: t is the digestion time; $m_{digestate}(t)$ is the mass of digestate grass, $m_g(t)$ is the mass of silage, and $m_{digestate}(0)$ is the mass of solid digestate at the beginning each batch; mass is expressed in gVS .

5.3.2 Lignocellulosic degradation

To further investigate the degradation of silage in the fermentation, digestate samples from the reactors' last batch in Phase V were characterised in terms of its lignocellulosic components, extractives and cell wall materials. The degradation of cellulose, hemicellulose, and lignin was determined based on the solid materials fed to the reaction (Batch 29's digestate and silage Phase V), and the digestate collected at the end of Batch 30 (Equation 23).

$$\eta_i = 1 - \frac{l_{30,i} \cdot m_{30}}{l_{29} \cdot m_{29,i} + l_{s,i} \cdot m_{sil}} \quad (23)$$

Where, η represents the degradation level of the lignocellulosic component, i (%); l is the content of a respective lignocellulosic component (%TS), and m is the amount of digestate/silage fed to or removed from the reactor (gTS). The index 29 stands for Batch 29's digestate, while the index 30 stands for Batch 30's digestate; 's' stands for silage. In the present study, i represents the components in the lignocellulosic matrix's cell wall – cellulose, hemicellulose and lignin. The calculation was performed for the three reactors.

5.3.3 Biomethane production

The volume of biogas and biomethane was normalised to standard conditions (101.3 kPa, 273 K) for all experiments proposed in this study (Equation 8, Section 3.3.4)⁶⁷. The cumulative biogas production was calculated considering the headspace volume ($v^h = 213.27$ NL for bottles), and the volume collected from the gas bags (v^b) at each sampling point (Equation 9a, Section 3.3.4). The reactors' headspace volume varied during the experiment, as the pH was controlled by the addition of acid and base, which varied depending on the batch and conditions. Therefore, the reactor headspace was calculated as $(6.0 - V_r)$ NL, where 6.0 is the reactor's nominal volume, and V_r is the reactor volume at the end of each batch. The cumulative production of methane considered the composition of methane in the biogas at each sampling point (Equation 9b, Section 3.3.4)⁶⁸. For the seed-inoculum selection experiment (Section 5.2.3, page 110), as the bottles were not vented between measurements, a

correction for the methane composition in the headspace from a previous sampling point was considered (Equation 9b, Section 3.3.4). The volumetric yield for methane and biogas was calculated in terms of VS of grassland biomass silage fed to the digestion (Equation 9c, Section 3.3.4). The production of methane and biogas from silage was corrected by subtracting the volume produced in the control-bottles. Depending on the mixture of seed-inocula used in the experiment, the composition of seed-inoculum (Table 5.2) was incorporated in the calculation, similarly to what was performed for the VS degradation (5.3.1).

5.3.4 COD of solid materials

The COD of solid materials, such as silages and digestates from Batch 29 and Batch 30, was determined based on the oxidative reaction of lignocellulosic samples with potassium dichromate ($K_2Cr_2O_7$, 1N, Panreac Applichem, ITW reagents), and a sulphuric acid reagent prepared with silver sulphate (Ag_2SO_4 , Thermo Scientific®) and pure sulphuric acid (H_2SO_4 , 96%, Sigma-Aldrich®). This assay was developed and explained in detail by Noguerol-Arias⁶⁹, but is summarised as follows. Samples of 100-300 mg cut to approximately 1-2 cm were transferred to digestion glass tubes, in ice, followed by 15 mL of dichromate, 45 mL of the H_2SO_4 reagent, and 20 mL of water. A blank was prepared with the addition of reagents, but no sample. The tubes were transferred to a thermoreactor (Velp Scientifica™ ECO6) and connected to condensation tubes; the reaction occurs at 150 °C for 2 hours. After cooled down, the digestion liquid was transferred to conical flasks with ferroin indicator and titrated with a Mohr's salt solution ($Fe(NH_4)_2(SO_4)_2 \cdot 6H_2O$, 0.25N). The COD in the samples is determined based on the volume of Mohr's salt solution used to titrated the remaining dichromate in blank and samples after the digestion in the thermoreactor (Equation 24).

$$COD_s = \frac{(V_{Mohr,blank} - V_{Mohr,sample}) \times N_{Mohr} \times 8000}{V_{sample}}, \quad (24)$$

Where: COD_s is the solids' COD ($mgO_2 \cdot L^{-1}$). The volume of Mohr's salt solution used to titrated the remaining dichromate in blank and samples is represented by $V_{Mohr,blank}$ and $V_{Mohr,sample}$ (mL), respectively. N_{Mohr} is the normality of the Mohr's solution (Equation 25). The exact normality of the Mohr's salt solution is obtained by titrating a solution composed of potassium dichromate (10 mL, 1N), distilled water (90 mL), and H_2SO_4 (30 mL, 96%).

$$N_{Mohr} = \frac{(V_{K_2Cr_2O_7} \times N_{K_2Cr_2O_7})}{V_{Mohr}}, \quad (25)$$

Where: N_{Mohr} is the normality of the Mohr's salt solution; $V_{K_2Cr_2O_7}$ is the volume of dichromate solution (10 mL); $N_{K_2Cr_2O_7}$ is the normality of the dichromate solution (1N); and V_{Mohr} is the volume of Mohr's salt solution used to titrate the mixture.

5.3.5 Acidification yield and VFA production

The VFA production in the silage fermentation in LBRs (Section 5.2.4, page 111), and in the inoculum phase study (Section 5.2.5, page 113) was evaluated in terms of acidification, VFA net production, VFA yield and total product yield (in the case of the reactor trial). The acidification yield was calculated based on the accumulation of VFAs and soluble COD in the leachate at the end of each batch (Equation 26)⁷. The net production of VFAs is calculated by discounting the amount of VFAs in the leachate at the beginning of the batch (Equation 27), and the yield is obtained by dividing the net production of VFAs by the initial quantity of grass silage fed to the experiment (Equation 28).

$$\chi = \frac{\text{VFA}_t}{\text{sCOD}}, \quad (26)$$

Where, χ represents the acidification yield (%), VFA_t represents the concentration of VFAs (in total) at the end of each batch (gCOD.L^{-1}), and sCOD represents the amount of soluble COD at the end of each batch (gCOD.L^{-1}).

$$\text{VFA}_{net}(t) = \text{VFA}(t) - \text{VFA}(0), \quad (27)$$

Where, VFA_{net} is the net concentration of VFAs (or any specific acid) at a time t , $\text{VFA}(t)$ is the VFA concentration in the leachate at a time t , and $\text{VFA}(0)$ is the VFA concentration in the leachate at the beginning of each batch. All concentrations are represented here in gCOD.L^{-1} .

$$Y_{\text{VFA}} = \frac{\text{VFA}_{net}(t)}{m_g(0)}, \quad (28)$$

Where, Y_{VFA} is the yield of VFAs produced at a time t (gCOD.gVS^{-1}) based on the VFA net concentration (VFA_{net}) at that time t , and the mass of silage supplied to the bottles or reactor ($m_g(0)$, in gVS).

To incorporate the methane production observed in the reactor run to the total product yield, methane volumes in STP were converted to COD using the theoretical conversion $1 \text{ gCOD} = 350 \text{ mL CH}_4$. Methane yield was calculated by dividing the gCOD of methane by the gVS of silage added. The total production yield was obtained by summing the VFA yield and methane yield.

5.4 Results

5.4.1 Mixing granular sludge with other seed-inocula improved the conversion of silage

Prior to the silage fermentation in LBRs, four sources of inoculum were assessed individually and as mixtures – rumen fluid (RF^a and RF^b), rumen solid (RS), cattle slurry (CS), and granular sludge (GS). From this assessment, three seed-inocula were selected based on their capability of degrading silage (Figure 5.3.a) and their potential to convert silage's biodegradable materials into methane (Figure 5.3.b).

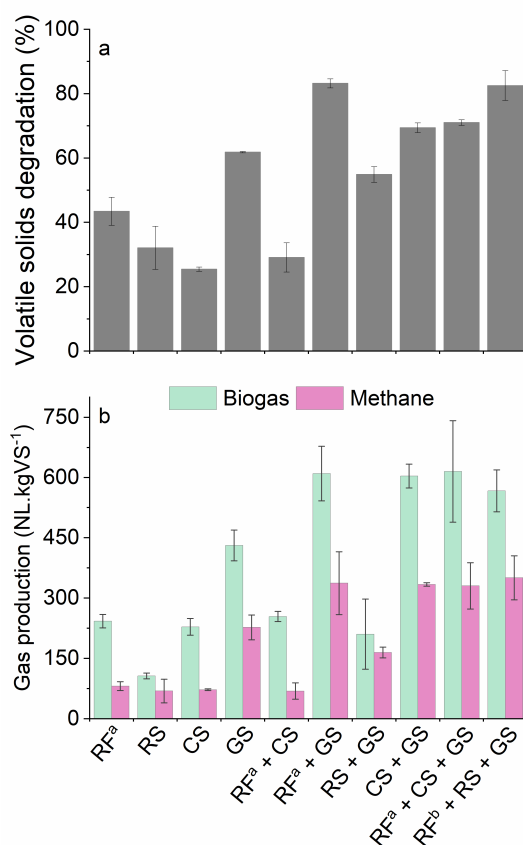


Figure 5.3: Volatile solids degradation (a) and gas production (b) in the seed-inoculum selection experiment for rumen fluid (RF^a and RF^b), rumen solid (RS), cattle slurry (CS), and granular sludge (GS). The error bars represent standard deviations.

The best degradation of silage was observed with mixtures of RF that incorporated GS (RF^a+GS: 83.2±1.3% VS), or incorporated both GS and RS (RF^b+RS+GS: 82.5±4.6% VS). Other mixtures that incorporated GS also presented degradation values around 70%, such as RF^a+CS+GS (71.0±0.6% VS) and CS+GS (69.4±1.5% VS). When comparing the silage degradation reached when using each inoculum source individually, the highest degradation level was observed using GS (61.8±0.2% VS) – this VS degradation was similar to other mixtures of inoculum sources using GS. The use of other inoculum sources individually (RF^a, RS, and CS) resulted in a silage degradation lower than 50%. Moreover, batches that had a VS degradation of 70% or more resulted in a methane yield ranging from 337.2±78.1 to 350.6 ±54.5 NL.kgVS⁻¹ (RF^a+GS, RF^b+RS+GS, CS+GS, and RF^b+CS+GS).

5.4.2 Silage degradation was not influenced by the inoculum source during its fermentation

According to the results from the seed-inoculum selection experiment (Section 5.4.1, page 120), the best degradation of silage was observed when GS was combined with other inoculum sources. Therefore, a combination of RF, RS and GS (Reactor 1), a combination of CS and GS (Reactor 2), and GS (Reactor 3) were chosen for the fermentation of silage. The fermentation trial was performed

for nine months in semi-continuous mode and divided in five phases: Phase I (n=5), Phase II (n=3), Phase III (n=3), Phase IV (n=6), and Phase V (n=6). The phases were based on different operational conditions such as organic loading rate (OLR), SRT, initial COD solution, and silage pH (Section 5.2.4, page 111). Besides these five phases, the reactor trial was also divided in Start up, which was the very beginning of the trial; Batch 16, where a silage of pH 8.1 was used; and transient batches (Batches 1 and 24), in which conditions were stabilising between phases.

Overall, the fermentation of grassland silage resulted in a similar VS degradation regardless of the reactor or phase analysed (Figure 5.4, Table 5.4). No difference was observed between reactors and phases, except for a small difference in the performance of Reactor 1 on Phases I and V ($10 \pm 8.5\%$ VS), and Reactors 2 and 3 on Phase V ($9.1 \pm 6.9\%$ VS). The conversion of silage was also assessed by computing the degradation of cellulose, hemicellulose, and lignin, considering both the starting digestate (from Batch 29) and fresh silage (Table C.1). The lignocellulosic degradation of silage during the last batch of fermentation (Phase V, Batch 30) represented 82.1% (Reactor 1), 67.3% (Reactor 2) and 72.8% (Reactor 3) of the dry matter content degraded in each reactor. Most of the lignocellulosic degradation corresponded to cellulose (above 50%), followed by the hemicellulose fraction. A small degree of degradation was observed for lignin in Reactor 1.

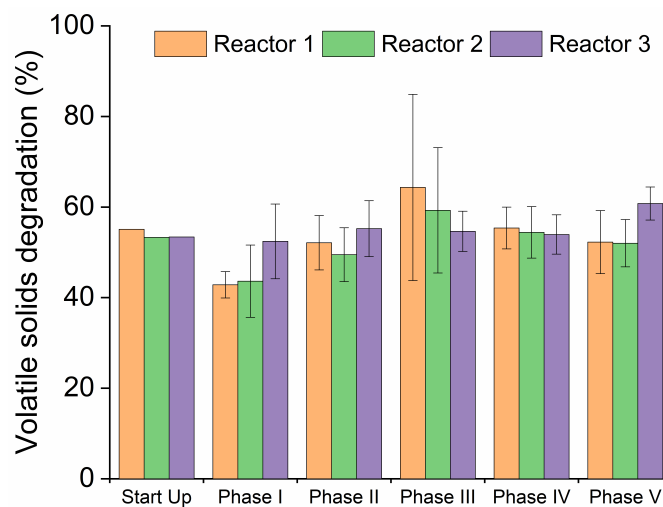


Figure 5.4: Volatile solids degradation in the fermentation of silage over the phases in Reactor 1 (left-bar), Reactor 2 (middle-bar), and Reactor 3 (right-bar). The error bars represent standard deviations – Phase I (n=4), Phases II and III (n=3), Phase IV and V (n=6).

5.4.3 The fermentation of silage resulted in a VFA mixture dominated by butyric acid in all Phases but Phase IV

After six days of fermentation, butyric acid was the VFA with the highest concentration in all reactors, except in Phase IV, where the proportion of propionic acid from the total VFAs was similar (Reactors 1 and 2) or higher (Reactor 3) than the proportion of butyric acid (Table 5.5; Figure 5.5.c). In fact, the accumulation of propionic acid was significantly higher in Phase IV compared to the other phases

(Table 5.5) – Phase I (R1–R3: p-value<0.01), Phase II (R1–R2: p-value<0.01; R3: p-value<0.05), Phase III (R1–R3: p-value<0.001), and Phase V (R1–R3 p-value<0.01).

Table 5.4: Reactor performance over phases in volatile solids (VS) degradation, acidification yield, and yield of VFAs, butyric acid and caproic acid.

Phase	Reactor	VS degradation (%)	Acidification (%)	VFA yield ^b (gCOD.gCOD ⁻¹)	VFA yield ^c (gCOD.gVS ⁻¹)	Butyric acid ^b (gCOD.gVS ⁻¹)	Caproic acid ^b (gCOD.gVS ⁻¹)
Start up	R1	55.1	97.5	0.24	0.36	0.15	0.03
	R2	51.9	92.5	0.24	0.36	0.12	0.04
	R3	53.4	72.0	0.16	0.25	0.15	0.03
Phase I	R1	42.8±2.9	87.4±2.9	0.11±0.01	0.28±0.03	0.16±0.02	0.00±0.00
	R2	43.6±8.0	82.8±8.8	0.10±0.01	0.27±0.01	0.15±0.03	0.01±0.01
	R3	52.4±8.2	87.2±9.8	0.13±0.02	0.33±0.03	0.16±0.03	0.03±0.02
Phase II	R1	52.1±6.0	91.2±4.3	0.12±0.01	0.27±0.04	0.12±0.02	0.01±0.02
	R2	49.5±5.9	85.3±14.5	0.09±0.02	0.24±0.03	0.11±0.02	0.03±0.00
	R3	52.2±6.2	76.9±1.3	0.08±0.03	0.19±0.07	0.04±0.04	0.01±0.01
Phase III	R1	64.3±20.6	80.3±8.6	0.07±0.02	0.23±0.04	0.11±0.02	0.01±0.01
	R2	59.3±13.8	85.0±1.2	0.08±0.02	0.25±0.03	0.11±0.01	0.01±0.00
	R3	54.6±4.4	72.0±3.1	0.03±0.01	0.14±0.03	0.06±0.01	0.01±0.00
Phase IV	R1	49.8±13.2	76.5±11.8	0.06±0.01	0.17±0.04	0.07±0.03	0.02±0.00
	R2	54.4±5.7	79.4±13.6	0.05±0.01	0.15±0.04	0.06±0.03	0.02±0.01
	R3	53.9±4.3	65.2±14.0	0.04±0.01	0.10±0.03	0.03±0.01	0.00±0.01
Batch 24 ^a	R1	57.4	91.5	0.31	0.60	0.28	0.03
	R2	51.9	92.5	0.25	0.50	0.15	0.00
	R3	50.5	89.6	0.25	0.48	0.25	0.00
Phase V	R1	52.3±7.0	86.3±6.2	0.17±0.03	0.36±0.04	0.14±0.04	0.07±0.03
	R2	52.0±5.2	81.4±3.1	0.16±0.02	0.33±0.04	0.11±0.03	0.07±0.02
	R3	60.8±3.7	83.7±4.2	0.15±0.04	0.32±0.07	0.13±0.03	0.05±0.04

Note: ^aBatch 24 was a transient batch between Phases IV and V. ^bYield in gCOD of silage. ^cYield in gVS fed to the reactors. ‘±’ symbols represents the standard deviation of duplicate to triplicate measurements.

Table 5.5: Average net production and profile of VFAs from reactors 1, 2, and 3 at the end of the batch in each fermentation phase.

Phase	Reactor	Total VFA (gCOD.L ⁻¹)	Acetic acid (%)	Butyric acid (%)	Caproic acid (%)	Propionic acid (%)	Valeric acid (%)
Start up	R1	14.1	28.3	42.1	9.0	14.9	5.7
	R2	14.3	26.3	34.0	10.6	21.3	7.8
	R3	8.6	24.2	61.9	11.1	2.7	0.0
Phase I	R1	6.2±0.4	26.8±4.2	57.2±5.7	1.6±1.4	11.5±3.4	2.9±1.3
	R2	6.1±0.4	19.3±10.9	53.7±10.9	2.2±0.5	14.6±0.6	6.3±2.3
	R3	6.7±0.5	27.0±2.2	51.0±2.0	8.3±4.0	12.2±1.2	2.3±0.2
Phase II	R1	6.2±0.8	33.7±11.1	44.4±3.4	3.2±5.6	15.1±2.3	5.4±3.4
	R2	5.6±0.8	20.2±1.2	46.1±4.5	11.2±0.8	14.3±0.5	6.5±1.4
	R3	4.5±1.6	25.9±3.1	51.1±6.2	*	18.9±2.7	2.3±3.2
Phase III	R1	4.2±0.7	18.4±17.8	47.8±13.9	2.8±2.4	26.1±2.8	5.0±0.9
	R2	4.4±0.7	22.2±12.5	41.9±6.2	3.5±0.6	22.0±1.8	4.1±0.8
	R3	2.2±0.4	5.9±8.3	45.5±2.8	6.1±0.8	34.6±4.1	7.8±0.6
Phase IV	R1	4.1±0.5	0.0	35.4±8.6	9.0±4.6	38.7±4.7	16.9±3.7
	R2	3.6±0.6	0.0	35.5±11.9	14.2±4.4	38.2±6.8	12.1±7.0
	R3	2.7±0.4	0.0	26.4±8.9	6.0±9.6	51.6±8.9	16.0±8.8
Batch 24	R1	13.3	22.7	46.8	5.5	12.9	12.0
	R2	9.7	31.2	33.3	0.0	23.0	12.5
	R3	10.7	19.9	52.4	0.0	17.8	9.9
Phase V	R1	7.9±1.3	16.2±4.4	40.0±5.7	19.8±7.7	13.6±1.9	10.4±1.1
	R2	7.2±0.8	18.5±2.9	36.0±4.1	21.2±5.4	14.1±2.7	10.2±2.6
	R3	7.2±1.6	14.9±2.8	41.4±9.2	14.7±11.0	19.4±7.9	15.5±4.2

Note: ^aBatch 24 was a transient batch. Isomeric forms of VFAs were not detected or acquired below the GC’s detection limit. * VFAs that were detected only in one batch of a phase. ‘±’ symbols represents the standard deviation of duplicate to triplicate measurements.

In Phase I, on average, the highest concentration of butyric acid was reached between the third day and the last day of fermentation, with a significant difference in butyric acid accumulation after two days and six days – R1: 1.8±0.8 gCOD.L⁻¹, R2: 1.7±1.1 gCOD.L⁻¹, and R3: 1.7±1.4 gCOD.L⁻¹, p-value<0.05. After Phase I, the highest mean concentration of butyric acid was constantly reached

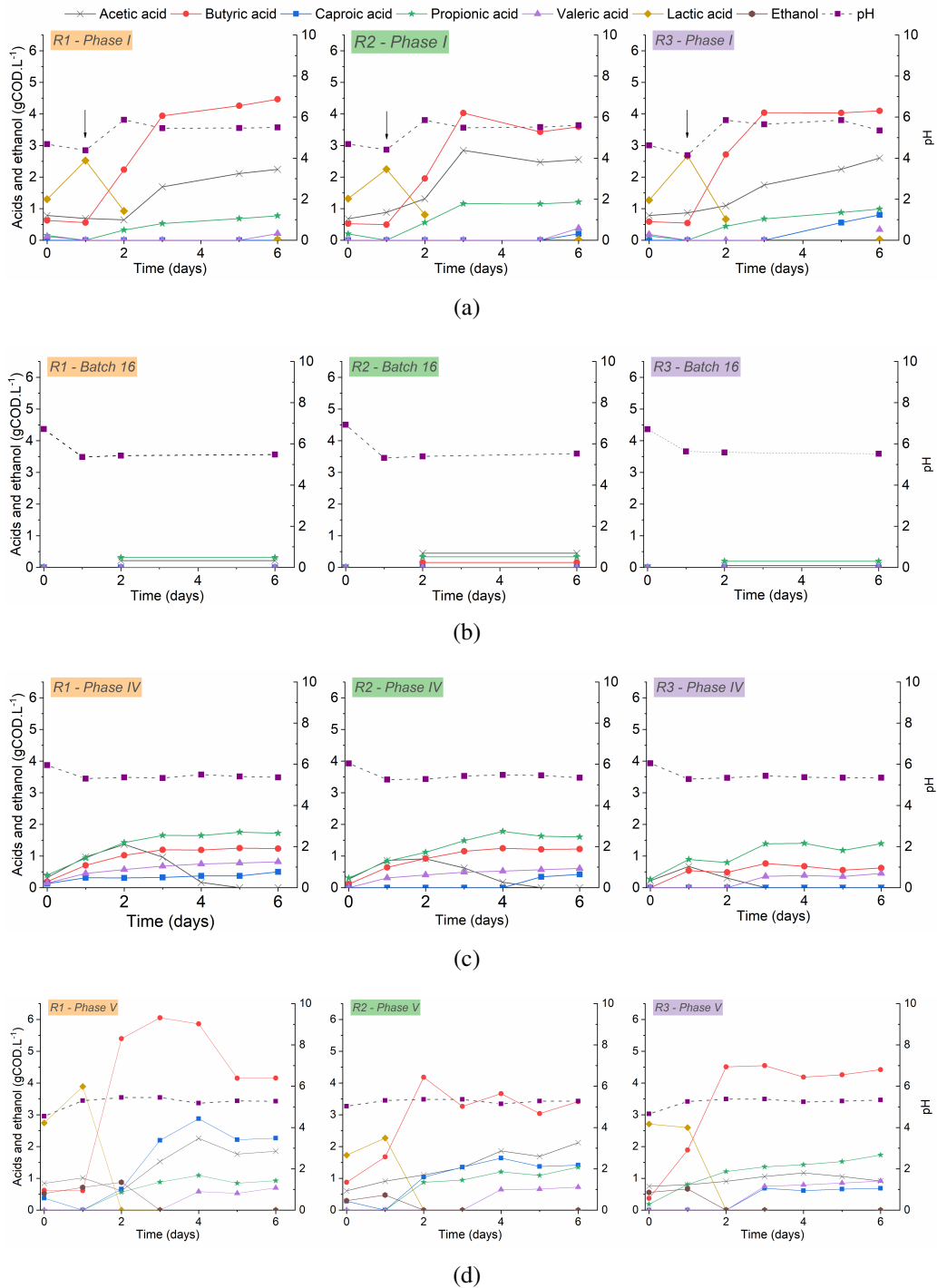


Figure 5.5: Profile of volatile fatty acids, lactic acid, ethanol, and pH profile at Phase I (Batch 3, a); Batch 16 (b); Phase IV (Batch 20, c); and Phase V (Batch 30, d). For Phase I, pH control started at day 1, while at the other phases it started at day 0.

after two days of fermentation, with no difference to days 3 or 6 (Figure 5.5). In Phase III, washing the solid mixture composed of digestate and silage, led to a lower accumulation of VFAs (Table 5.4) and to the production of methane (Figure 5.7), which resulted in a similar product yield to Phases I and II but with the participation of methane (Figure 5.6).

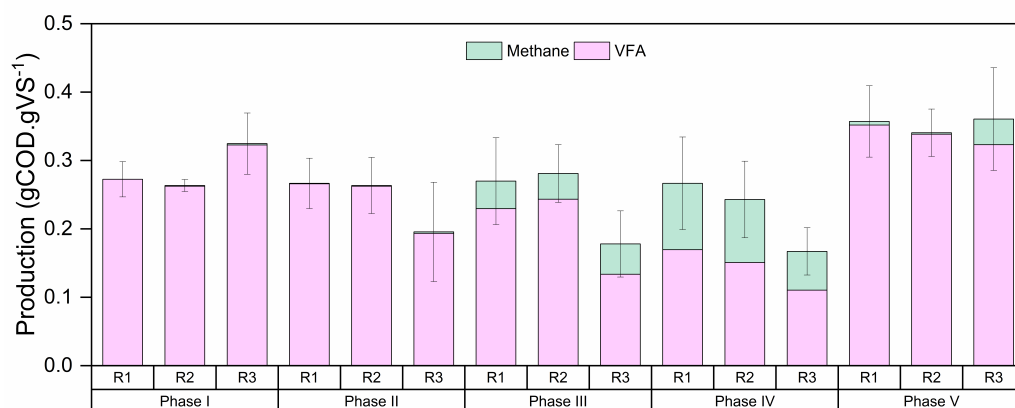


Figure 5.6: Production of VFAs and methane from the fermentation of silage through Phases I-V in Reactors 1, 2 and 3. The error bars represent standard deviations of the total production (VFAs and methane) – Phase I (n=4), Phases II and III (n=3), Phase IV and V (n=6).

The lowest production of VFAs observed in this study was detected between Phases III and IV (Batch 16, transient), in which a high-pH silage was loaded into the reactor (pH 8.1, Table 5.3), leading to a complete consumption of VFAs (Figure 5.5.b) and a methane production of 1.4 NL in Reactor 1 and 1.0 NL in Reactor 3 (no detection on Reactor 2 due to a leakage on the gas bag). Methane was consistently observed in Phase IV (Figure 5.7), when a silage with pH 6.6 was used. An average production of 4.8 (1.3) L, 3.3 (1.4) L, and 2.6 (0.7) L was detected for Reactors 1, 2 and 3, respectively. Alongside this methane production, a complete consumption of acetic acid (Figure 5.5.c) and a lower production of VFAs were also observed in Phase IV (Figure 5.8). Methane production decreased in Phase V for all reactors, except Reactor 3, in which an average production of 1.4 (0.6) L was detected.

Apart from the Start up, the highest accumulation of VFAs was observed in Phase V (Figure 5.8, Table 5.4). Phase V also presented the highest numerical total product yield (Figure 5.6). The production of VFAs and butyric acid was restored (Figure 5.8) after Phase IV, when a silage with acidic pH (pH 4.3) was fed again to reactors. When compared to Phase IV, a significantly higher production of VFAs (R1: 3.7 ± 1.5 , R2: 3.6 ± 1.0 , R3: 4.5 ± 1.7 gCOD.L⁻¹, p-value<0.001), and butyric acid (R1: 1.7 ± 0.9 , R2: 1.2 ± 0.7 , R3: 2.2 ± 0.7 gCOD.L⁻¹, p-value<0.002) was observed in Phase V. The maximum concentration of butyric acid was reached after the consumption of the lactic acid accumulated in the leachate, which seemed conditional to the silage pH (Phases I and V). Overall, the three reactors produced a similar concentration of VFAs and butyric acid during Phase V. Moreover, after six days of fermentation, the highest yield of caproic acid was achieved by Phase V in all reactors after six days of fermentation (Figure 5.8, and Table 5.4), with yields of 0.07 gCOD.gVS⁻¹ (Reactors 1 and 2), and 0.05 gCOD.gVS⁻¹ (Reactor 3).

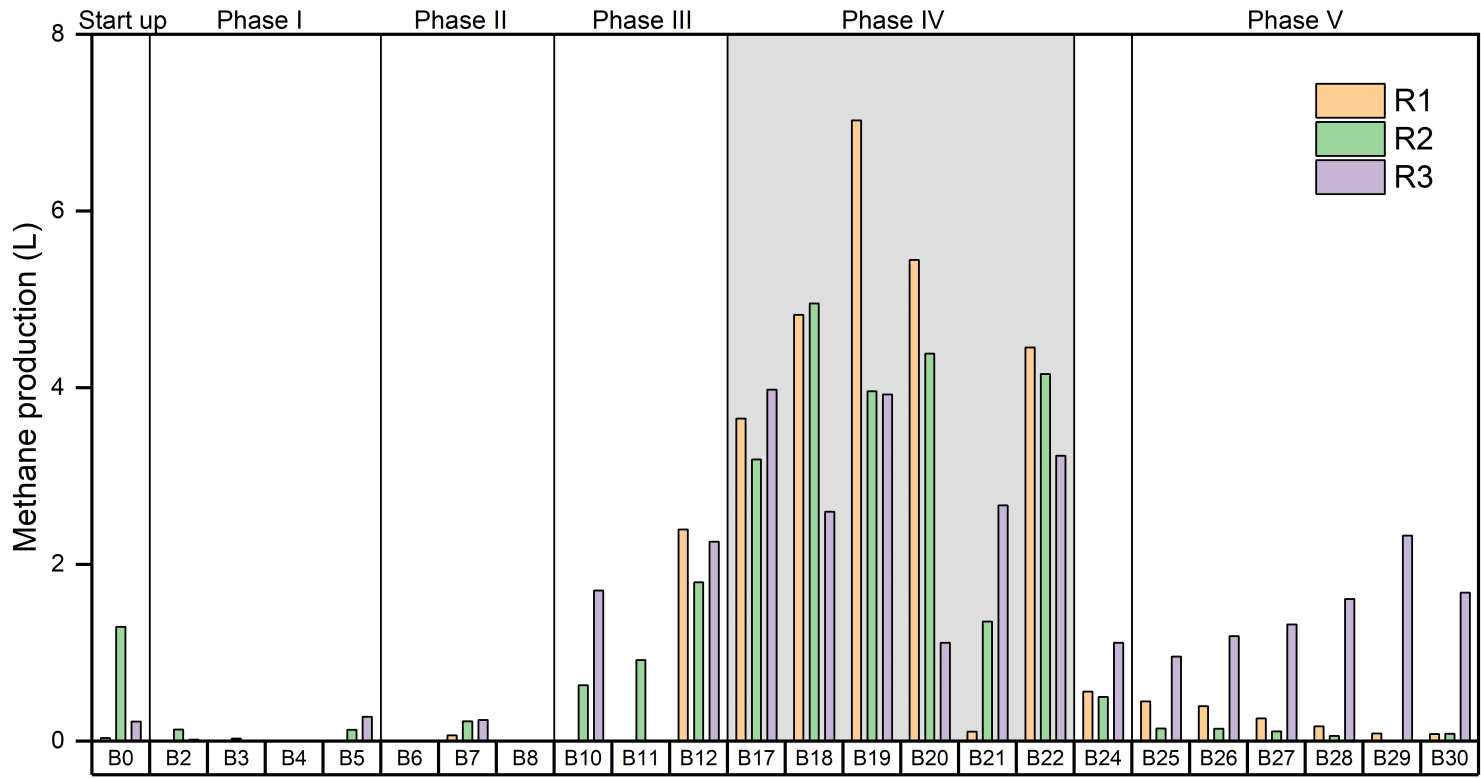


Figure 5.7: Methane production detected during the fermentation of silage in Reactor 1 (left-bar, orange), Reactor 2 (middle-bar, green), and Reactor 3 (right-bar, purple)

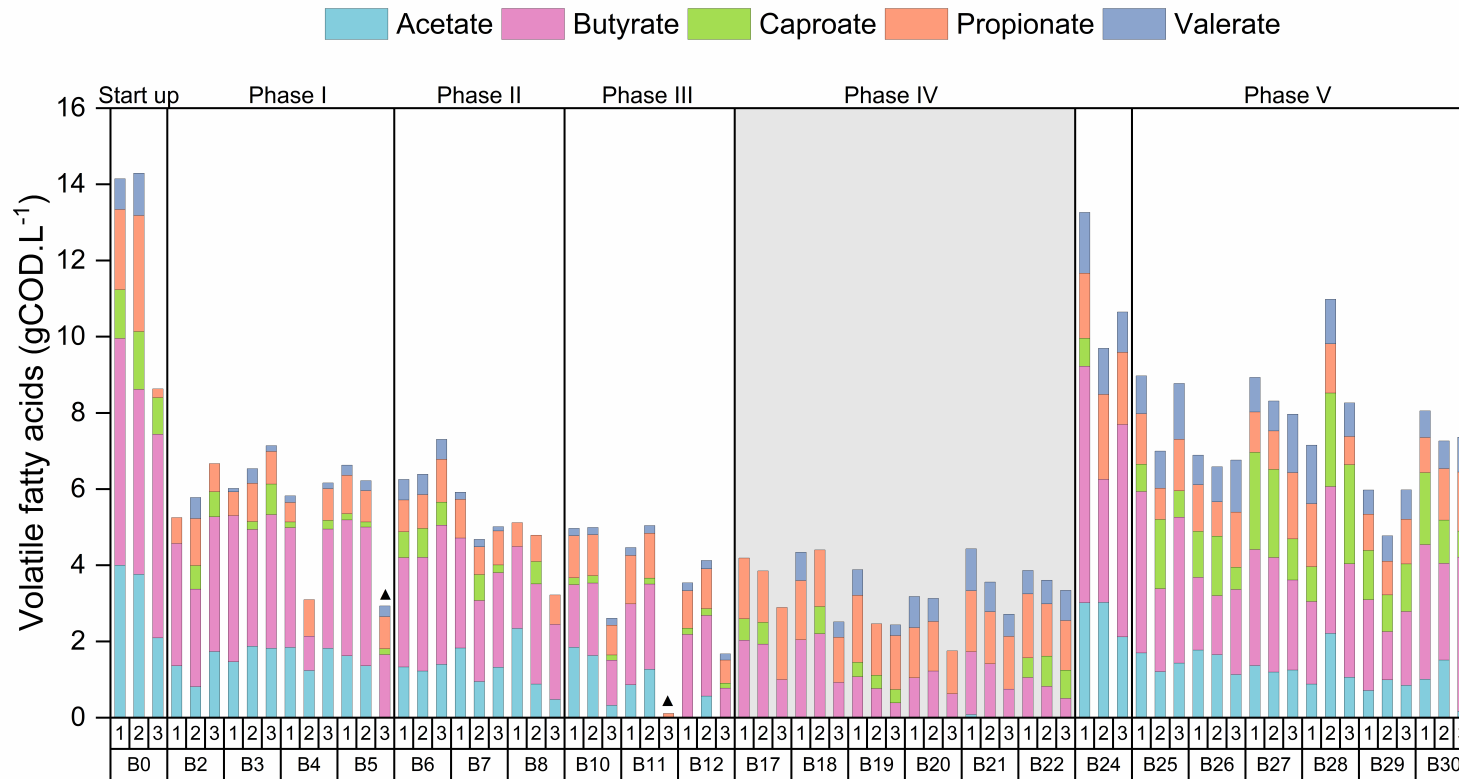


Figure 5.8: Net production of volatile fatty acids (VFA) from silage over phases in reactors 1, 2, and 3. Triangles mark batches that had a problem with the control system (e.g., overdosing of base or acids).

5.4.4 Digestate is important for the degradation of silage and production of VFAs

The differences in VS degradation seemed to be influenced more by the inoculum approach than the reactor from where the inoculum was collected (Figure 5.9). Silage degradation levels were lower when the fermentation was inoculated only with the leachate phase. Moreover, similar values of VS degradation were observed when the digestate was used as inoculum, mixed or on its own. No difference was observed between reactors, considering the same inoculum phase. In this fermentation, pH levels at day 0 were below 5.0 (Digestate + Leachate: 4.9 ± 0.1 ; Digestate: 4.7 ± 0.1 ; and Leachate: 4.4 ± 0.0). A correction to 5.3 was performed for the first two days as levels were consistently below 4.5. By the end of the fermentation, pH levels between 4.8-4.9 were observed when the digestate was used as inoculum, on its own or in a mixture with leachate. The pH increased, however, by the end of the fermentation when leachate was used as an inoculum (approximately 5.9 for the three reactors).

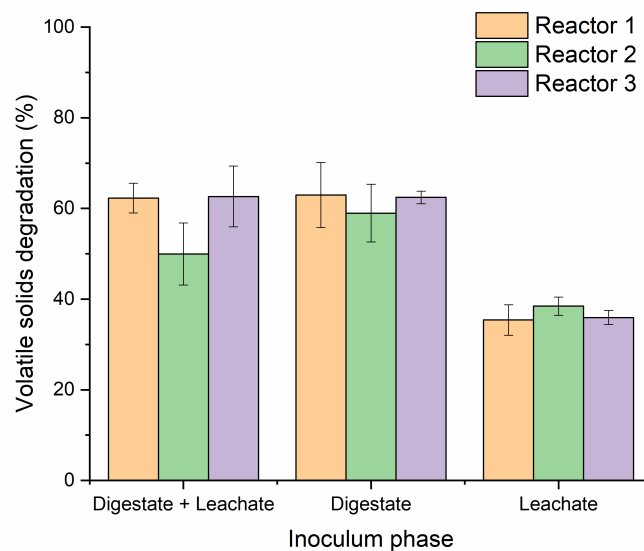


Figure 5.9: Silage degradation (in %VS) resulting from its fermentation using Batch 30's digestate + leachate, leachate, and digestate as inoculum. The error bars represent standard deviations.

The cumulative methane production was considered negligible, as a production below 7.5 mL and below 1.0 NmL.gVS^{-1} was detected for most conditions – except in the fermentation of silage using Reactor 3's digestate as inoculum (CH_4 : $77.8 \pm 1.7 \text{ mL}$, $9.8 \pm 0.2 \text{ NmL.gVS}^{-1}$). In terms of VFA production, a similar net production was reached after six days of fermentation, when using the digestate as inoculum, considering it a mixture or on its own (Table C.3, Figure 5.10). The highest VFA production rate was observed when using the mixture of digestate and leachate as inoculum (R1: $3.5 \pm 0.4 \text{ gCOD.L}^{-1}.\text{day}^{-1}$; R3: $3.8 \pm 0.7 \text{ gCOD.L}^{-1}.\text{day}^{-1}$). Considering the inoculum from Reactor 1, the VFA production rate for the mixture of inocula phases was higher than the production rate while using digestate-only (2.2x) or leachate-only (5.8x). Moreover, the VFA production rate was equivalent after two days of fermentation using digestate in the inoculum, as a mixture or on its own; the same was not observed using leachate-only as inoculum.

Butyric acid and caproic acid were the highest produced VFAs regardless of inoculum phase used

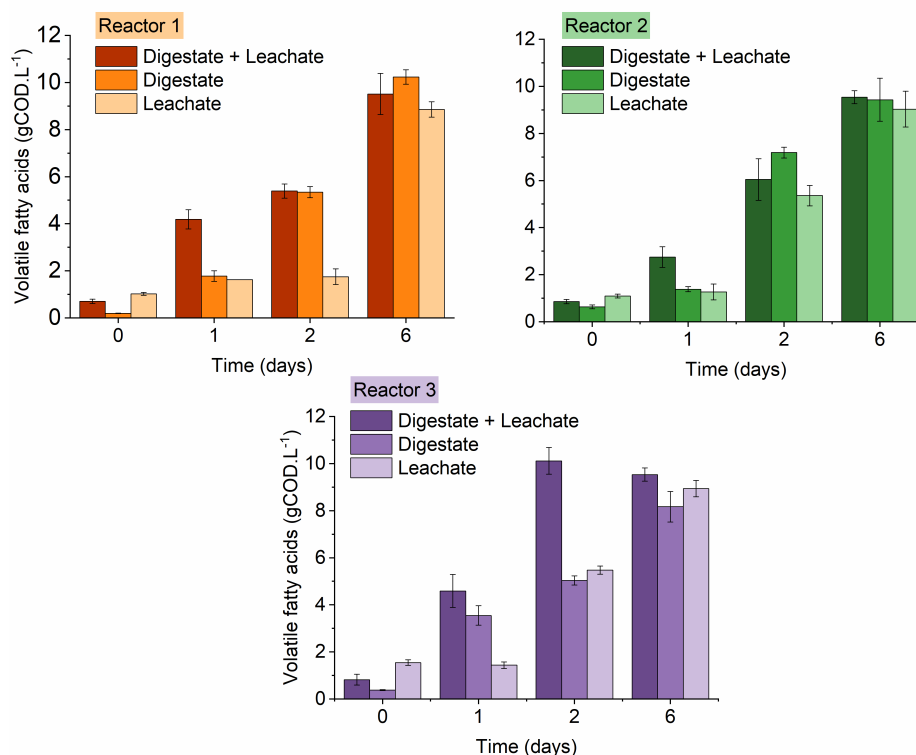


Figure 5.10: VFA production in the fermentation of silage using different inoculum approaches. The error bars represent standard deviations.

or reactor, followed by acetic acid and propionic acid (Table C.3). Numerically, the maximum net concentration of butyric acid was observed using Reactor 1's digestate (R1 D: 3.6 ± 0.7 gCOD.L⁻¹) as inoculum, which was higher than the concentration of butyric acid obtained when using leachate as inoculum (R1 L: 2.1 ± 0.1 gCOD.L⁻¹). Moreover, the highest production of caproic acid was also observed using Reactor 1's digestate (3.2 ± 0.2 gCOD.L⁻¹), leachate (3.2 ± 0.2 gCOD.L⁻¹), and the mixture of phases (3.0 ± 0.3 gCOD.L⁻¹).

5.4.5 Combining seed-inocula and silage was important to compose a richer microbial community

The microbial community dynamics in the fermentation of silage in LBRs was investigated considering (i) the three different silages used in Phases I, IV and V (silages PI, PIV and PV); (ii) the seed-inocula used at the start-up of each reactor; (iii) and the community extracted from leachate and digestate samples in Phases I, IV and V. For that, microbial samples were evaluated in terms of alpha diversity (rarefied richness and Shannon entropy), beta diversity (Bray-Curtis distance and HMS) and taxonomic composition (at DNA and cDNA level). Moreover, a quality-check was performed to investigate the effect of sonication times and RNAlater[®] in the quality of the DNA extracted. A discussion about this quality-check can be found in this chapter's appendix (Section C.1, page 158).

No difference in rarefied richness was observed between silages PI, PIV and PV (Figure 5.11). However, these silages had a significantly lower richness (p-value < 0.05) compared to the seed-

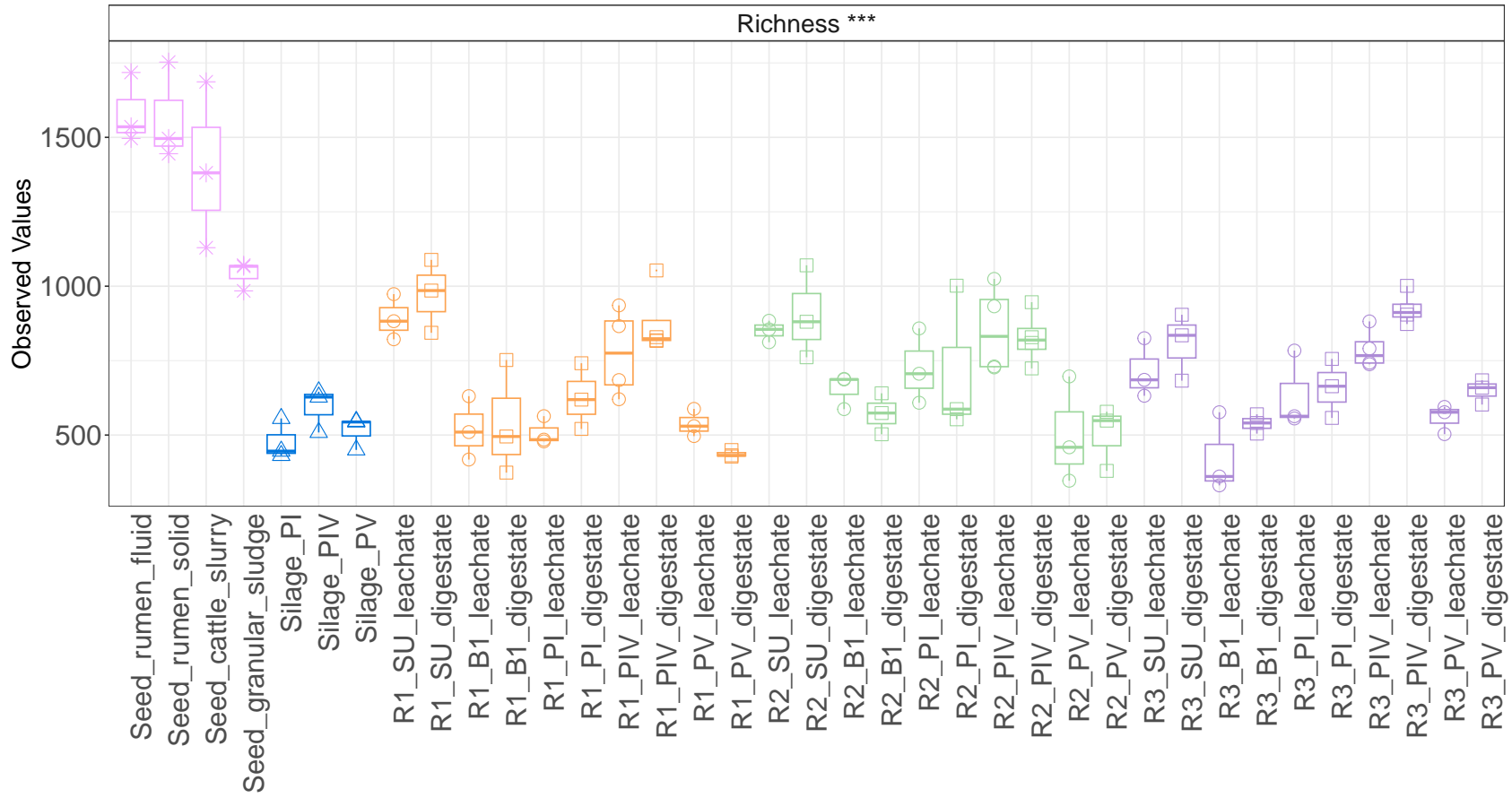


Figure 5.11: Rarefied richness profile based on the 16s rRNA sequences (DNA level) extracted from silage (triangle), seed-inocula (star), leachate (round) and digestate (square) samples – Reactor samples were extracted from the three reactors in the Start Up and Phases I, IV and V.

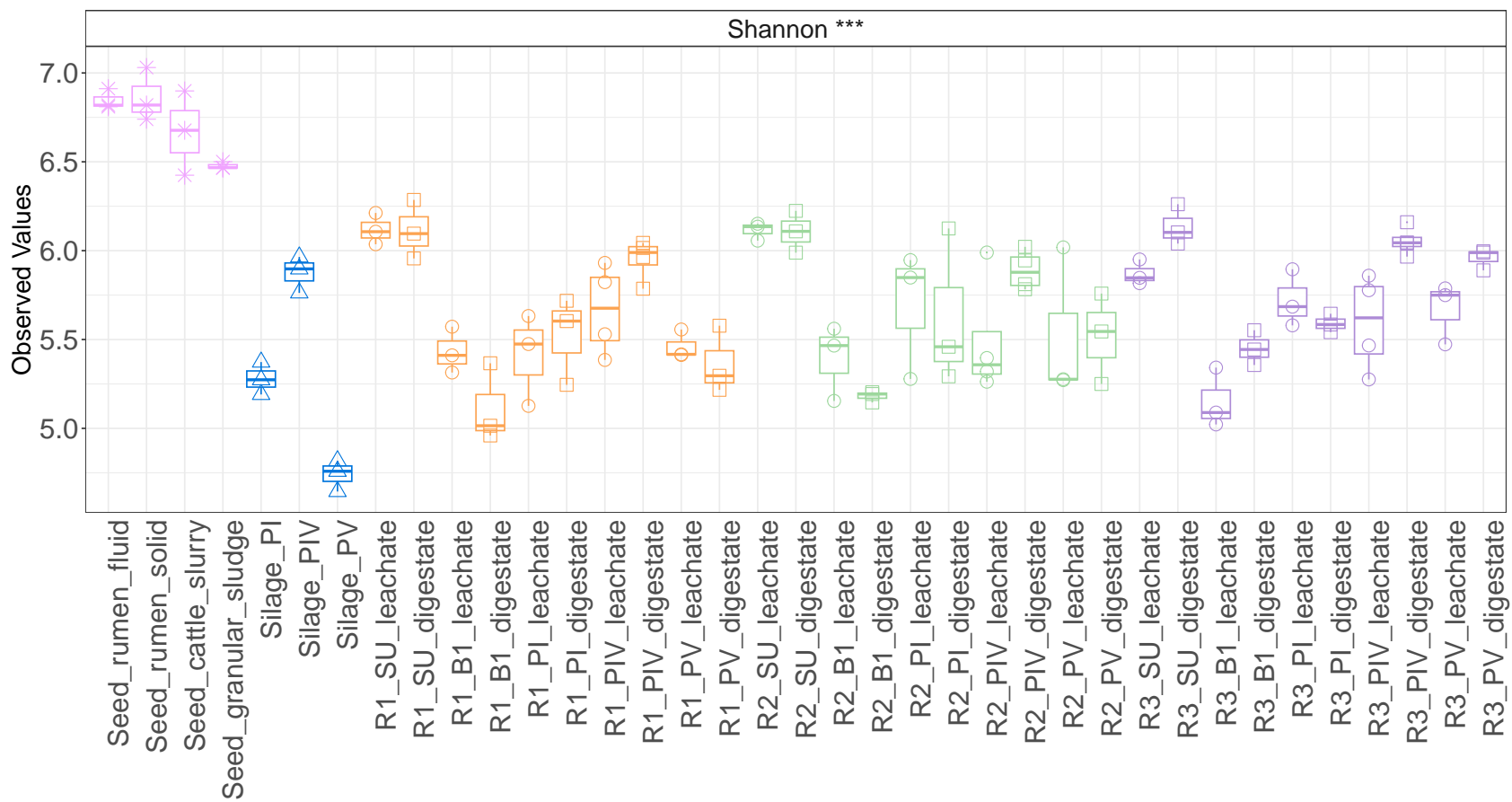


Figure 5.12: Shannon Entropy based on the 16s rRNA sequences (DNA level) extracted from silage (triangle), seed-inocula (star), leachate (round) and digestate (square) samples – Reactor samples were extracted from the three reactors in the Start Up and Phases I, IV and V.

inocula used in the start-up of the fermentation (GS, RF, RS, and CS). No difference in richness was observed between seed-inocula samples, except between GS and rumen material (RF and RS, p -value <0.01). Overall, changes in richness were observed across the different operational phases, but with the same trend for the three reactors. For example, richness was higher during the Start Up phase (SRT = 13 days), decreasing significantly at Batch 1, when the SRT was decreased to 6 days (p -value < 0.05). The decrease in richness between Phases IV and V was also significant (p -value <0.05). Moreover, the same richness was observed between digestate and leachate samples considering the same phase and reactor. Therefore, the fact that these changes were common to the three reactors over different phases indicated that the shift in richness was governed by supplying different silages and not by the different seed-inocula used at Start Up.

On the other hand, Shannon entropy results showed a difference between silages, with silages PI and PIV presenting a higher Shannon entropy compared to Silage PV (p -value <0.001 , Figure 5.12). Silage PIV also had a higher Shannon entropy than Silage PI (p -value <0.01). Moreover, all silages had a significantly lower Shannon entropy compared to the seed-inocula (p -value < 0.05). No difference in Shannon entropy was observed between seed-inocula samples, except between GS and rumen material (RS and RF, p -value <0.05). However, results for the Start Up phase of the three reactors showed no significant difference in Shannon entropy, despite using different mixtures of seed-inocula composed of GS. Over the phases, results showed a shift in the microbial community, with higher Shannon entropy values in Start Up compared to Batch 1, when the SRT was decreased to 6 days (p -value <0.01). For some reactors, this decrease in Shannon entropy was also observed between Start Up and Phase I (R1 and R3, p -value <0.05); and between Phases IV and V (R1, p -value <0.01). In terms of inocula source for a subsequent batch (leachate or digestate), Shannon entropy results showed that the microbial community abundance was similar in most phases and reactors. This was not the case for Reactor 3 in Start Up and Phase IV, where the abundance in the digestate was significantly higher (p -value <0.05) than in the leachate. However, this could be a statistical artefact due to the low amount of samples (triplicate) and data, leading to a lack of systematical difference because of the system's heterogeneity.

These results from richness and Shannon entropy indicated the importance of using a seed-inocula alongside the indigenous microbial community of silage. With a lower richness and lower Shannon entropy, the microbial community of silage itself may lack important organisms to the degradation of silage and production of VFAs. However, maintaining a more balanced and rich microbial community after the Start Up seemed to be a challenge in all reactors, as evidenced by the decrease in rarefied richness and Shannon entropy between the Start Up phase and Batch 1 (transient).

5.4.6 Shifts in microbial composition were correlated to the different silages

As indicated by the alpha diversity measures, the microbial community shift over the course of the fermentation seemed to be more related to the different silages used in Phases I, IV and V than the seed-inocula mixture supplied in the Start Up phase (i.e., different reactors). To better understand

the difference in diversity between samples (beta diversity), measures such as Bray-Curtis distance (Figure 5.13) and HMS (Figure C.2) were used. The beta diversity showed a compositional similarity between Silages PI and PV, and a dissimilarity between these two silages and Silage PIV (Figure 5.13). This pattern was also observed when comparing the operational phases supplied with Silages PI, PIV and PV. Each operational phase (I, IV and V) was clustered together, with no overlap between Phases I, IV and V, indicating a similarity between samples from the same operational phase, but a dissimilarity between samples in different phases. This was observed especially between Phases IV and V, where the distance indicates a compositional dissimilarity between Phases IV and V (p-value <0.001). A slight dissimilarity between Reactor 3 and the other two reactors can be observed in Phase V, but still lower than the difference between phases. The compositional similarity between seed-inocula may have contributed to the compositional similarity between reactors, especially at the Start Up phase, where the seed-inocula was fresh. Moreover, a slight difference in functionality can be observed between Phases IV and V based on the KOs abundances (Figure C.2), irrespective of the reactor. This dissimilarity was also observed between Silages PI, PIV and PV.

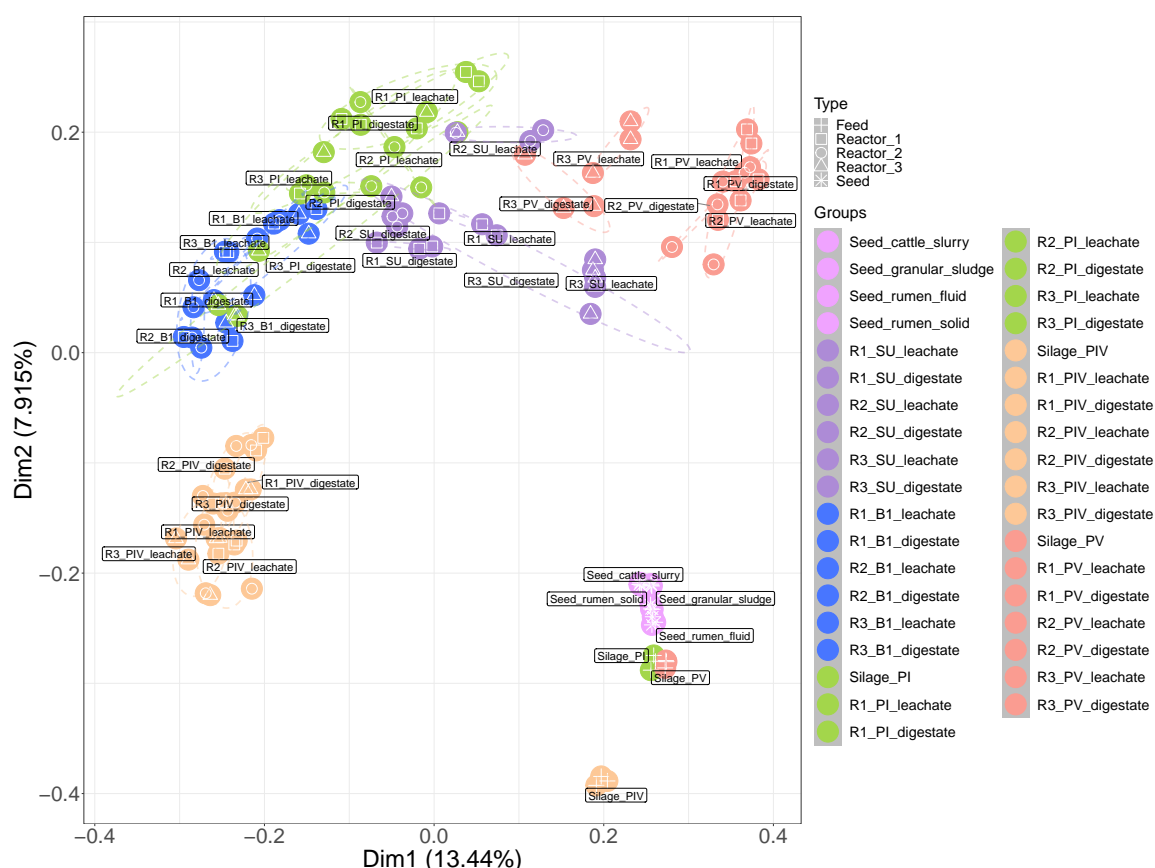


Figure 5.13: Principal Coordinate Analysis (PCoA) plot based on Bray-Curtis distance of 16s rRNA sequences (DNA level) extracted from seed-inocula (pink), Start Up (purple), Phase I (green), Phase IV (orange), and Phase V (red). Silage colour is represented according to the phase it was fed; p-value <0.001.

5.4.7 *Prevotella* and *Lactobacillus* as the most abundant genera, irrespective of the seed-inocula used

A difference in taxonomic composition can be observed when comparing the three silages fermented in LBRs (Figure 5.14). In Silage PI and Silage PV, bacteria from the *Lactobacillales* order (genera *Lactobacillus* and *Weisella*, 49.7% relative abundance) were more abundant in comparison to other bacteria. However, the relative abundance of bacteria from the *Lactobacillales* order (6.1% relative abundance) was lower in Silage PIV, especially when compared to the abundance of bacteria from the *Pseudomonadales* order (genera *Acinetobacter* and *Pseudomonas*, 30.5% relative abundance). In fact, the appearance of *Acinetobacter* and *Sphingobacterium* was observed in the leachate and digestate of all reactors in Phase IV. Compared to the other feed, Silage PV also presented two genera of relevance to this work, *Prevotella* and *Caproiciproducens*, at the top-25 most abundant genera, but in low relative abundance. The *Lactobacillus* genus represented 6.9% of the relative abundance (at the top-25 most abundant genera), with a relative abundance of others of 85%. Regarding the seed-inocula used to inoculate the reactors, the same taxonomic groups were found in rumen fluid, rumen solid and cattle slurry. Granular sludge, which was used as a seed-inoculum in all reactors, had two genera as most abundant – an uncultured genera of the *Rhodocyclaceae* family, and the saccharolytic genus *Christensenellaceae R-7 group* – which was also observed in the other seed-inoculum.

The most abundant phyla during the reactor trial were *Firmicutes*, *Bacteroidota*, *Proteobacteria*, and *Actinobacteriota* (Table C.2). However, a shift in relative abundance was observed over the operational phases, especially between *Firmicutes* and *Bacteroidota*. In Phase I, the relative abundance of *Firmicutes* was numerically higher than the relative abundance of *Bacteroidota* – a pattern that was reversed in Phase IV. In Phase V, *Firmicutes* was the most abundant phyla, with a relative abundance of 2-7x higher than the relative abundance of *Bacteroidota* (depending on the reactor and sample considered). The relative abundance of *Actinobacteriota* also increased in Phase V (Reactors 1 and 2). Bacteria from the genus *Lactobacillus* and *Prevotella* were observed consistently in all reactors, irrespective of the operational phase. The relative abundance of *Prevotella* was higher than *Lactobacillus* until Phase V, where a predominance of *Lactobacillus* was higher or similar to the relative abundance of *Prevotella*. Moreover, bacteria from genera *Acidaminococcus* and *Pseudoclavibacter* were observed in Phase V, but not the other phases. *Prevotella* bacteria can be observed since the beginning of the fermentation, irrespective of the reactor, but *Caproiciproducens* was the most abundant in Reactor 3's Start Up phase. Bacteria from the genera *Bacteroides* and *Rikenellaceae RC9 gut group* are also present at the start up, but their relative abundance decreased over the trial. The taxonomic composition at Phase V was similar at both DNA and cDNA levels (Figure 5.15), and when comparing leachate and digestate. However, different genera seemed more active in each reactor, with *Prevotella* more activate in Reactor 3, while *Lactobacillus* were more active in Reactors 1 and 2. Bacteria from the *Pseudoclavibacter* genus also seemed more active in Reactor 1, especially in digestate samples.

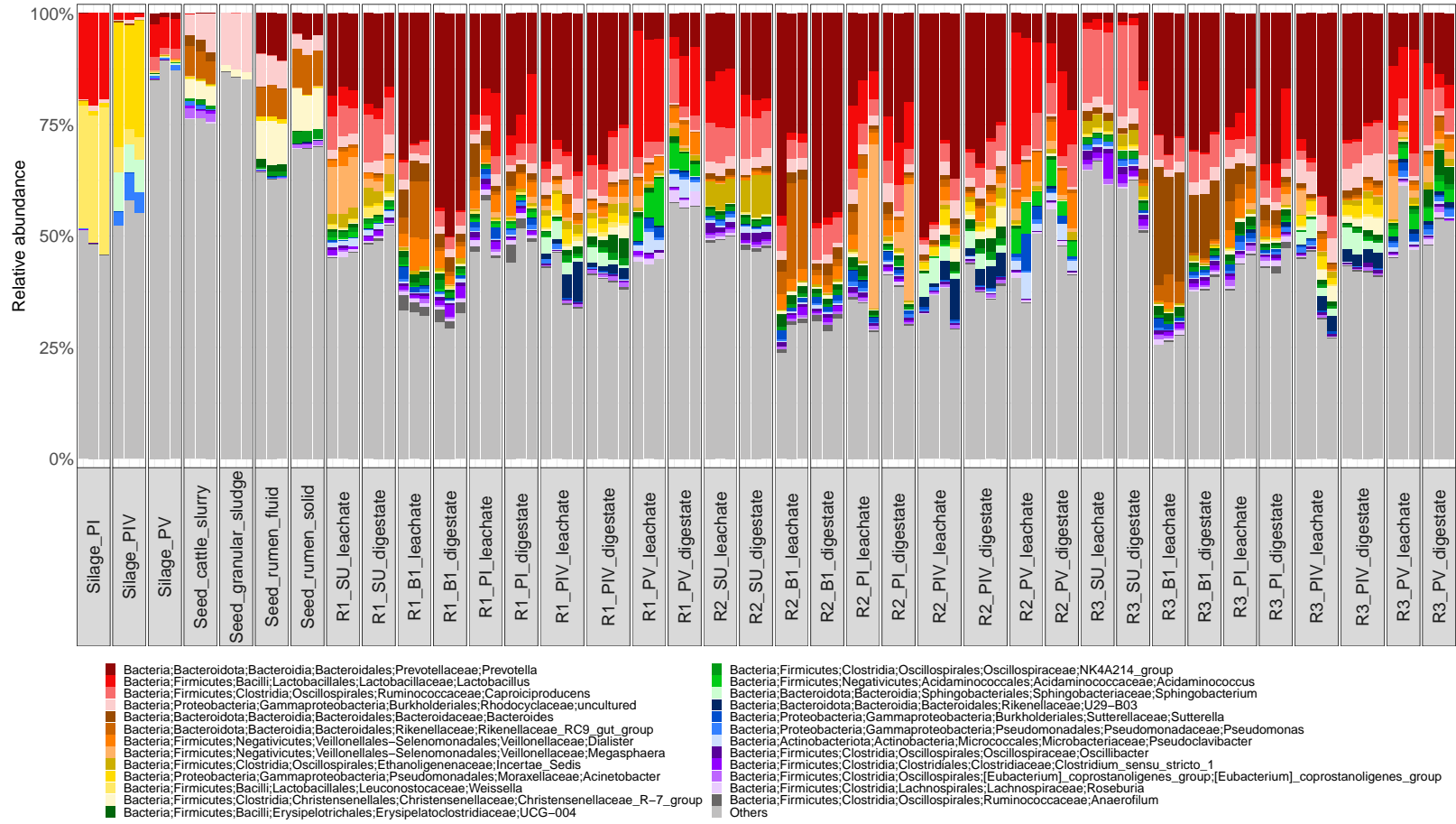


Figure 5.14: Taxonomic composition of the microbial community 16s rRNA gene (DNA level) extracted from silage, seed-inocula, leachate and digestate samples – Reactor samples were extracted from the three reactors in the Start Up and Phases I, IV and V.

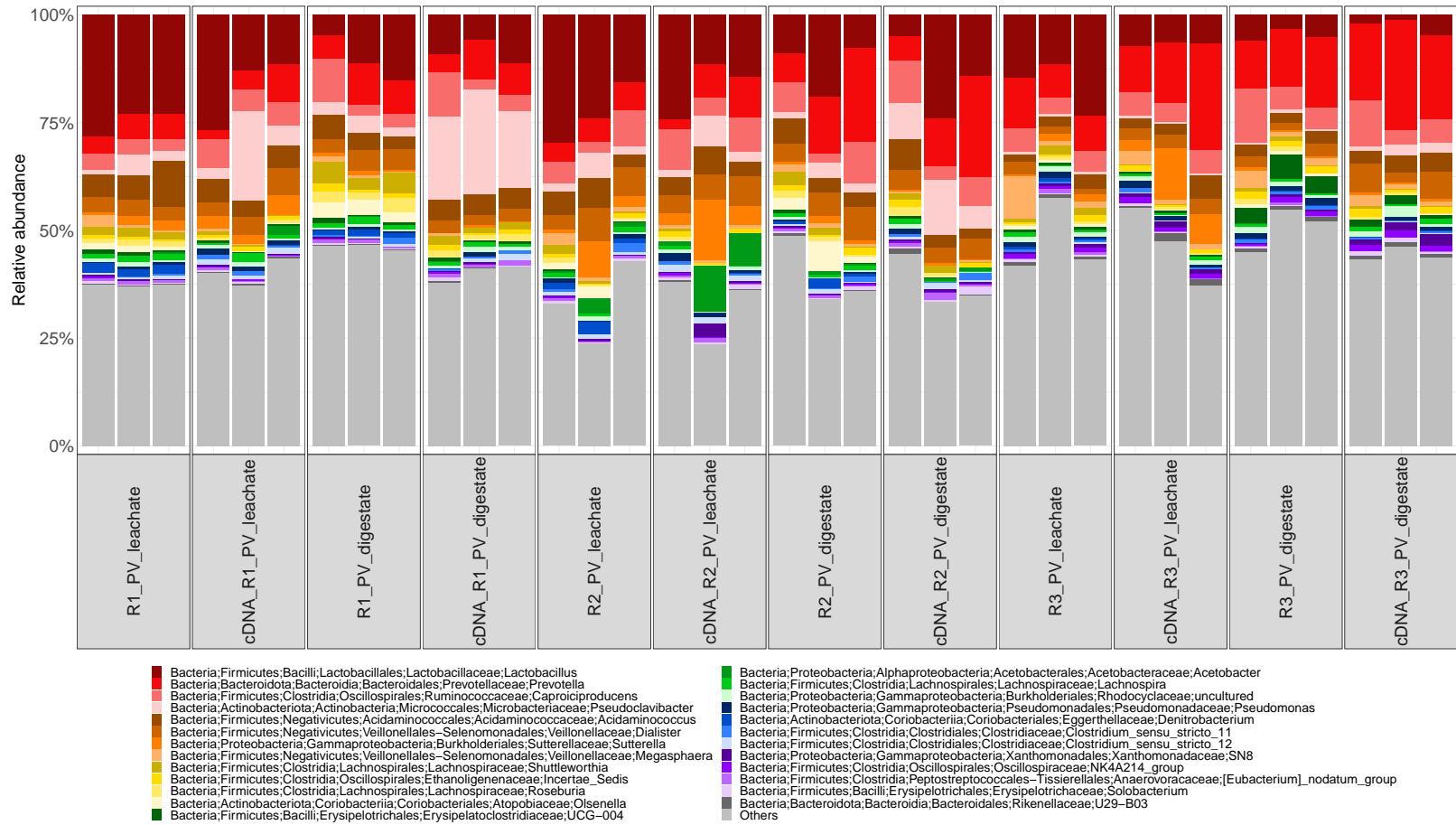


Figure 5.15: Taxonomic composition of the microbial community 16s rRNA gene (cDNA level) extracted from silage, seed-inocula, leachate and digestate samples – Reactor samples were extracted from the three reactors in Phase V.

5.5 Discussion

5.5.1 Efficient silage degradation achieved using a mixture of granular sludge with rumen material and cattle slurry

In previous chapters of this thesis, granular sludge (GS) has been employed successfully to convert the lignocellulosic matrix of fresh grassland biomass into methane while providing a sufficient biomass degradation (see Chapters 2 and 3). Therefore, the same source of granular sludge was used again in this chapter, alongside rumen material (RF and RS) and cattle slurry (CS). Our results showed that combining GS with RF, RS and CS was important to reach a higher degradation efficiency, especially compared to using each seed-inoculum individually (Figure 5.3.a). This higher degradation is a result of the hydrolytic capability of the microbial community present in RF, RS and CS, which has fibrolytic microorganisms that are responsible for degrading the lignocellulosic fibre^{44,45}. As a consequence, this higher silage degradation had a direct effect in biomass conversion, leading to an increased methane yield when using those combinations of seed-inocula in comparison to using each seed-inoculum individually (Figure 5.3.b).

Other studies have highlighted the hydrolytic capability of rumen fluid and cattle slurry and its potential to enhance productivity^{28,41-43}. Ozbayram et al.⁴² also achieved a higher methane yield in the digestion of cow manure by using a combination of rumen fluid and anaerobic seed sludge as inoculum. Moreover, adding a pre-treatment step with rumen fluid led to a 57% increase in methane production from rapeseed⁴¹. The use of cow manure and rumen fluid as inoculum or co-inoculum was responsible for increasing hydrolysis rate²⁸ and VFA accumulation in the fermentation of food waste²⁸ and different lignocellulosic biomasses⁴³. Therefore, combinations of GS with RF, RS and CS were selected as seed-inoculum for the fermentation of silage in LBRs. However, although a higher VS degradation was achieved with these mixtures of inoculum, lower values are expected from the fermentation of silage due to low pH.

5.5.2 Silage degradation evidenced by the reduction of cellulose and hemicellulose content

Overall, the degradation of silage was similar during the nine months of reactor operation and across different phases (Figure 5.4). As expected, the VS degradation of silage in LBRs was lower than what was observed in the inoculum selection experiment, irrespective of the seed-inocula used. Conditions in the Start Up phase were similar to the seed-inoculum experiment in terms of SRT (13 days) and the freshness of the inoculum source. However, after the Start Up phase, silage degradation decreased by 33% (Reactor 1), 25% (Reactor 2), and 14% (Reactor 3) in comparison to the seed-inoculum experiment.

A further decrease was observed in the following phase (Phase I) for Reactors 1 and 2, where pH levels were around 4.1 after one day of fermentation, which is a pH that can hinder the hydrolysis of biomass²⁸. Over the course of the fermentation, pH was kept around 5.5 (Figure 5.5), which is below the neutral to basic range that is preferable for solubilising lignocellulosic biomass^{7,70}, thus

explaining the silage degradation achieved. This pH range was chosen for accumulating VFAs from grassland biomass with minimal loss to methane, as results from Chapter 4 showed a consumption of acetic acid and VFA loss for methane accumulation when pH was above 6.0. Therefore, this lower degradation can be explained by the pH range applied in this fermentation, which was lower than the pH used for the seed-inoculum selection experiment (pH 7.5/8.0).

Two attempts were performed to improve the degradation of silage: (i) increase leachate dilution at the beginning of the batch (Phase II), and (ii) wash the solid mixture of digestate and leachate (Phase III). In Phase II, the dilution was performed to decrease the starting VFA concentration in the liquid phase, which led to a 35% dilution of the initial COD in the leachate. The hypothesis was that this dilution would lead to product removal from the starting leachate, which would increase silage degradation for VFA production. This strategy led to a slight increase in silage degradation, but no difference in VFA accumulation.

In Phase III, a washing of the solid mixture (silage and digestate) was performed as it was believed that the amount of solid COD supplied to the reactor was hindering the degradation of silage. The hypothesis was that the readily available material from the surface of silage and digestate was being used preferentially for VFA production, hindering the hydrolysis of the biomass. Alongside washing the solids, the OLR was also decreased as the reactor system was too packed with solids (Figure 5.2), leading to gas bubbles trapped inside the silage-digestate bed and poor mixing. However, neither of those changes significantly improved silage degradation. In fact, decreasing the OLR led to a lower accumulation of VFAs³⁴ despite controlling the pH, especially in Reactor 3, leading to methane accumulation (Figure 5.7), acetic acid consumption and propionic acid production (Table 5.5).

Despite the lower than optimum degradation levels, evidence for the degradation of silage's ligno-cellulosic matrix was found for all reactors in Phase V (Table C.1), with a higher degradation of cellulose followed by hemicellulose. A lignin degradation below 10% was observed in Reactor 1, but not in the other two reactors which had negative values for lignin degradation. These negative values indicate that the lignin content (in mass of dry weight) was higher at the end of Batch 30 than at the beginning, which is not possible as lignin cannot be generated in this system. There can be two explanation for these unusual values. One hypothesis is the heterogeneity of the silage biomass, as observed in Chapter 3, which means that the lignin content will not be evenly distributed so a particular sample is a representative sample of the whole structure. Moreover, the nature of the LBR operation, in a system heavily packed with digestate and grass silage, may not provide a homogeneous degradation of the biomass.

5.5.3 Silage pH was an important process indicator for acid accumulation efficiency and acid profile

Four different silages were used in our work with different pH values (Table 5.1), a characteristic that was crucial in the accumulation of VFAs and butyric acid (Figures 5.8; Figure 5.5). It is known that methane yields are affected by feedstock quality, which, in turn, are affected by grassland manage-

ment and preservation⁷¹. The silage pH is intrinsically connected with the conservation of silage, and lower pH values are important to guarantee a feedstock with a higher quality and nutritional value, as it is less prone to spoilage³⁸.

In this fermentation, Silage PI (pH 4.6), Silage B16 (pH 8.1), Silage PIV (pH 6.6), and Silage PV (pH 4.3) were supplied to reactors in Phases I, Batch 16 (transient), Phase IV, and Phase V, respectively, at similar retention times and loading rates (Table 5.3). Notably, Silage B16 and Silage PIV had patches of mould upon arrival, which were removed before storage and feed preparation. The presence of mould in Silage B16 resulted in the consumption of water-soluble compounds, such as water-soluble carbohydrates⁷², as indicated by the lower quantity of water-extractives and the silage with high pH (Table 5.1). After feeding the Silage B16, the reactor's pH was around 7.5 (Figure 5.5.b), which was higher than what was observed in Phases IV (around 6.0, Figure 5.5.c), Phases I (around 4.6, Figure 5.5.a), and Phase V (around 4.5, Figure 5.5.d). Attempts to decrease pH levels in Batch 16 included diluting the leachate to 65-70% of its initial COD and turning on the acid pumps only, leading to pH levels around 5.5 after one day with an acid consumption of 50 mL (3M HCl). However, the high-pH silage had several impacts on reactor performance: **(i)** the lowest production of VFAs was observed with concentrations below 1.0 gCOD.L⁻¹; **(ii)** very low concentrations of butyric acid (only detected in Reactor 2); **(iii)** silage degradation levels below 30%; **(iv)** and methane production in Reactors 1 and 3.

The silage pH also had an impact between Phases I, IV and V, but not as drastic as what was observed in Batch 16. The use of a silage with pH 6.6 led to a complete consumption of acetic acid and a significant increase in methane production in Phase IV compared to Phases I and V. This change in pH also led to a shift in the VFA profile, with propionic acid dominating the VFA mix after six days (Table 5.5). Shifts in VFA profile have been associated to operational conditions, such as operational pH, inoculum and feedstock type³. In our work, the silage pH, therefore its quality, was correlated with shifts in VFA profile and differences in acid yields with a pH 8.1 silage leading to no VFA accumulation, a pH 6.6 silage leading to low VFA accumulation, and pH 4.3 or 4.6 resulting in optimum VFA and butyric accumulation for this trial. In fact, when re-introducing a silage with similar pH to the beginning (Phase I vs Phase V), the production of VFAs, especially butyric acid, was restored and improved.

Moreover, despite the similar butyric acid yield, a higher accumulation of VFAs was detected due to the increased production of caproic acid (Table 5.4). Also, the rate of butyric acid production was higher in Phase V than Phase I, considering a maximum concentration of butyric acid was reached after 2 days of fermentation. Therefore, not only was the VFA production restored by Phase V, it was also improved for butyric acid accumulation and chain-elongation. It is also worth noting that Silage PI and PV were composed of different mixtures – Silage PI was composed mainly of *L. perenne* while Silage PV was composed of an equi-proportional mixture of six species of grassland biomass. The performance of Silage PV, therefore, validates the use of mixed-species silages for butyric acid production, with no significant difference from the silage composed mainly of *L. perenne*, and contributing to the sustainability of the process⁷³.

5.5.4 Butyric acid was the primary VFA produced from silage, with a significant accumulation of caproic acid

Overall, the three reactors presented a similar VFA profile (Figure 5.5) in each phase. However, in Phase III, the VFA yield from Reactor 3 was 41-45% lower (p -value <0.05) than Reactors 1 and 2 (Figure 5.6), which could be explained by the lower butyric acid yield observed for Reactor 3 in Phase III (Table 5.4). On the other hand, the difference in the production of VFAs in this fermentation seems to be more related to the silage pH than the seed-inocula mixture used in the Start Up phase (i.e., the different reactors). This could be a result of continuously feeding silage every six days, while the seed-inocula was only supplied to the fermentation at the Start Up phase. Although not tested, re-seeding the reactor with rumen material, cattle slurry and granular sludge could have affected the reactor performance and even improve the production of VFAs to the levels observed in the Start Up (Figure 5.8).

By Phase V, the system was selected for VFA production (around 7.5 gCOD.L^{-1}), reaching higher VFA yields (Figure 5.6) with lower methane accumulation and with butyric acid as the main produced acid followed by caproic acid and acetic acid (Table 5.5). The highest butyric acid concentration was obtained in Reactor 1 during Batch 24, a transient batch between Phase IV and V, where the silage PV was introduced for the first time. In Batch 24, a butyric acid concentration of 6.8 gCOD.L^{-1} (3.7 g.L^{-1} , 75.6%gVFA) was reached after two days of fermentation. This butyric acid concentration decreased slightly by the end of Batch 24 (6.2 gCOD.L^{-1} , 3.4 g.L^{-1} , 40.3%gVFA), but it remained the main produced VFA followed by acetic acid (33.3%gVFA). Butyric acid has been obtained previously as the main acid in the VFA mix from the anaerobic digestion of grass, but at lower concentrations (0.5 gCOD.L^{-1})⁷⁰. On average, the best production of butyric acid was observed in Phase V, after 2-3 days of fermentation (e.g., Reactor 1: $3.3\pm 0.9 \text{ gCOD.L}^{-1}$, $1.8\pm 0.5 \text{ g.L}^{-1}$, $72.24\pm 11.2\%$ gVFA). Afterwards, butyric acid concentration was constant or decreased (e.g., Reactor 1: $3.1\pm 0.8 \text{ gCOD.L}^{-1}$, $1.7\pm 0.4 \text{ g.L}^{-1}$, $36.5\pm 5.2\%$ gVFA), and caproic acid accumulated (e.g., Reactor 1: $1.5\pm 0.7 \text{ gCOD.L}^{-1}$, $0.7\pm 0.3 \text{ g.L}^{-1}$, $15.1\pm 6.2\%$ gVFA).

As VS degradation levels were similar over the fermentation trial (Figure 5.4), the higher production of VFAs by Phase V was not correlated to substrate degradation. In fact, the difference in VFA yield (Figure 5.6) and profile between phases (Figure 5.5) may be explained by the silage used, the initial accumulation of lactic acid and methane accumulation. The presence and accumulation of lactic acid at the first two days of fermentation was detected in Phase I (Figure 5.5.a) and Phase V (Figure 5.5.d), where a silage with low pH was used. This accumulation of lactic acid was important for the production of butyric acid¹⁹, which reached its maximum concentration after the complete consumption of lactic acid. Moreover, the VFA yield alone on Phases I and V was higher than the VFA yield reached in Phase IV (Table 5.6), and the difference between these phases was the silage pH. As no treatment was performed to inhibit methanogenic archaea (e.g., using BES or heat-shock)³, the process relied completely on the acidification of the system through VFA accumulation to inhibit methane production.

However, the use of a silage with pH 6.6 (Phase IV) resulted in a slower accumulation of VFAs, with no lactic acid accumulation at the beginning. This slower accumulation was favourable for VFA consumption to methane despite maintaining pH levels around 5.5, thus resulting in a lower VFA yield in Phase IV. Methane accumulation was also observed in Phase III, as a consequence of decreasing the OLR supplied to the reactors (Figure 5.7). However, the VFA concentration obtained in Phase III was the same as the VFA concentration obtained in Phase IV, indicating that using the Silage PIV (Phase IV) had the same effect in VFA concentration as using Silage PI at a lower OLR (Phase III). Residual methane was still observed in Reactor 3 by Phase V, even after changing the feed to Silage PV and maintaining pH levels around 5.5. In Phase V, methane production progressively decreased in Reactors 1 and 2, indicating that methane can indeed be detected when pH levels are 5.5²¹. However, consistent and continuous exposure to VFAs above a 0.3 gCODVFA.gVS⁻¹ was important to decrease methane accumulation.

The butyric acid production, however, was not limited to the accumulation of lactic acid, as butyric acid was still produced in Phase IV when no lactic acid was detected. Despite using Silage PI in Phases II and III, no lactic acid was detected in those phases, which can be a consequence of diluting the initial COD or washing the solid mixture. Moreover, the detection of butyric acid in Phases II and III was low compared to Phases I and V. Therefore, this indicates that the accumulation of lactic acid at the beginning or the consumption of the available lactic acid from day 0 was relevant to improve butyric acid yields, allowing a higher, quicker and selective conversion^{20,39} with a lower production of other acids in the metabolism, such as acetic acid. Reaching the highest concentrations of butyric acid from lactic acid in Phases I and V after 2-3 days of fermentation was an important indication to further optimise the process.

As discussed previously, lactic acid is commonly observed from well-preserved silage, so designing a step to maximise the production of lactic acid from grass can enhance butyric acid yields. This has been showed in Chapter 4 and other studies, when placing grass in water with no inoculum addition resulted in a sharp drop in pH and the accumulation of lactic acid^{8,11}. As this process occurs at low pH, however, hydrolysis of the lignocellulosic biomass may be hindered²⁸, so controlling the pH in this fermentation is important. In fact, pH control had a small effect in butyric acid production rate for Reactor 1 when comparing Phases I and V. In Phase I, pH levels were around 4.5 for the first two days of fermentation (days 0-1), which are not optimum for VFA production and biomass consumption^{3,28}. This drop in pH levels has been observed before in the fermentation of a pH 4.1 grass silage⁸ in LBRs, when pH levels were allowed to fluctuate for a day as well. Despite no change in butyric acid accumulation after six days, the accumulation after two days was significantly lower compared to Phase V (in R1: 1.6±1.1 gCOD.L⁻¹, p-value<0.01).

To the best of the authors' knowledge, our study has been the first to report butyric acid as the main VFA obtained from grass using AD technology after six days of fermentation in LBRs; most studies have reported acetic acid as main VFA produced over the course of the process^{7,12-14}. Silage fermentation for 24-32 days at pH 6.2-6.5 reached similar VS removal levels to our study, but with lower levels of acidification (60%) despite the higher VFA yield (0.3-0.4 gCOD.gtCOD⁻¹)⁷. Moreover,

after six days in that fermentation⁷, a VFA concentration of 4.6 g.L⁻¹ (25-28% butyric acid) at pH 6.2 was reached, which was similar to our study (R1: 4.7±0.8, R2: 4.4±0.5, R3: 4.3±1.1 g.L⁻¹) but lower in butyric acid proportion (Phase V, Table 5.5). The fermentation of Napier grass in LBRs¹² for 28 days at 28 °C and pH 6.4, using 20% cow manure as inoculum and leachate dilution, led to an average biomass degradation of 65% VS, 62% of acidification and 3.3 g.L⁻¹ of VFAs (butyric acid: 20% gVFA). In our study, concentrations of 4.7±0.8 g.L⁻¹ (R1, 36%gVFA of butyric), 4.4±0.5 g.L⁻¹ (R2, 32%gVFA of butyric), and 4.3±1.1 g.L⁻¹ (R3, 38%gVFA of butyric) were achieved at pH 5.5 and an 11x leachate dilution.

When comparing to the fermentation of grass pellets in 82.5 L bioreactors at pH 5.5 (287 mgVFA.gVS⁻¹, 15% butyric)¹³, the VFA yield in our work was lower (R1: 212.0, R2: 206.6 mgVFA.gVS⁻¹), but with higher butyric acid yields (R1: 36%, R2: 33%). VFA yield from grass pellets in 82.5 L at pH 5.5 has been improved with the in-line removal of VFAs using a combination of solid separation with electro dialysis (in 41%, recovering 4.8 gVFA.L⁻¹), despite a decrease of 20% in butyric acid yield¹³. Improvement in VFA production from grass pellets has also been observed when using a combination of solid separation with pervaporation and electro dialysis (in 24%, recovering 4.5 gVFA.L⁻¹)¹⁴. In-line VFA recovery is important to reduce inhibition due to acid accumulation^{13,27}, thus improving VFA yield.

Chain-elongation was observed in Phase V, where caproic acid and valeric acid were consistently produced after batch 25. The concentration of caproic acid obtained in Phase V was 15x higher in Reactor 1 when comparing Phase I and V, which contributed to the significantly higher VFA accumulation (28%). By Phase V, the conversion of silage seemed to start with its degradation to carbohydrates, which were first converted to lactic acid and then to butyric acid¹⁹; when butyric acid reached its maximum concentration, caproic acid was produced. In parallel, the already available lactic acid from the beginning of the fermentation was also converted to butyric acid. The consumption of lactic acid also seemed to be related to the production of propionic acid, but in lower quantities, indicating that the cyclic chain-elongation pathway²¹ may have been favoured in comparison to the acrylate pathway⁷⁴. This has been observed before, from the fermentation of chinese liquor, where lactic acid concentrations decreased with subsequent butyric acid and caproic acid increase¹⁹. In our study, when butyric acid concentrations reached values around 4 gCOD.L⁻¹, caproic acid was produced alongside acetic acid¹⁸, leading to caproic acid accumulation (R1: 6.0±2.7, R2: 6.0 ±2.0, and R3: 4.3±3.4 mM) after a maximum accumulation of butyric acid was reached (R1: 20.4±5.7, R2: 12.4±4.8, R3: 15.4±3.8 mM) in the leachate.

This caproic acid concentration, however, was lower than what has been observed using pure lactic acid as electron donor and butyric acid as electron acceptor. Nzeteu *et al.*¹⁸ reported a caproic acid concentration of 91.7 mM using 300 mM of butyric and lactic acid (1:1) in batch bottles, while Xie *et al.*¹⁷ achieved a concentration of 30.9 mM in a semi-continuous operation using 80 mM of butyric acid in a 4:1 ratio with lactic acid. The butyric acid concentration accumulated in our work was lower than what has been used in previous studies, and it was also lower than the butyric acid threshold proposed for the production of caproic acid (100-200 mM)¹⁸. Despite caproic acid being detected in the

fermentation of grass, some strategies would be beneficial to optimise its production by increasing the accumulation of butyric acid towards its threshold, such as supplementation of lactic acid¹⁸, constant removal of VFAs to decrease acid inhibition^{13,14}, and a second-stage focused on caproic acid accumulation. A higher SRT could also be beneficial, as a higher concentration of caproic acid was achieved in the semi-continuous fermentation of lactic acid at pH 5.5-6.2 after 15 days compared to what was obtained after 6 days¹¹. Moreover, dark fermentation studies have demonstrated the conversion of lactate and acetate to butyrate at pH 5.0-6.0 using *C. butyricum*^{31,32}; and bio-augmentation studies with the same species showed an improvement in butyric acid production (11x) and VFA production (3x) from the fermentation of dairy wastewater at pH 10 and 35 °C. Therefore, bio-augmentation with bacteria from the genus *Clostridium sensu stricto 1*, such as *Clostridium butyricum*, can also be a good approach to improve the production of butyric acid and caproic acid¹⁸.

5.5.5 Silage indigenous community and pH were the driving forces shifting the reactor performance

As stated previously, silage quality and pH are intrinsically connected³⁸ and these factors can be a reflection of the silage's microbiome³⁷. A good quality silage has pH values around 4, which are reached when LAB ferment the sugars available in the surface of the silage³⁷. This was the case for Silages PI (pH 4.6) and PV (pH 4.3), where LAB such as *Weisella* and *Lactobacillus* were detected, as well as concentrations of lactic acid in the leachate at the beginning of the fermentation in Phases I and V (Figure 5.5).

However, the presence of *Lactobacillus* in Silage PV was considerably lower in comparison with Silage PI, and the presence of other genera that were not among the top-25 most abundant represented approximately 85% of the community. In terms of relative abundance distribution at class-level, 59.5% of the bacterial class in Silage PV corresponded to *Enterobacterales*. Enterobacteria are known to be the highest competitor to *Lactobacillus* in ensiling fermentation, and responsible for the accumulation of acetic acid in the resulting silage³⁸. However, acetic levels at day 0 in Phase V were not higher than the acetic levels in Phase I. Moreover, Silage PV still presented a low pH, which resulted in the accumulation and production of lactic acid in the first days of fermentation.

On the other hand, when the biomass is contaminated with soil and manure, the resulting silage will have a higher pH due to the predominance of bacteria from other classes, such as *Clostridia* and *Bacilli*³⁷, which ferment the surface sugars to other carboxylic acids. Silage PIV (pH 6.6) presented a more balanced (Figure 5.12) and richer (Figure 5.13) community, but with a lower presence of LAB when compared to other genera, such as *Acinetobacter* (18x higher). The bacterial class with the highest relative abundance in Silage PIV was *Gammaproteobacteria* (genera *Acinetobacter* and *Pseudomonas*)⁷⁵, a class known for breaking down lignin⁷⁶. Also present in Silage PIV, the *Sphingobacterium* genus was correlated to the degradation of lignocellulosic biomass in submerged fermentation for the production of biofuels using a mixed-species culture⁷⁶ and pure-culture⁷⁷. The presence of those genera on the surface of Silage PIV may indicate a certain level of lignocellulosic

degradation when the feedstock was received and supplied to the reactors. Therefore, the difference in genera and diversity may explain the difference in pH observed when comparing Silage PIV with Silages PI and PV, indicating different fermentation processes occurred leading to silages with different qualities³⁷.

The use of those three Silages PI, PIV and PV was correlated to the shift in VFA production and methane accumulation in Phases I, IV and V. On the other hand, no difference in VFA accumulation was observed between reactors over the phases, indicating that the mixtures of seed-inocula proposed were not a major factor in the shift of VFA production compared to the silage. In fact, the microbial community dynamics of the three reactors presented a similar trend, with differences in diversity driven by the different phases (Figures 5.13 and C.2). It is important to highlight that the seed-inocula was only added at the beginning of the Start Up phase and, despite differences in taxonomic composition and diversity, the constant feeding of silage may be a stronger driving force to the microbial community dynamics than the seed-inocula. Nevertheless, the addition of an external source of inoculum has proved to be important in improving VFA production⁷. In fact, combining an inoculum source with the silage community led to butyric acid yields (Phase V – R1: 77.7, R2: 66.9, R3: 71.6 g.kgVS⁻¹) that were higher than what has been observed from the ensiling process (20.1 g.kgVS⁻¹)⁴⁰.

Moreover, adding an inoculum source (digestate from the lab-scale treatment of pig manure and silage) led to an increase in VS removal compared to using the silage's community only⁷. In our study, similar diversities (Figures 5.11-5.13) were observed for the ruminal seed-inocula (rumen material and cattle slurry), with similar genera such as *Christensenellaceae R-7 group*, *Rikenellaceae RC9 gut group*, *Prevotella*, and *Prevotellaceae UCG-001*, indicating the hydrolytic capability of these seed-inocula⁴⁴. This similarity in microbial community between rumen material and cattle slurry may explain the similar VS degradation observed throughout the reactor performance (Figure 5.4). *Prevotella* is an hydrolytic genus present in the rumen microbial community⁴⁴. Most species of the *Christensenellaceae R-7 group* are capable of decomposing fibrous material⁷⁸ and fermenting carbohydrates to SCCAs⁷⁹, while members of the *Rikenellaceae* family can produce acetic acid and propionic acid from lactic acid⁴², and butyric acid and propionic acid from unabsorbed polysaccharides⁸⁰. Most of these genera, however, were not detected throughout the reactor trial, or were detected at low relative abundances – the exception was *Prevotella*, which was present over Phases I, IV and V (Figure 5.14).

When considering the phylum distribution over the phases (Table C.2), it was observed that the relative abundance of *Firmicutes* was higher than the relative abundance of *Bacteroidota* in Phases I and V – a pattern that was reversed in Phase IV. This distribution correlates with the profile of VFAs produced in this study, as propionate (and acetate) are mainly produced by *Bacteroidota*⁸¹, and butyrate⁸¹ and caproate^{11,21} are mainly produced by *Firmicutes*. In this work, the lower accumulation of acetic acid in Phase IV was correlated to the production of methane (Figure 5.10). The higher production of propionic acid in Phase IV (e.g. R1: 44.5±5.1% gVFA or 38.7±4.7% gCOD, Table 5.5) may be associated with the higher relative abundance of *Prevotella* compared to the other phases,

such as Phase V (e.g. R1: $14.9 \pm 2.0\%$ gVFA or $13.6 \pm 1.9\%$ gCOD), as well as the appearance of members of the *Rikenellaceae* family. The *Prevotellaceae* family is known for the degradation of lignocellulosic biomass in the rumen⁴³, and *Prevotella* is considered an important genus for hemicellulose and cellulose degradation, consuming especially xylan polymers⁴¹ to produce organic acids, such as acetic acid⁹ and propionic acid²³. The lower relative abundance (<1%) of LAB in Phase IV and the absence of lactic acid at the earlier days of the fermentation, however, indicates that the VFA production is mainly coming from the carbohydrates hydrolysed from the grass silage. Moreover, the lower presence of LAB in Phase IV may be an indication of the lower production of butyric acid in comparison to Phases I and V.

The higher relative abundance of *Lactobacillus* at Phase V, especially in the leachate (vs *Prevotella*: R1: 4.7x; R2: 4.2x; and R3: 80%), led to an increase in lactic acid accumulation. In fact, *Lactobacillus* was still active by the end of the fermentation (Figure 5.15), despite not necessarily being the most abundant genus. This is an indication that the production of lactic acid was still occurring after 6 days of fermentation. This activity of *Lactobacillus* may explain the chain-elongation observed for valeric acid after 4 days of fermentation, if lactic acid was being used as an electron donor and the propionic acid produced from the acrylate pathway was being used as electron acceptor²¹. The presence of both *Lactobacillus* and *Caproiciproducens* has been associated with the production of lactic acid (by the former), and the utilisation of said lactic acid in the production of butyric acid and caproic acid²⁰. Both genera were also associated to achieving a VFA-mix dominated by butyric acid in the fermentation of dairy manure at pH 5.5²⁰. Moreover, the presence of lactic acid in the media at pH 5-6 has been considered a stimulating factor for the growth of butyric acid producers, with a balance between LAB and butyric acid producers considered important for the conversion of lactate to butyrate³².

In previous studies²⁵, *Caproiciproducens* was correlated to the production of acetic, propionic and butyric acids in the acidogenesis of agave biomass, with *Prevotella* and *Pseudoclavibacter* correlated to the solids' destruction. *Pseudoclavibacter*, which was especially active in Reactor 1 (Figure 5.15), produces α - and β - glucosidases which are responsible for degrading the lignocellulosic material⁸². The activity of *Lactobacillus*, *Pseudoclavibacter*, *Prevotella*, and *Caproiciproducens* may suggest that longer SRTs may improve silage degradation as well as VFA yield. Members of the *Clostridiaceae* family (DNA: *Clostridium sensu stricto 1*; cDNA: *Clostridium sensu stricto 11*, and *Clostridium sensu stricto 12*) were observed in this fermentation (Phases I and V), but with relative abundances that corresponded to less than 1%. On the other hand, other genera known for the production of butyric acid, such as *Megasphaera*¹⁶ (higher in Phase I), *Roseburia*^{16,23,24}, *Caproiciproducens*^{20,25}, and *Acidaminococcus*²⁶ were detected. Some of these genera have been identified in the chain-elongation of acids or carbohydrates producing caproic acid, such as *Roseburia*⁸³ and *Caproiciproducens*²¹.

Bacteria from the *Roseburia* genus produce butyric and lactic acids from carbohydrates²⁴. In this way, *Roseburia* may be contributing to the production of butyric acid associated with the conversion of the already present lactic acid, but from the carbohydrates released from grass after hydrolysis.

On another note, *Roseburia* was identified as the genus responsible for caproic acid production in a community dominated by *Lactobacillus* in a xylose-rich stream from switchgrass stillage⁸³. In our system, we also observed the production of caproic acid in Phase V, where a higher presence of *Lactobacillus* and the presence of *Roseburia* were detected. Silage PV (30.2%Ts glucan, 7.6 %TS xylan, 0.8%TS mannan) has a xylan backbone, indicating that its hemicellulose degradation (Table C.1) will generate xylose in the leachate, although in lower quantities than glucose due to the higher glucan content in that silage. Therefore, there is a possibility of caproic acid generation from xylose conversion. However, the conversion of cellulose was higher than hemicellulose, indicating a higher accumulation of glucose in the system than other cellulolytic sugars, as cellulose is glycan-polymer⁴⁶. Moreover, the relative abundance of *Caproiciproducens* was higher than the relative abundance of *Roseburia* (Digestate R1: 2.5x, R2: 5.8x, R3:9.4x; Leachate R1: 2.7x, R2 and R3: 7.5x) – this higher relative abundance was observed at both DNA-level (Figure 5.14) and cDNA-level (Figure 5.15). *Caproiciproducens* is a well-known caproic acid producing bacteria, and has been highlighted in media where butyric acid and lactic acid accumulates¹⁸. Therefore, the higher abundance of *Caproiciproducens* associated to the accumulation of lactic acid and its conversion to butyric acid leads to the hypothesis that the majority of the caproic acid generated in this study may come from the *Caproiciproducens* genus. However, both *Roseburia* and *Caproiciproducens* may be important for the production of butyric acid and caproic acid, but the level of importance and its association with *Lactobacillus* should be further investigated in this system.

5.5.6 Combining digestate and leachate as inoculum is more important for biomass degradation than acids production

In the fermentation of silage, leachate and digestate from a previous batch were used as inoculum in a semi-continuous process for VFA accumulation. This design was proposed to improve the residence of hydrolytic and acidogenic bacteria enriched over the fermentation, thus improving or maintaining the silage degradation levels and VFA production. However, the role of each portion of inoculum (digestate or leachate) was unclear in the process.

The most important difference in inoculum approach was observed in terms of VS degradation, as using the leachate-only as inoculum led to a lower silage degradation. In fact, the introduction of the digestate as an inoculum was important to improve silage degradation (Figure 5.9) in 76-78% (R1), 30-53% (R2), and 74% (R3). This could be explained by the presence of hydrolysers that attached previously to the digestate for degradation, and would be mixed directly with the silage before feeding the bottles. The use of leachate and digestate as inoculum also affected the VFA production rate, which was faster in comparison to choosing one only digestate or leachate as inoculum. Despite these differences in VFA production rate and VS degradation, VFA net production and profile was similar irrespective of the inoculum approach, with lower values observed when only leachate was used as inoculum (Figure 5.10 and Table C.3). The results for VFA production showed that the combination of digestate and leachate was acclimatised for the selective production of butyric acid and caproic

acid from silage, which were the highest produced VFAs in all conditions tested. The similarities in the production of VFAs using both digestate and leachate as inoculum was not surprising, as the microbiology analysis shows similarity in the distribution of bacterial genus (Figure 5.14) between digestate and leachate, as well as similar abundances (Figure 5.13) and functionality (Figure C.2). However, using both digestate and leachate as inoculum can improve the inoculum density thus improving the VFA production rate. Therefore, using both digestate and leachate seems advantageous to the process, for both silage degradation and butyric acid production.

5.6 Conclusions

The present work was successful in obtaining a VFA-mix dominated by butyric acid in the fermentation of silage. Despite selecting three combinations of seed-inocula for the reactor trial (R1 – rumen fluid + rumen solid + granular sludge; R2 – cattle slurry + granular sludge; R3 – granular sludge), no major difference was observed between reactors in terms of VFA production and silage degradation. Moreover, the use of digestate as an inoculum for the next batch in a semi-continuous process was important to guarantee silage degradation, but no major difference was observed in terms of the final VFA concentration in comparison to using only leachate or digestate as inoculum. However, the use of both leachate and digestate seemed to improve the rate of VFA production. Silage pH and quality was established as the driving forces responsible for shifting the reactor performance in terms of butyric acid and VFA production. In fact, the use of a silage with acidic pH was crucial to restore the reactor performance, leading to the highest production of VFAs (7.2-7.9 gCOD.L⁻¹) and caproic acid (1.1-1.5 gCOD.L⁻¹) after 6 days, and the highest concentration of butyric acid (2.0-3.3 gCOD.L⁻¹). Therefore, silage pH can be an important process indicator, as pre-testing the pH may give an indication of which conversion products to be expected and aid in selecting the appropriate process for that type of silage. Moreover, the constant feeding of silage seemed to have a higher impact in the microbial community dynamics than the seed-inocula, which was added only at the beginning of the reactor run. *Prevotella* was observed during the nine months of fermentation, and may be correlated with the degradation of silage and propionic accumulation in Phase IV. The production of butyric acid seemed to be associated with the production and consumption of lactic acid at the early stages of fermentation. The higher presence of *Lactobacillus* at Phase V, associated to the presence of *Caproiciproducens* may explain the production of caproic acid from butyric acid. However, further studies are needed to identify the metabolism and kinetics in place for both butyric acid and caproic acid accumulation in their fermentation of silage.

5.7 Acknowledgement and contribution

This work was financially supported by Science Foundation Ireland (SFI). The authors would like to acknowledge the BiOrbic (Bioeconomy SFI Research Centre) for the technical and financial support; Dr. Paolo Dessi for the support with the pH control system assembling; and Stephen Nolan, Michael

Dineen, Aidan Lawless, Stuart Kirwan, Shaun Connolly, and Dawn Meats Ballyhaunis factory for the supplying the silages and seed-inoculum used in this work. This work was possible due to the technical support of Alejandra Villa, Sandra O'Connor and Andrew Bartle. Microbial data analysis was assisted by Dr. Anna Trego and Dr. Umer Ijaz. The study was conceptualised in collaboration with Dr. Corine Nzeteu and Prof. Vincent O'Flaherty.

5.8 References

1. European comission. *A European Green Deal - Striving to be the first climate-neutral continent* Dec. 2019. <https://ec.europa.eu/newsroom/know4pol/items/664852>.
2. Ravindran, R. *et al.* Biogas, Biomethane and Digestate Potential of By-Products from Green Biorefinery Systems. *Clean Technologies* **4**, 35–50 (Jan. 2022).
3. Nzeteu, C., Coelho, F., Davis, E., Trego, A. & O'flaherty, V. Current Trends in Biological Valorization of Waste-Derived Biomass: The Critical Role of VFAs to Fuel a Biorefinery. **8**, 445 (2022).
4. Cherubini, F. *et al.* Toward a common classification approach for biorefinery systems. *Biofuels, Bioproducts and Biorefining* **3**, 534–546 (Sept. 2009).
5. Nizami, A.-S. & Murphy, J. D. Optimizing the Operation of a Two-Phase Anaerobic Digestion System Digesting Grass Silage. *Environmental Science & Technology* **45**, 7561–7569 (Sept. 2011).
6. Nizami, A.-S., Korres, N. E. & Murphy, J. D. Review of the Integrated Process for the Production of Grass Biomethane. *Environmental Science & Technology* **43**, 8496–8508 (Nov. 2009).
7. Xie, S., Lawlor, P. G., Frost, J. P., Wu, G. & Zhan, X. Hydrolysis and acidification of grass silage in leaching bed reactors. *Bioresource Technology* **114**, 406–413 (2012).
8. Lehtomäki, A., Huttunen, S., Lehtinen, T. M. & Rintala, J. A. Anaerobic digestion of grass silage in batch leach bed processes for methane production. *Bioresource Technology* **99**, 3267–3278 (May 2008).
9. Wang, H. *et al.* Development of microbial populations in the anaerobic hydrolysis of grass silage for methane production. *FEMS Microbiology Ecology* **72**, 496–506 (Feb. 2010).
10. Wall, D. M., Allen, E., Shea, R. O., Kiely, P. O. & Murphy, J. D. Investigating two-phase digestion of grass silage for demand-driven biogas applications: Effect of particle size and rumen fluid addition. *Renewable Energy* **86**, 1215–1223 (2016).
11. Khor, W. C., Andersen, S., Vervaeren, H. & Rabaey, K. Electricity-assisted production of caproic acid from grass. *Biotechnology for Biofuels* **10**, 1–11 (Dec. 2017).

12. Kullavanijaya, P. & Chavalparit, O. The production of volatile fatty acids from Napier grass via an anaerobic leach bed process: The influence of leachate dilution, inoculum, recirculation, and buffering agent addition. *Journal of Environmental Chemical Engineering* **7**, 103458 (Dec. 2019).
13. Jones, R. J., Massanet-Nicolau, J., Fernandez-Feito, R., Dinsdale, R. M. & Guwy, A. J. Recovery and enhanced yields of volatile fatty acids from a grass fermentation via in-situ solids separation and electrodialysis. *Journal of cleaner production* **296**, 126430 (2021).
14. Jones, R. J., Massanet-Nicolau, J., Fernandez-Feito, R., Dinsdale, R. M. & Guwy, A. J. Fermentative volatile fatty acid production and recovery from grass using a novel combination of solids separation, pervaporation, and electrodialysis technologies. *Bioresource technology* **342**, 125926 (2021).
15. Jones, R., Massanet-Nicolau, J. & Guwy, A. A review of carboxylate production and recovery from organic wastes. *Bioresource Technology Reports* **16**, 100826 (Dec. 2021).
16. Liberato, V. *et al.* Clostridium sp. as Bio-Catalyst for Fuels and Chemicals Production in a Biorefinery Context. *Catalysts* **9**, 962 (Nov. 2019).
17. Xie, S. *et al.* Anaerobic caproate production on carbon chain elongation: Effect of lactate/butyrate ratio, concentration and operation mode. *Bioresource Technology* **329**, 1–8 (June 2021).
18. Nzeteu, C. o. *et al.* Development of an enhanced chain elongation process for caproic acid production from waste-derived lactic acid and butyric acid. *Journal of Cleaner Production* **338**, 130655 (Mar. 2022).
19. Gao, M. *et al.* Production of medium-chain fatty acid caproate from Chinese liquor distillers' grain using pit mud as the fermentation microbes. *Journal of Hazardous Materials* **417** (Sept. 2021).
20. Ingle, A. T., Fortney, N. W., Walters, K. A., Donohue, T. J. & Noguera, D. R. Mixed Acid Fermentation of Carbohydrate-Rich Dairy Manure Hydrolysate. *Frontiers in Bioengineering and Biotechnology* **9** (Aug. 2021).
21. Candry, P. & Ganigué, R. Chain elongators, friends, and foes. *Current Opinion in Biotechnology* **67**, 99–110 (Feb. 2021).
22. Atasoy, M. & Cetecioglu, Z. Butyric acid dominant volatile fatty acids production: Bio-augmentation of mixed culture fermentation by Clostridium butyricum. *Journal of Environmental Chemical Engineering* **8**, 104496 (2020).
23. Flint, H. J., Bayer, E. A., Rincon, M. T., Lamed, R. & White, B. A. Polysaccharide utilization by gut bacteria: potential for new insights from genomic analysis. *Nature Reviews Microbiology* **6**, 121–131 (Feb. 2008).

24. Duncan, S. H., Hold, G. L., Barcenilla, A., Stewart, C. S. & Flint, H. J. *Roseburia intestinalis* sp. nov., a novel saccharolytic, butyrate-producing bacterium from human faeces. *International Journal of Systematic and Evolutionary Microbiology* **52**, 1615–1620 (Sept. 2002).
25. Dudek, K., Buitrón, G. & Valdez-Vazquez, I. Nutrient influence on acidogenesis and native microbial community of Agave bagasse. *Industrial Crops and Products* **170** (Oct. 2021).
26. Rogosa, M. *Acidaminococcus* gen. n., *Acidaminococcus fermentans* sp. n., Anaerobic Gram-negative Diplococci Using Amino Acids as the Sole Energy Source for Growth tech. rep. (1969), 756–766.
27. Nzeteu, C. O., Trego, A. C., Abram, F. & O’Flaherty, V. Reproducible, high-yielding, biological caproate production from food waste using a single-phase anaerobic reactor system. *Biotechnology for Biofuels* **11**, 1–14 (Dec. 2018).
28. Yan, B. H., Selvam, A. & Wong, J. W. C. Application of rumen microbes to enhance food waste hydrolysis in acidogenic leach-bed reactors. eng. *Bioresource technology* **168**, 64–71 (Sept. 2014).
29. Atasoy, M. & Cetecioglu, Z. The effects of pH on the production of volatile fatty acids and microbial dynamics in long-term reactor operation. *Journal of Environmental Management* **319**, 115700 (Oct. 2022).
30. Lee, W. S., Chua, A. S. M., Yeoh, H. K. & Ngoh, G. C. A review of the production and applications of waste-derived volatile fatty acids. *Chemical Engineering Journal* **235**, 83–99 (2014).
31. Detman, A. *et al.* Cell factories converting lactate and acetate to butyrate: *Clostridium butyricum* and microbial communities from dark fermentation bioreactors. *Microbial Cell Factories* **18**, 36 (Dec. 2019).
32. Detman, A. *et al.* Dynamics of dark fermentation microbial communities in the light of lactate and butyrate production. *Microbiome* **9**, 158 (Dec. 2021).
33. Atasoy, M., Owusu-Agyeman, I., Plaza, E. & Cetecioglu, Z. Bio-based volatile fatty acid production and recovery from waste streams: Current status and future challenges. *Bioresource Technology* **268**, 773–786 (2018).
34. Magdalena, J. A., Greses, S. & González-Fernández, C. Impact of Organic Loading Rate in Volatile Fatty Acids Production and Population Dynamics Using Microalgae Biomass as Substrate. *Scientific Reports* **9**, 18374 (Dec. 2019).
35. Ramos-Suarez, M., Zhang, Y. & Outram, V. Current perspectives on acidogenic fermentation to produce volatile fatty acids from waste. *Reviews in Environmental Science and Bio/Technology* **20**, 439–478 (2021).

36. Atasoy, M., Eyice, O., Schnürer, A. & Cetecioglu, Z. Volatile fatty acids production via mixed culture fermentation: Revealing the link between pH, inoculum type and bacterial composition. *Bioresource Technology* **292**, 121889 (2019).
37. Pahlow, G., Muck, R. E., Driehuis, F., Elferink, S. J. W. H. O. & Spoelstra, S. F. in *Silage Science and Technology* 31–93 (Jan. 2003).
38. Kung Jr, L., Shaver, R. D., Grant, R. J. & Schmidt, R. J. Silage review: Interpretation of chemical, microbial, and organoleptic components of silages. *Journal of Dairy Science* **101**, 4020–4033 (2018).
39. Steinbrenner, J., Nägele, H.-J., Buschmann, A., Hülsemann, B. & Oechsner, H. Testing different ensiling parameters to increase butyric acid concentration for maize silage, followed by silage separation and methane yield potential of separated solids residues. *Bioresource Technology Reports* **7**, 100193 (Sept. 2019).
40. Steinbrenner, J., Mueller, J. & Oechsner, H. Combined Butyric Acid and Methane Production from Grass Silage in a Novel Green Biorefinery Concept. *Waste and Biomass Valorization* **13**, 1873–1884. <https://doi.org/10.1007/s12649-021-01626-4> (2022).
41. Baba, Y. *et al.* Pretreatment of Lignocellulosic Biomass with Cattle Rumen Fluid for Methane Production: Fate of Added Rumen Microbes and Indigenous Microbes of Methane Seed Sludge. *Microbes and Environments* **34**, 421–428 (2019).
42. Ozbayram, E. G., Akyol, Ince, B., Karakoç, C. & Ince, O. Rumen bacteria at work: bioaugmentation strategies to enhance biogas production from cow manure. *Journal of Applied Microbiology* **124**, 491–502 (2018).
43. Nguyen, L. N. *et al.* Application of rumen and anaerobic sludge microbes for bio harvesting from lignocellulosic biomass. *Chemosphere* **228**, 702–708 (Aug. 2019).
44. Bayané, A. & Guiot, S. R. *Animal digestive strategies versus anaerobic digestion bioprocesses for biogas production from lignocellulosic biomass* 2011.
45. Krause, D. O. *et al.* Opportunities to improve fiber degradation in the rumen: microbiology, ecology, and genomics. *FEMS Microbiology Reviews* **27**, 663–693 (Dec. 2003).
46. Sharma, H. K., Xu, C. & Qin, W. Biological Pretreatment of Lignocellulosic Biomass for Biofuels and Bioproducts: An Overview. *Waste and Biomass Valorization* **10**, 235–251 (2019).
47. Buswell, A. M. & Neave, S. L. *Laboratory studies of sludge digestion* tech. rep. (Department of registration and education. Division of the state Water survey, Urbana, Illinois, 1930).
48. Zehnder, A. J. B., Huser, B. A., Brock, T. D. & Wuhrmann, K. Characterization of an acetate-decarboxylating, non-hydrogen-oxidizing methane bacterium. *Archives of Microbiology* **124**, 1–11 (Jan. 1980).
49. Zhu, X. *et al.* The synthesis of n-caproate from lactate: a new efficient process for medium-chain carboxylates production. *Scientific Reports* **5**, 1–9 (Nov. 2015).

50. APHA. *Standard Methods for the Examination of Water and Wastewater* 20th ed. (eds Eaton, A. D., Clesceri, L. S., Franson, M. A. H. F., Rice, E. W. & Greenberg, A. E.) *Standard Methods for the Examination of Water and Wastewater* v. **21** (American Public Health Association, 2005).
51. Selvakumar, T. *et al.* Process optimization of biogas energy production from cow dung with alkali pre-treated coffee pulp. *3 Biotech* **7** (Aug. 2017).
52. Hames, B., Scalata, C. & Sluiter, A. *Determination of protein content in biomass* (eds Sluiter, A., Scarlata, C. & (U.S.), N. R. E. L.) (National Renewable Energy Laboratory, Golden, Colo, 2005).
53. Gerike, P. The biodegradability testing of poorly water soluble compounds. *Chemosphere* **13**, 169–190 (Jan. 1984).
54. Hames, B. *et al.* *Preparation of samples for compositional analysis* (eds Hames, B. & (U.S.), N. R. E. L.) (National Renewable Energy Laboratory, Golden, Colo, 2008).
55. Sluiter, A., Ruiz, R. O., Scarlata, C., Sluiter, J. & Templeton, D. *Determination of Extractives in Biomass* tech. rep. July (Golden, Colo., National Renewable Energy Laboratory./, 2005), 1–9.
56. Sluiter, A. *et al.* *Determination of structural carbohydrates and lignin in biomass* (eds Sluiter, A. & (U.S.), N. R. E. L.) (National Renewable Energy Laboratory, Golden, Colo, 2008).
57. Griffiths, R. I., Whiteley, A. S., O'Donnell, A. G. & Bailey, M. J. Rapid method for coextraction of DNA and RNA from natural environments for analysis of ribosomal DNA- and rRNA-based microbial community composition. *Applied and Environmental Microbiology* **66**, 5488–5491 (2000).
58. Caporaso, J. G. *et al.* Global patterns of 16S rRNA diversity at a depth of millions of sequences per sample. *Proceedings of the National Academy of Sciences* **108**, 4516–4522 (Mar. 2011).
59. Caporaso, J. G. *et al.* QIIME allows analysis of high-throughput community sequencing data. *Nature Methods* **7**, 335–336 (May 2010).
60. Callahan, B. J. *et al.* DADA2: High-resolution sample inference from Illumina amplicon data. *Nature Methods* **13**, 581–583 (July 2016).
61. Batool, M. *et al.* A Cross-Sectional Study of Potential Antimicrobial Resistance and Ecology in Gastrointestinal and Oral Microbial Communities of Young Normoweight Pakistani Individuals. *Microorganisms* **11**, 279 (Jan. 2023).
62. Douglas, G. M. *et al.* PICRUSt2 for prediction of metagenome functions. *Nature Biotechnology* **38**, 685–688 (June 2020).
63. Oksanen, J. *et al.* The vegan package: community ecology package. *R package version* **1**, 1–190 (2007).

64. Zhang, Y., Jing, G., Chen, Y., Li, J. & Su, X. <i>Hierarchical Meta-Storms</i> enables comprehensive and rapid comparison of microbiome functional profiles on a large scale using hierarchical dissimilarity metrics and parallel computing. *Bioinformatics Advances* **1** (ed Forslund, S.) vbab003 (June 2021).
65. McMurdie, P. J. & Holmes, S. phyloseq: An R Package for Reproducible Interactive Analysis and Graphics of Microbiome Census Data. *PLoS ONE* **8** (ed Watson, M.) e61217 (Apr. 2013).
66. Browne, J. D., Allen, E. & Murphy, J. D. Assessing the variability in biomethane production from the organic fraction of municipal solid waste in batch and continuous operation. *Applied Energy* **128**, 307–314 (Sept. 2014).
67. Pham, C. H., Triolo, J. M., Cu, T. T., Pedersen, L. & Sommer, S. G. Validation and recommendation of methods to measure biogas production potential of animal manure. *Asian-Australasian Journal of Animal Sciences* **26**, 864–873 (2013).
68. Filer, J., Ding, H. H. & Chang, S. Biochemical Methane Potential (BMP) Assay Method for Anaerobic Digestion Research. *Water* **11**, 921 (May 2019).
69. Noguerol-Arias, J., Rodríguez-Abalde, A., Romero-Merino, E. & Flotats, X. Determination of chemical oxygen demand in heterogeneous solid or semisolid samples using a novel method combining solid dilutions as a preparation step followed by optimized closed reflux and colorimetric measurement. *Analytical Chemistry* **84**, 5548–5555 (July 2012).
70. Cysneiros, D. *et al.* Temperature effects on the trophic stages of perennial rye grass anaerobic digestion. *Water Science and Technology* **64**, 70–76 (2011).
71. Prochnow, A. *et al.* Bioenergy from permanent grassland - A review: 1. Biogas. *Bioresource Technology* **100**, 4931–4944 (2009).
72. Han, X., Hong, F., Liu, G. & Bao, J. An Approach of Utilizing Water-Soluble Carbohydrates in Lignocellulose Feedstock for Promotion of Cellulosic <sc>l</sc>-Lactic Acid Production. *Journal of Agricultural and Food Chemistry* **66**, 10225–10232 (Oct. 2018).
73. Bråthen, K. A., Pugnaire, F. I. & Bardgett, R. D. The paradox of forbs in grasslands and the legacy of the mammoth steppe. *Frontiers in Ecology and the Environment* **19**, 584–592 (Dec. 2021).
74. Kucek, L. A., Nguyen, M. & Angenent, L. T. Conversion of l-lactate into n-caproate by a continuously fed reactor microbiome. *Water Research* **93**, 163–171 (Apr. 2016).
75. Tsegaye, B., Balomajumder, C. & Roy, P. Microbial delignification and hydrolysis of lignocellulosic biomass to enhance biofuel production: an overview and future prospect. *Bulletin of the National Research Centre* **43** (Dec. 2019).
76. Chukwuma, O. B., Rafatullah, M., Tajarudin, H. A. & Ismail, N. A Review on Bacterial Contribution to Lignocellulose Breakdown into Useful Bio-Products. *International Journal of Environmental Research and Public Health* **18**, 6001 (June 2021).

77. Neelkant, K. S., Shankar, K., Jayalakshmi, S. K. & Sreeramulu, K. Optimization of conditions for the production of lignocellulolytic enzymes by *Sphingobacterium* sp. ksn-11 utilizing agro-wastes under submerged condition. *Preparative Biochemistry and Biotechnology* **49**, 927–934 (2019).
78. Evans, N. J. *et al.* Characterization of novel bovine gastrointestinal tract *Treponema* isolates and comparison with bovine digital dermatitis treponemes. *Applied and Environmental Microbiology* **77**, 138–147 (Jan. 2011).
79. Tavella, T. *et al.* Elevated gut microbiome abundance of *Christensenellaceae*, *Porphyromonadaceae* and *Rikenellaceae* is associated with reduced visceral adipose tissue and healthier metabolic profile in Italian elderly. *Gut Microbes* **13**, 1–19 (Jan. 2021).
80. Su, X. L. *et al.* *Acetobacteroides hydrogenigenes* gen. nov., Sp. nov., An anaerobic hydrogen-producing bacterium in the family *Rikenellaceae* isolated from a reed swamp. *International Journal of Systematic and Evolutionary Microbiology* **64**, 2986–2991 (Sept. 2014).
81. Feng, W., Ao, H. & Peng, C. Gut Microbiota, Short-Chain Fatty Acids, and Herbal Medicines. *Frontiers in Pharmacology* **9** (Nov. 2018).
82. Cho, S. L. *et al.* *Pseudoclavibacter chungangensis* sp. nov., isolated from activated sludge July 2010.
83. Scarborough, M. J. *et al.* Increasing the economic value of lignocellulosic stillage through medium-chain fatty acid production. *Biotechnology for Biofuels* **11** (July 2018).
84. Wang, M., Ji, X., Wang, B., Li, Q. & Zhou, J. Simultaneous Evaluation of the Preservative Effect of RNAlater on Different Tissues by Biomolecular and Histological Analysis. *Biopreservation and Biobanking* **16**, 426–433 (Dec. 2018).
85. Lebuhn, M. *et al.* DNA and RNA extraction and quantitative real-time PCR-based assays for biogas biocenoses in an interlaboratory comparison. *Bioengineering* **3** (Mar. 2016).
86. Dominianni, C., Wu, J., Hayes, R. B. & Ahn, J. Comparison of methods for fecal microbiome biospecimen collection. *BMC Microbiology* **14**, 103 (Dec. 2014).
87. Hallmaier-Wacker, L. K., Lueert, S., Roos, C. & Knauf, S. The impact of storage buffer, DNA extraction method, and polymerase on microbial analysis. *Scientific Reports* **8**, 6292 (2018).

C Appendices

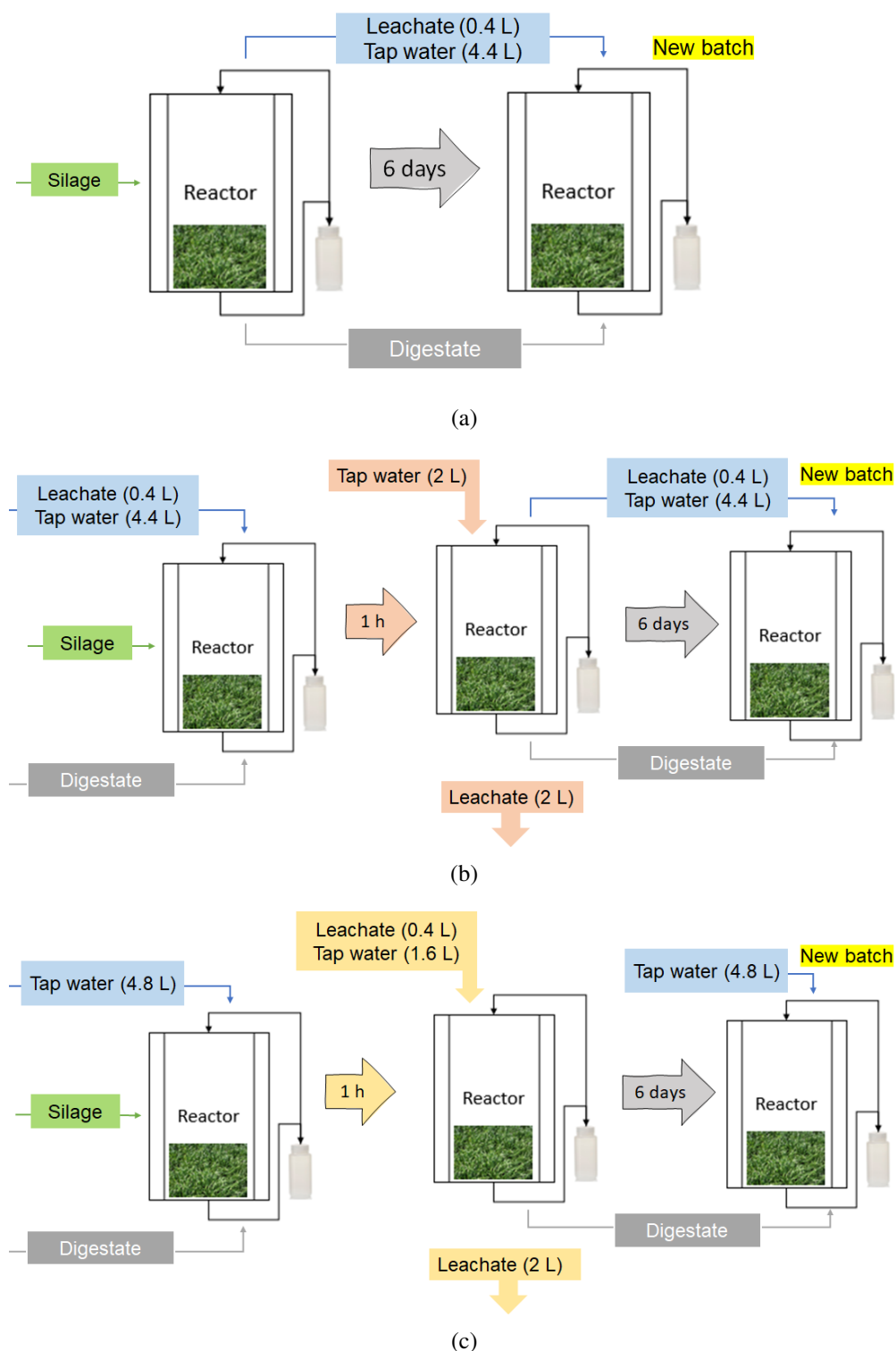


Figure C.1: Schematic diagram illustrating the feeding regime for all phases of silage fermentation in LBRs: Phase I, IV and V (a), Phase II (b) and Phase III (c). Batch 16 was fed in a similar way to Phase II, but with two washes.

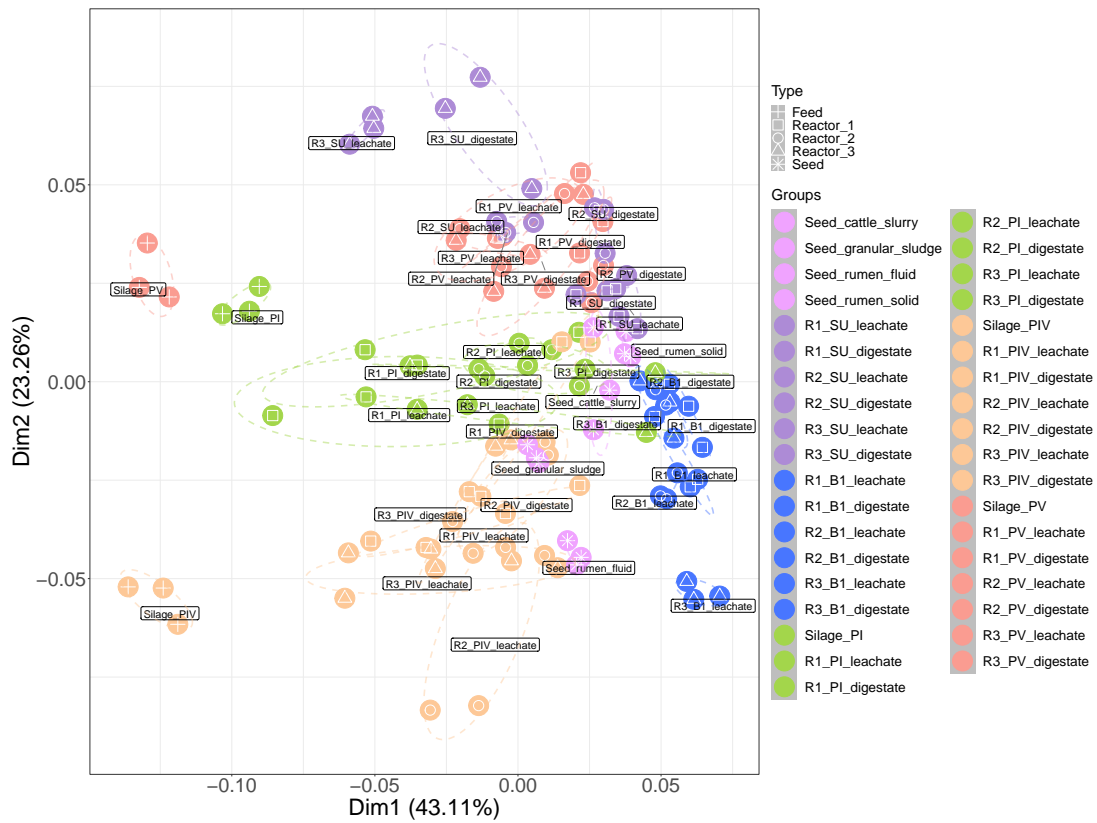


Figure C.2: Principal Coordinate Analysis (PCoA) plot based on Hierarchical Meta-Storms distances of the 16s rRNA sequences (DNA level) extracted from seed-inocula (pink), Start Up (purple), Phase I (green), Phase IV (orange), and Phase V (red). Silage colour is represented according to each phase it was fed (I, IV and V); p-value<0.001.

Table C.1: Lignocellulosic and total solids degradation of silage and the starting mix of silage and digestate during Phase V Batch 30.

Reactor	Lignocellulosic degradation (%) ^a				Total solids degradation (%)	
	Cellulose (%)	Hemicellulose (%)	Lignin (%)	Total (%)	Silage+digestate ^b (%)	Grass-only ^c (%)
1	53.3±0.3	27.2±1.2	7.7±1.4	33.5	26.1	48.6
2	59.1±0.6	30.6±0.8	-5.6±1.5	33.2	31.8	60.1
3	62.4±0.5	33.8±0.3	2.0±4.5	36.1	33.3	61.7

Note: ^aFor the lignocellulosic degradation, both Batch 29's digestate and silage were considered (Section 5.3.2, page 118). ^bThe same consideration was made for the TS degradation of grass+digestate^b. ^cThe TS degradation for grass only followed the same calculations of VS degradation (Section 5.3.1, page 117). '±' symbols represents the standard deviation of duplicate to triplicate measurements..

Table C.2: Relative abundances (% , at DNA-level) of the phylum observed in the fermentation of silage over phases and reactors.

Phase	Source	<i>Actinobacteriota</i>	<i>Bacteroidota</i>	<i>Firmicutes</i>	<i>Proteobacteria</i>
Reactor 1					
I	Digestate	3.8 (1.7)	31.5 (7.3)	45.1 (5.3)	18.7 (10.1)
	Leachate	3.8 (1.6)	31.7 (5.9)	39.8 (5.8)	24.2 (10.5)
IV	Digestate	3.2 (1.2)	41.1 (5.9)	41.9 (3.7)	12.7 (8.3)
	Leachate	2.9 (1.8)	46.5 (5.3)	30.1 (11.0)	19.0 (5.0)
V	Digestate	14.8 (3.2)	16.0 (2.1)	64.7 (4.4)	3.4 (3.7)
	Leachate	11.6 (1.8)	9.7 (2.4)	71.0 (7.5)	7.2 (0.8)
Reactor 2					
I	Digestate	6.8 (0.6)	33.8 (7.2)	48.3 (6.0)	9.2 (2.2)
	Leachate	3.4 (1.0)	27.8 (5.2)	56.6 (8.8)	11.4 (2.9)
IV	Digestate	3.5 (1.3)	45.7 (8.6)	35.2 (9.5)	13.6 (5.0)
	Leachate	1.7 (0.3)	57.9 (4.2)	19.5 (7.0)	19.0 (3.9)
V	Digestate	13.6 (4.4)	25.3 (0.9)	55.3 (10.3)	5.3 (7.7)
	Leachate	12.3 (3.7)	10.3 (4.7)	63.1 (4.6)	13.8 (1.7)
Reactor 3					
I	Digestate	5.8 (5.2)	38.0 (9.2)	46.1 (3.5)	9.3 (7.8)
	Leachate	5.2 (1.9)	38.6 (6.7)	41.9 (2.2)	13.5 (8.6)
IV	Digestate	4.4 (1.3)	43.6 (9.5)	32.5 (3.8)	16.9 (9.9)
	Leachate	3.2 (2.0)	48.6 (4.9)	23.5 (9.2)	22.2 (3.9)
V	Digestate	5.5 (1.7)	21.3 (2.4)	63.7 (1.6)	8.7 (3.7)
	Leachate	5.6 (1.5)	13.5 (3.4)	68.4 (6.9)	11.9 (2.4)

Note: Mean values of relative abundance of each phylum with its standard deviation in brackets.

Table C.3: Mean values (and standard deviation) for the net production and profile of VFAs obtained in the fermentation of silage using Batch30's digestate and leachate as inoculum.

Inoculum phase		Total VFA (gCOD.L ⁻¹)	Acetic acid (%)	Butyric acid (%)	Caproic acid (%)	Propionic acid (%)	Valeric acid (%)
Reactor 1	Digestate + Leachate	8.8 (0.9)	18.1 (2.6)	27.9 (9.5)	33.8 (4.9)	10.9 (1.1)	9.3 (1.6)
	Digestate	10.0 (0.3)	15.8 (1.4)	35.4 (2.0)	31.9 (2.4)	9.6 (0.3)	7.3 (0.4)
	Leachate	7.8 (0.3)	15.5 (2.8)	27.5 (2.2)	40.9 (3.0)	8.7 (1.0)	7.4 (0.7)
Reactor 2	Digestate + Leachate	8.7 (0.3)	12.2 (1.1)	32.0 (3.3)	34.9 (1.3)	12.9 (0.5)	8.1 (0.3)
	Digestate	8.8 (0.9)	14.2 (6.4)	33.2 (8.4)	32.7 (3.9)	12.5 (3.1)	7.4 (1.2)
	Leachate	7.9 (0.8)	8.8 (3.8)	38.8 (7.3)	34.3 (6.9)	9.9 (1.8)	8.4 (0.8)
Reactor 3	Digestate + Leachate	8.7 (0.4)	13.9 (2.6)	29.9 (2.5)	28.4 (2.6)	14.5 (0.8)	13.2 (0.7)
	Digestate	7.8 (0.6)	12.1 (3.0)	35.6 (5.9)	26.0 (5.8)	14.4 (2.3)	12.0 (1.9)
	Leachate	7.4 (0.4)	13.4 (1.9)	33.6 (4.1)	38.8 (3.2)	10.0 (0.5)	7.8 (0.5)

Note: Isomeric forms of VFAs were not detected or acquired below the GC's detection limit.

C.1 Quality-check for the microbial community extraction: Sonication and RNAlater

Two small tests were performed before DNA and RNA were co-extracted from reactors samples and send for sequencing. The first test aimed to evaluate the effect of different sonication times in the DNA quality extracted from the biofilm detached to digestate samples. Six sonication times were tested – 0, 5, 10, 15, 20 and 30 min. Despite seeing the nucleic acid bands in the electrophoresis gel (Figure C.3), though vaguely at samples sonicated for 0 and 5 min, the quality and quantity of the DNA extracted was different depending on the duration of the sonication (Table C.4). Lower quantity was observed when digestate samples were sonicated for less than 10 min, and lower quality when samples were sonicated for less than 20 min. Similar values of quantity and quality were observed when samples were sonicated for 20 min and 30 min. In order to decrease the experimental time due to the amount of samples to be sonicated, a 20 min sonication was chosen to extract the biofilm from digestate samples.



Figure C.3: Electrophoresis gel after the DNA/RNA co-extraction of samples testing different sonication times (1 to 6), and the use of RNAlater® in digestate and leachate samples.

The second test evaluated the influence of adding RNAlater® as a preservative to leachate and digestate samples. In the present study, samples from Phase I were preserved with RNAlater® and liquid nitrogen, while samples from Phase IV and V were preserved directly flash-freezing in liquid nitrogen. One sample from Phase IV (Batch 20) was preserved in RNAlater® because no liquid nitrogen was available at the sampling time. RNAlater® is a commercial mix composed of quaternary ammonium salts that stabilises RNA, especially when collecting and transporting samples can affect RNA integrity⁸⁴ (e.g., long-distance travels, lack of liquid nitrogen for flash-freezing). However, there is no common agreement regarding the effects of stabilisation agents, such as RNAlater®, in the quality of the nucleic acids extracted or the yield⁸⁵. The importance of RNAlater® to obtain high-quality nucleic acids in animal tissue⁸⁴ has been reported. However, although some studies have

Table C.4: Quality check of sonication and RNAlater[®] samples in terms of DNA concentration (Qubit[®]) and Nanodrop ratios.

Test	Sample	Code	Concentration (ng.nL ⁻¹)	Nanodrop	
				260/280	260/230
Sonication	Sample 0 min	1	6.72	0.6	-1.0
	Sample 5 min	2	5.91	0.5	-0.5
	Sample 10 min	3	14.4	1.2	-15.6
	Sample 15 min	4	15.7	1.5	6.1
	Sample 20 min	5	12.2	1.9	1.7
	Sample 30 min	6	11.9	2.0	1.9
RNAlater	Digestate with RNAlater	7	22.6	2.0	1.7
	Digestate without RNAlater	8	29.9	1.9	1.7
	Leachate with RNAlater	9	16.9	2.1	2.0
	Leachate without RNAlater	10	7.5	2.0	1.8

shown decreased DNA purity and yield⁸⁶, others have reported no influence in richness or evenness while using the storage buffer in bacterial strains⁸⁷ or significant difference between using liquid nitrogen or RNAlater[®] in conservation⁸⁵.

In the present study, no difference in DNA quality and yield was observed when preserving the samples directly by flash-freezing in liquid nitrogen or using RNAlater[®] before flash-freezing, especially for the digestate samples. Regarding leachate samples preserved without the addition of RNAlater[®], the low DNA concentration when compared to using RNAlater[®] was due to the loss of sample while removing the ethanol at the precipitation step of the Phenol-Chloroform extraction⁵⁷. Moreover, the same taxonomic composition with similar relative abundances was observed when comparing the samples treated with and without RNAlater[®] (Figure C.4). Therefore, the present test did not show a massive influence of using or not RNAlater[®] when conserving the samples, and almost no difference in terms of DNA. The effects on RNA were not studied, as it did not impact this particular study. More details on richness and evenness were not performed due to the lack of replicates for a robust statistical analysis.

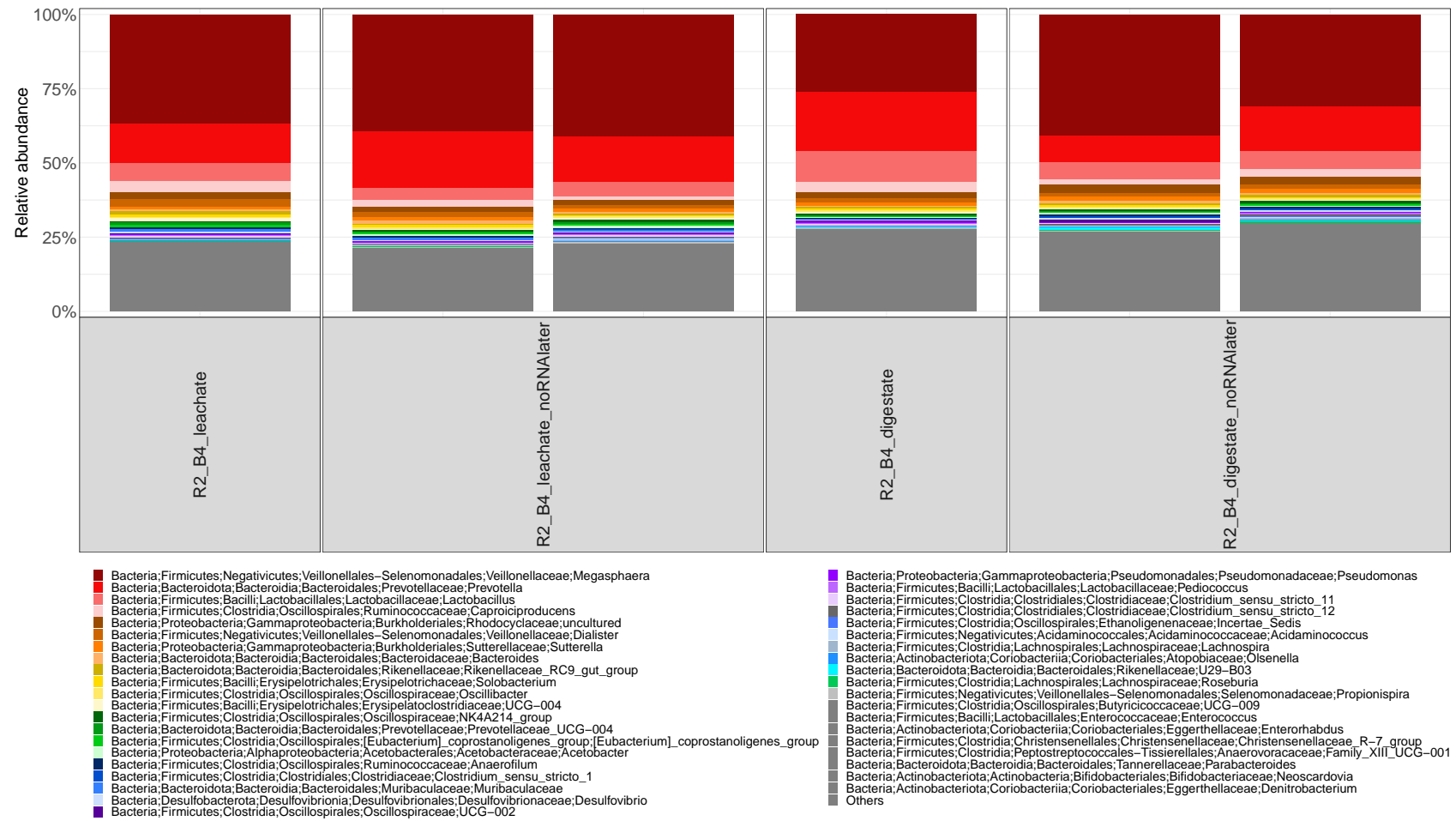


Figure C.4: Taxonomic composition of the microbial community 16S rRNA gene (DNA level) extracted from Phase I Batch 4 leachate and digestate with and without RNaLater[®].

Chapter 6: Conclusions and Perspective

6.1 Final Discussion and Conclusions

In this chapter, an overview of the main conclusions are compiled as a final discussion based on the results obtained in each individual paper. The main goal of this Ph.D was to investigate the valorisation of permanent grasslands by converting these feedstocks to biomethane and butyric acid using AD technology. Alongside feedstock-type, pH is also an important parameter in the production of VFAs (yields and profile), and both can affect the microbial community, which is the central actor in this process. Based on the hypotheses drawn in the first chapter and the methodology applied in this work, it was concluded that:

- (i) Different permanent grasslands can be used in the production of methane and VFAs, and the use of different feedstock-types can lead to different product yields.
- (ii) Mixed species of grassland biomass can improve forage yield and product yield at lower nitrogen fertilisation rates.
- (iii) Butyric acid can be the primary VFA produced from grassland biomass, especially when fermenting or co-fermenting the *Lolium perenne* species.
- (iv) pH is a determinant factor in the fermentation of grassland biomass, and the process benefits from a pH control especially when nitrogen-rich feedstocks are fermented.
- (v) Different inoculum sources did not affect the VFA production as much as the use of different silages, which was correlated with the feeding regime of silage opposed to the seed-inoculum feeding regime.
- (vi) Silage pH is an important process indicator, which was responsible for shifting the VFA production and microbial community.

6.1.1 Permanent grassland for the production of methane

Here we showed the importance of using multiple species of grassland biomass for both AD and the environment. As explained in Chapters 3 and 4, maintaining the biodiversity of permanent grassland fields is crucial for the sustainable production of forages with higher yields^{1,2} and better nitrogen intake at a lower input of nitrogen fertiliser³ and a lower emission of N₂O⁴. In Chapter 3, a systematic study was performed to link the sustainable production of grassland biomass to methane yield. The aim was to understand the differences and similarities in mono- and co-digesting different species of grassland biomass. We observed that an **improved methane yield was achieved in the mono-digestion of species that had a balanced C:N ratio and fibre content**, such as *P. pratense*. Indeed, the poor nutrient availability in *L. perenne* (150 kgN.ha⁻¹.yr⁻¹) resulted in a lower production of methane compared to the other grasses – *P. pratense* and *L. perenne* supplied with 300 kgN.ha⁻¹.yr⁻¹.

In fact, the unbalanced C:N ratio from *L. perenne* as well as the heterogeneity of these grassland biomasses were evident with the BMP results of Chapter 4. In Chapter 4, the same species (*L. perenne*) with the same nitrogen fertiliser dose ($150 \text{ kgN}\cdot\text{ha}^{-1}\cdot\text{yr}^{-1}$) but from a different plot was digested at similar conditions to Chapter 3, except the substrate was not sorted in any way. We observed a higher methane yield when digesting the $150 \text{ kgN}\cdot\text{ha}^{-1}\cdot\text{yr}^{-1}$ *L. perenne* from Chapter 4, compared to the results from the same substrate in Chapter 3. This was correlated to the C:N ratio of the $150 \text{ kgN}\cdot\text{ha}^{-1}\cdot\text{yr}^{-1}$ *L. perenne*, which was higher in Chapter 3 compared to Chapter 4. Moreover, the production of methane from *L. perenne* in Chapter 4 was the same irrespective of the nitrogen fertiliser dose supplied to those forages. In this way, we concluded that **a balanced C:N ratio for *L. perenne* was as effective as a higher nitrogen fertilisation rate.**

This unbalanced nutrient availability in *L. perenne* has been highlighted as a major issue in its mono-digestion, leading to lower product yield and process failure^{5,6}. Therefore, studies have proposed the co-digestion with animal slurry^{7,8} and forbs⁹⁻¹¹, as these feedstocks have a more balanced nutrient content. The co-digestion with slurries can mitigate an environmental burden from the GHG emissions associated to land-spreading animal slurry/manure¹². However, the methane yield from co-digesting grass and slurries is lower than the methane yield obtained in the mono-digestion of grass^{8,13}, while the co-digestion with forbs increased methane yield due to synergistic effects⁹. In the Chapter 3 of this thesis, we concluded that **synergistic and antagonistic effects were species-dependent, and the identity of each species was important in methane accumulation.** For example, synergistic effects were important in the co-digestion of *T. repens* and *C. intybus*, resulting in a higher methane yield. On the other hand, antagonistic effects were detected in the co-digestion of grass species (*L. perenne* and *P. pratense*), despite the mono-digestion of *P. pratense* resulting in the highest methane yield from all monocultures. Moreover, despite being both species of herbs, the co-digestion of *C. intybus* and clovers synergistically enhance methane yield, while the co-digestion with *P. lanceolata* and clovers had the opposite effect.

Antagonistic and synergistic effects are a result of the difference in trace elements, surface sugars and fibre content between species⁸. Therefore, mapping those interspecific effects can be important to optimise the production of VFAs and methane from grassland biomass, thus helping to design the forage production and management to meet product criteria in AD. This was evident in the digestion of clovers (*T. pratense* and *T. repens*) in Chapter 4, where **weed intrusion was deemed as the factor hindering the accumulation of methane from clover fields.** Different from Chapter 3, substrates in Chapter 4 were not sorted. Therefore, intended species and unsown species were added to the experiment as they were received from the field. The weed intrusion in clovers, thus the presence of other species than *T. pratense* or *T. repens*, was indeed higher compared to the grass substrates in Chapter 4. The presence of unsown species in the substrate could have resulted in antagonistic or synergistic effects, indicating how important it is to know which species are present in the field and the effect of their interactions to product yield. In reality, despite cultivated in the same field and under the same conditions, each field plot of the same species of grassland biomass may have a different species composition due to weed intrusion, which contributes to the heterogeneity of the feedstock.

However, manually sorting species to compose a substrate may be unfeasible when operations are scaled up to a pilot-plant or full-scale anaerobic digestion plant, indicating that field management and design can be crucial to eliminate or decrease antagonistic effects.

An important trait of combining different grassland species is the increased forage yield^{1,2} and the possibility of mitigating drought effects¹⁴. Securing feedstock quantity and quality is important to guarantee a reliable supply chain for a green biorefinery. Therefore, estimating the methane production in terms of forage yield was important. In Chapter 3, we observed a **comparable area-specific methane yield while co-digesting six species of grassland biomass or mono-digesting a higher fertilised *L. perenne***. The synergistic effects from species that had a higher forage yield played an important role in improving the methane yield per area in the co-digestion of six grassland species. The same was observed in the area-specific methane yield when co-digesting *L. perenne* and *T. pratense*, indicating the importance of mixing clovers to other species. Therefore, results from Chapter 3 indicate that combining grassland species can synergistically improve methane yield, providing an alternative to using higher dosages of nitrogen fertiliser leading to a more sustainable process. It may be beneficial to increase the proportion of species that synergistically increased methane production, such as *C. intybus*, *T. pratense* and *T. repens*, to observe if a higher methane yield could be reached.

6.1.2 Permanent grasslands in the production of butyric acid and other VFAs

In Chapter 3, we saw that using clovers as a feedstock or co-feedstock in AD was important to provide the nutrition needed for methane production⁹. Clovers have a higher nitrogen content than grasses, which leads to a higher accumulation of ammonia in the liquid upon substrate degradation (Chapters 3 and 4). Although the accumulation of ammonia can lead to a slower degradation¹⁵, as seen in Chapter 4, **clover's buffering capacity was associated to its higher VS degradation under fermentation conditions**. In fact, the slower degradation of clovers was beneficial to the slower accumulation of acids, decreasing possible inhibitory effects of a fast acid accumulation¹⁶. However, the two-stage fermentation assay showed that adding an external source of inoculum acclimatised to VFA production from grass silage was crucial for substrate degradation as well. After placed in water in the first-stage, pH levels dropped to 4.0 after two days of fermentation, which are levels that hinders biomass hydrolysis¹⁷. After adding the acclimatised inoculum and correcting pH to mildly acidic levels (second-stage), the biomass degradation reached was the same as the one observed in the one-stage fermentation. Therefore, an acclimatised inoculum was crucial for increasing degradation levels, indicating the importance of selecting an appropriate inoculum source not only for the production of VFAs, but also for substrate degradation.

This higher degradation of clovers, however, did not necessarily result in the highest production of VFAs in the one-stage fermentation. In fact, the slow accumulation of acids provided a buffered system in the fermentation of *T. pratense*, which led a higher accumulation of methane instead of VFAs. Despite having the same total product yield (methane + VFA) as *T. pratense*, the one-stage

fermentation of *T. repens* led to a higher VFA yield, which was associated to the weed intrusion in the *T. repens* field. Therefore, identifying those unsown species in the *T. repens* field is important, as they may have synergistically favoured the production of VFAs, especially butyric acid. Methane accumulation was observed in the fermentation and co-fermentation of all substrates, contributing to the higher product yield from the 300 kgN.ha⁻¹.yr⁻¹ *L. perenne*, for example. This methane accumulation was correlated to the pH profile, which was left to fluctuate, leading to a potential loss in VFA yield. The highest accumulation of VFAs was observed from the fermentation of *L. perenne*, irrespective of the nitrogen fertiliser dosage applied. In fact, no significant difference in butyric acid yield or VFA yield was observed when comparing the fermentation of both *L. perenne* substrates, indicating that **using a double dose of nitrogen fertiliser was not needed to improve acid yield**. Moreover, **the selective production of butyric acid was mainly observed from the fermentation of *L. perenne*, as a single substrate or in a co-fermentation with *T. repens***. This is an important result for the sustainable production of VFAs in AD, considering the negative environmental impact of monocultures and high nitrogen fertilisation rates to forage production.

pH is a very important parameter in the production of VFAs not only because it affects biomass hydrolysis¹² and VFA yield¹⁸, but also the VFA profile^{12,17}. In the one-stage fermentation study, the fermentation of *T. pratense* resulted in a different VFA profile when compared to the fermentation of *L. perenne* and the co-fermentation of *L. perenne* and *T. repens*. This was both correlated to the feedstock-type as well as the pH profile shift to neutral levels, which was previously associated with the ammonia accumulation. In the two-stage fermentation of grassland biomass, some species were placed in water for 7 days before inoculation. At that moment, it was observed a **sharp drop in pH as a consequence of lactic acid accumulation**. This pH drop and lactic acid accumulation observed in Chapter 4 was the first indication that the microbial community present in the surface of grass could influence the fermentation process. The idea of accumulating lactic acid in the first-stage was to provide an important intermediary for the production of butyric acid^{19,20} in the second-stage. However, **no difference in VFA production was observed when comparing the one-stage and two-stage fermentations**. Again, controlling pH levels below 6.0 was considered important to produce butyric acid from precursors such as lactic acid and readily available sugars, as pH levels above 6.0 can lead to a predominant accumulation of propionic^{21,22} and acetic acid¹⁷. By the end of the second-stage fermentation, the accumulation of propionic acid and acetic acid was favoured in comparison to butyric acid, especially when *T. repens* was fermented or co-fermented with *L. perenne*.

6.1.3 Silage pH – an important process indicator for VFA accumulation

The need for pH control in the fermentation of grassland biomass as well as an appropriate inoculum that combined biomass degradation and VFA production motivated the reactor trial in Chapter 5. Three combinations of seed-inoculum were selected based on the **efficient silage degradation achieved when mixtures of granular sludge with rumen material and cattle slurry were used**. Rumen fluid, rumen solid and granular sludge composed the seed-inoculum used in Reactor 1, while

cattle slurry and granular sludge composed the mixture used in Reactor 2. In Reactor 3, as a basis of comparison, granular sludge was used as seed-inoculum. Our results showed that combining rumen material with granular sludge was imperative to reach a higher degradation efficiency and product conversion, which was correlated to the hydrolytic capability of the rumen microbiome²³. In fact, DNA analysis showed the presence of bacterial genera correlated to the hydrolysis of lignocellulosic biomass in the rumen material, such as *Christensenellaceae R-7 group*, *Rikenellaceae RC9 gut group*, *Prevotella*, and *Prevotellaceae UCG-001*. Improved biomass hydrolysis and product conversion using rumen fluid and cow manure has been observed in the anaerobic digestion of rapeseed²⁴, cow manure²⁵, lignocellulosic biomass²⁶, and food waste²⁷.

These inoculum mixtures were named seed-inoculum as they were used in the Start Up phase of the reactor trial, therefore, only used at the beginning of the trial. Afterwards, the leachate and digestate from a previous batch was used to inoculate the subsequent batch, alongside fresh silage. A small batch study was designed to investigate the need for using both leachate and digestate as inoculum for a subsequent batch. From this, we discovered that **combining digestate and leachate as inoculum is more important for biomass degradation than acids production**. This result for acid production was associated with the similarity in distribution of bacterial genus as well as abundances in both leachate and digestate. However, a difference in microbial density of hydrolysers in the digestate compared to the leachate could explain the higher VS degradation when the digestate is used. Moreover, using both leachate and digestate was considered advantageous for the fermentation of silage, since it was considered that the combination can lead to a higher microbial density, which may explain the improvement in VFA production rate.

Despite using different sources of seed-inoculum at the Start Up phase, **no major difference in VS degradation was observed** during the reactor trial. Even increasing leachate dilution at the beginning of each batch (Phase II) or washing the solid mixture of silage and digestate (Phase III) did not significantly impact silage degradation. Moreover, the different sources of seed-inoculum, hence the different reactors, had close to no difference in terms of VFA yield or butyric acid yield in each phase. In fact, the changes in VFA yield and methane accumulation were correlated to the **silage indigenous community and pH, which were deemed the driving forces shifting the reactor performance**. This was concluded based on the four silage used in this work, which had different pHs – 4.6 (Silage PI), 8.1 (Silage B16), 6.6 (Silage PIV), and 4.3 (Silage PV). The silage pH is intrinsically connected with the conservation of silage and its microbiome²⁸, and lower pH values are important to guarantee a feedstock with a higher quality and nutritional value²⁹. Our work showed that using a silage with pH 8.1 resulted in the lowest accumulation of VFAs and the lowest silage degradation. Moreover, when the silage with pH 6.6 was introduced in the process (Phase IV), it favoured methane accumulation, resulting in VFA mix dominated by propionic acid. The use of a silage with low pH was considered important for VFA production, leading to the highest concentration of VFA, especially caproic acid and butyric acid. Therefore, **silage pH was an important process indicator for acid accumulation efficiency and acid profile**, which can aid in selecting the appropriate process for each type of silage.

Based on the results of Chapter 5, VFA production was restored by re-introducing a low pH silage (Silage PV, pH 4.3) in the fermentation. By Phase V, **butyric acid was obtained as the primary VFA from silage, with a significant accumulation of caproic acid.** The highest concentration of butyric acid was reached after 2-3 days of fermentation upon complete consumption of the lactic acid that was quickly produced or already available from the surface of silage. This was considered relevant to improve butyric acid yields, allowing a higher, quicker and selective conversion^{30,31} with a lower production of other acids in the metabolism, such as acetic acid.

Production of lactic acid from grass, followed by its fast and complete consumption to butyric acid was also observed in the Chapter 4 in the two-stage fermentation of *L. perenne* and in other studies^{32,33}. Therefore, the conversion of silage seemed to start with its degradation to carbohydrates, which were first converted to lactic acid and then to butyric acid¹⁹; when butyric acid reached its maximum concentration, caproic acid was produced. In our study, when butyric acid concentrations reached values around 4 gCOD.L⁻¹, caproic acid was produced alongside acetic acid³⁴, leading to caproic acid accumulation after a maximum accumulation of butyric acid was reached in the leachate. This caproic acid concentration, however, was lower than what has been observed using pure lactic acid as electron donor and butyric acid as electron acceptor^{34,35}. Despite caproic acid being detected in the fermentation of grass, some strategies would be beneficial to optimise its production by increasing the accumulation of butyric acid towards its threshold. Some of these strategies are the supplementation of lactic acid³⁴, the constant removal of VFAs to decrease acid inhibition^{36,37}, the bioaugmentation with *Clostridium* species to improve butyric acid yield^{20,38}, and the introduction of a second-stage focused on caproic acid accumulation.

The production of lactic acid from grass was associated with the predominance of LAB in the surface of silages PI and PV, especially *Lactobacillus*, which is a characteristic of well-preserved silages²⁹. In the case of Silage PIV (pH 6.6), a lower presence of LAB was detected, with a predominance of hydrolytic bacteria from the class *Gammaproteobacteria* and the genus *Sphingobacterium*. Moreover, the shift in the microbial community dynamics was associated with the balance between *Firmicutes* and *Bacteroidota* in Phases I, IV and V. A higher relative abundance of the *Firmicutes* compared to *Bacteroidota* was observed in Phases I and V, and the opposite was observed in Phase IV. This distribution correlates with the profile of VFAs produced in this study, as propionate (and acetate) are mainly produced by *Bacteroidota*³⁹, and butyrate³⁹ and caproate^{32,40} are mainly produced by *Firmicutes*. *Prevotella* was observed during the nine months of fermentation, but it was predominant in Phase IV, where propionic acid dominated the VFA mix. The higher presence of *Lactobacillus* in Phase V, associated to the presence of *Caproiciproducens* was correlated to the production of caproic acid from butyric acid.

Last, but not least, Silage PV consisted of a mix of grassland species, while Silage PI was composed mainly of *L. perenne*. Therefore, the reactor performance in Phase V validates the use of mixed-species silages for butyric acid production, with no significant difference from a silage composed mainly of *L. perenne*, and contributing to the sustainability of the process⁴¹.

6.2 Future Recommendations and Perspectives

This thesis provides new insights in the use of grassland species and nitrogen fertiliser in the production of methane, butyric acid and VFAs. Although it contributes to the overall knowledge regarding those species, some recommendations are proposed here for the continued development of the field:

- (i) a systematic study at nutrient level to maximise the product conversion from grassland species;
- (ii) a faster and simple chemical assay to understand solid degradation, such as the solid's COD proposed in Chapter 5, as current methods can take from two days (solids content) to a week (lignocellulosic characterisation);
- (iii) a simplex design similarly to Chapter 3, but expanded to different species proportions using methane yield, VFA yield, and butyric acid yield as response variables (manual separation would be advisable to understand the interaction between species);
- (iv) the fermentation of clovers in LBRs using a pH control system similarly to what was performed for silage in Chapter 5;
- (v) a fermentation study to maximise the production of lactic acid from grassland biomass in a first-step, with constant recovery of lactic acid. This lactic acid would be fermented in second-step for butyric acid under controlled pH and using an inoculum bio-augmented with *Clostridium* species;
- (vi) a fermentation study similarly to Chapter 5 but re-seeding the reactor to observe its effects on biomass degradation and VFA production;
- (vii) an in-line recovery of VFAs, provided the drop in acidic pressure does not impact the production of butyric acid.

6.3 References

1. Grange, G., Brophy, C. & Finn, J. A. Grassland legacy effects on yield of a follow-on crop in rotation strongly influenced by legume proportion and moderately by drought. *European Journal of Agronomy* **138**, 126531 (2022).
2. Finn, J. A. *et al.* Ecosystem function enhanced by combining four functional types of plant species in intensively managed grassland mixtures: a 3-year continental-scale field experiment. *Journal of Applied Ecology* **50** (ed Wilsey, B.) 365–375 (Apr. 2013).
3. Connolly, J. *et al.* Weed suppression greatly increased by plant diversity in intensively managed grasslands: A continental-scale experiment. *Journal of Applied Ecology* **55** (ed Inderjit) 852–862 (Mar. 2018).
4. Rahman, M. M. *et al.* in *Advances in Legumes for Sustainable Intensification* (eds Meena, R. S. & Kumar, S.) 381–402 (Academic Press, 2022).

5. Thamsiroj, T., Nizami, A. S. & Murphy, J. D. Why does mono-digestion of grass silage fail in long term operation? *Applied Energy* **95**, 64–76 (2012).
6. Wall, D. M., Allen, E., Straccialini, B., Kiely, P. O. & Murphy, J. D. The effect of trace element addition to mono-digestion of grass silage at high organic loading rates. *Bioresource Technology* **172**, 349–355 (2014).
7. Murphy, J. D. *et al.* *The Potential for Grass Biomethane as a Biofuel: Compressed Biomethane Generated from Grass , Utilised as a Transport Biofuel* tech. rep. (Environmental Research Institute, 2011), 1–69.
8. Himanshu, H., Murphy, J., Grant, J. & O’Kiely, P. Antagonistic effects on biogas and methane output when co-digesting cattle and pig slurries with grass silage in in vitro batch anaerobic digestion. *Biomass and Bioenergy* **109**, 190–198 (Feb. 2018).
9. Cong, W.-F., Moset, V., Feng, L., Møller, H. B. & Eriksen, J. Anaerobic co-digestion of grass and forbs – Influence of cattle manure or grass based inoculum. *Biomass and Bioenergy* **119**, 90–96 (Dec. 2018).
10. Wahid, R., Ward, A. J., Møller, H. B., Sjøgaard, K. & Eriksen, J. Biogas potential from forbs and grass-clover mixture with the application of near infrared spectroscopy. *Bioresource Technology* **198**, 124–132 (2015).
11. Wahid, R. *et al.* Anaerobic mono-digestion of lucerne, grass and forbs – Influence of species and cutting frequency. *Biomass and Bioenergy* **109**, 199–208 (Feb. 2018).
12. Nzeteu, C., Coelho, F., Davis, E., Trego, A. & O’flaherty, V. Current Trends in Biological Valorization of Waste-Derived Biomass: The Critical Role of VFAs to Fuel a Biorefinery. **8**, 445 (2022).
13. Wall, D. M., O’Kiely, P. & Murphy, J. D. The potential for biomethane from grass and slurry to satisfy renewable energy targets. *Bioresource Technology* **149**, 425–431 (Dec. 2013).
14. Grange, G., Brophy, C. & Finn, J. *Drought and plant diversity effects on the agronomic multifunctionality of intensively managed grassland* in *Grassland Science in Europe, Vol. 27 - Grassland at the heart of circular and sustainable food systems* (2022), 403–405.
15. Fischer, M. A. *et al.* Immediate Effects of Ammonia Shock on Transcription and Composition of a Biogas Reactor Microbiome. *Frontiers in Microbiology* **10** (Sept. 2019).
16. Magdalena, J. A., Greses, S. & González-Fernández, C. Impact of Organic Loading Rate in Volatile Fatty Acids Production and Population Dynamics Using Microalgae Biomass as Substrate. *Scientific Reports* **9**, 18374 (Dec. 2019).
17. Lee, W. S., Chua, A. S. M., Yeoh, H. K. & Ngoh, G. C. A review of the production and applications of waste-derived volatile fatty acids. *Chemical Engineering Journal* **235**, 83–99 (2014).

18. Nagarajan, S., Jones, R. J., Oram, L., Massanet-Nicolau, J. & Guwy, A. Intensification of Acidogenic Fermentation for the Production of Biohydrogen and Volatile Fatty Acids—A Perspective. *Fermentation* **8**, 325 (July 2022).
19. Gao, M. *et al.* Production of medium-chain fatty acid caproate from Chinese liquor distillers' grain using pit mud as the fermentation microbes. *Journal of Hazardous Materials* **417** (Sept. 2021).
20. Detman, A. *et al.* Cell factories converting lactate and acetate to butyrate: *Clostridium butyricum* and microbial communities from dark fermentation bioreactors. *Microbial Cell Factories* **18**, 36 (Dec. 2019).
21. Bengtsson, S., Hallquist, J., Werker, A. & Welander, T. Acidogenic fermentation of industrial wastewaters: Effects of chemostat retention time and pH on volatile fatty acids production. *Biochemical Engineering Journal* **40**, 492–499 (July 2008).
22. Atasoy, M. & Cetecioglu, Z. The effects of pH on the production of volatile fatty acids and microbial dynamics in long-term reactor operation. *Journal of Environmental Management* **319**, 115700 (Oct. 2022).
23. Bayané, A. & Guiot, S. R. *Animal digestive strategies versus anaerobic digestion bioprocesses for biogas production from lignocellulosic biomass* 2011.
24. Baba, Y. *et al.* Pretreatment of Lignocellulosic Biomass with Cattle Rumen Fluid for Methane Production: Fate of Added Rumen Microbes and Indigenous Microbes of Methane Seed Sludge. *Microbes and Environments* **34**, 421–428 (2019).
25. Ozbayram, E. G., Akyol, Ince, B., Karakoç, C. & Ince, O. Rumen bacteria at work: bioaugmentation strategies to enhance biogas production from cow manure. *Journal of Applied Microbiology* **124**, 491–502 (2018).
26. Nguyen, L. N. *et al.* Application of rumen and anaerobic sludge microbes for bio harvesting from lignocellulosic biomass. *Chemosphere* **228**, 702–708 (Aug. 2019).
27. Yan, B. H., Selvam, A. & Wong, J. W. C. Application of rumen microbes to enhance food waste hydrolysis in acidogenic leach-bed reactors. *eng. Bioresource technology* **168**, 64–71 (Sept. 2014).
28. Paudel, S. R. *et al.* Pretreatment of agricultural biomass for anaerobic digestion: Current state and challenges. *Bioresource Technology* **245**, 1194–1205 (2017).
29. Kung Jr, L., Shaver, R. D., Grant, R. J. & Schmidt, R. J. Silage review: Interpretation of chemical, microbial, and organoleptic components of silages. *Journal of Dairy Science* **101**, 4020–4033 (2018).

30. Steinbrenner, J., Nägele, H.-J., Buschmann, A., Hülsemann, B. & Oechsner, H. Testing different ensiling parameters to increase butyric acid concentration for maize silage, followed by silage separation and methane yield potential of separated solids residues. *Bioresource Technology Reports* **7**, 100193 (Sept. 2019).
31. Ingle, A. T., Fortney, N. W., Walters, K. A., Donohue, T. J. & Noguera, D. R. Mixed Acid Fermentation of Carbohydrate-Rich Dairy Manure Hydrolysate. *Frontiers in Bioengineering and Biotechnology* **9** (Aug. 2021).
32. Khor, W. C., Andersen, S., Vervaeren, H. & Rabaey, K. Electricity-assisted production of caproic acid from grass. *Biotechnology for Biofuels* **10**, 1–11 (Dec. 2017).
33. Lehtomäki, A., Huttunen, S., Lehtinen, T. M. & Rintala, J. A. Anaerobic digestion of grass silage in batch leach bed processes for methane production. *Bioresource Technology* **99**, 3267–3278 (May 2008).
34. Nzeteu, C. o. *et al.* Development of an enhanced chain elongation process for caproic acid production from waste-derived lactic acid and butyric acid. *Journal of Cleaner Production* **338**, 130655 (Mar. 2022).
35. Xie, S. *et al.* Anaerobic caproate production on carbon chain elongation: Effect of lactate/butyrate ratio, concentration and operation mode. *Bioresource Technology* **329**, 1–8 (June 2021).
36. Jones, R. J., Massanet-Nicolau, J., Fernandez-Feito, R., Dinsdale, R. M. & Guwy, A. J. Recovery and enhanced yields of volatile fatty acids from a grass fermentation via in-situ solids separation and electro dialysis. *Journal of cleaner production* **296**, 126430 (2021).
37. Jones, R. J., Massanet-Nicolau, J., Fernandez-Feito, R., Dinsdale, R. M. & Guwy, A. J. Fermentative volatile fatty acid production and recovery from grass using a novel combination of solids separation, pervaporation, and electro dialysis technologies. *Bioresource technology* **342**, 125926 (2021).
38. Detman, A. *et al.* Dynamics of dark fermentation microbial communities in the light of lactate and butyrate production. *Microbiome* **9**, 158 (Dec. 2021).
39. Feng, W., Ao, H. & Peng, C. Gut Microbiota, Short-Chain Fatty Acids, and Herbal Medicines. *Frontiers in Pharmacology* **9** (Nov. 2018).
40. Candry, P. & Ganigué, R. Chain elongators, friends, and foes. *Current Opinion in Biotechnology* **67**, 99–110 (Feb. 2021).
41. Bråthen, K. A., Pugnaire, F. I. & Bardgett, R. D. The paradox of forbs in grasslands and the legacy of the mammoth steppe. *Frontiers in Ecology and the Environment* **19**, 584–592 (Dec. 2021).